UNIVERSITY OF ANTWERP
Faculty of Medicine and Health Sciences

Contribution to elucidating the genetic aetiology of thoracic aortic aneurysms

Contributie tot de opheldering van de genetische etiologie van thoracale aorta aneurysma's

Thesis submitted for the degree of
Doctor of Medical Sciences
at the University of Antwerp to be defended by

Elisabeth Gillis
Supervisors:
Prof. Dr. Bart Loeys
Prof. Dr. Lut Van Laer
Dr. Aline Verstraeten
Antwerp, 2019

Members of the jury

Prof. Dr. Bart Loeys, promotor
Center of Medical Genetics, University of Antwerp and Antwerp University Hospital,
Antwerp, Belgium

Prof. Dr. Lut Van Laer, promotor
Center of Medical Genetics, University of Antwerp and Antwerp University Hospital,
Antwerp, Belgium

Dr. Aline Verstraeten, promotor
Center of Medical Genetics, University of Antwerp, Antwerp, Belgium

Prof. Dr. Inez Rodrigus, chair of the doctoral committee
Cardiac surgery, Antwerp University Hospital, Antwerp, Belgium

Prof. Dr. Bernard Paelinck
Cardiology, Antwerp University Hospital, Antwerp, Belgium

Prof. Dr. Paul Coucke
Center for Medical Genetics Ghent, Ghent University Hospital, Ghent, Belgium

Dr. Fleur Van Dijk
Clinical genetics, North West Thames Regional Genetics Service (Kennedy-Galton
centre), London, UK

Summary

The aorta is the largest artery in the human body. It starts from the heart and supplies the rest of the body with oxygen-carrying blood. The aorta can abnormally enlarge in diameter, this is called an aortic aneurysm. The aneurysm can then lead to dissection or rupture which is often deadly, accounting for 1-2% of all deaths in Western Europe. There are two kinds of aortic aneurysms depending on the position: thoracic aortic aneurysms (TAA) at the level of the chest cavity and abdominal aortic aneuryms in the abdomen. In this thesis, we focused on TAA, because it has a strong genetic component. About 20% of patients have a positive family history. The goal of this thesis was to contribute to the elucidation of the genetic aetiology of TAA, because many patients remain genetically undiagnosed. A genetic diagnosis is beneficial for the patient's treatment, follow-up and counselling. To better understand the genetic cause and underlying mechanism, researchers have focused on syndromic TAA, such as Marfan syndrome (MFS), Loeys-Dietz syndrome and Shprintzen-Goldberg syndrome. MFS is caused by mutations in the *FBN1* gene. Although this gene was already discovered in 1991, Chapter 1 tells the scientific story of a family with MFS and a mutation in *FBN1* only diagnosed during this thesis. Even though the affected members showed clear symptoms of MFS, they did not have a molecular genetic confirmation for 10 years. By using a myriad of techniques, such as whole exome sequencing and cDNA sequencing, we were able to finally identify the causal intronic *FBN1* mutation. The contribution of the TGF-β pathway to the pathomechanism of MFS was discovered in 2003. Since then, numerous TGF-β genes, such as *TGFBR1/2*, *TGFB2*, etc. have been linked to TAA-related syndromes. An extra gene was added to this list during this thesis; Chapter 2 describes the discovery of *TGFB3* as an additional TAA gene. The fourth chapter describes the finding and preliminary functional experiments of a possible new TAA gene, *KLF15*. This gene encodes a transcription factor which might affect

the TGF-β pathway as well. Chapter 3 focusses on bicuspid aortic valve (BAV) associated TAA. Between the heart and the aorta, the aortic valve prevents blood flowing back into the heart. Normally the aortic valve has three leaflets, but the aortic valve of 1-2% of the general population only contains two aortic valve leaflets. This condition is often accompanied by an increased risk for the development of TAA. Unfortunately, it has been very difficult to pinpoint causal genes for isolated BAV. Because TAA and BAV most possibly share a genetic cause, we focused on BAV/TAV patients to unravel more genetic determinants. A targeted gene panel helped to identify the *SMAD6* gene as a new causal gene for BAV/TAA.

Samenvatting

De aorta is het grootste bloedvat in het menselijk lichaam. Deze begint vanaf het hart om dan de rest van het lichaam van zuurstofrijk bloed te voorzien. De aorta kan toenemen in diameter, wat een aorta aneurysma wordt genoemd. Een aneurysma kan leiden tot een dissectie of ruptuur van de aorta wat dodelijk kan zijn. Dit is de doodsoorzaak van 1-2% van de West-Europese bevolking. Er zijn twee soorten aorta aneurysma's afhankelijk van de positie in het lichaam: thoracale aorta aneurysma's (TAA), ter hoogte van de borstkast, en abdominale aorta aneurysma's, ter hoogte van de buikholte. In deze thesis lag de focus op TAA, omdat deze vorm een sterke genetische component heeft. Maar liefst 20% van de patiënten heeft een familielid met TAA. Het doel van deze thesis was om bij te dragen aan het ophelderen van de genetische oorzaak van TAA, omdat veel patiënten nog steeds geen genetische diagnose hebben gekregen. Als men de genetische oorzaak kent kan de patiënt beter behandeld, opgevolgd en gecounceld worden. Om de genetische oorzaak te onderzoeken, focussen wetenschappers op syndromale vormen van TAA. Aandoeningen zoals Marfan syndroom (MFS), Loeys-Dietz syndroom en Shprintzen-Goldberg syndroom hebben allemaal TAA als één van de belangrijkste symptomen. Al in 1991 werd ontdekt dat MFS veroorzaakt wordt door mutaties in het *FBN1* gen. Nochtans vertelt hoofdstuk 1 het verhaal van een MFS familie die pas na 10 jaar moleculair werd gediagnosticeerd. Met behulp van verschillende technieken zoals exoom-wijde sequenering en cDNA sequenering werd de causale intronische *FBN1* variant geïdentificeerd. Door middel van verder onderzoek op het *FBN1* gen in MFS werd het belang van de TGF-β signalisatie pathway opgehelderd in 2003. Sindsdien zijn al verschillende TGF-β pathway genen, zoals *TGFBR1/2*, *TGFB2*, etc., gelinkt aan TAA syndromen. Een nieuw gen werd aan deze lijst toegevoegd tijdens deze thesis, namelijk het *TGFB3* gen (zie hoofdstuk 2). Het vierde hoofdstuk beschrijft dan weer de ontdekking van mogelijk nog een nieuw TAA gen, *KLF15*, en de prelimi-

naire functionele experimenten die werden uitgevoerd. Dit gen wordt omgeschreven als een transcriptie factor die ook effect zou kunnen hebben op de TGF-β pathway. Hoofdstuk 3 daarentegen focust op bicuspide aortaklep met geassocieerd TAA. Tussen het hart en de aorta zit de aorta klep die voorkomt dat het bloed terugstroomt naar het hart. Normaal gezien heeft deze klep drie klepblaadjes, maar in 1-2% van de algemene bevolking zijn dit maar twee klepblaadjes. Vaak is TAA een extra complicatie bij deze aandoening. Het is heel moeilijk om causale genen te ontdekken voor geïsoleerde BAV, daarom focusten we op BAV/TAA patiënten om de genetische oorzaken te zoeken. Een targeted genen panel heeft geholpen om het *SMAD6* gen aan te duiden als een nieuw gen voor BAV/TAA.

Abbreviations

Table 1: List of abbreviations

Abbreviation	Explanation
AAA	Abdominal aortic aneurysms
ACE	Angiotensin-converting enzyme
AD	Autosomal dominant
ADPKD	Autosomal dominant polycystic kidney disease
ANG	Angiotensin
AOVD1	Aortic valve disease 1
AR	Autosomal recessive
ASD	Atrial septal defect
AVM	Arteriovenous malformations
BAPN	β-aminopropionitrile
BAV	Bicuspid aortic valve
BSA	Bovine serum albumine
CAD	Coronary artery disease
CADD	Combined Annotation Dependent Depletion
CCB	Calcium channel blockers
cDNA	Complementary DNA
CNC	Cardiac neural crest
CTA	Computed tomographic angiography
DMEM	Dulbecco's Modified Eagle Medium
DNA	Deoxyribonucleic acid
EBP	Elastin-binding protein
ECM	Extracellular matrix
EDS	Ehlers-Danlos syndrome

EGM	Endothelial Cell Growth medium
ERK	Extracellular signal-regulated kinase
ExAC	Exome Aggregation Consortium
FAA	Familial aortic aneurysm
FBLN4	Fibulin-4
FBN1	Fibrillin-1
FBS	Fetal bovine serum
FFPE	Formalin-fixed Paraffin-embedded
FTAAD	Familial thoracic aortic aneurysms and dissection
GATK	Genome Analysis Toolkit
gDNA	Genomic DNA
GI	Gastrointestinal
GOF	Gain of function
HDAC	Histone deacetylase
HEK	Human embryonic kidney
HHT	Hemorrhagic telangiectasia syndrome
JNK	Jun N-terminal kinase
JPS	Juvenile polyposis syndrome
KLF	Krüppel-like factors
L-R	Left-non-coronary
LDS	Loeys-Dietz syndrome
LOF	Loss of function
LTBP	Latent TGF-β-binding protein
mAC	Mutant allele count
MAF	Minor allele frequency
MAPK	Mitogen activated protein kinase
MEK	Mitogen activated protein kinase/extracellular signal-regulated kinase kinase
MFS	Marfan syndrome
MIP	Molecular Inversion Probes
miRNA	Micro RNA
MLCK	Myosin light chain kinase
MMP	Matrix metalloproteinase
MRA	Magnetic resonance angiography

MRI	Magnetic resonance imaging
MYLK	Myosin light chain kinase
NCBI	National Center for Biotechnology Information
NMD	Nonsense mediated mRNA decay
OFT	Outflow tract
OMIM/MIM	Online Mendelian Inheritance in Man
PAI	Plasminogen acivator inhibitor
PCR	Polymerase chain reaction
PDA	Patent ductus arteriosus
PFO	Patent foramen ovale
R-L	Right-left coronary
R-N	Right-non-coronary
SGS	Shprintzen-Goldberg syndrome
SKI	V-ski avian sarcoma viral oncogene homolog
SMAD	Mother against decapentaplegic homolog 4 [drosophila]
SNP	Single-nucleotide polymorphism
STAAD	Sporadic thoracic aortic aneurysms and dissections
SVAS	Supravalvular aortic stenosis
TAA	Thoracic aortic aneurysms
tAC	Total allele count
TAV	Thoracic aortic valve
TBS	Tris buffered saline
TEVAR	Thoracic EndoVascular Aortic Repair
TGF	Transforming growth factor
TGFBR	Transforming growth factor-β receptor
TSP	Thrombospondin
TVP	Tricuspid valve prolapse
VSD	Ventricular septal defect
VSMC	Vascular smooth muscle cells
VVG	Verhoeff-Van Gieson
WES	Whole genome sequencing
WT	Wild-type
XD	X-linked dominant
XL	X-linked

Contents

3 Candidate gene resequencing in a large bicuspid aortic valve-associated thoracic aortic aneurysm cohort: *SMAD6* as an important contributor   **116**

4 Mutations in the transcriptional regulator, *KLF15*, are associated with thoracic aortic aneurysms   **154**

IV   Discussion   179

PART I

Introduction

The introduction is partially modified from

Genetics of Thoracic Aortic Aneurysm: At the Crossroad of Transforming Growth Factor-β Signaling and Vascular Smooth Muscle Cell Contractility

Elisabeth Gillis[1], Lut Van Laer[1] and Bart L. Loeys[1,2]

[1]*Center for Medical Genetics, Faculty of Medicine and Health Sciences, University of Antwerp and Antwerp University Hospital, Antwerp, Belgium*

[2]*Department of Human Genetics, Radboud University Nijmegen Medical Center, Nijmegen, The Netherlands*

The aorta is the largest artery in the human body and supplies oxygen-carrying blood to all organs. It can become abnormally widened, called an aortic aneurysm. When left untreated, these aneurysms can dissect or rupture, accounting for 1% to 2% of all deaths in the Western countries[1]. Because acute aortic dissections might be disguised as heart attacks, true incidence numbers could even be significantly higher[2]. Aortic aneurysms are categorized into two main groups depending on their location: thoracic aortic aneurysms (TAA) and abdominal aortic aneurysms (AAA). Abdominal aortic aneurysms are most common in the population and are linked to various lifestyle-associated risk factors, including smoking, hyperlipidemia, hypertension, sex, and age[3, 4]. Heritability estimates as high as 70% have been found, and recently, several genes and loci have been associated with AAA (*DAB2IP*, *LRP1*, *CDKN2B-AS1*, *CNTN3*, *LPA*, *IL6R*, *LDLR*, *SORT1*, *MMP3* and *AGTR1* [5–19]). In this thesis, the focus lies on TAA, which has an even stronger genetic component, with 20% of patients having a positive family history[20, 21]. This number is also likely to be underestimated because developing TAA usually remain asymptomatic. TAA can develop at the level of the ascending (60%) or descending aorta (40%), the aortic arch (10%), or the upper abdomen (10%)[22]. These numbers do not add up to 100% because patients with TAA frequently experience aneurysms at multiple locations.

Life expectancy in TAA patients is mainly determined by the risk of aortic dissection. The main predictor of aortic dissection is the aortic diameter[23, 24]. Historically, aortic diameters >5.5 cm were regarded as at high risk for dissection. Aortas with a diameter >6 cm had a 3.6% risk of rupture, and 10.8% of such patients die because of dissection within a year[25]. Recent studies demonstrated that aortic diameter significantly correlates with age, weight, and sex and should be adjusted as such[26]. Several studies have developed reference values, expressed as Z scores, for children and adults[27, 28]. Recent findings suggest that the risk for aortic dissection is also determined by the specific underlying gene defect. As such, treatment strategies are increasingly tailored according to the underlying genetic cause.

In many TAA cases, a typical histopathologic finding of the aortic wall is observed, which previously was referred to as cystic medial necrosis, but is now more

accurately called medial degeneration. Medial degeneration is not the cause of a
dissection, but rather a consequential pathological finding or a side effect caused by
a primary syndrome[29]. Medial degeneration is characterized by disruption of the
lamellar organization of elastic fibers, accumulation of basophilic ground substance
with cyst-like lesions, degradation of the extracellular matrix (ECM), including
elastin fragmentation and disruptions of collagen, and apoptosis of vascular smooth
muscle cells (VSMC)[29]. In patients with TAA undergoing surgery (replacement of
a part of the aorta or the placing of a stent-graft inside the aorta), the prevalence
of medial degeneration is 6%, whereas it rises up to 100% after having undergone
combined aortic and aortic valve surgery[29, 30]. Although it is clear that excessive
matrix degradation is involved in the development of TAA, the exact underlying
mechanisms are not yet fully unraveled. One possible hypothesis focuses on matrix
metalloproteinases (MMPs)[22]. MMPs are zinc endopeptidases that can degrade
the ECM of aortic tissue[31]. An imbalance between MMPs and their inhibitors,
possibly caused by an excess of reactive oxygen species, could induce medial
degeneration and aneurysm development[32, 33]. In addition, some chronic condi-
tions, such as systemic arterial hypertension, can lead to thickening and fibrosis
of the intimal layer and degradation and apoptosis of VSMC in the media, re-
sulting in wall stiffness and weakness, and eventually in dissections and ruptures[34].

During the past two decades, it has become clear that genetic factors lie at the
basis of TAA formation. Important progress has been made since the discovery of
fibrillin-1 (*FBN1*) as the causal gene for Marfan syndrome[35]. The study of this hu-
man syndromic form of TAA and its counterpart in mouse has served as a paradigm
for a better understanding of TAA in general and revealed the transforming growth
factor (TGF)-β signaling pathway as a key culprit in the pathogenesis of TAA. Sev-
eral other syndromic aneurysmal conditions (Loeys-Dietz syndrome [LDS], arterial
tortuosity syndrome, autosomal recessive cutis laxa) and numerous additional genes
have been identified and confirmed a strong basis for the dysregulation of TGF-β
signaling as the common final pathway in aortic aneurysm development. Most inter-
estingly, these findings have led to putative new therapeutic strategies for patients
with TAA.

1 Study of Syndromic TAA: A Key Role for TGF-β Signaling

1.1 Marfan Syndrome

Marfan syndrome (MFS; Online Mendelian Inheritance in Man [OMIM] 154700) is an autosomal dominant connective tissue disorder, with a prevalence of 2 to 3 per 10000 individuals[36]. It is a multisystemic disorder affecting the skeletal (disproportionate overgrowth, joint laxity, vertebral column deformity), ocular (lens dislocation and myopia), and cardiovascular system (aortic root aneurysm and dissection, mitral valve disease)[37]. Other symptoms include dural ectasia, striae distensae, recurrent inguinal hernias, pneumothorax, and lung emphysema. The cardiovascular manifestations cause the most important morbidity and mortality in patients with MFS. In the majority of patients with MFS, the primary dilatation occurs at the aortic root at the level of the sinuses of Valsalva. To facilitate the clinical diagnosis of MFS, first the Berlin[38], later the Ghent[39], and most recently the revised Ghent nosology[40] have been proposed. These guidelines, formulated by international experts in the field, facilitate the accurate recognition of MFS and the differential diagnosis with other TAA syndromes, thereby improving patient management, follow-up, and counseling. Four possible scenarios can lead to a diagnosis of MFS in a proband: aortic root dilatation (Z score >2) and ectopia lentis, aortic root dilatation with an *FBN1* mutation, aortic root dilatation with sufficient systemic findings (score of ≥ 7 on the systemic scale; for details see Loeys et al[40]), or finally ectopia lentis with an *FBN1* mutation that has been previously associated with aortic root dilatation.

Table 1: Genes/Disorders Associated With Thoracic Aortic Aneurysm as a Recurrent Feature

				Clinical Features			
Gene	Protein	Inheritance	Associated disorder	Cardiovascular	Non-cardiovascular	OMIM (pheno-type)	PMID[Ref]
FBN1	Fibrillin-1	AD	MFS	TAA (typically at sinuses of Valsalva), aortic regurgitation, mitral regurgitation, mitral valve prolapse	Disproportional overgrowth, lens dislocation	154700	1852208[35]
FBN1	Fibrillin-1	AD	Weill-Marchesani syndrome 2	Mitral valve insufficiency, aortic valve stenosis	Short stature, joint stiffness, lens abnormalities	608328	12525539[41]
FBN1 (fourth LTBP domain)	Fibrillin-1	AD	Stiff skin syndrome	/	Short stature, thick skin	184900	20375004[42]
FBN1 (fifth LTBP domain)	Fibrillin-1	AD	Geophysic dysplasia 2, Acromicric dysplasia	Mitral valve insufficiency, aortic valve stenosis	Short stature, thick skin	614185, 102370	21683322[43]

Gene	Protein	Inheritance	Associated disorder	Clinical Features		OMIM (phenotype)	PMID[Ref]
				Cardiovascular	Non-cardiovascular		
FBN2	Fibrillin-2	AD	Congenital contractural arachnodactyly	Mitral valve prolapse, BAV, atrial septal defect, TAA occasionally	Arachnodactyly, Marfanoid features, crumpled ears	121050	7493032[44]
TGFBR1	TGF-β receptor type 1 (ALK5)	AD	LDS type 1	TAA (sinuses and beyond), arterial tortuosity, PDA, widespread aortic and arterial aneurysms	Marfanoid features, hypertelorism, cleft palate, bifid uvula, craniosynostosis, club feet, dystrophic scarring, easy bruising	609192, 608967	15731757[45]
TGFBR2	TGF-β receptor type 2	AD	LDS type 2	TAA, arterial tortuosity, PDA, widespread aortic and arterial aneurysm	Marfanoid features, hypertelorism, cleft palate, bifid uvula, craniosynostosis, club feet, dystrophic scarring, easy bruising	610168, 610380	15731757[45]
SMAD2	SMAD2	AD	LDS type 6	Arterial aneurysms and dissections	Joint anomalies	NA	26247899[46]
SMAD3	SMAD3	AD	LDS type 3 (aneurysm-osteoarthritis syndrome)	TAA, arterial aneurysm, arterial tortuosity	Hypertelorism, bifid uvula, osteo-arthritis	613795	21217753[47]

Gene	Protein	Inheritance	Associated disorder	Clinical Features		OMIM (phenotype)	PMID[Ref]
				Cardiovascular	Non-cardiovascular		
TGFB2	TGFB2	AD	LDS type 4	TAA, arterial tortuosity, PDA, mitral valve prolapse	Mild marfanoid features, hypertelorism, cleft palate, bifid uvula	614816	22772368[48]
TGFB3	TGFB3	AD	LDS type 5	TAA, AAA, mitral valve disease	Cleft palate, bifid uvula, skeletal overgrowth, cervical spine instability	615582	25835445[49]
SKI	SKI	AD	Shprintzen-Goldberg syndrome	TAA	Craniosynostosis, marfanoid skeletal built, intellectual disability	182212	23023332[50]
EFEMP2	Fibulin-4	AR	Cutis laxa with arterial tortuosity and aortic aneurysm	TAA, arterial tortuosity, aortic/arterial stenosis	Arachnodactyly, hypertelorism, high-arched palate	614437	16685658[51]
ELN (GOF)	Elastin	AD	Cutis laxa	Mitral valve regurgitation, aortic valve regurgitation, BAV, TAA occasionally	Loose redundant skin, premature aged appearance, emphysema	123700	9873040, 9580666[52, 53]
ELN (LOF)	Elastin	AD	Supravalvular aortic stenosis (SVAS)	SVAS, pulmonary valvular and artery stenosis	/	185500	8132745[54]

Gene	Protein	Inheritance	Associated disorder	Clinical Features		OMIM (phenotype)	PMID[Ref]
				Cardiovascular	Non-cardiovascular		
ELN (contiguous gene deletion)	Elastin and others	AD	Williams-Beuren	SVAS, pulmonary valvular and artery stenosis, ASD, VSD	Friendly personality, hypercalcemia, puffy eyelids, thick lips, joint limitations and hyperlaxity	194050	7693128[55]
SLC2A10	Glucose trans-porter type 10	AR	Arterial tortuosity syndrome	Arterial tortuosity, arterial aneurysms, pulmonary artery stenosis	High-arched palate, hypertelorism, arachnodactyly	208050	16550171[56]
COL3A1	Collagen III α-1	AD	EDS, vascular type	TAA, AAA, mitral valve prolapse, arterial rupture without aneurysm	Intestinal ruptures, small joint hypermobility, thin translucent skin	130050	10652271[57]
COL1A1[*] (Arg to Cys)	Collagen I α-1	AD	EDS, vascular like type	Arterial aneurysm, typically infrarenal	Osteoporosis and joint hypermobility	130060	4031065[58]
COL1A2	Collagen I α-2	AR	EDS, valvular type	Severe aortic valve, mitral and tricuspid valve insufficiency, borderline aortic enlargement	Joint laxity, skin hyperextensibility	225320	15077201, 2767050[59, 60]

| Gene | Protein | Inheritance | Associated disorder | Clinical Features | | OMIM (phenotype) | PMID[Ref] |
				Cardiovascular	Non-cardiovascular		
PLOD1	Lysyl hydroxylase 1	AR	EDS, kyphoscoliotic type	Rare TAA, arterial rupture	Marfanoid features	225400	8449506[61]
FLNA	Filamin-A	XL	EDS with periventricular nodular heteropia	TAA, BAV, mitral valve disease	Seizures, coagulopathy, joint hypermobility	300049	9883725[62]
BGN	Biglycan	XL	Meester-Loeys syndrome	Early-onset TAAD, mild mitral or aortic insufficiency	Facial dysmorphism, pectus deformities, joint hypermobility, skin striae, bifid uvula, cervical spine instability	300989	7632686[63]
ACTA2	α-smooth muscle actin	AD	FTAAD	TAA, PDA, premature stroke, CAD	Livedo reticularis, iris flocculi, Moya-Moya disease[†]	611788	17994018[64]
ACTA2 (Arg179)	α-smooth muscle actin	De novo	Generalized smooth cell dysfunction	TAA, PDA, arterial aneurysm	Mydriasis, GI malrotation, bladder hypotonia	613834	20734336[65]

				Clinical Features		OMIM (phenotype)	PMID[Ref]
Gene	Protein	Inheritance	Associated disorder	Cardiovascular	Non-cardiovascular		
MYH11	Smooth muscle myosin heavy chain 11	AD	FTAAD	TAA, PDA	/	132900	16444274[66]
MYLK	Myosin light chain kinase	AD	FTAAD	TAA	/	613780	21055718[67]
MFAP5	Microfibrillar-associated protein 5	AD	FTAAD	TAA, arterial tortuosity	/	616166	25434006[68]
MAT2A	Methionine adenosyl-transferase II α	AD	FTAAD	TAA, BAV	/	NA	25557781[69]
PRKG1	cGMP-dependent protein kinase α	AD	FTAAD	TAA, arterial tortuosity	/	615436	23910461[70]
LOX	Lysyl oxidase	AD	FTAAD	TAA	/	NA	26838787[71]

Gene	Protein	Inheritance	Associated disorder	Clinical Features		OMIM (phenotype)	PMID[Ref]
				Cardiovascular	Non-cardiovascular		
FOXE3	FOXE3	AD	FTAAD	TAA	/	NA	26854927[72]
NOTCH1	NOTCH1	AD	BAV	Early calcified BAV, TAA (low penetrance)	/	109730	16025100[73]

AAA indicates abdominal aortic aneurysm; AD, autosomal dominant; AR, autosomal recessive; ASD, atrial septal defect; BAV, bicuspid aortic valve; CAD, coronary artery disease; EDS, Ehlers–Danlos syndrome; FTAAD, familial thoracic aortic aneurysm and dissection; GI, gastrointestinal tract; GOF, gain of function; LDS, Loeys-Dietz syndrome; LOF, loss of function; MFS, Marfan syndrome; PDA, patent ductus arteriosus; SVAS, supravalvular aortic stenosis; TAA, thoracic aortic aneurysm; TGF, transforming growth factor; VSD, ventricular septal defect; and XL, X-linked.

[*] For COL1A1 mutations related to osteogenesis imperfecta, see Supplementary Table 2.

[†] Other genes responsible for Moya-Moya disease have been identified (see OMIM252350 for review).
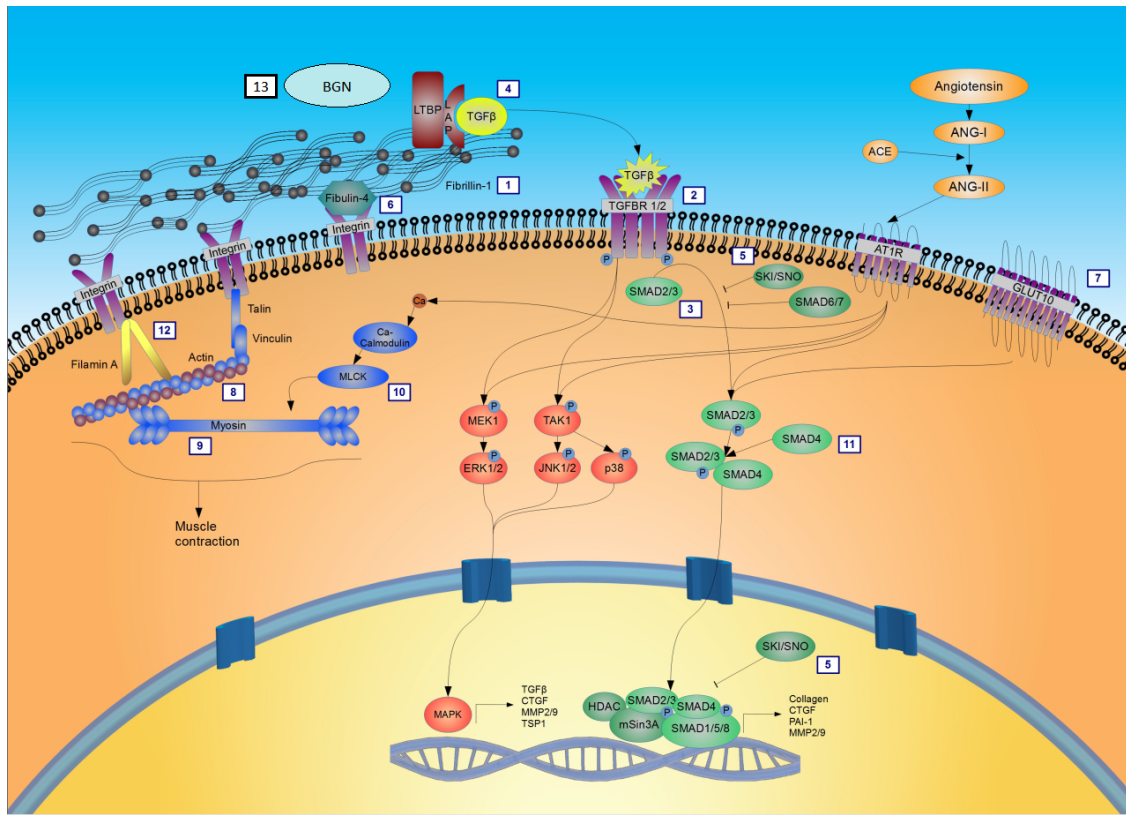
Figure 1: Pathways implicated in thoracic aortic aneurysm. Numbers indicate the corresponding syndrome caused by mutations in the protein, 1, Marfan syndrome; 2, Loeys-Dietz syndrome type 1/2; 3, Loeys-Dietz syndrome type 3; 4, Loeys-Dietz syndrome type 4; 5, Shprintzen-Goldberg syndrome; 6, Cutis laxa type 1B; 7, Arterial tortuosity syndrome; 8 to 10, Familial thoracic aortic aneurysms and dissections; 11, Myhre syndrome, juvenile polyposis syndrome and hemorrhagic telangiectasia syndrome; 12, Ehlers-Danlos-related syndrome with periventricular nodular heterotopia; 13, Meester-Loeys syndrome. ACE indicates angiotensin-converting enzyme; ANG, angiotensin; ERK, extracellular signal–regulated kinase; HDAC, histone deacetylase; JNK, Jun N-terminal kinase; MAPK, mitogen-activated protein kinase; MEK, mitogen-activated protein kinase/extracellular signal-regulated kinase kinase; MLCK, myosin light chain kinase; MMP, matrix metalloproteinase; PAI, plasminogen activator inhibitor; TAK, transforming growth factor-β-activated kinase; TGF, transforming growth factor; TGFBR, transforming growth factor-β receptor; and TSP, thrombospondin.

The causative gene of MFS, *FBN1*, encoding fibrillin-1 (Table 1), an important component of the ECM, was identified in 1991[35]. More than 1800 *FBN1* mutations spread throughout the entire 65 exon-containing gene have been described ever since [35, 37, 74, 75]. Fibrillin-1 molecules assemble into microfibrils, which have an important structural function, both in the aortic wall and in the ciliary

apparatus supporting the ocular lens[76]. This knowledge for a long time supported the 'weak tissue' model, which hypothesized that *FBN1* mutations cause a purely structural deficiency. Weakening of the connective tissues and hence weakening of the aortic wall would make it prone to ruptures[77, 78], whereas weakening of the ciliary apparatus would cause ectopia lentis. However, the weak tissue model never provided a complete explanation for the skeletal overgrowth, and this challenged the idea of a purely structural role for fibrillin-1. A new vision on the pathogenesis of MFS was developed through the study of MFS mouse models (Supplementary Table 1), specifically of the lung phenotype[79]. The hypothesis that *FBN1* mutations might have adverse effects on the functioning of the latent TGF-β -binding protein (LTBP) complexes, because LTBP and fibrillin proteins were known interaction partners[80–82], formed the basis of these experiments. Investigation of the developmental impairment of pulmonary alveolar septation in the $Fbn1^{tm1Rmz}$ mouse model (alias $Fbn1^{mg\triangle}$) demonstrated that fibrillin-1 deficiency alters matrix sequestration of the TGF-β latent complex, leading to uncontrolled release of TGF-β and as a consequence activation of the TGF-β pathway (Figure 1). Most interestingly, increased TGF-β signaling could be countered by perinatal administration of a polyclonal TGF-β neutralizing antibody[79]. The findings of dysregulated TGF-β signaling were later confirmed through the study of the mitral valve prolapse phenotype[83] and the aortic aneurysmal phenotype[84], both in the $Fbn1^{C1039G}$ transgenic mouse. Originally, only the canonical (mother against decapentaplegic homolog 4 [drosophila], [SMAD]-dependent) TGF-β pathway was evaluated in aneurysmal disease, but more recently it became clear that the non-canonical (SMAD-independent) TGF-β pathway is also associated with aneurysm formation[85]. The latter involves signaling through the mitogen-activated protein kinases (MAPK), including the extracellular signal-regulated kinase (ERK)1/2, p38, and the Jun N-terminal kinase (Figure 1).

1.2 Loeys-Dietz Syndrome

In 2005, a new syndrome, related to MFS, was described and designated as Loeys-Dietz syndrome (LDS; OMIM 609192 and OMIM 608967; Table 1)[45]. In its most typical presentation, LDS is characterized by a triad of hypertelorism,

cleft palate or bifid uvula, and arterial tortuosity, combined with widespread aneurysms. The aortic aneurysms tend to be more aggressive than in patients with MFS, leading to dissection and rupture at smaller diameters and at younger ages[45]. Additional MFS-like cardiovascular, craniofacial, and skeletal symptoms are often observed. Distinguishing features between LDS and MFS include hypertelorism, cleft palate/bifid uvula, craniosynostosis, cervical spine instability, arterial tortuosity, and aneurysm beyond the aortic root. Initially 2 types of LDS were distinguished. LDS type 1 patients presented with typical craniofacial features, whereas LDS type 2 patients lacked the craniofacial features, but presented with skin abnormalities, including frail and velvety skin[86]. Nowadays, the 2 types of LDS are thought to be part of a continuum of disease. Patients with LDS experience increased risk for aneurysms and dissections of other vessels, including cerebral aneurysms[87]. This illustrates the necessity of broad clinical follow-up in patients with LDS. Medial degeneration in patients with LDS is often more diffuse with more collagen deposition, elastic fiber fragmentation, and glycosaminoglycan deposition[29].

Based on the findings of *TGFBR2* mutations in MFS-like patients[88, 89] and the similarities of the human clinical phenotype and an existing conditional *Tgfbr2* knockout mouse model with cleft palate, calvarial defects, and outflow tract defects, *TGFBR2* was suggested as a candidate gene for LDS[90–92]. Indeed, mutations in both genes encoding the TGF-β receptors 1 and 2 (*TGFBR1/2*) were identified. Most LDS mutations are missense mutations found in the serine/threonine kinase domain of both receptors[89, 93], which suggests loss-of-function as the relevant mechanism of pathogenesis. These findings provided further proof of the association between TAA and dysregulated TGF-β signaling (Figure 1)[93]. In addition to LDS and MFS-like patients, *TGFBR1/2* mutations have also been described in familial TAA and dissection (FTAAD) families[94]. The large majority of patients with *TGFBR1/2* mutations do not fulfill the diagnostic criteria for MFS, but rare exceptions with aortic aneurysm and ectopia lentis have been described[89].

Recently, four additional LDS genes have been identified (Table 1): *SMAD2*[46], *SMAD3*[47], *TGFB2*[48, 95] and *TGFB3*[49] (see Chapter 2). *SMAD3* mutations were initially described in the aneurysm-osteoarthritis syndrome, which is, based

on the many clinical similarities (hypertelorism, bifid uvula, arterial tortuosity) with LDS, now also classified as LDS type 3[47, 96]. *SMAD2* mutations mostly lead to arterial aneurysms and joint abnormalities. SMAD2 and SMAD3 are both intracellular downstream effectors of the TGF-β pathway. Similar to other receptor (R-)SMADs (including SMAD1, 2, 5, and 8), they are activated by phosphorylation by the type 1 TGF-β receptor. Further signalization and translocation to the nucleus are achieved through the formation of heteromeric complexes with comediator SMAD proteins, such as SMAD4[97]. Most interestingly, despite the loss-of-function *SMAD3* mutations, the overall effect was an increase of TGF-β signaling as evidenced by increased pSMAD2 immunohistochemical staining of aortic wall tissues (Figure 1)[96].

Similarly, *SMAD2* mutations were observed to enhance TGF-β signaling. Both pSMAD2 and pSMAD3 protein levels were proven to be elevated after addition of exogenous *TGFB1* in fibroblasts from affected individuals[46]. Identification of causal *TGFB2* mutations in patients with LDS[48, 95] implicated for the first time the involvement of a TGF-β ligand in the development of TAA (Table 1). The clinical phenotype of *TGFB2* mutant patients demonstrates both features of MFS and LDS, including aortic aneurysm, mitral valve disease, club foot, bifid uvula, and skeletal features. TGFB2 is one of the three TGF-β cytokines. These are all highly expressed in the cardiovascular system, both during embryonic development and adult life[98], and are kept in a latent state in the ECM. Haploinsufficient *Tgfb2* mice recapitulated the human phenotype with aortic dilatations (aortic annulus and root), which were observed around the age of 8 months (Supplementary Table 1)[48, 91]. Western blot and immunohistochemical analysis of aortic wall tissues revealed a signature of increased canonical (pSMAD2) and noncanonical (phosphorylated extracellular signal-regulated kinase) signaling pathways (Figure 1). Another cytokine, TGFB3, was identified as a causal LDS gene during this thesis and will be discussed more detailed in Chapter 2.

1.3   Disorders related to MFS and LDS

Shprintzen-Goldberg syndrome (OMIM 182212) is characterized by craniosynostosis, skeletal changes (arachnodactyly, camptodactyly, scoliosis, joint hypermobility),

and aortic aneurysms. Shprintzen-Goldberg syndrome shows considerable phe-
notypic overlap with MFS and LDS but presents with additional manifestations,
including mental retardation and severe skeletal muscle hypotonia[99, 100]. Re-
cently, v-ski avian sarcoma viral oncogene homolog (SKI) was identified as the
causal gene for this rare TAA syndrome (Table 1)[50, 101]. The oncogene *SKI*
encodes a protein that plays an important role in the negative feedback loop of
the TGF-β signaling pathway (Figure 1). SKI itself cannot bind to DNA, but SKI
and the SKI-related protein SKI-like homolog are able to regulate transcription by
competing with other transcription factors. SKI and SKI-like homolog bind to the
SMAD2/SMAD3/SMAD4 complex, which subsequently binds to DNA and causes
repression of transcription of TGF-β-responsive genes. The aneurysm phenotype
in Shprintzen-Goldberg syndrome is less penetrant and less severe in comparison
with that observed in MFS and LDS, possibly because of the temporal and regional
expression pattern of SKI.

Aortic aneurysmal disease has been linked to altered TGF-β signaling in two other
rare recessive connective tissue disorders: autosomal recessive cutis laxa type 1B
and arterial tortuosity syndrome (Table 1). Both disorders are characterized by
arterial tortuosity and aneurysms, and share skin and skeletal findings with MFS
and LDS[102]. Autosomal recessive cutis laxa type 1B (OMIM 614437) is caused
by mutations in the *EFEMP2* gene[51], coding for fibulin-4 (FBLN4), a molecule
involved in elastic fiber assembly and highly expressed in the medial layers of blood
vessel walls, including the aortic media. FBLN4 and LTBP1 bind with high affinity,
which suggests a key role for FBLN4 in the association of LTBP1 with microfibrils
and the latent TGF-β cytokine[103]. Indeed, upregulated TGF-β signaling was
found both in fibroblasts of cutis laxa patients with *EFEMP2* mutations and in
the aortic wall of *Fbln-4* hypomorphic mice (Figure 1)[102]. Interestingly, FBLN4
is also involved in recruiting lysyl oxidase to the elastic fiber, and lysyl oxidase is
known to inhibit TGF-β enzymatically[104].

The gene responsible for the arterial tortuosity syndrome (OMIM 208050) is
SLC2A10[56], which codes for glucose transporter 10, a member of the facilitative
glucose transporter family (Table 1). Although it is still unclear what the substrate
for this transporter is, a link to TGF-β signaling has been suggested (Figure 1).

By mechanisms that are not well understood, a deficiency of functional glucose transporter 10 protein leads to upregulation of TGF-β signaling, potentially mediated by altered expression of decorin, a known TGF-β antagonist[56]. In addition, and more recently, studies in zebrafish suggested that glucose transporter 10 is involved in cardiovascular development and that it functions through both stimulation of the mitochondrial respiratory chain and TGF-β signaling[105].

Another rare, autosomal dominant Marfan-like disorder, congenital contractual arachnodactyly (OMIM 121050), is caused by heterozygous mutations in *FBN2* (Table 1)[44]. Patients with *FBN2* mutations present with marfanoid features, including arachnodactyly, contractures, marfanoid body habitus, and mitral valve prolapse. Arterial aneurysms are not frequently observed in this condition[106].

Most recently, mutations in the *BGN* gene have been identified to cause a severe form of TAAD[63]. Other recurrent findings among these patients are hypertelorism, pectus deformity, joint hypermobility, contractures, and mild skeletal dysplasia, which are also observed in MFS and LDS[37, 45]. The *BGN* gene encodes the proteoglycan biglycan which plays an important mechanical role in the ECM, and possibly in growth factor binding and regulation of signalling as well. Unlike aortic tissue of MFS or LDS patients, almost normal ECM architecture is observed in these patients. Possibly, BGN plays a bigger role in the association of collagens instead of regulating their abundance. When staining for pSMAD2, an increase of pSMAD2 in the nuclei was observed, confirming that biglycan's role goes beyond ECM structure. Additionally, it confirms biglycan's possible involvement in regulating TGF-β signalling.

1.4   Other syndromic forms of aortic aneurysmal disease

TAA can also be an important complication of different subtypes of Ehlers–Danlos syndrome (EDS). EDS is a heterogeneous group of disorders with cutaneous (skin hyperextensibility and atrophic scars), skeletal (joint hypermobility and luxations), and vascular features (vascular rupture and easy bruising).

The most life-threatening form is the vascular type of EDS (former type 4 EDS, OMIM 130050), which is caused by a deficiency of type III collagen (Table 1). The clinical phenotype is characterized by rupture of middle-sized arteries and intestines[107]. Aortic dissections have also been described and seem to occur without significant preceding aneurysm formation. Although it is known that collagen production is TGF-β dependent, there is no evidence that mutations in COL3A1 do affect TGF-β pathway regulation in a direct way. Nevertheless, Brooke[108] suggested that the celiprolol effect seen in vascular EDS treatment[109] might be related to its TGF-β expression-suppressing effects. Alternatively, indirect cross-talk between bone morphogenetic protein and TGF-β signaling could contribute to further ECM degeneration[110].

Specific arginine-to-cysteine mutations in *COL1A1* have been identified in a subset of affected individuals who typically present with aneurysms of the abdominal aorta and iliac arteries reminiscent of vascular EDS (Table 1)[111]. For these cases, distinct abnormalities on collagen electrophoresis have been observed.

The valvular type of EDS (OMIM 225320) is a rare form of EDS with early-onset cardiac valvular dysfunction. This autosomal recessive condition is caused by nonsense mutations in *COL1A2*[59]. Other recurrent findings include joint hypermobility and skin hyperextensibility. Borderline aortic root dilatations have been described.

Aortic aneurysm and arterial rupture can also occur in the kyphoscoliotic form of EDS (the former type VI or ocular-scoliotic type, OMIM 225400). This generalized connective tissue disorder is characterized by kyphoscoliosis, joint laxity, muscle hypotonia, and, in some individuals, ocular problems. This autosomal recessive form of EDS is caused by deficient activity of the enzyme procollagen-lysine, 2-oxoglutarate 5-dioxygenase 1 (also called lysyl hydroxylase 1), and mutations in the encoding gene, *PLOD1*, are causative (Table 1)[112]. The diagnosis of the kyphoscoliotic form of EDS relies on the demonstration of an increased ratio of deoxypyridinoline to pyridinoline crosslinks in urine. Alternatively, an assay of lysyl hydroxylase enzyme activity in skin fibroblasts is diagnostic.

Mildly dilated aortas have been described in the hypermobile form of EDS, but these do not seem to progress over time, and aortic dissection is almost never encountered in hypermobile EDS[113]. Finally, a spectrum of EDS-like findings has been associated with *FLNA* mutations (Table 1). Filamin A is an intermediate filament that connects the contractile apparatus of the VSMC to the cell membrane (Figure 1). Filamin A has numerous interaction partners, including membrane receptors, transcription factors, and intermediate signaling proteins[114, 115]. Although *FLNA* mutations were initially associated with periventricular nodular heterotopias (OMIM 300049), more recently, *FLNA* patients have been observed with additional mitral valve disease, aortic root dilatation, and joint hypermobility[62].

Occasionally, aortic root aneurysms have been described in other rare genetic syndromes (Supplementary Table 2). Several other signaling pathways seem to be involved. First, aortic aneurysms have been described sporadically in patients with mutations involving the rat sarcoma-ERK signaling pathway, including Noonan syndrome (eg, *PTPN11*)[116, 117] and neurofibromatosis (*NF1*)[118]. This finding suggests links between these RASopathies and the noncanonical TGF-β signaling pathway involved in several common syndromic forms of aortic aneurysms, such as MFS and LDS. Second, the Notch signaling pathway has been implicated in the Alagille syndrome[119, 120] (see also section on bicuspid aortic valve (BAV)/TAA). Third, aortic aneurysm has been occasionally implicated in several forms of hereditary hemorrhagic telangiectasia, caused by mutations in *ENG*, activin A receptor, type II-like 1 (*ACVRL1*), and *SMAD4*[121–123]. The latter genes either encode for components of the TGF-β signaling pathway (SMAD4) or for a receptor of the TGF-β superfamily of ligands (ENG, ACVRL1). Mainly, patients with mutations in *SMAD4*, associated with juvenile polyposis syndrome (OMIM 174900) and a combined juvenile polyposis syndrome–hereditary hemorrhagic telangiectasia (OMIM 175050), were described to have TAA[124]. Fourth, mutations in other genes encoding collagens or enzymes involved in collagen maturation (*COL1A1/A2*, *COL4A1*, *COL4A3/4/5*, *PLOD3*)[58, 125–132] have been associated with aortic aneurysm, but overall the incidence of aortic aneurysm in these disorders (osteogenesis imperfecta, hereditary angiopathy with nephropathy, aneurysms and muscle cramps syndrome, Alport syndrome) seems very low. Finally, an association of TAAD with autosomal dominant polycystic kidney disease (ADPKD) has been reported. In

1% to 10% of patients with ADPKD, aortic aneurysms are found[133–135]. Furthermore, dissection of the thoracic aorta is seven times more frequent in patients with ADPKD[136]. The causal ADPKD genes, *PCD1* and *PCD2*, encode for polycystines, which are transmembrane molecules. Interestingly, polycystin-1 has several ECM motifs that may function in cell-cell and cell-matrix interactions[137]. Finally, dysregulated TGF-β signaling has also been shown to be involved in the pathogenesis of ADPKD[138].

2   Nonsyndromic TAA: Components of the VSMC contractile apparatus. . . and once again TGF-β dysregulation

Sporadic nonsyndromic TAA and dissections (sporadic TAAD(STAAD)) is a complex and multifactorial disease, mostly affecting the ascending aorta[139]. Twenty percent of patients with TAAD have affected family members, designated as FTAAD. The latter is usually inherited in an autosomal dominant fashion with variable expression and reduced penetrance[140]. STAAD occurs at a mean age of 66 years, whereas FTAAD cases are diagnosed at $\approx$ 56 years of age[139].

Several candidate loci for FTAAD have been found (Table 2). The responsible gene for the TAAD2 locus (3p24-25) was shown to be *TGFBR2*[89, 141]. Indeed, mutations in *TGFBR2* can cause a broad spectrum of disease, from nonsyndromic TAAD to full-blown LDS. Another LDS gene, *SMAD3*, can cause FTAAD as well[96], whereas *FBN1* mutations have also been identified in patients with FTAAD[142]. Many of the reported families present skeletal syndromic features and might represent the mildest end of the syndromic spectrum. This demonstrates the variable expression of symptoms caused by mutations in TAA genes, which may implicate the presence of modifying genes that may exaggerate or suppress the development of additional symptoms.

Besides the genes previously involved in syndromic types of TAA, several other genes have been implicated in nonsyndromic FTAAD. *ACTA2* mutations are responsible

for 14% of patients with FTAAD (Table 1 and Table 2)[64]. The *ACTA2* gene encodes a VSMC-specific isoform of the α-actin protein and is involved in VSMC contraction (Figure 1). Other vascular manifestations caused by mutations in this gene include premature coronary artery disease and stroke[143]. Surprisingly, one specific *ACTA2* missense mutation (p.Arg179His) also causes generalized smooth muscle dysfunction with patent ductus arteriosus (OMIM 613834), which includes symptoms such as mydriasis, intestinal malrotation, hypotonic bladder, and periventricular white matter hyperintensities. It was shown that the ACTA2 p.Arg179His mutation alters the formin regulation of actin filament polymerization, resulting in filament instability[144].

Mutations in *MYH11* are associated with FTAAD and patent ductus arteriosus (locus on 16p; Table 1 and Table 2)[67, 139]. *MYH11* encodes a myosin heavy chain, which is involved in VSMC contraction (Figure 1). It should be noted, however, that many of the *MYH11* mutations do not fully segregate with TAAD/patent ductus arteriosus in affected families. Additional modifying genetic factors are thus expected to contribute to the phenotype[145]. In the autosomal recessive Myh11 zebrafish model (meltdown; mlt), constitutive activation of the Myh11 ATPase part, which subsequently results in disruption of the VSMC surrounding the posterior intestine, leads to high mortality. These findings implicated that smooth muscle signaling could play an essential role in the maintenance of the epithelial wall[146]. Indeed, one TAAD patient with a mutation affecting the *MYH11* ATPase part, homologous to the region affected in the mlt zebrafish, showed an early and severe decrease in the elasticity of the aortic wall[66].

The contraction of VSMC is initiated by phosphorylation of myosin light chains. This process is catalyzed by myosin light chain kinase (MYLK), which in turn is activated by binding of calcium-calmodulin complexes. MYLK is thus another key player in VSMC contraction. Building on the previous identification of two important components of the VSMC contractile apparatus (*ACTA2* and *MYH11*), *MYLK* mutation analysis was performed in patients with FTAAD[67]. *MYLK* mutations were found in a minority of TAAD and FTAAD cases (<1%)[147, 148]. Loss of MYLK function could lead to alteration of its calcium-calmodulin-binding capacity, which is required for MYLK activation and phosphorylation of myosin.

Patients with *MYLK* mutations often develop aneurysms in the ascending thoracic aorta, which is the part of the aorta exposed to the highest biomechanical force. It has been suggested that MYLK haploinsufficiency may decrease the VSMC contractile function and that, as a consequence, the aorta will not be able to withstand the biomechanical forces for long[67].

On the other hand, VSMC relaxation is aided by proteins such as cGMP-dependent protein kinases (PKG). A gain of function variant (p.Arg177Gln) in *PRKG1*, encoding PKG-1, was identified in four FTAAD families[70]. Functional analysis showed that the increased activity of PKG-1 causes decreased phosphorylation of the myosin regulatory light chains, leading to decreased vascular VSMC contraction. This downstream result is also observed in *MYLK* mutations.

The absence of other VSMC problems in patients with mutations in components of the VSMC contractile apparatus demonstrates that the VSMC itself is not majorly affected and that aneurysms mainly develop at locations where the biomechanical forces are greatest. This may mean that one working allele might be sufficient for smooth muscle cell contraction but that it leaves the aortic wall in a weaker position.

Intriguingly, upregulation of TGF-β signaling has also been observed in the aortic walls of TAA patients with *ACTA2* and *MYH11* mutations[149]. This might not be completely surprising because the VSMC contractile apparatus is linked via the intermediate filaments to the cell surface integrins, which are known major regulators of TGF-β activity. These findings suggest a possible link between TGF-β upregulation and VSMC contractility alterations.

Recently, more FTAAD genes have been discovered that can be linked to the TGF-β pathway. *LOX*[71], which encodes for a lysyl oxidase, was identified in several FTAAD families. This enzyme has an important role in forming crosslinks in elastin and collagen fibers. Like biglycan, this gene is crucial for ECM structure. More importantly, lysyl oxidase is also known to inhibit TGF-β enzymatically[104]. Another matrix alteration gene was identified to cause FTAAD development. Mutations in *MFAP5*, which encodes for a microfibril-associated glycoprotein[68],

were found in two families. A nonsense and missense variant were discovered that lead to inherited TAAD. Once again, upregulation of TGF-β signalling was observed in aortic tissue of the patient with the missense mutation. Both enhancement of TGFB1 and pSMAD2/3 expression were observed.

Furthermore, enzymes are also found to be playing a role in FTAAD development. Missense mutations in *MAT2A* have been identified in two families[69]. This gene encodes for a methionine adenosyltransferase II and its downstream role involves methylation reactions. This finding raises questions about possible epigenetic involvement in TAAD.

Another recently discovered FTAAD gene is *FOXE3*[72]. FOXE3 works as a transcription factor. Surprisingly, FOXE3 is not expressed in adult mouse aorta, but it is briefly expressed during development in the pharyngeal arches. Apparently, expression is also induced by increased biomechanical forces in ascending aortic VSMC[72]. In this way, *FOXE3* might be expressed in critical aortic tissue. In this thesis, we propose another transcription factor, *KLF15*, as a possible candidate gene for TAA (Chapter 4).

The genetic basis for STAAD has been explored as well. A first genome-wide association study was performed, which, surprisingly, identified a region of linkage disequilibrium that contained the *FBN1* gene. Thus, it seems that common variation at the *FBN1* locus may explain part of the susceptibility to aneurysm formation in STAAD[150]. Genome-wide copy number variant analysis in a large number of STAAD cases further suggested the involvement of VSMC adhesion and contraction in the development of TAA[151, 152]. Exome array studies additionally associated *LRP1* and *ULK4* SNPs with non-familial TAAD patients[153].

Table 2: Familial Thoracic Aortic Aneurysms and Dissections or Bicuspid Aortic Valve With Thoracic Aortic Aneurysms and Dissections Locus

Locus	Gene	Human Condition	Initial Locus Name	OMIM Locus	OMIM Number (Phenotype)	PubMed Identifier[Ref]
3p24-25	*TGFBR2*	FTAAD	TAAD2	AAT3	610380	15235604, 12821554[89, 141]
3q21	*MYLK*	FTAAD		AAT7	613780	21055718[67]
5q13-14		FTAAD	TAAD1	AAT2	607087	11369686[154]
9q22.33	*TGFBR1*	FTAAD		AAT5	608967	19542084[155]
10q22-24	*ACTA2*	FTAAD		AAT6	611788	17994018[64]
11q23.3-24		FTAAD (single family)	FAA1	AAT1	607086	11369687[156]
12q13-14		Low-risk FTAAD	TAAD5			21163914[157]
15q21	Potentially *FBN1*	FTAAD				20937124[158]
15q21.1	*FBN1* SNPs rs10519177, rs4774517, rs755251, rs1036477, rs2118181	STAAD predisposition				21909107[150]
15q22.33	*SMAD3*	FTAAD				21778426[96]
15q24-26		FTAAD	TAAD3			17182941[159]

Locus	Gene	Human Condition	Initial Locus Name	OMIM Locus	OMIM Number (Phenotype)	PubMed Identifier[Ref]
16p13.12-13	*MYH11*	FTAAD with PDA	FAA4	AAT4	132900	16444274, 15998682[66, 160]
16p13.12 duplication	*MYH11*	FTAAD				21092924, 21698135 [151, 152]
5q15-21		BAV/TAAD				17203300[161]
9q34.3	*NOTCH1*	BAV with low penetrance TAA		AOVD1	109730	16025100[73]
13q33-qter		BAV/TAAD				17203300[161]
15q25-26		BAV/TAAD				[162]

AAT indicates aortic aneurysm, familiar thoracic; AOVD1, aortic valve disease 1; BAV, bicuspid aortic valve; FAA, familia aortic aneurysms; FTAAD, familial thoracic aortic aneurysm and dissection; PDA, patent ductus arteriosus; SNP, single-nucleotide polymorphism; STAAD, sporadic thoracic aortic aneurysm and dissection; and TAAD, thoracic aortic aneurysm and dissection.

3 BAV-Associated TAA: Polygenic or Complex Genetic Phenotype?

BAV (OMIM 109730), a condition in which the aortic valve consists of two valve leaflets instead of the normal three, is the most common congenital heart disorder. Curiously, BAV often remains asymptomatic, but the risk of developing TAA is 9 times higher in patients with BAV than in patients with a tricuspid aortic valve (TAV). Aneurysms most commonly occur in the ascending aorta distal to the sinotubular junction; however, dilatation can occur anywhere between the aortic root and the aortic isthmus[33]. Very little is known at the molecular level about the development of BAV and BAV-associated TAA, demonstrating the complexity of the disease. Although several linked loci have been identified (5q, 13q, 18q; Table 2)[161] and a set of candidate genes/proteins (*ACTA2*, *TGFBR2*, nitric oxide synthase 3, ubiquitin fusion degradation 1-like, etc)[45, 163–165] have been proposed, until now, mutations in only a single gene (*NOTCH1*) have been consistently associated with BAV[73]. NOTCH1 is a key component of the Notch signaling pathway, important in transcriptional regulation and in cell growth and differentiation. Notch signaling also promotes epithelial–mesenchymal transition during cardiac development[166]. Investigations on the role of Notch signaling in TAAD, more specifically in descending aneurysms, showed a complex signaling pattern, with activation in fibroblasts but impairment in medial VSMCs[167]. One other gene was linked to BAV more recently, *MAT2A* which causes FTAAD[69]. Several of the mutation-carrying patients within the *MAT2A* family also had BAV. In Chapter 3, the identification of the BAV/TAA gene, *SMAD6*, is described.

Although studies have shown that TAA formation is different in BAV and TAV[168], at least some disease mechanisms may be shared. Most interestingly, increased TGF-β activity was demonstrated in BAV-associated TAA[169]. BAV and TAV have slightly different mRNA expression profiles, as well as alternative splicing of genes involved in the TGF-β pathway[170]. In contrast to the TAV aortic aneurysms, BAV aneurysms were associated with a relative lack of inflammation, normal MMP9 levels, and elevated MMP2 expression[171–173]. Because the latter is an activator of TGF-β signaling[174], this provides indirect evidence of the

involvement of TGF-β dysregulation in the pathogenesis of BAV/TAA. Medial degeneration is also observed in BAV-associated dilated aortic tissue, including elastic fiber degeneration and fragmentation, non-inflammatory VSMC loss, and accumulation of basophilic ground substance[33]. In women with Turner syndrome, aortic dilatation at the level of the sinuses of Valsalva has been reported in 25% of the patients with BAV and in 5% of the patients with TAV[175]. This data suggests that if there would be a responsible gene, it would most likely be located on the short arm of the X-chromosome.

4 Supplementary material

Supplementary Table 1: Mouse models most commonly used in TAA research

| Gene | Allele symbol/ Common name | Phenotype | | PMID[Ref] |
		Heterozygous	Homozygous	
FBN1				
	$Fbn1^{tm1Rmz}/mg\triangle$	Normal phenotype	Perinatal death because of vascular complications	9326947[78]
	$Fbn1^{tm2Rmz}/mgR$	Normal phenotype	Survive longer than mg△ mice, medial calcification, inflammatory responses	23239472[176]
	$Fbn1^{tm1Hcd}/$ $Fbn1^{C1039G/+}$	Elastic fiber fragmentation (from 2 months of age), thickening of aortic wall, no aortic dissection	Die at P7 - P10 from aortic dissection	16601194[84]
	$Fbn1^{Tsk}/Tsk$	Thickened skin, bone overgrowth, lung emphysema, no vascular abnormalities	Die at 7-8 days of gestation	[177]
TGFB2				
	$Tgfb2^{tm1Doe}/ Tgfb2^-$	Elastic fiber fragmentation, dilation of aortic root and annulus (from 8 months of age), aortic root aneurysm	Neonatal lethality	9217007[91]

| Gene | Allele symbol/Common name | Phenotype | | PMID[Ref] |
		Heterozygous	Homozygous	
TGFBR1				
	$Tgfbr1^{tm1Karl}$/ $TbetaRI^-$	/	Embryonic lethality during organogenesis, severe defects in yolk sac and placenta vascular development	11285230[178]
	$Tgfbr1^{tm1Karl}$/ $TbetaRI^-$ (Wnt1-neural crest)	/	Outflow tract defects	17078885[179]
	M318R KI	Aortic root and diffuse aneurysm	/	21593863[1]
TGFBR2				
	$Tgfbr2^{tm1Mmt}$	Developmentally normal	Defects in the yolk sac hematopoiesis and vasculogenesis	8873772[180]
	$Tgfbr2^{tm1Karl}$/ $Tgfbr2^{fl}$ (Interferon induced)	/	Lethal inflammatory disorder	12091349[181]
	$Tgfbr2^{tm1Hlm}$ (Wnt1-neural crest)	/	Outflow tract defect, abnormal aortic arch and aortic branch attachment, ventricular septal defect cleft palate, calvarial defects	12975342, 16332365[92, 182]

| Gene | Allele symbol/Common name | Phenotype | | PMID[Ref] |
		Heterozygous	Homozygous	
	$Tgfbr2^{tm1Hlm}$ (Mesp1/Dermo1/ Mef2c-VSMC)	/	Decreased lysyl oxidase, impaired elastogenesis and aneurysm	19165826[183]
	G357W KI	Aortic root and diffuse aneurysm	/	21593863[1]
EFEMP2				
	$Mus81^{tm1Esse}$/ $Fbln4^{R}$	Abnormal aorta wall morphology	Abnormal aorta and valve morphology, aortic aneurysm and dilatation	17293478, 21858106[184, 185]

EDS: Ehlers-Danlos syndrome; TAA: thoracic aortic aneurysm; PDA: patent ductus arteriosis; AVM: arteriovenous malformation; JPS: Juvenile polyposis syndrome; HHT: Hemorrhagic telangiectasia syndrome; GI: gastrointestinal tract; AD: autosomal dominant; AR: autosomal recessive; XD: X-linked dominant.

Supplementary Table 2: Syndromes with low penetrance of aneurysms and their corresponding genes

Gene	Protein	Inheritance	Associated syndrome	Clinical Features		OMIM (phenotype)	PMID^{Ref}
				Cardiovascular	Non-cardiovascular		
PTPN11	Protein-tyrosine phosphatase 2C	AD	Noonan syndrome	Coronary artery aneurysms, atrial septal defect, PDA	Short stature, hypertelorism	163950	11704759[116]
			LEOPARD syndrome	Coronary artery aneurysms	Short stature, hypertelorism, cleft palate	151100	12058348[117]
NF1	Neurofibromin-1	AD	Neurofibromatosis type 1	Arterial aneurysms and stenosis	Hypertelorism, scoliosis, café-au-lait spots, neurofibroma, freckling	162200	2134734[118]
JAG1	JAGGED1	AD	Alagille syndrome	TAA, intracranial aneurysms, coarctation of the aorta	Hypertelorism, embryotoxon, myopia, renal involvement, vertebral anomalies	118450	9207787, 9207788[119, 120]

Gene	Protein	Inheritance	Associated disorder	Clinical Features		OMIM (pheno-type)	PMID[Ref]
				Cardiovascular	Non-cardiovascular		
ENG	Endoglin	AD	Hereditary hemorrhagic telangiectasia type 1	TAA, AVM	Telangiectasia, nose bleeding	187300	7894484[121]
ACVRL1	Activin receptor-like kinase I	AD	Hereditary hemorrhagic telangiectasia type 2	TAA, AVM	Telangiectasia, nose bleeding	600376	8640225[122]
SMAD4	SMAD4 (Ile500)	AD	Myhre syndrome	PDA, septal defects	Cleft palate, hypertelorism, short stature	139210	22158539[123]
	SMAD4	AD	JPS/JPS-HHT	Mitral valve prolapse, TAA, AVM	Hamartomatous polyps in GI tract, telangiectasia	175050	15031030[125]
COL1A1	Collagen I α-1	AD	Osteogenesis imperfecta	Rare TAA, mitral valve disease	Mild joint hypermobility, hearing loss, short stature, thin velvety skin, fractures	166200	4031065[58]
COL1A2	Collagen I α-2	AD	Osteogenesis imperfecta	Rare TAA, mitral valve disease	Mild joint hypermobility, hearing loss, short stature, thin velvety skin, fractures	166210, 259420, 166220	2745420, 2794057, 1054840 [126–128]

| Gene | Protein | Inheritance | Associated disorder | Clinical Features | | OMIM (phenotype) | PMID[Ref] |
				Cardiovascular	Non-cardiovascular		
COL4A1	Collagen IV α-1	AD	Hereditary angiopathy	Aneurysms in right internal carotid artery and right middle cerebral artery	Retinal arteriolar tortuosity, renal cysts, muscle cramps	611773	18160688[129]
COL4A5	Collagen IV α-5	XD	Alport syndrome	TAA, AAA, hypertension	Deafness, myopia, renal failure	301050	2339699, 2349482[186, 187]
COL4A3 *COL4A4*	Collagen IV α-3 Collagen IV α-4	AR	Alport syndrome	TAA, AAA, hypertension	Deafness, myopia, renal failure	203780	7987301, 7783412[130, 131]
PLOD3	Lysyl hydroxylase 3	AR	Bone fragility with contractures, arterial rupture and deafness	Arterial aneurysms	Scoliosis, myopia, growth retardation, deafness	612394	18834968[132]
PKD1	Polycystin-1	AD	Polycystic kidney disease 1	Intracranial aneurysm	Polycystic kidney, renal failure	173900	8004675[188]
PKD2	Polycystin-2	AD	Polycystic kidney disease 2	Intracranial aneurysm	Polycystic kidney, renal failure	613095	8650545[189]

| Gene | Protein | Inheritance | Associated disorder | Clinical Features | | OMIM (phenotype) | PMID[Ref] |
				Cardiovascular	Non-cardiovascular		
TSC2	Tuberin	AD	Tuberous sclerosis	Thoraco-abdominal aneurysms	Renal cysts, seizures, mental retardation	613254	7581393, 8825048[190, 191]
GAA	Lysosomal α-glucosidase	AR	Glycogen storage disease II	Intracranial aneurysms	Muscle weakness, hearing loss	232300	2203258[192]

EDS: Ehlers-Danlos syndrome; TAA: thoracic aortic aneurysm; PDA: patent ductus arteriosis; AVM: arteriovenous malformation; JPS: Juvenile polyposis syndrome; HHT: Hemorrhagic telangiectasia syndrome; GI: gastrointestinal tract; AD: autosomal dominant; AR: autosomal recessive; XD: X-linked dominant.

References

1. Lindsay, M. E. & Dietz, H. C. Lessons on the pathogenesis of aneurysm from heritable conditions. *Nature* **473,** 308–16. ISSN: 1476-4687 (May 2011).

2. Elefteriades, J. a. Thoracic aortic aneurysm: reading the enemy's playbook. *World J Surg* **32,** 366–74. ISSN: 0364-2313 (Mar. 2008).

3. Blanchard, J. F., Armenian, H. K. & Friesen, P. P. Risk factors for abdominal aortic aneurysm: results of a case-control study. *Am J Epidemiol* **151,** 575–83. ISSN: 0002-9262 (Mar. 2000).

4. Lederle, F. A. *et al.* Prevalence and associations of abdominal aortic aneurysm detected through screening. Aneurysm Detection and Management (ADAM) Veterans Affairs Cooperative Study Group. *Ann Intern Med* **126,** 441–9. ISSN: 0003-4819 (Mar. 1997).

5. Wahlgren, C. M., Larsson, E., Magnusson, P. K. E., Hultgren, R. & Swedenborg, J. Genetic and environmental contributions to abdominal aortic aneurysm development in a twin population. *J Vasc Surg* **51,** 3–7, discussion 7. ISSN: 1097-6809 (Jan. 2010).

6. Gretarsdottir, S. *et al.* Genome-wide association study identifies a sequence variant within the DAB2IP gene conferring susceptibility to abdominal aortic aneurysm. *Nat Genet* **42,** 692–7. ISSN: 1546-1718 (Aug. 2010).

7. Bown, M. J. *et al.* Abdominal aortic aneurysm is associated with a variant in low-density lipoprotein receptor-related protein 1. *Am J Hum Genet* **89,** 619–27. ISSN: 1537-6605 (Nov. 2011).

8. Helgadottir, A. *et al.* The same sequence variant on 9p21 associates with myocardial infarction, abdominal aortic aneurysm and intracranial aneurysm. *Nat Genet* **40,** 217–24. ISSN: 1546-1718 (Feb. 2008).

9. Bown, M. J. *et al.* Association between the coronary artery disease risk locus on chromosome 9p21.3 and abdominal aortic aneurysm. en. *Circ Genetics* **1,** 39–42. ISSN: 1942-3268 (Oct. 2008).

10. Elmore, J. R. *et al.* Identification of a genetic variant associated with abdominal aortic aneurysms on chromosome 3p12.3 by genome wide association. *J Vasc Surg* **49,** 1525–31. ISSN: 1097-6809 (June 2009).

11. Hinterseher, I., Tromp, G. & Kuivaniemi, H. Genes and abdominal aortic aneurysm. *Ann Vasc Surg* **25,** 388–412. ISSN: 1615-5947 (Apr. 2011).

12. Harrison, S. C. *et al.* Interleukin-6 receptor pathways in abdominal aortic aneurysm. *Eur Heart J* **34,** 3707–16. ISSN: 1522-9645 (Oct. 2012).

13. Jones, G. T. *et al.* A sequence variant associated with sortilin-1 (SORT1) on 1p13.3 is independently associated with abdominal aortic aneurysm. *Hum Mol Genet* **In-press.** ISSN: 1460-2083. doi:`10.1093/hmg/ddt141` (Apr. 2013).

14. Helgadottir, A. *et al.* Apolipoprotein(a) genetic sequence variants associated with systemic atherosclerosis and coronary atherosclerotic burden but not with venous thromboembolism. *J Am Coll Cardiol* **60,** 722–9. ISSN: 1558-3597 (Aug. 2012).

15. Bradley, D. T. *et al.* A variant in LDLR is associated with abdominal aortic aneurysm. *Circulation. Cardiovascular genetics* **6,** 498–504. ISSN: 1942-3268 (Oct. 2013).

16. Jones, G. T. *et al.* Angiotensin II type 1 receptor 1166C polymorphism is associated with abdominal aortic aneurysm in three independent cohorts. *Arteriosclerosis, thrombosis, and vascular biology* **28,** 764–70. ISSN: 1524-4636 (Apr. 2008).

17. Deguara, J. *et al.* An increased frequency of the 5A allele in the promoter region of the MMP3 gene is associated with abdominal aortic aneurysms. *Human molecular genetics* **16,** 3002–7. ISSN: 0964-6906 (Dec. 2007).

18. Yoon, S. *et al.* Genetic Analysis of MMP3, MMP9, and PAI-1 in Finnish Patients with Abdominal Aortic or Intracranial Aneurysms. *Biochemical and Biophysical Research Communications* **265,** 563–568. ISSN: 0006291X (Nov. 1999).

19. Jones, G. T. *et al.* Meta-Analysis of Genome-Wide Association Studies for Abdominal Aortic Aneurysm Identifies Four New Disease-Specific Risk Loci-Novelty and Significance. *Circulation Research* **120,** 341–353. ISSN: 0009-7330 (Jan. 2017).

20. Biddinger, A., Rocklin, M., Coselli, J. & Milewicz, D. M. Familial thoracic aortic dilatations and dissections: A case control study. *J Vasc Surg* **25,** 506–511. ISSN: 07415214 (Mar. 1997).

21. Albornoz, G. *et al.* Familial thoracic aortic aneurysms and dissections–incidence, modes of inheritance, and phenotypic patterns. *Ann Thorac Surg* **82,** 1400–5. ISSN: 1552-6259 (Oct. 2006).

22. Danyi, P., Elefteriades, J. a. & Jovin, I. S. Medical therapy of thoracic aortic aneurysms: are we there yet? *Circulation* **124,** 1469–76. ISSN: 1524-4539 (Sept. 2011).

23. Losenno, K. L., Goodman, R. L. & Chu, M. W. a. Bicuspid aortic valve disease and ascending aortic aneurysms: gaps in knowledge. *Cardiol Res Pract* **2012,** 145202. ISSN: 2090-0597 (Jan. 2012).

24. Bonderman, D. *et al.* Mechanisms underlying aortic dilatation in congenital aortic valve malformation. *Circulation* **99,** 2138–43. ISSN: 1524-4539 (Apr. 1999).

25. Elefteriades, J. A. Natural history of thoracic aortic aneurysms: indications for surgery, and surgical versus nonsurgical risks. *Ann Thorac Surg* **74,** S1877–80, discussion S1892–8. ISSN: 0003-4975 (Nov. 2002).

26. Mirea, O. *et al.* Effects of aging and body size on proximal and ascending aorta and aortic arch: Inner edge-to-inner edge reference values in a large adult population by two-dimensional transthoracic echocardiography. *J Am Soc Echocardiogr* **26,** 419–27. ISSN: 1097-6795 (Jan. 2013).

27. Kaiser, T., Kellenberger, C. J., Albisetti, M., Bergsträsser, E. & Valsangiacomo Buechel, E. R. Normal values for aortic diameters in children and adolescents–assessment in vivo by contrast-enhanced CMR-angiography. *J Cardiovasc Magn Reson* **10,** 56. ISSN: 1532-429X (Jan. 2008).

28. Devereux, R. B. *et al.* Normal limits in relation to age, body size and gender of two-dimensional echocardiographic aortic root dimensions in persons ≥15 years of age. *Am J Cardiol* **110,** 1189–94. ISSN: 1879-1913 (Oct. 2012).

29. Yuan, S.-M. & Jing, H. Cystic medial necrosis: pathological findings and clinical implications. *Rev Bras Cir Cardiovasc* **26,** 107–15. ISSN: 1678-9741 (Mar. 2011).

30. Bickerstaff, L. K. *et al.* Thoracic aortic aneurysms: a population-based study. en. *Surgery* **92,** 1103–8. ISSN: 0039-6060 (Dec. 1982).

31. Palombo, D. *et al.* Matrix metalloproteinases. Their role in degenerative chronic diseases of abdominal aorta. en. *J Cardiovasc Surg* **40,** 257–60. ISSN: 0021-9509 (Apr. 1999).

32. Nagasawa, A. *et al.* Important role of the angiotensin II pathway in producing matrix metalloproteinase-9 in human thoracic aortic aneurysms. *J Surg Res* **In-press.** ISSN: 1095-8673. doi:`10.1016/j.jss.2012.12.012` (Jan. 2013).

33. Braverman, A. C. *et al.* The bicuspid aortic valve. *Curr Probl in Cardiol* **30,** 470–522. ISSN: 0146-2806 (Sept. 2005).

34. Ramanath, V. S., Oh, J. K., Sundt, T. M. & Eagle, K. A. Acute aortic syndromes and thoracic aortic aneurysm. *Mayo Clin Proc* **84,** 465–81. ISSN: 1942-5546 (May 2009).

35. Dietz, H. C. *et al.* Marfan syndrome caused by a recurrent de novo missense mutation in the fibrillin gene. *Nature* **352,** 337–9. ISSN: 0028-0836 (July 1991).

36. Pyeritz, R. E. & McKusick, V. A. The Marfan Syndrome: Diagnosis and Management. *N Engl J Med* **300,** 772–777 (1979).

37. Loeys, B. *et al.* Comprehensive molecular screening of the FBN1 gene favors locus homogeneity of classical Marfan syndrome. *Hum Mutat* **24,** 140–6. ISSN: 1098-1004 (Aug. 2004).

38. Beighton, P. *et al.* International nosology of heritable disorders of connective tissue, Berlin, 1986. *Am J Med Genet* **29,** 581–94. ISSN: 0148-7299 (Mar. 1988).

39. De Paepe, A., Devereux, R. B., Dietz, H. C., Hennekam, R. C. & Pyeritz, R. E. Revised diagnostic criteria for the Marfan syndrome. *Am J Med Genet* **62,** 417–26. ISSN: 0148-7299 (Apr. 1996).

40. Loeys, B. L. *et al.* The revised Ghent nosology for the Marfan syndrome. *J Med Genet* **47,** 476–85. ISSN: 1468-6244 (July 2010).

41. Faivre, L. *et al.* In frame fibrillin-1 gene deletion in autosomal dominant Weill-Marchesani syndrome. *J Med Genet* **40,** 34–6. ISSN: 1468-6244 (Jan. 2003).

42. Loeys, B. L. *et al.* Mutations in fibrillin-1 cause congenital scleroderma: stiff skin syndrome. *Sci Transl Med* **2,** 23ra20. ISSN: 1946-6242 (Mar. 2010).

43. Le Goff, C. *et al.* Mutations in the TGFβ binding-protein-like domain 5 of FBN1 are responsible for acromicric and geleophysic dysplasias. en. *Am J Hum Genet* **89,** 7–14. ISSN: 1537-6605 (July 2011).

44. Putnam, E. A., Zhang, H., Ramirez, F. & Milewicz, D. M. Fibrillin-2 (FBN2) mutations result in the Marfan-like disorder, congenital contractural arachnodactyly. *Nat Genet* **11,** 456–8. ISSN: 1061-4036 (Dec. 1995).

45. Loeys, B. L. *et al.* A syndrome of altered cardiovascular, craniofacial, neurocognitive and skeletal development caused by mutations in TGFBR1 or TGFBR2. *Nat Genet* **37,** 275–81. ISSN: 1061-4036 (Mar. 2005).

46. Micha, D. *et al.* SMAD2 Mutations Are Associated with Arterial Aneurysms and Dissections. *Human Mutation* **36,** 1145–1149. ISSN: 10597794 (Dec. 2015).

47. Van de Laar, I. M. B. H. *et al.* Mutations in SMAD3 cause a syndromic form of aortic aneurysms and dissections with early-onset osteoarthritis. *Nature genetics* **43,** 121–126. ISSN: 1061-4036 (Feb. 2011).

48. Lindsay, M. E. *et al.* Loss-of-function mutations in TGFB2 cause a syndromic presentation of thoracic aortic aneurysm. *Nat Genet* **44,** 922–7. ISSN: 1546-1718 (Aug. 2012).

49. Bertoli-Avella, A. M. *et al.* Mutations in a TGF-β Ligand, TGFB3, Cause Syndromic Aortic Aneurysms and Dissections. *Journal of the American College of Cardiology* **65,** 1324–36. ISSN: 1558-3597 (Apr. 2015).

50. Doyle, A. J. *et al.* Mutations in the TGF-β repressor SKI cause Shprintzen-Goldberg syndrome with aortic aneurysm. *Nat Genet* **44,** 1249–54. ISSN: 1546-1718 (Sept. 2012).

51. Hucthagowder, V. *et al.* Fibulin-4: a novel gene for an autosomal recessive cutis laxa syndrome. *Am J Hum Genet* **78,** 1075–80. ISSN: 0002-9297 (June 2006).

52. Zhang, M. C. *et al.* Cutis laxa arising from frameshift mutations in exon 30 of the elastin gene (ELN). *J Biol Chem* **274,** 981–6. ISSN: 0021-9258 (Jan. 1999).

53. Tassabehji, M. *et al.* An elastin gene mutation producing abnormal tropoelastin and abnormal elastic fibres in a patient with autosomal dominant cutis laxa. *Hum Mol Genet* **7,** 1021–8. ISSN: 0964-6906 (June 1998).

54. Ewart, A. K., Jin, W., Atkinson, D., Morris, C. A. & Keating, M. T. Supravalvular aortic stenosis associated with a deletion disrupting the elastin gene. *J Clin Invest* **93,** 1071–7. ISSN: 0021-9738 (Mar. 1994).

55. Ewart, A. K. *et al.* Hemizygosity at the elastin locus in a developmental disorder, Williams syndrome. *Nat Genet* **5,** 11–6. ISSN: 1061-4036 (Sept. 1993).

56. Coucke, P. J. *et al.* Mutations in the facilitative glucose transporter GLUT10 alter angiogenesis and cause arterial tortuosity syndrome. *Nat Genet* **38,** 452–7. ISSN: 1061-4036 (Apr. 2006).

57. Superti-Furga, A., Steinmann, B., Ramirez, F. & Byers, P. H. Molecular defects of type III procollagen in Ehlers-Danlos syndrome type IV. *Hum Genet* **82,** 104–8. ISSN: 0340-6717 (May 1989).

58. Rowe, D. W., Shapiro, J. R., Poirier, M. & Schlesinger, S. Diminished type I collagen synthesis and reduced alpha 1(I) collagen messenger RNA in cultured fibroblasts from patients with dominantly inherited (type I) osteogenesis imperfecta. *J Clin Invest* **76,** 604–11. ISSN: 0021-9738 (Aug. 1985).

59. Schwarze, U. *et al.* Rare autosomal recessive cardiac valvular form of Ehlers-Danlos syndrome results from mutations in the COL1A2 gene that activate the nonsense-mediated RNA decay pathway. *Am J Hum Genet* **74,** 917–30. ISSN: 0002-9297 (May 2004).

60. Weil, D. *et al.* A base substitution in the exon of a collagen gene causes alternative splicing and generates a structurally abnormal polypeptide in a patient with Ehlers-Danlos syndrome type VII. *EMBO J* **8,** 1705–10. ISSN: 0261-4189 (June 1989).

61. Hautala, T., Heikkinen, J., Kivirikko, K. I. & Myllylä, R. A large duplication in the gene for lysyl hydroxylase accounts for the type VI variant of Ehlers-Danlos syndrome in two siblings. *Genomics* **15,** 399–404. ISSN: 0888-7543 (Feb. 1993).

62. Fox, J. W. *et al.* Mutations in filamin 1 prevent migration of cerebral cortical neurons in human periventricular heterotopia. *Neuron* **21,** 1315–25. ISSN: 0896-6273 (Dec. 1998).

63. Meester, J. A. *et al.* Loss-of-function mutations in the X-linked biglycan gene cause a severe syndromic form of thoracic aortic aneurysms and dissections. *Genetics in Medicine.* ISSN: 1098-3600. doi:`10.1038/gim.2016.126` (2016).

64. Guo, D.-C. *et al.* Mutations in smooth muscle α-actin (ACTA2) lead to thoracic aortic aneurysms and dissections. *Nature Genetics* **39,** 1488–1493. ISSN: 1061-4036 (Dec. 2007).

65. Milewicz, D. M. *et al.* De novo ACTA2 mutation causes a novel syndrome of multisystemic smooth muscle dysfunction. *Am J Hum Genet* **152A,** 2437–43. ISSN: 1552-4833 (Oct. 2010).

66. Zhu, L. *et al.* Mutations in myosin heavy chain 11 cause a syndrome associating thoracic aortic aneurysm/aortic dissection and patent ductus arteriosus. *Nat Genet* **38,** 343–9. ISSN: 1061-4036 (Mar. 2006).

67. Wang, L. *et al.* Mutations in myosin light chain kinase cause familial aortic dissections. *Am J Hum Genet* **87,** 701–7. ISSN: 1537-6605 (Nov. 2010).

68. Barbier, M. *et al.* MFAP5 Loss-of-Function Mutations Underscore the Involvement of Matrix Alteration in the Pathogenesis of Familial Thoracic Aortic Aneurysms and Dissections. *The American Journal of Human Genetics* **95,** 736–743. ISSN: 00029297 (Dec. 2014).

69. Guo, D.-c. *et al.* MAT2A Mutations Predispose Individuals to Thoracic Aortic Aneurysms. *The American Journal of Human Genetics* **96,** 170–177. ISSN: 00029297 (Jan. 2015).

70. Guo, D.-c. *et al.* Recurrent gain-of-function mutation in PRKG1 causes thoracic aortic aneurysms and acute aortic dissections. *American journal of human genetics* **93,** 398–404. ISSN: 1537-6605 (Aug. 2013).

71. Guo, D.-c. *et al.* LOX Mutations Predispose to Thoracic Aortic Aneurysms and DissectionsNovelty and Significance. *Circulation Research* **118,** 928–934. ISSN: 0009-7330 (Mar. 2016).

72. Kuang, S.-Q. *et al.* FOXE3 mutations predispose to thoracic aortic aneurysms and dissections. *Journal of Clinical Investigation* **126,** 948–961. ISSN: 0021-9738 (Feb. 2016).

73. Garg, V. *et al.* Mutations in NOTCH1 cause aortic valve disease. *Nature* **437,** 270–4. ISSN: 1476-4687 (Sept. 2005).

74. Collod-Béroud, G. *et al.* Update of the UMD-FBN1 mutation database and creation of an FBN1 polymorphism database. *Hum Mutat* **22,** 199–208. ISSN: 1098-1004 (Sept. 2003).

75. Baetens, M. *et al.* Applying massive parallel sequencing to molecular diagnosis of Marfan and Loeys-Dietz syndromes. *Hum Genet* **32,** 1053–1062. ISSN: 1098-1004 (May 2011).

76. Hayward, C., Porteous, M. E. & Brock, D. J. Mutation screening of all 65 exons of the fibrillin-1 gene in 60 patients with Marfan syndrome: report of 12 novel mutations. *Hum Mutat* **10,** 280–9. ISSN: 1059-7794 (Jan. 1997).

77. Fleischer, Md, K. J., Nousari, Md, H. C., Anhalt, Md, G. J., Stone, Md, C. D. & Laschinger, Md, J. C. Immunohistochemical abnormalities of fibrillin in cardiovascular tissues in Marfan's syndrome. *Ann Thorac Surg* **63,** 1012–17. ISSN: 00034975 (Apr. 1997).

78. Pereira, L. *et al.* Targetting of the gene encoding fibrillin-1 recapitulates the vascular aspect of Marfan syndrome. *Nat Genet* **17,** 218–22. ISSN: 1061-4036 (Oct. 1997).

79. Neptune, E. R. *et al.* Dysregulation of TGF-beta activation contributes to pathogenesis in Marfan syndrome. *Nat Genet* **33,** 407–11. ISSN: 1061-4036 (Mar. 2003).

80. Dallas, S. L., Miyazono, K., Skerry, T. M., Mundy, G. R. & Bonewald, L. F. Dual role for the latent transforming growth factor-beta binding protein in storage of latent TGF-beta in the extracellular matrix and as a structural matrix protein. *J Cell Biol* **131,** 539–49. ISSN: 0021-9525 (Oct. 1995).

81. Dallas, S. L. *et al.* Role of the latent transforming growth factor beta binding protein 1 in fibrillin-containing microfibrils in bone cells in vitro and in vivo. *J Bone Miner Res* **15,** 68–81. ISSN: 0884-0431 (Jan. 2000).

82. Isogai, Z. *et al.* Latent transforming growth factor beta-binding protein 1 interacts with fibrillin and is a microfibril-associated protein. *J Biol Chem* **278,** 2750–7. ISSN: 0021-9258 (Jan. 2003).

83. Ng, C. M. *et al.* TGF-beta-dependent pathogenesis of mitral valve prolapse in a mouse model of Marfan syndrome. *J Clin Invest* **114,** 1586–92. ISSN: 0021-9738 (Dec. 2004).

84. Habashi, J. P. *et al.* Losartan, an AT1 antagonist, prevents aortic aneurysm in a mouse model of Marfan syndrome. *Science* **312,** 117–121. ISSN: 1095-9203 (Apr. 2006).

85. Holm, T. M. *et al.* Noncanonical TGFbeta signaling contributes to aortic aneurysm progression in Marfan syndrome mice. *Science* **332,** 358–361 (2011).

86. Van Hemelrijk, C., Renard, M. & Loeys, B. The Loeys-Dietz syndrome: an update for the clinician. *Curr Opin Cardiol* **25,** 546–51. ISSN: 1531-7080 (Nov. 2010).

87. Rahme, R. J. *et al.* Association of intracranial aneurysm and Loeys-Dietz syndrome: case illustration, management, and literature review. *Neurosurgery* **69,** E488–92, discussion E492–3. ISSN: 1524-4040 (Aug. 2011).

88. Singh, K. K. *et al.* TGFBR1 and TGFBR2 mutations in patients with features of Marfan syndrome and Loeys-Dietz syndrome. *Hum Mutat* **27,** 770–7. ISSN: 1098-1004 (Aug. 2006).

89. Mizuguchi, T. *et al.* Heterozygous TGFBR2 mutations in Marfan syndrome. *Nat Genet* **36,** 855–60. ISSN: 1061-4036 (Aug. 2004).

90. Azhar, M. *et al.* Transforming growth factor beta in cardiovascular development and function. *Cytokine Growth Factor Rev* **14,** 391–407. ISSN: 1359-6101 (Oct. 2003).

91. Sanford, L. P. *et al.* TGFbeta2 knockout mice have multiple developmental defects that are non-overlapping with other TGFbeta knockout phenotypes. *Development* **124,** 2659–70. ISSN: 0950-1991 (July 1997).

92. Ito, Y. *et al.* Conditional inactivation of Tgfbr2 in cranial neural crest causes cleft palate and calvaria defects. *Development* **130,** 5269–80. ISSN: 0950-1991 (Nov. 2003).

93. Loeys, B. L. *et al.* Aneurysm syndromes caused by mutations in the TGF-beta receptor. *N Engl J Med* **355,** 788–98. ISSN: 1533-4406 (Aug. 2006).

94. Pannu, H. *et al.* Mutations in transforming growth factor-beta receptor type II cause familial thoracic aortic aneurysms and dissections. *Circulation* **112,** 513–20. ISSN: 1524-4539 (July 2005).

95. Boileau, C. *et al.* TGFB2 mutations cause familial thoracic aortic aneurysms and dissections associated with mild systemic features of Marfan syndrome. *Nat Genet* **44,** 916–21. ISSN: 1546-1718 (Aug. 2012).

96. Regalado, E. S. *et al.* Exome sequencing identifies SMAD3 mutations as a cause of familial thoracic aortic aneurysm and dissection with intracranial and other arterial aneurysms. *Circ Res* **109,** 680–6. ISSN: 1524-4571 (Sept. 2011).

97. Heldin, C. H., Miyazono, K. & ten Dijke, P. TGF-beta signalling from cell membrane to nucleus through SMAD proteins. *Nature* **390,** 465–71. ISSN: 0028-0836 (Dec. 1997).

98. Bujak, M. & Frangogiannis, N. G. The role of TGF-beta signaling in myocardial infarction and cardiac remodeling. *Cardiovasc Res* **74,** 184–95. ISSN: 0008-6363 (May 2007).

99. Shprintzen, R. J. & Goldberg, R. B. A recurrent pattern syndrome of craniosynostosis associated with arachnodactyly and abdominal hernias. en. *J Craniofac Genet Dev Biol* **2,** 65–74. ISSN: 0270-4145 (Jan. 1982).

100. Robinson, P. N. *et al.* Shprintzen-Goldberg syndrome: fourteen new patients and a clinical analysis. *Am J Hum Genet* **135,** 251–62. ISSN: 1552-4825 (June 2005).

101. Carmignac, V. *et al.* In-frame mutations in exon 1 of SKI cause dominant Shprintzen-Goldberg syndrome. *Am J Hum Genet* **91,** 950–957. ISSN: 1537-6605 (Nov. 2012).

102. Renard, M. *et al.* Altered TGFbeta signaling and cardiovascular manifestations in patients with autosomal recessive cutis laxa type I caused by fibulin-4 deficiency. *Eur J Hum Genet* **18,** 895–901. ISSN: 1476-5438 (Aug. 2010).

103. Massam-Wu, T. *et al.* Assembly of fibrillin microfibrils governs extracellular deposition of latent TGF beta. *J Cell Sci* **123,** 3006–18. ISSN: 1477-9137 (Sept. 2010).

104. Horiguchi, M. *et al.* Fibulin-4 conducts proper elastogenesis via interaction with cross-linking enzyme lysyl oxidase. *Proc Natl Acad Sci U S A* **106,** 19029–34. ISSN: 1091-6490 (Nov. 2009).

105. Willaert, A. *et al.* GLUT10 is required for the development of the cardiovascular system and the notochord and connects mitochondrial function to TGFβ signaling. *Hum Mol Genet* **21,** 1248–59. ISSN: 1460-2083 (Mar. 2012).

106. Callewaert, B. L. *et al.* Comprehensive clinical and molecular assessment of 32 probands with congenital contractural arachnodactyly: report of 14 novel mutations and review of the literature. *Hum Mutat* **30,** 334–41. ISSN: 1098-1004 (Mar. 2009).

107. Lum, Y. W., Brooke, B. S. & Black, J. H. Contemporary management of vascular Ehlers-Danlos syndrome. *Curr Opin Cardiol* **26,** 494–501. ISSN: 1531-7080 (Nov. 2011).

108. Brooke, B. S. Celiprolol therapy for vascular Ehlers-Danlos syndrome. *Lancet* **376,** 1443–4. ISSN: 1474-547X (Oct. 2010).

109. Ong, K.-T. *et al.* Effect of celiprolol on prevention of cardiovascular events in vascular Ehlers-Danlos syndrome: a prospective randomised, open, blinded-endpoints trial. *Lancet* **376,** 1476–84. ISSN: 1474-547X (Oct. 2010).

110. Ramirez, F. & Sakai, L. Y. Biogenesis and function of fibrillin assemblies. *Cell Tissue Res* **339,** 71–82. ISSN: 1432-0878 (Jan. 2010).

111. Malfait, F. *et al.* Three arginine to cysteine substitutions in the pro-alpha (I)-collagen chain cause Ehlers-Danlos syndrome with a propensity to arterial rupture in early adulthood. *Hum Mutat* **28,** 387–95. ISSN: 1098-1004 (Apr. 2007).

112. Yeowell, H. N. & Walker, L. C. Mutations in the lysyl hydroxylase 1 gene that result in enzyme deficiency and the clinical phenotype of Ehlers-Danlos syndrome type VI. *Mol Genet Metab* **71,** 212–24. ISSN: 1096-7192 (2000).

113. McDonnell, N. B. *et al.* Echocardiographic findings in classical and hypermobile Ehlers-Danlos syndromes. *Am J Med Genet A* **140,** 129–36. ISSN: 1552-4825 (Jan. 2006).

114. Nakamura, F., Osborn, T. M., Hartemink, C. A., Hartwig, J. H. & Stossel, T. P. Structural basis of filamin A functions. *J Cell Biol* **179,** 1011–25. ISSN: 1540-8140 (Dec. 2007).

115. Popowicz, G. M., Schleicher, M., Noegel, A. A. & Holak, T. A. Filamins: promiscuous organizers of the cytoskeleton. *Trends Biochem Sci* **31,** 411–9. ISSN: 0968-0004 (July 2006).

116. Tartaglia, M. *et al.* Mutations in PTPN11, encoding the protein tyrosine phosphatase SHP-2, cause Noonan syndrome. *Nat Genet* **29,** 465–8. ISSN: 1061-4036 (Dec. 2001).

117. Digilio, M. C. *et al.* Grouping of multiple-lentigines/LEOPARD and Noonan syndromes on the PTPN11 gene. *Am J Hum Genet* **71,** 389–94. ISSN: 0002-9297 (Aug. 2002).

118. Wallace, M. R. *et al.* Type 1 neurofibromatosis gene: identification of a large transcript disrupted in three NF1 patients. *Science* **249,** 181–6. ISSN: 0036-8075 (July 1990).

119. Oda, T. *et al.* Mutations in the human Jagged1 gene are responsible for Alagille syndrome. *Nat Genet* **16,** 235–42. ISSN: 1061-4036 (July 1997).

120. Li, L. *et al.* Alagille syndrome is caused by mutations in human Jagged1, which encodes a ligand for Notch1. *Nat Genet* **16,** 243–51. ISSN: 1061-4036 (July 1997).

121. McAllister, K. A. *et al.* Endoglin, a TGF-beta binding protein of endothelial cells, is the gene for hereditary haemorrhagic telangiectasia type 1. *Nat Genet* **8,** 345–51. ISSN: 1061-4036 (Dec. 1994).

122. Johnson, D. W. *et al.* Mutations in the activin receptor-like kinase 1 gene in hereditary haemorrhagic telangiectasia type 2. *Nat Genet* **13,** 189–95. ISSN: 1061-4036 (June 1996).

123. Le Goff, C. *et al.* Mutations at a single codon in Mad homology 2 domain of SMAD4 cause Myhre syndrome. *Nat Genet* **44,** 85–8. ISSN: 1546-1718 (Jan. 2012).

124. Teekakirikul, P. *et al.* Thoracic aortic disease in two patients with juvenile polyposis syndrome and SMAD4 mutations. *Am J Med Genet* **161A,** 185–91. ISSN: 1552-4833 (Dec. 2012).

125. Gallione, C. J. *et al.* A combined syndrome of juvenile polyposis and hereditary haemorrhagic telangiectasia associated with mutations in MADH4 (SMAD4). *Lancet* **363,** 852–9. ISSN: 1474-547X (Mar. 2004).

126. Marini, J. C., Grange, D. K., Gottesman, G. S., Lewis, M. B. & Koeplin, D. A. Osteogenesis imperfecta type IV. Detection of a point mutation in one alpha 1(I) collagen allele (COL1A1) by RNA/RNA hybrid analysis. *J Biol Chem* **264,** 11893–900. ISSN: 0021-9258 (July 1989).

127. Starman, B. J. *et al.* Osteogenesis imperfecta. The position of substitution for glycine by cysteine in the triple helical domain of the pro alpha 1(I) chains of type I collagen determines the clinical phenotype. *J Clin Invest* **84,** 1206–14. ISSN: 0021-9738 (Oct. 1989).

128. Penttinen, R. P., Lichtenstein, J. R., Martin, G. R. & McKusick, V. A. Abnormal collagen metabolism in cultured cells in osteogenesis imperfecta. *Proc Natl Acad Sci U S A* **72,** 586–9. ISSN: 0027-8424 (Feb. 1975).

129. Plaisier, E. *et al.* COL4A1 mutations and hereditary angiopathy, nephropathy, aneurysms, and muscle cramps. *N Engl J Med* **357,** 2687–95. ISSN: 1533-4406 (Dec. 2007).

130. Lemmink, H. H. *et al.* Mutations in the type IV collagen alpha 3 (COL4A3) gene in autosomal recessive Alport syndrome. *Hum Mol Genet* **3,** 1269–73. ISSN: 0964-6906 (Aug. 1994).

131. Gubler, M. C. *et al.* Autosomal recessive Alport syndrome: immunohistochemical study of type IV collagen chain distribution. *Kidney Int* **47,** 1142–7. ISSN: 0085-2538 (Apr. 1995).

132. Salo, A. M. *et al.* A connective tissue disorder caused by mutations of the lysyl hydroxylase 3 gene. *Am J Hum Genet* **83,** 495–503. ISSN: 1537-6605 (Oct. 2008).

133. Chapman, J. & Hilson, A. Polycystic kidneys and abdominal aortic aneurysms. *Lancet* **315,** 646–647. ISSN: 01406736 (Mar. 1980).

134. Roodvoets, A. P. Aortic aneurysms in presence of kidney disease. *Lancet* **1,** 1413–4. ISSN: 0140-6736 (June 1980).

135. Torra, R. *et al.* Abdominal aortic aneurysms and autosomal dominant polycystic kidney disease. *J Am Soc Nephrol* **7,** 2483–6. ISSN: 1046-6673 (Nov. 1996).

136. Torres, V. E. in *The Cystic kidney* (eds Gardner, K. D. & Berstein, J.) 295–326 (Kluwer, Dordrecht, 1990).

137. Calvet, J. P. & Grantham, J. J. The genetics and physiology of polycystic kidney disease. *Semin Nephrol* **21,** 107–23. ISSN: 0270-9295 (Mar. 2001).

138. Hassane, S. *et al.* Elevated TGFbeta-Smad signalling in experimental Pkd1 models and human patients with polycystic kidney disease. *J Pathol* **222,** 21–31. ISSN: 1096-9896 (Sept. 2010).

139. Cury, M., Zeidan, F. & Lobato, A. C. Aortic disease in the young: genetic aneurysm syndromes, connective tissue disorders, and familial aortic aneurysms and dissections. *Int J Vasc Med* **2013,** 267215. ISSN: 2090-2824 (Jan. 2013).

140. Milewicz, D. M. *et al.* Reduced penetrance and variable expressivity of familial thoracic aortic aneurysms/dissections. en. *Am J Cardiol* **82,** 474–479. ISSN: 00029149 (Aug. 1998).

141. Hasham, S. N. *et al.* Mapping a locus for familial thoracic aortic aneurysms and dissections (TAAD2) to 3p24-25. *Circulation* **107,** 3184–90. ISSN: 1524-4539 (July 2003).

142. Milewicz, D. M. *et al.* Fibrillin-1 (FBN1) mutations in patients with thoracic aortic aneurysms. *Circulation* **94,** 2708–11. ISSN: 0009-7322 (Dec. 1996).

143. Al-Mohaissen, M. *et al.* Brachial artery occlusion in a young adult with an ACTA2 thoracic aortic aneurysm. *Vasc Med* **17,** 326–9. ISSN: 1477-0377 (Oct. 2012).

144. Malloy, L. E. *et al.* Thoracic aortic aneurysm (TAAD)-causing mutation in actin affects formin regulation of polymerization. *J Biol Chem* **287,** 28398–408. ISSN: 1083-351X (Aug. 2012).

145. Harakalova, M. *et al.* Incomplete segregation of MYH11 variants with thoracic aortic aneurysms and dissections and patent ductus arteriosus. *Eur J Hum Genet* **21,** 487–93. ISSN: 1476-5438 (Sept. 2013).

146. Wallace, K. N. *et al.* Mutation of smooth muscle myosin causes epithelial invasion and cystic expansion of the zebrafish intestine. *Dev Cell* **8,** 717–26. ISSN: 1534-5807 (May 2005).

147. Kamm, K. E. & Stull, J. T. Dedicated myosin light chain kinases with diverse cellular functions. *J Biol Chem* **276,** 4527–30. ISSN: 0021-9258 (Feb. 2001).

148. Luyckx, I. *et al.* Two novel MYLK nonsense mutations causing thoracic aortic aneurysms/dissections in patients without apparent family history. *Clinical Genetics,* 4–6. ISSN: 00099163 (2017).

149. Renard, M. *et al.* Novel MYH11 and ACTA2 mutations reveal a role for enhanced TGFβ signaling in FTAAD. *Int J Cardiol* **165,** 314–21. ISSN: 1874-1754 (Sept. 2013).

150. Lemaire, S. A. *et al.* Genome-wide association study identifies a susceptibility locus for thoracic aortic aneurysms and aortic dissections spanning FBN1 at 15q21.1. *Nat Genet* **43,** 996–1000. ISSN: 1546-1718 (Oct. 2011).

151. Prakash, S. K. *et al.* Rare copy number variants disrupt genes regulating vascular smooth muscle cell adhesion and contractility in sporadic thoracic aortic aneurysms and dissections. *Am J Hum Genet* **87,** 743–56. ISSN: 1537-6605 (Dec. 2010).

152. Kuang, S.-Q. *et al.* Recurrent chromosome 16p13.1 duplications are a risk factor for aortic dissections. *PLoS Genet* **7** (ed Hakonarson, H.) e1002118. ISSN: 1553-7404 (June 2011).

153. Guo, D.-c. *et al.* Genetic Variants in LRP1 and ULK4 Are Associated with Acute Aortic Dissections. *The American Journal of Human Genetics,* 1–8. ISSN: 00029297 (2016).

154. Guo, D. *et al.* Familial thoracic aortic aneurysms and dissections: genetic heterogeneity with a major locus mapping to 5q13-14. *Circulation* **103,** 2461–8. ISSN: 1524-4539 (May 2001).

155. Tran-Fadulu, V. *et al.* Analysis of multigenerational families with thoracic aortic aneurysms and dissections due to TGFBR1 or TGFBR2 mutations. *J Med Genet* **46,** 607–13. ISSN: 1468-6244 (Sept. 2009).

156. Vaughan, C. J. *et al.* Identification of a chromosome 11q23.2-q24 locus for familial aortic aneurysm disease, a genetically heterogeneous disorder. *Circulation* **103,** 2469–75. ISSN: 1524-4539 (May 2001).

157. Guo, D.-C. *et al.* Familial thoracic aortic aneurysms and dissections: identification of a novel locus for stable aneurysms with a low risk for progression to aortic dissection. *Circ Genetics* **4,** 36–42. ISSN: 1942-3268 (Feb. 2011).

158. Keramati, A. R., Sadeghpour, A., Farahani, M. M., Chandok, G. & Mani, A. The non-syndromic familial thoracic aortic aneurysms and dissections maps to 15q21 locus. *BMC Med Genet* **11,** 143. ISSN: 1471-2350 (Jan. 2010).

159. Pannu, H., Avidan, N., Tran-Fadulu, V. & Milewicz, D. M. Genetic basis of thoracic aortic aneurysms and dissections: potential relevance to abdominal aortic aneurysms. *Ann NY Acad Sci* **1085,** 242–55. ISSN: 0077-8923 (Nov. 2006).

160. Khau Van Kien, P. *et al.* Mapping of familial thoracic aortic aneurysm/dissection with patent ductus arteriosus to 16p12.2-p13.13. *Circulation* **112,** 200–6. ISSN: 1524-4539 (July 2005).

161. Martin, L. J. *et al.* Evidence in favor of linkage to human chromosomal regions 18q, 5q and 13q for bicuspid aortic valve and associated cardiovascular malformations. *Hum Genet* **121,** 275–84. ISSN: 0340-6717 (Apr. 2007).

162. Loscalzo, M. L. *et al.* Familial thoracic aortic dilation and bicommissural aortic valve: a prospective analysis of natural history and inheritance. *Am J Med Genet* **143A,** 1960–7. ISSN: 1552-4825 (Sept. 2007).

163. Guo, D.-C. *et al.* Mutations in smooth muscle alpha-actin (ACTA2) cause coronary artery disease, stroke, and Moyamoya disease, along with thoracic aortic disease. *Am J Hum Genet* **84,** 617–27. ISSN: 1537-6605 (May 2009).

164. Lee, T. C., Zhao, Y. D., Courtman, D. W. & Stewart, D. J. Abnormal aortic valve development in mice lacking endothelial nitric oxide synthase. *Circulation* **101,** 2345–8. ISSN: 1524-4539 (May 2000).

165. Mohamed, S. A., Hanke, T., Schlueter, C., Bullerdiek, J. & Sievers, H.-H. Ubiquitin fusion degradation 1-like gene dysregulation in bicuspid aortic valve. *J Thorac Cardiovasc Surg* **130,** 1531–6. ISSN: 1097-685X (Dec. 2005).

166. Timmerman, L. A. *et al.* Notch promotes epithelial-mesenchymal transition during cardiac development and oncogenic transformation. *Gene Dev* **5,** 99–115 (2004).

167. Zou, S. *et al.* Notch signaling in descending thoracic aortic aneurysm and dissection. *PloS one* **7,** e52833. ISSN: 1932-6203 (Jan. 2012).

168. Tadros, T. M., Klein, M. D. & Shapira, O. M. Ascending aortic dilatation associated with bicuspid aortic valve: pathophysiology, molecular biology, and clinical implications. *Circulation* **119,** 880–90. ISSN: 1524-4539 (Feb. 2009).

169. Gomez, D. *et al.* Syndromic and non-syndromic aneurysms of the human ascending aorta share activation of the Smad2 pathway. *J Pathol* **218,** 131–42. ISSN: 1096-9896 (May 2009).

170. Kjellqvist, S. *et al.* A combined proteomic and transcriptomic approach shows diverging molecular mechanisms in thoracic aortic aneurysm development in patients with tricuspid and bicuspid aortic valve. *Mol Cell Proteomics* **12,** 1–51 (2012).

171. Fedak, P. W. M. *et al.* Vascular matrix remodeling in patients with bicuspid aortic valve malformations: implications for aortic dilatation. *J Thorac Cardiovasc Surg* **126,** 797–806. ISSN: 0022-5223 (Sept. 2003).

172. Nataatmadja, M. *et al.* Abnormal extracellular matrix protein transport associated with increased apoptosis of vascular smooth muscle cells in Marfan syndrome and bicuspid aortic valve thoracic aortic aneurysm. *Circulation* **108 Suppl,** II329–34. ISSN: 1524-4539 (Sept. 2003).

173. LeMaire, S. A. *et al.* Matrix metalloproteinases in ascending aortic aneurysms: bicuspid versus trileaflet aortic valves. *J Surg Res* **123,** 40–8. ISSN: 0022-4804 (Jan. 2005).

174. Yu, Q. & Stamenkovic, I. Cell surface-localized matrix metalloproteinase-9 proteolytically activates TGF-beta and promotes tumor invasion and angiogenesis. *Gene Dev* **14,** 163–76. ISSN: 0890-9369 (Jan. 2000).

175. Sachdev, V. *et al.* Aortic valve disease in Turner syndrome. *J Am Coll Cardiol* **51,** 1904–9. ISSN: 1558-3597 (May 2008).

176. Pereira, L. *et al.* Pathogenetic sequence for aneurysm revealed in mice underexpressing fibrillin-1. *Proc Natl Acad Sci U S A* **96,** 3819–23. ISSN: 0027-8424 (Mar. 1999).

177. Green, M. & Sweet, H. Tight skin (Tsk). *Mouse News Lett* **48** (1973).

178. Larsson, J. *et al.* Abnormal angiogenesis but intact hematopoietic potential in TGF-beta type I receptor-deficient mice. *EMBO J* **20,** 1663–73. ISSN: 0261-4189 (Apr. 2001).

179. Wang, J. *et al.* Defective ALK5 signaling in the neural crest leads to increased postmigratory neural crest cell apoptosis and severe outflow tract defects. *BMC Dev Biol* **6,** 51. ISSN: 1471-213X (Jan. 2006).

180. Oshima, M., Oshima, H. & Taketo, M. M. TGF-beta receptor type II deficiency results in defects of yolk sac hematopoiesis and vasculogenesis. *Dev Biol* **179,** 297–302. ISSN: 0012-1606 (Oct. 1996).

181. Levéen, P. *et al.* Induced disruption of the transforming growth factor beta type II receptor gene in mice causes a lethal inflammatory disorder that is transplantable. *Blood* **100,** 560–8. ISSN: 0006-4971 (July 2002).

182. Choudhary, B. *et al.* Cardiovascular malformations with normal smooth muscle differentiation in neural crest-specific type II TGFbeta receptor (Tgfbr2) mutant mice. *Dev Biol* **289,** 420–9. ISSN: 0012-1606 (Jan. 2006).

183. Choudhary, B. *et al.* Absence of TGFbeta signaling in embryonic vascular smooth muscle leads to reduced lysyl oxidase expression, impaired elastogenesis, and aneurysm. *Genesis* **47,** 115–21. ISSN: 1526-968X (Feb. 2009).

184. Hanada, K. *et al.* Perturbations of vascular homeostasis and aortic valve abnormalities in fibulin-4 deficient mice. *Circ Res* **100,** 738–46. ISSN: 1524-4571 (Mar. 2007).

185. Moltzer, E. *et al.* Impaired vascular contractility and aortic wall degeneration in fibulin-4 deficient mice: effect of angiotensin II type 1 (AT1) receptor blockade. *PloS one* **6,** e23411. ISSN: 1932-6203 (Jan. 2011).

186. Myers, J. C. *et al.* Molecular cloning of alpha 5(IV) collagen and assignment of the gene to the region of the X chromosome containing the Alport syndrome locus. *Am J Hum Genet* **46,** 1024–33. ISSN: 0002-9297 (June 1990).

187. Barker, D. F. *et al.* Identification of mutations in the COL4A5 collagen gene in Alport syndrome. *Science* **248,** 1224–7. ISSN: 0036-8075 (June 1990).

188. European Polycystic Kidney Disease, T. The polycystic kidney disease 1 gene encodes a 14 kb transcript and lies within a duplicated region on chromosome 16. The European Polycystic Kidney Disease Consortium. *Cell* **77,** 881–94. ISSN: 0092-8674 (June 1994).

189. Mochizuki, T. *et al.* PKD2, a gene for polycystic kidney disease that encodes an integral membrane protein. *Science* **272,** 1339–42. ISSN: 0036-8075 (May 1996).

190. Kumar, A. *et al.* A de novo frame-shift mutation in the tuberin gene. *Hum Mol Genet* **4,** 1471–2. ISSN: 0964-6906 (Aug. 1995).

191. Vrtel, R. *et al.* Identification of a nonsense mutation at the 5' end of the TSC2 gene in a family with a presumptive diagnosis of tuberous sclerosis complex. *J Med Genet* **33,** 47–51. ISSN: 0022-2593 (Jan. 1996).

192. Martiniuk, F., Bodkin, M., Tzall, S. & Hirschhorn, R. Identification of the base-pair substitution responsible for a human acid alpha glucosidase allele with lower "affinity" for glycogen (GAA 2) and transient gene expression in deficient cells. *Am J Hum Genet* **47,** 440–5. ISSN: 0002-9297 (Sept. 1990).

PART II

Aim of the Thesis

The aim of this thesis can be summarized in two specific research questions:

1. To identify the causal gene in previously undefined syndromic and non-syndromic forms of thoracic aortic aneurysm (Chapters 1, 2, 4).

2. Elucidating the genetic background of bicuspid aortic valve with associated thoracic aortic aneurysm (Chapter 3).

PART III

Results

Chapter 1

An *FBN1* Deep Intronic Mutation in a Familial Case of Marfan Syndrome: An Explanation for Genetically Unsolved Cases?

Elisabeth Gillis[1], Marlies Kempers[2], Simone Salemink[2], Janneke Timmermans[3], Emile C. Cheriex[4], Sebastiaan C.A.M. Bekkers[4], Erik Fransen[1], Christine E.M. De Die-Smulders[5], Bart L. Loeys[1,2] and Lut Van Laer[1]

1 Center for Medical Genetics, Faculty of Medicine and Health Sciences, University of Antwerp, Antwerp, Belgium
2 Department of Human Genetics, Radboud University Nijmegen Medical Centre, Nijmegen, The Netherlands
3 Department of Cardiology, Radboud University Medical Center, Nijmegen, The Netherlands
4 Department of Cardiology, Maastricht University Medical Center, Maastricht, The Netherlands
5 Department of Clinical Genetics, Maastricht University Medical Center, Maastricht, The Netherlands

Contribution: Whole exome sequencing analysis, RNA extraction from fibroblast cells, cDNA sequencing and analysis, analysis of splice-site scores, Sanger sequencing of introns

1.1 Abstract

Marfan syndrome (MFS) is caused by mutations in the *FBN1* (fibrillin-1) gene, but approximately 10% of MFS cases remain genetically unsolved. Here, we report a new *FBN1* mutation in an MFS family that had remained negative after extensive molecular genomic DNA *FBN1* testing, including denaturing high-performance liquid chromatography, Sanger sequencing, and multiplex ligation-dependent probe amplification. Linkage analysis in the family and cDNA sequencing of the proband revealed a deep intronic point mutation in intron 56 generating a new splice donor site. This mutation results in the integration of a 90-bp pseudo-exon between exons 56 and 57 containing a stop codon, causing nonsense-mediated mRNA decay. Although more than 90% of *FBN1* mutations can be identified with regular molecular testing at the genomic level, deep intronic mutations will be missed and require cDNA sequencing or whole-genome sequencing.

1.2 Introduction

Marfan syndrome (MFS) is a multisystemic autosomal dominant connective tissue disorder caused by mutations in the *FBN1* gene (MIM 134797). Its estimated prevalence is 2–3 per 10 000 individuals. MFS is characterized by a myriad of features occurring mainly in the skeletal, ocular, and cardiovascular systems, such as disproportionate overgrowth, pectus and vertebral column deformity, lens dislocation, mitral valve disease, and aortic root aneurysms[1]. The latter manifestations are the most life-threatening, as aneurysms may lead to fatal dissections. *FBN1* encodes fibrillin-1, which is a vital protein of the extracellular matrix (ECM). Fibrillin-1 also functions as an important regulator of the TGF-β (transforming growth factor beta) pathway[2–4]. Fibrillin-1 containing fibers can, together with the latent TGF-β binding protein and the latency associated peptide, keep TGF-β in a latent state. Thus, in contrast to the former belief that MFS is caused by the weakening of the ECM due to structural fibrillin-1 deficiency, it is now clear that many of the pathological manifestations of MFS can be explained by dysregulated TGF-β signaling. Since 1991, more than 1500 different *FBN1* mutations have been identified that can cause MFS[5–8]. However, in general, no disease causing mutation can be identified in approximately 10% of MFS patients.

1.3 Methods

DNA was extracted using standard methods. Standard molecular testing of *FBN1* (including MLPA), *TGFBR1*, *TGFBR2*, *SMAD3* and *ACTA2* and CNV analysis was performed in several diagnostic labs. Eleven family members were genotyped using the Linkage-24 DNA Analysis BeadChip (Illumina, CA, USA) according to the manufacturers' guidelines (Illumina, CA, USA). Linkage analysis was carried out using Merlin version 1.1.2[9]. Microsatellite markers were analysed by fragment analysis on the ABI Prism Genetic Analyzer 3130xl (Applied Biosystems Inc, CA, USA). Whole exome sequencing was performed on a HiSeq 1500 using the TruSeq Exome Enrichment Kit (Illumina, CA, USA). An in-house developed automated data analysis pipeline and a variant interpretation tool were used for data analysis.

Fibroblasts were cultured from a skin biopsy of the proband (IV:4). Before RNA extraction, 200μg/ml puromycine (Sigma-Aldrich, MO, USA) was added to inhibit nonsense-mediated mRNA decay. RNA was isolated using the miRNeasy Mini kit (Qiagen, Valencia, CA, USA), followed by reverse transcription with the SuperScript III First-Strand Synthesis System for RT-PCR (Invitrogen, UK). *FBN1* cDNA was amplified using 16 cDNA primerpairs (Supplementary Table 1.2) and standard touch-down PCR conditions. PCR products were sequenced with the ABI 3130XL Genetic Analyser (Applied Biosystems, CA, USA) using a BigDye terminator v1.1 cycle sequencing kit (Applied Biosystems, CA, USA). The deep intronic variant was analyzed with Alamut mutation interpretation software (Interactive Biosoftware, Rouen, France), which includes ESEfinder, SpliceSiteFinder-like, MaxEntScan, GeneSplicer and known constitutive signals. Splice site analysis of all existing refseq splice sites was performed with Human Splicing Finder[10]. Introns 25, 37 and 56 were sequenced with the primerpairs described in Supplementary table 1.2.

1.4 Results

Here, we report on an extended family that presented with skeletal and cardiovascular clinical features (Figure 1.1A, Table 1.1) that fulfilled the diagnostic criteria for MFS[11]. As usually seen in Marfan families, we did not observe nonpenetrance and most affected members of the family display strong clinical expression. Molecular *FBN1* testing of the proband and other family members was performed multiple times in a diagnostic setting. This consisted of denaturing high-pressure liquid chromatography and Sanger sequencing at the genomic DNA level, including intron–exon borders, and multiplex ligation-dependent probe amplification analysis but no causative *FBN1* mutation was identified. Subsequently, *TGFBR1* (MIM 190181), *TGFBR2* (MIM 190182), *SMAD3* (MIM 603109), and *ACTA2* (MIM 102620) were also excluded as causative genes by Sanger sequencing of genomic DNA. Finally, microarray analysis for copy-number variation gave normal results. Next, we performed linkage analysis using the Linkage-24 DNA Analysis BeadChip (Illumina, Hayward, CA) and Merlin version 1.1.2 [9] on 11 living family members from two generations (indicated with asterisks in Figure 1.1A). This revealed a unique large linked region on chromosome 15, with a

maximum LOD score reaching 2.6 at 29.4Mb (Figure 1.1B). This linkage result was confirmed by analysis of microsatellite markers located in or in the vicinity of the linked region, which also delineated the linked haplotype between 20.5 and 78.9 Mb (D15S1035–D15S983), containing the *FBN1* gene (Figure 1.1C). In addition, this large part of chromosome 15 harbored other interesting candidate genes, such as *TJP1* (MIM 601009), *AVEN* (MIM 605265), *ACTC1* (MIM 102540), *THBS1* (MIM 188060), *MAPKBP1*, *MFAP1* (MIM 600215), and *MAPK6* (MIM602904). Subsequently, we performed whole-exome sequencing on the proband (IV:4) using the TruSeq Exome Enrichment Kit (Illumina), followed by sequencing on a HiSeq 1500 (Illumina). An in-house developed automated data analysis pipeline and variant interpretation tool were used for data analysis. We did not find any promising variants in the linked region. Coverage analysis showed that all interesting positional candidate genes were sufficiently covered. In addition, no variants outside of the linkage region were considered to be plausible causal variants.

Because *FBN1* resided within the candidate region and the clinical phenotype completely fitted with a diagnosis of MFS, we sequenced *FBN1* cDNA derived from the proband's fibroblasts cultured with and without puromycin (Sigma–Aldrich, St. Louis, MO). The electropherogram from the amplicon containing exons 55–58 revealed a double-peak pattern starting from the exons 56–57 junction (Supplementary Figure 1.1), suggesting the presence of a pseudo-exon (Figure 1.1D). The insertion of a 90 bp pseudo-exon was confirmed by purification of the aberrant PCR fragment and Sanger sequencing of the cDNA sequence between exon 56 and 57. Sequencing of intron 56 identified a ENST00000316623:c.6872-961A>G mutation (NG 008805.2:g.221357A>G; Supplementary Figure 1.2). Splice-site predictions showed significantly increased 5' donor splice-site scores for the sequence surrounding the mutation (Alamut mutation interpretation software v2.3: SpliceSiteFinder-like 87.6 out of 100; MaxEntScan 8.6 out of 12; NNSPLICE 1 out of 1; Human Splicing Finder 87.7 out of 100; compared with zero for the wild-type sequence in each of the prediction programs). Segregation analysis confirmed that all affected family members were heterozygous for the mutation, whereas none of the unaffected family members carried the mutation. The mutation was not found in the 1000 Genomes Project [12] or the dbSNP database [13]. The insertion of the pseudo-exon between exons 56 and 57 introduced a premature
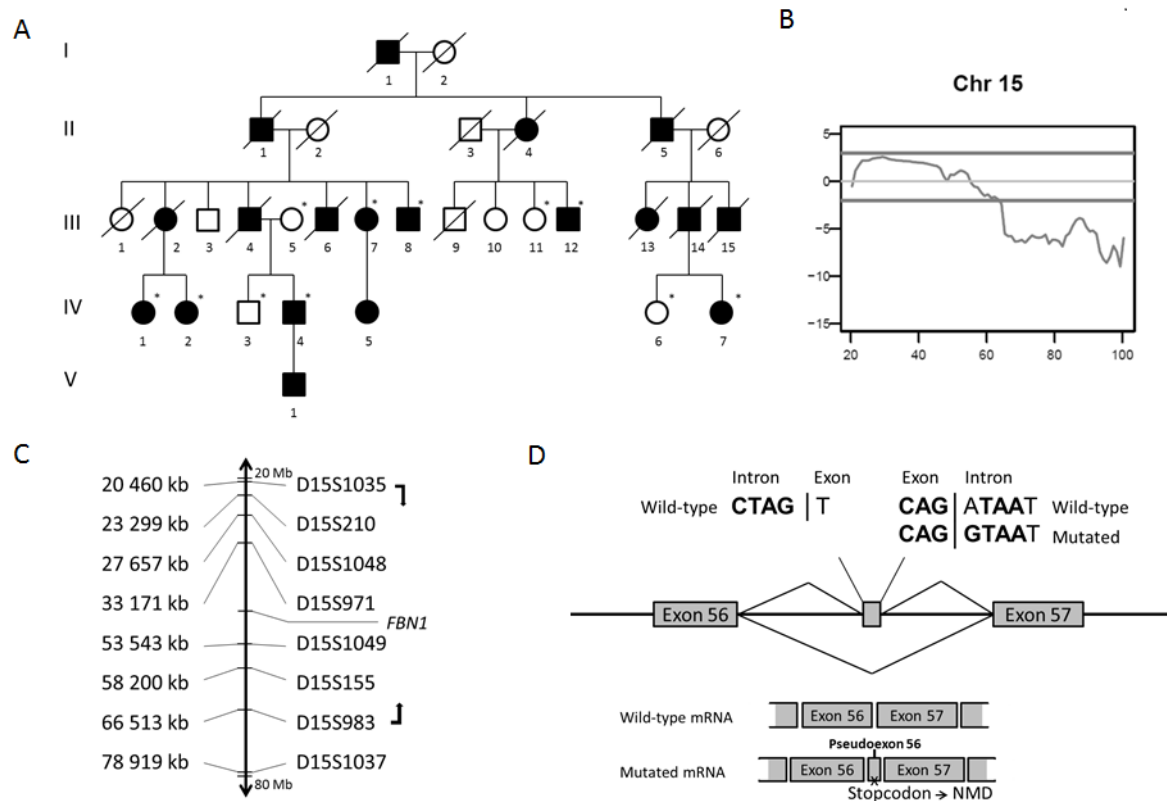
Figure 1.1: **A**: Pedigree of the family; asterisks indicate family members included in the linkage and segregation analyses. **B**: LOD scores on chromosome 15. The X-axis represents the genomic distance (in Mb). **C**: Microsatellite analysis delineates the linked region on chromosome 15. The position of *FBN1* is indicated. **D**: Introduction of the pseudo-exon between exons 56 and 57 caused by a deep intronic mutation. Both wild-type and mutated splice-site sequences are shown. NMD: nonsense-mediated mRNA decay.

stop codon. Comparison of cDNA derived from fibroblasts cultured in the presence or absence of puromycin confirmed that the mutated mRNA sequence was eliminated by nonsense-mediated mRNA decay (Supplementary Figure 1.1). The mutation was submitted to the Universal Mutation Database (www.umd.be/FBN1).

Subsequently, we performed a theoretical analysis of all donor and acceptor splice-site scores for all *FBN1* introns (*FBN1* transcript ENST00000316623) based on the Human Splicing Finder v2.4.1 (http://www.umd.be/HSF)[10]. The score of the 3' acceptor splice site of intron 56 was lower than the average score observed in *FBN1*. Besides intron 56, three additional introns had low-scoring splice sites (<76): introns 25, 37, and 63 (Supplementary Table 1.1). Next, we sequenced the

low-scoring introns with a maximum length of 2,000 bp (intron 25, 37, and 56; primer pairs described in Supplementary Table 1.2) in 25 additional *FBN1*-negative MFS patients, but we did not detect possible causal variants.

In general, known deep intronic mutations causing disorders are rare. Of course, a huge analytical bias exists and in reality deep intronic mutations may not be that uncommon. Indeed, deep intronic mutations are systematically missed when mutation analysis is restricted to exons and exon-intron boundaries. In a standard molecular diagnostic setting, only the 20-bp immediately adjacent to the exons is sequenced, whereas introns can span thousands of bases. For the deep intronic mutation described here, it was striking that *FBN1* intron 56 had a naturally occurring low-scoring splice acceptor site. This may suggest that the chance that deep intronic variants lead to the insertion of a pseudo-exon may be higher when the existing splice-site scores low. Based on that assumption, we performed an *FBN1* splice-site score analysis and screened unexplained MFS cases for selected (relatively small) introns (25, 37, and 56) adjacent to low-scoring splice sites, but we did not identify any additional deep intronic mutations. However, within the current report, we did not explore the possibility that even in introns with relatively high-scoring splice sites, pseudo-exons could be introduced.

Table 1.1: Clinical features of the presented family.

Ped Id	Current age or age of death	Surgery/major complication/cause of death	Last echocardiographic evaluation	Other
II:1	44 yrs[a]	Sudden death (no autopsy)		Severe pectus excavatum
II:4	74 yrs[a]	Cause of death unknown		Marfanoid skeletal features
II:5	49 yrs[a]	Sudden death (also had lung cancer)		Marfanoid skeletal features
III:2	51 yrs[a]	Underwent three surgeries (Ao valve and root, MVP, and TVP) prior to cardiac and respiratory failure		Pneumothorax Scoliosis
III:4	41 yrs[a]	40 yrs: acute type B dissection with ascending Ao replacement 41 yrs: Ao valve insufficiency, aneurysm arcus and descendens, died during surgery		
III:6	21 yrs[a]	Sudden death (no autopsy)		
III:7	59 yrs	46 yrs: type B dissection with intramural hematoma from left arteria. Subclavia to abdominal	59 yrs: Ao root 42 mm (stable for many years), MVP	Cataract with bilateral lens replacement
III:8[b]	52 yrs	21 yrs: Ao root (12 cm) and Ao ascendens: Bentall surgery 32 yrs: ascending surgery 41 yrs: arch surgery 42 yrs: descending aorta surgery		
III:9	48 yrs[a]	Sudden death (no autopsy)		
III:12	62 yrs	48 yrs: Bentall surgery 50 yrs: type B dissection		Pneumothorax Inguinal hernia Dural ectasia

Ped Id	Current age or age of death	Surgery/major complication/cause of death	Last echocardiographic evaluation	Other
III: 13	35 yrs[a]	Sudden death (no autopsy)		
III:14	30 yrs[a]	Sudden death (autopsy: aortic dissection)		
III:15	18 yrs[a]	Sudden death (no autopsy)		
IV:1	39 yrs		39 yrs: Ao root 39 mm and MVP, without insufficiency	Pneumothorax 14 yrs: Scoliosis surgery 29 yrs: fixation sternoclavicular dislocation
IV:2	37 yrs		37 yrs: Ao sinus 38 mm, MVP	22 yrs: spondylodesis Th5-S1 32 yrs: scoliosis surgery
IV:4	34 yrs	23 yrs: Ao ascendens replacement 32 yrs: valve sparing Ao root replacement (47 mm)		Asymmetric pectus Mild scoliosis
IV:5	33 yrs		32 yrs: Ao sinus 35 mm, MVP	10 yrs: scoliosis surgery (Th4-L5)
IV:7	28 yrs		28 yrs: Ao sinus 32 mm	
V:1	4 yrs		4 yrs: Ao sinus 19.8 mm (Z = 1.4)	Pectus excavatum

[a]Deceased. [b]Patient already reported [14]. Ped ID, pedigree ID; Ao, Aorta; MVP, mitral valve prolapse; Th, thoracic segment of spinal cord; TVP, tricuspid valve prolapse; L, lumbar segment of spinal cord; yrs, years.

1.5   Discussion

Splicing mutations account for up to 18.5% of *FBN1* mutations[15]. The most common are mutations affecting the wild-type splice sites, leading to exon skipping[16, 17]. Occasionally, activation of a cryptic splice site within the exon or intron, causing, respectively, a partial exon deletion[18] or a partial intron insertion or complete intron retention[17, 19], have been described. To the best of our knowledge, this is only the second identification of a pseudo-exon in *FBN1*. Guo et al.[20] identified a mutation creating a donor splice site in intron 64 leading to pseudo-exon retention. Other pseudo-exon mutations caused by activated donor or acceptor splice sites have been described in Duchenne and Becker muscular dystrophies[21, 22], neurofibromatosis type 1[23, 24], and cystic fibrosis[21, 25]. A study comparing authentic and cryptic 5' splice sites revealed that the differences in splice-site strength are not always that different and that these cryptic sites can be scattered throughout exons and introns[26]. Another possible cause of pseudo-exon insertions can be increased binding of splicing enhancer elements to a mutated recognition sequence. For example, a type of homocystinuria is caused by an intronic *MTRR* mutation that creates an exonic splicing enhancer sequence and activates SF2/ASF binding, thus introducing a pseudo-exon[27]. Interestingly, ESEfinder also predicted that our intronic *FBN1* mutation created a new binding site for SF2/ASF. As such, this might also contribute to the pathogenic mechanism in this family.

The noncoding genome becomes increasingly important. Our finding demonstrates again the necessity of the analysis of regions outside of the coding exons, which is currently not routinely done. With the increasing importance of whole-genome sequencing within the molecular diagnostic setting, this shortcoming will soon be overcome.

1.6 Supplementary material
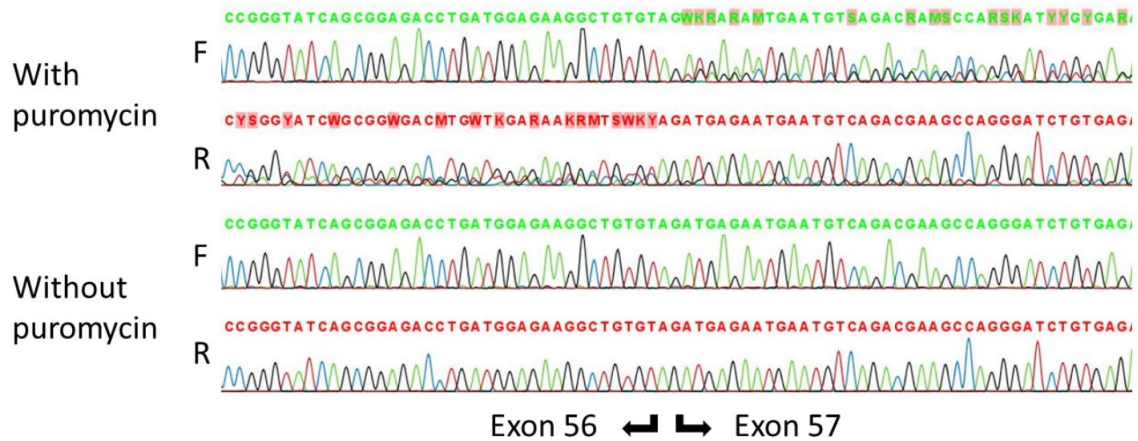
Supplementary Figure 1.1: Electropherogram of FBN1 cDNA ex55-58. A double peak pattern, only seen in the puromycin-treated FBN1 cDNA, starts on the exon 56-57 border. F: Forward strand; R: Reverse strand.
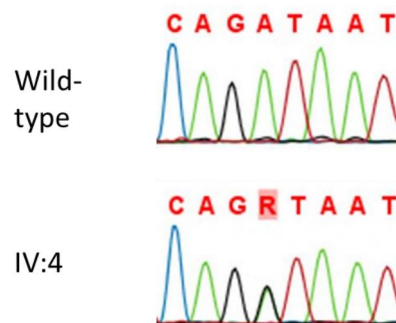
Supplementary Figure 1.2: Electropherogram of the deep intronic $NG\_008805.2 : g.221357A > G$ mutation. R denotes the nucleotides G or A. Due to the heterozygous nature of the mutation, both nucleotides are present in the patient at that position.

Supplementary Table 1.1: Splice site scores of reference splice sites in *FBN1*

	Splice site type	Motif	Consensus value (0-100)
Ex2	Donor	AGGgtaaag	80.09
Ex3	Acceptor	tttttgttttagAC	83.8
	Donor	TCCgtaagt	82.26
Ex4	Acceptor	gtttattcacagCC	86.71
	Donor	CCAgtaagt	84.67
Ex5	Acceptor	ttttttttcaagTA	83.86
	Donor	AACgtaagt	88.03
Ex6	Acceptor	cttattttacagCT	89.13
	Donor	GAGgtaatg	83.99
Ex7	Acceptor	ctttattttcagAT	91.28
	Donor	AAGgtaaac	84.71
Ex8	Acceptor	gtaatctgacagAT	81.85
	Donor	AAGgtaaga	96.71
Ex9	Acceptor	tttatattccagAT	89.82
	Donor	TAGgtaggt	89.68
Ex10	Acceptor	ctttgtcctcagAT	91.1
	Donor	CCGgtaaga	92.91
Ex11	Acceptor	gtgtttttctagAG	80.66
	Donor	CAAgtaaga	87.09
Ex12	Acceptor	atgttcttctagGG	84.02
	Donor	TTGgtacgt	84.46
Ex13	Acceptor	tgtgctttgcagAT	88.42
	Donor	GAGgtatgg	87.5
Ex14	Acceptor	ctttgattttagAC	80.66
	Donor	AAGgtaata	84.39
Ex15	Acceptor	ttgtattttcagAT	89.46
	Donor	AAGgttcgt	85.22
Ex16	Acceptor	tctctgccacagAC	88.31
	Donor	TTGgtaaga	90.93
Ex17	Acceptor	cttcctgtttagAC	81.34
	Donor	CAGgtatgt	91.2
Ex18	Acceptor	aatttattgcagCG	83.51
	Donor	GTGgtaagg	91.56
Ex19	Acceptor	tttgtggtgcagAT	86.43
	Donor	TTGgtgaga	89.77
Ex20	Acceptor	ttgactttgcagAT	88.88
	Donor	AAGgtaaac	84.71
Ex21	Acceptor	tttttgtttcagAC	91.48
	Donor	TAGgtattt	76.9

	Splice site type	Motif	Consensus value (0-100)
Ex22	Acceptor	cctcctctgcagAA	90.77
	Donor	TTGgtaaga	90.93
Ex23	Acceptor	tttttattacagAT	92.48
	Donor	AAGgtattt	77.92
Ex24	Acceptor	ttttctttttagAT	87.46
	Donor	TTGgtaaat	81.1
Ex25	Acceptor	tccctctgacagAT	87.69
	Donor	AAGgtacaa	75.74
Ex26	Acceptor	ttattcttgaagAT	82.4
	Donor	CAGgtcagt	94.98
Ex27	Acceptor	gtttttgtgcagAC	87.73
	Donor	TGGgtaagt	93.16
Ex28	Acceptor	tccattttgcagAT	88.79
	Donor	TCGgtaagg	91.34
Ex29	Acceptor	ttttcccgacagAC	91.85
	Donor	TTGgtaagt	93.27
Ex30	Acceptor	catttcttttagAC	81.25
	Donor	CCGgtgagt	94.09
Ex31	Acceptor	tattctttgcagAC	90.42
	Donor	TAGgtaagc	95.84
Ex32	Acceptor	tatgttttacagAT	87.62
	Donor	CAGgtgtgt	90.04
Ex33	Acceptor	tcatttttccagAC	89.3
	Donor	CTGgtgagt	94.09
Ex34	Acceptor	tttttctataagAT	82
	Donor	CAGgtatgt	91.2
Ex35	Acceptor	ttctggctgtagAC	81.85
	Donor	AAGgtaact	87.03
Ex36	Acceptor	cctccccccaagAT	82.3
	Donor	CAGgtaaga	97.66
Ex37	Acceptor	gttcggttttagAT	78.37
	Donor	TTGgtaaga	90.93
Ex38	Acceptor	tatggtaaatagAT	71.69
	Donor	CATgtaagt	89.13
Ex39	Acceptor	ttgtttcaatagCC	79.09
	Donor	AAGgtaatt	86.73
Ex40	Acceptor	tgattttgatagAT	76.47
	Donor	ATGgtaaat	82.13
Ex41	Acceptor	tttggattatagAT	79.77
	Donor	TGGgtaagt	93.16

	Splice site type	Motif	Consensus value (0-100)
Ex42	Acceptor	cctcccttctagAT	84.25
	Donor	CAGgtgagt	98.84
Ex43	Acceptor	taatcattgcagAT	85.91
	Donor	TTGgtgagt	92.11
Ex44	Acceptor	ctctgtctctagAT	84.27
	Donor	AAGgtaagt	99.05
Ex45	Acceptor	ttctgctcgtagAT	83.77
	Donor	ATGgtatgt	85.49
Ex46	Acceptor	tcttatttacagAT	90.79
	Donor	TGGgtaagt	93.16
Ex47	Acceptor	tcttcctactagAC	82.29
	Donor	TAGgtgcgt	88.06
Ex48	Acceptor	atttttctgcagAT	91.87
	Donor	TGGgtaagt	93.16
Ex49	Acceptor	ttttctttgcagAT	95.18
	Donor	AAGgtagga	88.37
Ex50	Acceptor	tgattcttttagAT	80.41
	Donor	AAGgtaagt	99.05
Ex51	Acceptor	tttatgctgcagAT	89.8
	Donor	ATGgtatgt	85.49
Ex52	Acceptor	tctccaccacagAG	89.22
	Donor	TTGgtcagt	88.24
Ex53	Acceptor	ctcttgcttaagAT	81.63
	Donor	TAGgtgagt	96.86
Ex54	Acceptor	ggtttcttgcagAT	88.16
	Donor	AAGgtacat	78.08
Ex55	Acceptor	cctctgctgcagAT	88.73
	Donor	AAGgtgagt	97.89
Ex56	Acceptor	catttttttacagAT	89.46
	Donor	TAGgtaaga	95.68
Ex57	Acceptor	aaaatcaaacagAT	75.05
	Donor	TTGgtgagt	92.11
Ex58	Acceptor	tgtcccttccagAC	90.53
	Donor	CAGgtactt	78.88
Ex59	Acceptor	gttaaattacagAT	84.11
	Donor	TAGgtaagt	98.02
Ex60	Acceptor	ctttgatcatagAT	80.72
	Donor	AAGgtaaag	84.95
Ex61	Acceptor	attttcttgtagAT	83.95
	Donor	TTGgtgagt	92.11

	Splice site type	Motif	Consensus value (0-100)
Ex62	Acceptor	tgcttctcatagAT	82.11
	Donor	AAGgtgggt	89.55
Ex63	Acceptor	cttcttttcagAC	91.24
	Donor	TTGgcaagt	66.43
Ex64	Acceptor	ttttgcctgcagAT	93.71
	Donor	AGGgtaagc	92.02
Ex65	Acceptor	cttctgctgcagGC	92.86
	Donor	GAGgtgggt	88.74
Ex66	Acceptor	gtgtctttccagGA	91.92

Supplementary Table 1.2: List of *FBN1* cDNA and genomic DNA primers

Primer name	Sense primer	Antisense primer
FBN1 cDNA ex1-5	5'-GCCGAGCAGTGGCTGTAG-3'	5'-TGAGTCCCTATGTATCCTTTCTGG-3'
FBN1 cDNA ex4-9	5'-TCAGATAGCTCCTTCCTGTGG-3'	5'-AGTATCCTGGGCGAACATCTAT-3'
FBN1 cDNA ex8-13	5'-CCTGCTGGACACAAACTTAATG-3'	5'-CCCTGGTTGTTAATACACTCACC-3'
FBN1 cDNA ex12-18	5'-CCGGTGTGAGTGCAACAA-3'	5'-GTCATTCCTGGCCCACTG-3'
FBN1 cDNA ex17-22	5'-CACACATGCGGAGCACAT-3'	5'-GGAGCAGCACTGGGACTTTA-3'
FBN1 cDNA ex21-27	5'-GCCCAGGCTCTTTTATTTGTG-3'	5'-TGCCACAGAGGTCAGGAGAT-3'
FBN1 cDNA ex26-31	5'-ATGATACCCAGCCTCTGCAC-3'	5'-TGCACTGACCACCATCACA-3'
FBN1 cDNA ex30-36	5'-AGCCGGGATTTGCACTAA-3'	5'-GGAAGGGAGCACTCATCAAT-3'
FBN1 cDNA ex35-41	5'-TGCACCAGGAGGATACCG-3'	5'-TTGCATGTAGTCTGGAGGACAG-3'
FBN1 cDNA ex40-46	5'-CCAACCGGCTACTACCTGAA-3'	5'-CACTGCCCATGACTGCATA-3'
FBN1 cDNA ex45-50	5'-CTACCGCTTCACCTCCACA-3'	5'-GGAAAACCCTTCTGGACACA-3'
FBN1 cDNA ex49-55	5'-TCAAAACTTGGATGGGTCCT-3'	5'-CAGAGGATTCTGGGCACATT-3'
FBN1 cDNA ex54-59	5'-GGAAATGGAACCTGCAAGAA-3'	5'-TCGGCAAACATCGTGAATAA-3'
FBN1 cDNA ex58-63	5'-AAATCGGAATGCTGCTGTG-3'	5'-TGGTAGTGCTGGAGGTAGCC-3'
FBN1 cDNA ex62-66	5'-GAAGACGTGGACGAGTGTGA-3'	5'-CCTTGTTACTGACGTGGGAAAT-3'
FBN1 cDNA ex65-66	5'-ACTCTCCCCAGAGGCTTGTT-3'	5'-TCACCTGTACCTTGCTTTGGT-3'
FBN1 DNA Intron 25-1	5'-TGCACCCTGCCTATTGCT-3'	5'-CCAAAACAAGACCAAACACTCA-3'
FBN1 DNA Intron 25-2	5'-GGACTTGGTGTTCTGGAGATTT-3'	5'-CAAGCAGTCAGGAGGTCTCA-3'
FBN1 DNA Intron 25-3	5'-TTGAAAGGCTAGAAATGTTTACAAAGT-3'	5'-AACAGCAAGTGGCAGCAAAT-3'
FBN1 DNA Intron 25-4*	5'-CCTTGATGACAGAGCAGATCC-3'	5'-GGATCTGCTCTGTCATCAAGG-3'
FBN1 DNA Intron 37	5'-TGGCTCAGGTGATAACTCCA-3'	5'GGGAATAAGGTCCCCTCTACA-3'
FBN1 DNA Intron 56-1	5'-TGAAAAACAAATGGAATGCAAG-3'	5'-TGCCAACTCCTGGTCTAAGG-3'
FBN1 DNA Intron 56-2	5'-TGGGATCTACCTCCAGAAAATC-3'	5'-GTTCAAAACCCCAATGCAA-3'

*Internal primers.

Primer name	Sense primer	Antisense primer
FBN1 DNA Intron 56-3	5'-CAAAAAGTTTCCTGACCTCTGC-3'	5'-TTGATCTGGGGGAGTTTGTC-3'
FBN1 DNA Intron 56-4	5'-CTGTTCTGGATTCACCTTCCA-3'	5'-AGACACCAAACTCCCCTCCT-3'
FBN1 DNA Intron 56-5	5'-CACTTGAAATAACACTTTGAGAGTCC-3'	5'-TGTAGCTCCCACGGGTGT-3'
FBN cDNA pseudo-exon	5'-ACCTGATGGAGAAGGCTGTG-3'	5'-AGATCCCTGGCTTCGTCTG-3'

*Internal primers.

References

1. Bolar, N., Van Laer, L. & Loeys, B. L. Marfan syndrome: from gene to therapy. *Curr Opin Pediatr* **24,** 498–504. ISSN: 1531-698X (Aug. 2012).

2. Isogai, Z. *et al.* Latent transforming growth factor beta-binding protein 1 interacts with fibrillin and is a microfibril-associated protein. *J Biol Chem* **278,** 2750–7. ISSN: 0021-9258 (Jan. 2003).

3. Neptune, E. R. *et al.* Dysregulation of TGF-beta activation contributes to pathogenesis in Marfan syndrome. *Nat Genet* **33,** 407–11. ISSN: 1061-4036 (Mar. 2003).

4. Chaudhry, S. S. *et al.* Fibrillin-1 regulates the bioavailability of TGFbeta1. *J Cell Biol* **176,** 355–67. ISSN: 0021-9525 (Jan. 2007).

5. Dietz, H. C. *et al.* Marfan syndrome caused by a recurrent de novo missense mutation in the fibrillin gene. *Nature* **352,** 337–9. ISSN: 0028-0836 (July 1991).

6. Collod-Béroud, G. *et al.* Update of the UMD-FBN1 mutation database and creation of an FBN1 polymorphism database. *Hum Mutat* **22,** 199–208. ISSN: 1098-1004 (Sept. 2003).

7. Loeys, B. *et al.* Comprehensive molecular screening of the FBN1 gene favors locus homogeneity of classical Marfan syndrome. *Hum Mutat* **24,** 140–6. ISSN: 1098-1004 (Aug. 2004).

8. Baetens, M. *et al.* Applying massive parallel sequencing to molecular diagnosis of Marfan and Loeys-Dietz syndromes. *Hum Genet* **32,** 1053–1062. ISSN: 1098-1004 (May 2011).

9. Abecasis, G. R., Cherny, S. S., Cookson, W. O. & Cardon, L. R. Merlin–rapid analysis of dense genetic maps using sparse gene flow trees. *Nat Genet* **30,** 97–101. ISSN: 1061-4036 (Jan. 2002).

10. Desmet, F.-O. *et al.* Human Splicing Finder: an online bioinformatics tool to predict splicing signals. *Nucleic acids research* **37,** e67. ISSN: 1362-4962 (May 2009).

11. Loeys, B. L. *et al.* The revised Ghent nosology for the Marfan syndrome. *J Med Genet* **47,** 476–85. ISSN: 1468-6244 (July 2010).

12. Abecasis, G. R. *et al.* An integrated map of genetic variation from 1,092 human genomes. *Nature* **491,** 56–65. ISSN: 1476-4687 (Nov. 2012).

13. Sherry, S. T. *et al.* dbSNP: the NCBI database of genetic variation. *Nucleic Acids Res* **29,** 308–11. ISSN: 1362-4962 (Jan. 2001).

14. Janssen, J. H. P., Leiner, T. & Cheriex, E. C. Bilobar apical pseudoaneurysm after left ventricular venting in a Marfan's patient. *European journal of echocardiography : the journal of the Working Group on Echocardiography of the European Society of Cardiology* **10,** 154–5. ISSN: 1532-2114 (Jan. 2009).

15. Howarth, R., Yearwood, C. & Harvey, J. F. Application of dHPLC for mutation detection of the fibrillin-1 gene for the diagnosis of Marfan syndrome in a National Health Service Laboratory. *Genetic testing* **11,** 146–52. ISSN: 1090-6576 (Jan. 2007).

16. Nijbroek, G. *et al.* Fifteen novel FBN1 mutations causing Marfan syndrome detected by heteroduplex analysis of genomic amplicons. *American journal of human genetics* **57,** 8–21. ISSN: 0002-9297 (July 1995).

17. Hutchinson, S., Wordsworth, B. P. & Handford, P. A. Marfan syndrome caused by a mutation in FBN1 that gives rise to cryptic splicing and a 33 nucleotide insertion in the coding sequence. *Human genetics* **109,** 416–20. ISSN: 0340-6717 (Oct. 2001).

18. McGrory, J. & Cole, W. G. Alternative splicing of exon 37 of FBN1 deletes part of an 'eight-cysteine' domain resulting in the Marfan syndrome. *Clinical Genetics* **55,** 118–121. ISSN: 0009-9163 (Feb. 1999).

19. Chao, S.-C. *et al.* Novel exon nucleotide substitution at the splice junction causes a neonatal Marfan syndrome. *Clinical genetics* **77,** 453–63. ISSN: 1399-0004 (May 2010).

20. Guo, D.-c. *et al.* An FBN1 pseudoexon mutation in a patient with Marfan syndrome: confirmation of cryptic mutations leading to disease. *Journal of human genetics* **53,** 1007–11. ISSN: 1434-5161 (Jan. 2008).

21. Tuffery-Giraud, S., Saquet, C., Chambert, S. & Claustres, M. Pseudoexon activation in the DMD gene as a novel mechanism for Becker muscular dystrophy. *Human mutation* **21,** 608–14. ISSN: 1098-1004 (June 2003).

22. Gurvich, O. L. *et al.* DMD pseudoexon mutations: splicing efficiency, phenotype, and potential therapy. *Annals of neurology* **63,** 81–9. ISSN: 1531-8249 (Jan. 2008).

23. Perrin, G., Morris, M. A., Antonarakis, S. E., Boltshauser, E. & Hutter, P. Two novel mutations affecting mRNA splicing of the neurofibromatosis type 1 (NF1) gene. *Human mutation* **7,** 172–5. ISSN: 1059-7794 (Jan. 1996).

24. Raponi, M., Upadhyaya, M. & Baralle, D. Functional splicing assay shows a pathogenic intronic mutation in neurofibromatosis type 1 (NF1) due to intronic sequence exonization. *Human mutation* **27,** 294–5. ISSN: 1098-1004 (Mar. 2006).

25. Ikezawa, M., Nishino, I., Goto, Y., Miike, T. & Nonaka, I. Newly recognized exons induced by a splicing abnormality from an intronic mutation of the dystrophin gene resulting in Duchenne muscular dystrophy. Mutations in brief no. 213. Online. *Hum Mutat* **13,** 170 (1999).

26. Roca, X., Sachidanandam, R. & Krainer, A. R. Intrinsic differences between authentic and cryptic 5' splice sites. *Nucleic acids research* **31,** 6321–33. ISSN: 1362-4962 (Nov. 2003).

27. Homolova, K. *et al.* The deep intronic c.903+469T¿C mutation in the MTRR gene creates an SF2/ASF binding exonic splicing enhancer, which leads to pseudoexon activation and causes the cblE type of homocystinuria. *Hum Mutat* **31,** 437–44. ISSN: 1098-1004 (Apr. 2010).

Chapter 2

Mutations in a TGF-β Ligand, *TGFB3*, Cause Syndromic Aortic Aneurysms and Dissections

Aida M. Bertoli-Avella[1,2,3], Elisabeth Gillis[2], Hiroko Morisaki[4], Judith M.A. Verhagen[1], Bianca M. de Graaf[1], Gerarda van de Beek[2], Elena Gallo[5], Boudewijn P.T. Kruithof[6], Hanka Venselaar[7,8], Loretha A. Myers[5], Steven Laga[9], Alexander J. Doyle[5,10,11], Gretchen Oswald[5,10], Gert W.A. van Cappellen[12,13], Itaru Yamanaka[14], Robert M. van der Helm[1], Berna Beverloo[1], Annelies de Klein[1], Luba Pardo[15], Martin Lammens[16], Christina Evers[17], Koenraad Devriendt[18], Michiel Dumoulein[19], Janneke Timmermans[20], Hennie T. Bruggenwirth[1], Frans Verheijen[1], Inez Rodrigus[9], Gareth Baynam[21,22], Marlies Kempers[23], Johan Saenen[24], Emeline M. Van Craenenbroeck[24], Kenji Minatoya[25], Ritsu Matsukawa[26], Takuro Tsukube[26], Noriaki Kubo[26], Robert Hofstra[1], Marie Jose Goumans[6], Jos A. Bekkers[27], Jolien W. Roos-Hesselink[3], Ingrid M.B.H. van de Laar[1], Harry C. Dietz[5,10,28], Lut Van Laer[2], Takayuki Morisaki[4,29], Marja W. Wessels[1], Bart L. Loeys[2,23]

1 Department of Clinical Genetics, Erasmus University Medical Center, Rotterdam, the Netherlands
2 Center of Medical Genetics, Faculty of Medicine and Health Sciences, University of Antwerp and Antwerp University Hospital, Antwerp, Belgium
3 Department of Cardiology, Erasmus University Medical Center, Rotterdam, the Netherlands
4 Departments of Bioscience and Genetics, and Medical Genetics, National Cerebral and Cardiovascular Center, Suita, Osaka, Japan

5 McKusick-Nathans Institute of Genetic Medicine, Johns Hopkins University School of Medicine, Baltimore, Maryland

6 Department of Molecular Cell Biology, Leiden University Medical Center, Leiden, the Netherlands

7 Nijmegen Center for Molecular Life Sciences (NCMLS), Radboud University Nijmegen Medical Center, Nijmegen, the Netherland

8 Center for Molecular and Biomolecular Informatics (CMBI), Nijmegen, the Netherlands

9 Department of Cardiac Surgery, Antwerp University Hospital, Antwerp, Belgium

10 Howard Hughes Medical Institute, Baltimore, Maryland

11 William Harvey Research Institute, Queen Mary University of London, London, United Kingdom

12 Erasmus Optical Imaging Centre, Erasmus University Medical Center, Rotterdam, the Netherlands

13 Department of Pathology, Erasmus University Medical Center, Rotterdam, the Netherlands

14 Department of Bioscience and Genetics, National Cerebral and Cardiovascular Center, Suita, Osaka, Japan

15 Department of Dermatology, Erasmus University Medical Center, Rotterdam, the Netherlands

16 Department of Pathology, Antwerp University Hospital, University of Antwerp, Antwerp, Belgium

15 Institute of Human Genetics, Heidelberg University, Heidelberg, Germany

18 Center for Human Genetics, Leuven, Belgium

19 Department of Cardiology, AZ Groeninge Kortrijk, Kortrijk, Belgium

20 Department of Cardiology, Radboud University Medical Centre, Nijmegen, the Netherlands

21 Genetic Services of Western Australia, Subiaco, Western Australia, Australia

22 School of Paediatrics and Child Health, The University of Western Australia, Crawley, Western Australia, Australia

23 Department of Human Genetics, Radboud University Medical Centre, Nijmegen, the Netherlands

24 Department of Cardiology, University Hospital Antwerp, Antwerp, Belgium

25 Department of Cardiovascular Surgery, National Cerebral and Cardiovascular Center, Suita, Osaka, Japan

26 Department of Cardiovascular Surgery, Japanese Red Cross Kobe Hospital, Kobe, Japan

27 Department of Pediatrics, Urakawa Red Cross Hospital, Urakawa, Hokkaido, Japan

28 Department of Cardio-Thoracic Surgery, Erasmus University Medical Center, Rotterdam, the Netherlands

28 Department of Pediatrics, Division of Pediatric Cardiology, Johns Hopkins University School of Medicine, Baltimore, Maryland

29 Department of Molecular Pathophysiology, Pathophysiology, Osaka University Graduate School of Pharmaceutical Sciences, Suita, Osaka, Japan

Contribution: Sequencing and mutation analysis

2.1   Abstract

Aneurysms affecting the aorta are a common condition associated with high mortality as a result of aortic dissection or rupture. Investigations of the pathogenic mechanisms involved in syndromic types of thoracic aortic aneurysms, such as Marfan and Loeys-Dietz syndromes, have revealed an important contribution of disturbed transforming growth factor TGF-β signaling. This study sought to discover a novel gene causing syndromic aortic aneurysms in order to unravel the underlying pathogenesis. We combined genome-wide linkage analysis, exome sequencing, and candidate gene Sanger sequencing in a total of 470 index cases with thoracic aortic aneurysms. Extensive cardiological examination, including physical examination, electrocardiography, and transthoracic echocardiography was performed. In adults, imaging of the entire aorta using computed tomography or magnetic resonance imaging was done. Here, we report on 43 patients from 11 families with syndromic presentations of aortic aneurysms caused by *TGFB3* mutations. We demonstrate that *TGFB3* mutations are associated with significant cardiovascular involvement, including thoracic/abdominal aortic aneurysm and dissection, and mitral valve disease. Other systemic features overlap clinically with Loeys-Dietz, Shprintzen-Goldberg, and Marfan syndromes, including cleft palate, bifid uvula, skeletal overgrowth, cervical spine instability and clubfoot deformity. In line with previous observations in aortic wall tissues of patients with mutations in effectors of TGF-β signaling (TGFBR1/2, SMAD3, and TGFB2), we confirm a paradoxical up-regulation of both canonical and noncanonical TGF-β signaling in association with up-regulation of the expression of TGF-β ligands. Our findings emphasize the broad clinical variability associated with *TGFB3* mutations and highlight the importance of early recognition of the disease because of high cardiovascular risk.
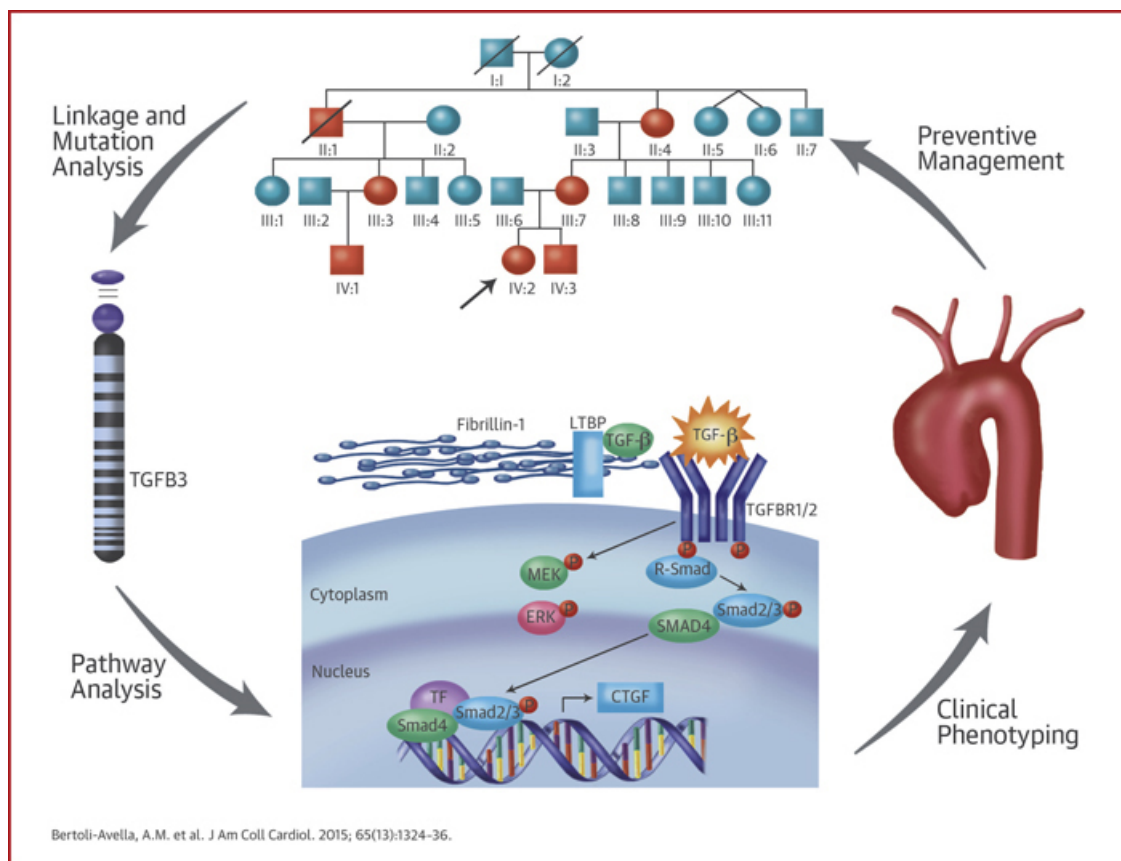
Figure 2.1: The Pathway From Patient to Gene and Back. The figure summarizes how initial identification of patients and families, followed by linkage and mutation analysis led to the discovery of *TGFB3* mutations. Further exploration of the TGF-β pathway allowed a better phenotypical delineation and characterization that will have implications in personalized clinical management.

2.2 Introduction

The transforming growth factor TGF-β pathway plays an important role in many medically relevant processes, including immunologic maturity, inflammation, cancer and fibrosis, as well as skeletal, vascular and hematopoietic homeostasis[1]. With the discovery of dysregulated TGF-β signaling in *Fbn1* knockout mice, the TGF-β pathway was revealed as a key player in the pathogenesis of thoracic aortic aneurysm development in Marfan syndrome (MFS; [Mendelian Inheritance in Man (MIM) 154700])[2, 3]. MFS is a multisystemic disease characterized by cardiovascular, ocular, and skeletal features caused by mutations in the *FBN1*

gene[4]. More recently, we and others identified pathogenic mutations in the genes encoding the TGF-β receptor (TGFBR) subunits TGFBR1 and TGFBR2[5, 6], the signaling transducer SMAD3[7], the ligand TGFB2[8, 9], and the inhibitor SKI [10], occurring predominantly in patients with syndromic presentations of thoracic aortic aneurysms and dissections (TAAD), designated Loeys-Dietz syndrome (LDS1 [MIM 609192][11]; LDS2 [MIM 610168][11]; LDS3 [MIM 613795] [also known as aneurysms-osteoarthritis syndrome] [7, 12, 13],LDS4[MIM614816] [8], and Shprintzen-Goldberg syndrome (SGS [MIM82212]) [10, 14]. The finding of human mutations in a ligand, receptors, a signaling transducer, and an inhibitor of the TGF-β pathway confirms the essential role of TGF-β signaling in aortic aneurysm development.

Recently, de novo mutations in the gene encoding the TGFB3 ligand (*TGFB3*) were reported in two girls exhibiting a syndrome affecting body growth (either short or tall stature) accompanied by skeletal features reminiscentof MFS or LDS, but without significant vascular involvement[15–17]. Here, we report that *TGFB3* mutations cause a syndromic form of aortic aneurysms and dissections, characterized by cardiovascular, craniofacial, cutaneous, and skeletal anomalies that significantly overlap with other TGF-β vasculopathies, particularly those within the LDS clinical spectrum.
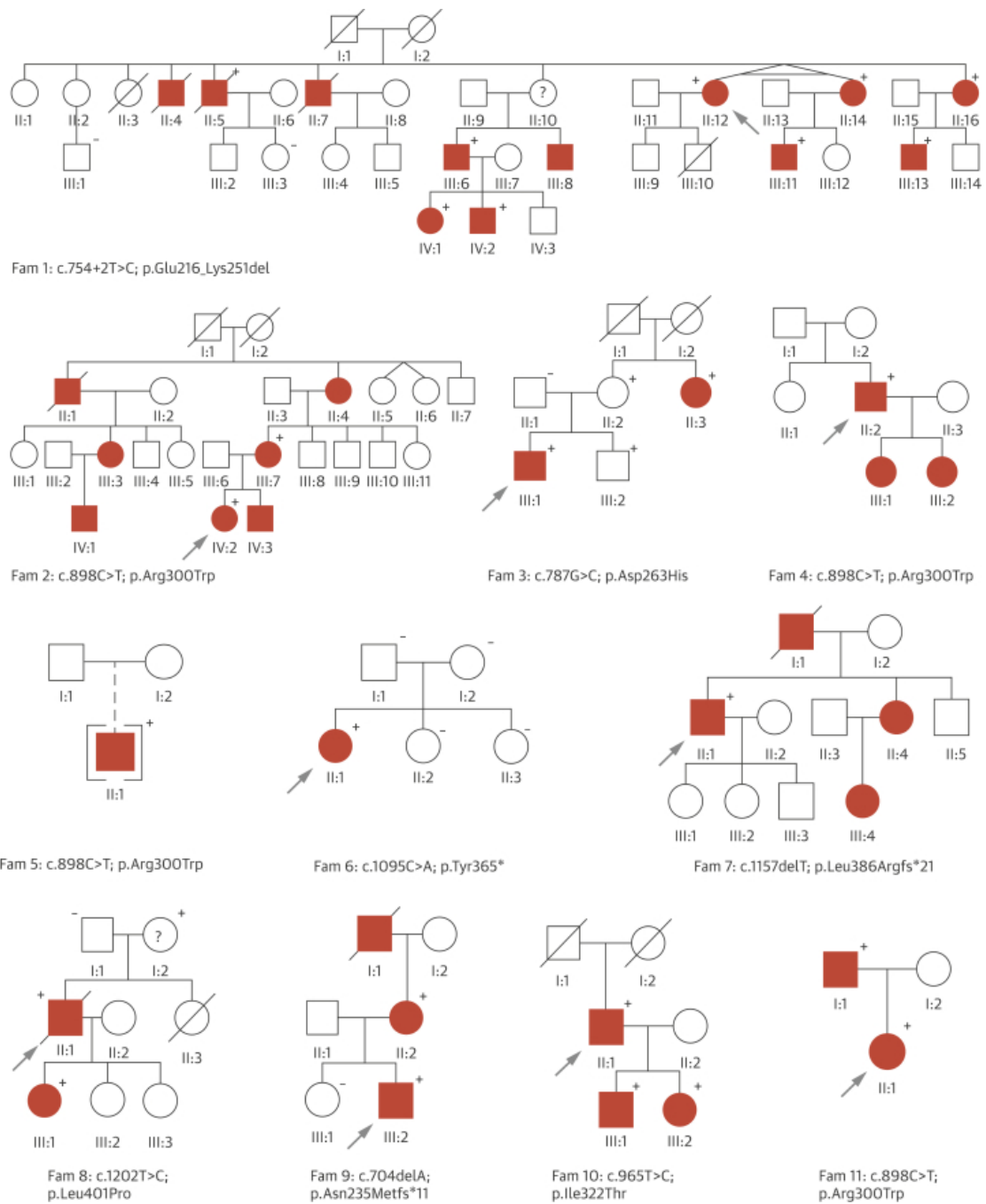
Figure 2.2: The causal *TGFB3* mutation is shown for each family. Probands are indicated with an arrow. Circle: female; square: male; open symbol: unaffected; solid symbol: affected; diagonal line: deceased; brackets: adopted; question mark: clinical affection status unknown. Plus and minus signs indicate presence or absence of a *TGFB3* mutation, respectively.

2.3 Methods

2.3.1 Patients

All patients or relatives provided written informed consent for participation in this study and, if applicable, publication of photographs. Family 1 was investigated by the department of Clinical Genetics (Erasmus University Medical Center, Rotterdam, the Netherlands) and Center for Medical Genetics (Antwerp University Hospital/University of Antwerp, Belgium) after previous surgical interventions. Clinical geneticists (M.W.W., B.L.L.) examined family members, with special attention to skeletal, joint, skin, and craniofacial features. Medical records from deceased patients were obtained for review. Extensive cardiological examination, including physical examination, electrocardiography, and transthoracic echocardiography, was performed. In adults, imaging of the entire aorta using computed tomography or magnetic resonance imaging was performed. Measurements of the aortic diameter were obtained at the level of the aortic annulus, sinuses of Valsalva, sinotubular junction, proximal ascending aorta, aortic arch, descending aorta, and suprarenal and infrarenal abdominal aorta. An aneurysm was defined as an arterial diameter >1.96 SDs (standard deviation) above the predicted diameter[18, 19]. Probands from families 2 through 8 and 9 through 11 were referred for molecular and/or clinical evaluation to Antwerp (Belgium) or Osaka (Japan), respectively.

Screening of the entire coding region of *TGFB3* was performed in 470 additional probands (120 probands had whole-exome sequencing), presenting both with syndromic and nonsyndromic forms of TAAD. The majority of these patients had been screened previously for all known TAAD genes. Family members of mutation-positive patients were ascertained and submitted to clinical investigations.

2.3.2 Genotyping and linkage analysis

Genomic DNA was extracted from peripheral blood samples (Gentra Systems, Qiagen, Hilden, Germany). RNA from two patients (Family 1; II:12 and III:11) (Figure 2.2) was extracted from peripheral blood (collected in PAXgene tubes,

PreAnalyliX, Qiagen) according to the manufacturer's protocol (PreAnalyliX, Qiagen).

Genome-wide genotyping was conducted using DNA from six family members (Figure 2.2, family 1) with Illumina Human SNP-Cyto12 Arrays (Illumina, San Diego, California), containing >262,000 genomic markers, as recommended by the manufacturer. The statistical package, easyLINKAGE Plus v5.08[20], Merlin v1.0.1 software (Abecasis Lab, University of Michigan), was used to perform single-point and multipoint parametric linkage analysis as previously described[21, 22]. Logarithm of odds scores were obtained using a dominant model of inheritance, with 90% penetrance and disease allele frequency of 1:1000. Allele frequencies of genotyped single nucleotide polymorphisms (SNPs) were set to codominant, and spacing of 0.25 Mb to 0.15 Mb between SNPs was used. Haplotype blocks containing 100 SNPs were constructed with Merlin (option BEST) and they were visualized using HaploPainter (v1.042, H. Thiele, University of Cologne, Germany).

2.3.3 Sequencing and mutation analysis

Exome sequencing was performed for 120 patients after TruSeq Exome enrichment on HiSeq (Illumina). In 350 other probands, bidirectional Sanger sequencing of exons and exon–intron boundaries was undertaken using polymerase chain reaction primers designed by Primer3 software (v.4.0.0, S. Rozen, Howard Hughes Medical Institute and the National Institutes of Health, National Human Genome Research Institute) (Supplementary Table 2.1). Polymerase chain reaction products were purified and sequenced using BigDye Terminator chemistry v3.1 on an ABI Prism3130xl (Applied Biosystems, Foster City, California). Sequences were aligned (SeqScape v2.5 software, Applied Biosystems) and compared with consensus sequences obtained from the human genome databases (Ensembl and NCBI). For annotation of DNA and protein changes, the Mutation Nomenclature guidelines from the Human Genome Variation Society were followed[23]. To describe mutations at the cDNA level, the A from the ATG start codon of the reference sequences is numbered as 1 (mRNA NM_003239.2 and protein NP_003230.1).

2.3.4   In silico analysis of novel variants

The effects of the mutations on protein structure and function were predicted using SIFT BLink (v.5.2.2) and Mutation Taster2. Population frequencies in controls were obtained from dbSNP, Exome Variant Server (EVS)[24], 1000Genomes[25], and Genome of the Netherlands[26]. To assess the putative effects on splicing, the Splice Site Prediction by Neural Network[27], the Net-Gene2[28] and Alamut Software Suite were used. Protein IDs used for conservation were gij148342461 (ABQ59024.1), gij135685 (P17125.1), gij18266825 (P16047.2), gij135682 (P17247.1), gij52138563 (NP_919367.2), gij410898023 (XP_003962498.1), gij351050916 (CCD74236.1), (NP_477340.1), gij135674 (P01137.2), and gij48429157 (P61812.1).

2.3.5   Homology modeling

A homology model was built using the experimentally solved structure of TGFB1 (PDB file [29] 3rjr, 60% identity) as a template. The model was built using an automatic YASARA script[30] with standard parameters. The model contains contains a homodimer of residues 14 to 412.

2.3.6   Immunohistochemistry

The protocol for staining of formalin-fixed, paraffin-embedded sections was adapted from Baschong et al.[31] with modifications (Detailed Methods, see supplements in 2.7). Slides were stained overnight at 4°C with anti-pSmad2 antibody (clone A5S, 1:100, Millipore, Billerica, Massachusetts) and anti-pERK1/2 (cloneD13.14.4E, 1:100, CellSignaling Technology, Danvers, Massachusetts) in 0.1% Triton/TBS buffer, washed 3 x 10 mininPerm/Staining buffer, and then stained with anti-rabbit Alexa594 (Molecular Probes, Life Technologies, Carlsbad, California) at 1:200 for 1 h at RT. Slides were then washed 3 x 10 min in Perm/Staining buffer and mounted with Hard Set VECTASHIELD Mounting Media (Vector Laboratories, Burlingame, California) with 2-(4-amidinophenyl)-1H-indole-6-carboxamidine (DAPI). Images were acquired on a Zeiss Axio-Examiner (Carl Zeiss, Oberkochen, Germany) with 710NLO-Meta multiphoton confocal microscope at 25x magnification.

2.3.7   In situ RNA with ACD RNAscope probes

The ACD RNAscope probe Hs-TGFB1 probe (Advanced Cell Diagnostics [ACD], Hayward, California) was used to detect human *TGFB1* transcript in conjunction with the RNAscope2.0 HD ReagentKit (RED) from ACD (Detailed Methods, see Supplements in 2.7).

2.3.8   Histology

Slides were histologically examined after hematoxylin-eosin, Elastica van Gieson (elastin), Alcian blue (proteoglycans), or Masson's trichrome (collagen) staining using standard techniques.

2.4   Results

We studied a large Dutch family (family 1) with clinical features overlapping with MFS and LDS consistent with an autosomal dominant inheritance pattern. Seven family members, between 40 and 68 years of age, presented with aneurysms and dissections, mainly involving the descending thoracic and abdominal aorta (Figure 2.2, Supplementary Table 2.2). Three patients died from aortic dissection and rupture of the descending thoracic or abdominal aorta (1-II:4, II:5, and II:7) (Figure 2.2), confirmed by autopsy in 2 cases (1-II:4, age 57 years and II:5, 56 years). In addition, 4 members had mitral valve abnormalities, ranging from mild prolapse to severe regurgitation requiring surgical intervention. Craniofacial abnormalities were rather subtle, including a long face, high-arched palate, and retrognathia (Figure 2.3). Pectus deformity and scoliosis were frequently observed (Figure 2.3). Other recurrent findings included velvety skin, varices, and hiatal hernia. Several family members presented with autoimmune features including (HLA-B27 positive) spondyloarthritis, Graves' disease, and celiac disease.

Figure 2.3: Phenotypic characteristics of patients with a *TGFB3* mutation observed. Observed clinical features include: long face (1-III:11, 5-II:1, 7-II:1, 8-II:1); pectus carinatum (1-IV:2); hypertelorism (2-III:7, 2-IV:2, 2-IV:3, 7-II:1, 8-II:1); bifid uvula (2-III:7, 2-IV:3, 7-II:1); joint hypermobility (2-IV:2); arachnodactyly (5-II:1); and metatarsus adductus (8-III:1). All affected individuals or parents gave permission to publish these photographs.

Sequencing of all known TAAD genes (*ACTA2*, *COL3A1*, *EFEMP2*, *FBN1*, *FLNA*, *MYH11*, *MYLK*, *NOTCH1*, *PRKG1*, *SKI*, *SLC2A10*, *SMAD3*, *TGFB2*, *TGFBR1*, *TGFBR2*) failed to identify a causal mutation. Linkage analysis using SNP genotypes from 6 patients of the family identified 2 large genomic regions on chromosomes 14 and 15 shared by all affected patients (Supplementary Figure 2.1. Detailed inspection of the genes in the regions identified several candidates,

most prominently the *TGFB3* gene on 14q24. Subsequent Sanger sequencing of all 7 exons and intron boundaries identified a heterozygous intronic variant affecting the highly conserved (PhastCons: 1, PhyloP: 4.97) canonical donor splice site of exon 4 (c.754+2T>C), which is absent from variant databases (Variant Server, Genome of the Netherlands, 1000Genomes). Sequencing of the cDNA for 2 patients (1-II:12 and III:11) confirmed skipping of exon 4, leading to an in-frame deletion of 108 nucleotides (Supplementary Figure 2.2). At the protein level, a deletion of 36 amino acids is expected (p.Glu216_ Lys251del). This *TGFB3* mutation (c.754+2T>C) segregated with the clinical phenotype and was also present in 1 young individual (1-IV:1, 17 years old) without documented cardiovascular features (Figure 2.2, Supplementary Table 2.2), but with mild systemic manifestations including craniofacial features, easy bruising, and scoliosis.

To further investigate the role of *TGFB3* in TAAD etiology, DNA samples from 350 syndromic and non-syndromic TAAD probands were Sanger sequenced for mutations in all exon–intron boundaries and the coding region of *TGFB3*. Additionally, in 120 TAAD patients, a targeted analysis of TAAD candidate genes after whole-exome sequencing was performed. This revealed additional heterozygous *TGFB3* mutations in 10 other probands (7 from Sanger sequencing and 3 from the exome sequencing cohort): 4 different missense mutations, p.Asp263His (family 3), p.Arg300Trp (families 2, 4, 5, 11), p.Ile322Thr (family 10), p.Leu401Pro (family 8); 1 nonsense mutation, p.Tyr365* (family 6); and 2 single-base deletions leading to a frameshift and premature stop codon, p.Leu386Argfs*21 (family 7) and p.Asn235Metfs*11 (family 9) (Figure 2.4). All missense mutations were predicted as deleterious by SIFT [32] and as disease causing by Mutation Taster [33]. The 2 missense mutations in exon 5 (p.Asp263His and p.Arg300Trp) both affect highly conserved amino acids of the latency-associated peptide (LAP) domain, which are also conserved among the TGFB1, TGFB2, and TGFB3 proteins (Figure 2.4). The p.Asp263His alteration disrupts the Arg-Gly-Asp (RGD) motif, which is essential for binding to the $\alpha_v\beta_3$, $\alpha_v\beta_6$, $\alpha_v\beta_1$,and $\alpha_v\beta_5$ integrins [34–36]. Mutations of the RGD motif in LAPβ3 were demonstrated to abolish binding to $\alpha_v\beta_3$, $\alpha_v\beta_5$,and $\alpha_v\beta_6$ [36]. The second missense mutation in exon 5, p.Arg300Trp, affects the last amino acid of the LAP domain, disrupting the last residue of the RKKR minimal recognition motif of the furin or related protease cleavage site [37]. Mutations

affecting similar amino acids in TGFB2 have been shown to be causal in syndromic forms of aortic aneurysms[8]. The 2 other missense mutations, p.Ile322Thr and p.Leu401Pro, affect highly conserved amino acids located in the region of the active cytokine. The 3 other mutations create premature stop codons, either in the LAP domain or in the active TGFB3 (cytokine) domain, leading to nonsense-mediated decay or truncated proteins, which probably lose their cytokine activity.
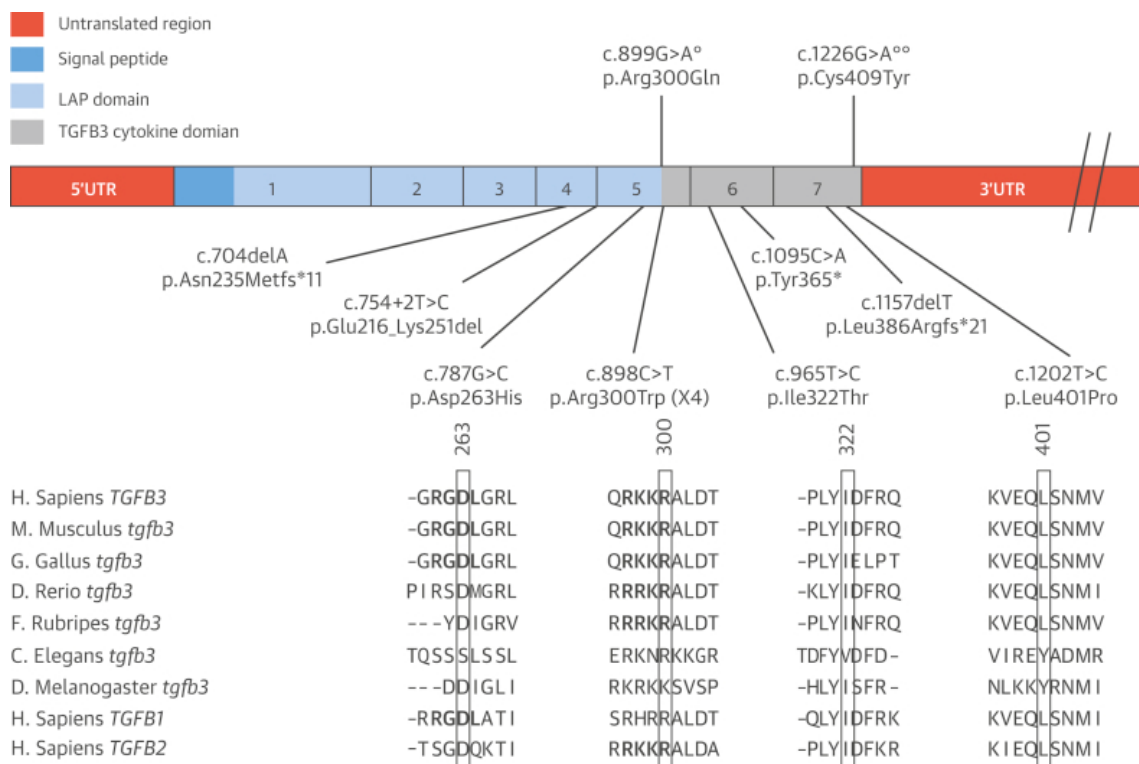

Figure 2.4: Mutation overview of the *TGFB3* gene. Exons are represented by rectangles. Exon numbering is given, and different colors denote the different protein domains. Mutations found in this study are indicated below the gene in the respective domains. Evolutionary conservation in TGFB3 and its related proteins is given for the 4 missense mutations (p.Arg300Trp: Family 2, 4, 5 and 11; p.Asp263His: Family 3; p.Leu401Pro: Family 8; p.Ile322Thr: Family 10). Previously published mutations are shown above the gene, with a single degree symbol indicating mutation described in Matyas et al.[17] and double degree symbols indicating mutation from Rienhoff et al.[16].

The causal nature of the *TGFB3* mutations was further supported by de novo occurrence (family 6) (Figure 2.2) and absence from controls (all mutations) in EVS, 1000Genomes, and the Genome of the Netherlands. Although p.Tyr365* in

family 6 occurred de novo, we previously identified a *SMAD3* variant (p.Ala250Thr) of unknown significance in the proband. This *SMAD3* variant was also present in the proband's mother, who presented with variable connective tissue findings and mild cardiovascular involvement, making its precise contribution to pathogenesis unclear.

We studied the molecular effects of these mutations in more detail using a homology model of the TGFB3 dimer. Asp263 is located in a surface loop where it is accessible for integrins (Figure 2.5). Mutation p.Glu216_Lys251del results in deletion of a central beta-strand and subsequent surface loop in the LAP domain (Figure 2.5). This will severely affect this domain's conformation, including the position of the RGD motif, and thereby affect dimerization and inhibition of the TGFB3 domain.

Missense mutations p.Arg300Trp, p.Ile322Thr, and p.Leu401Pro are also predicted to alter TGFB3 function. Besides participating in the cleavage site, Arg300 is involved in several ionic interactions that will be lost with the substitution to tryptophan, and this bulky residue will likely induce steric rearrangements. Ile322Thr is predicted to alter the positioning of Arg325, an important amino acid residue for binding with TGFBR2. In addition, hydrophobic contacts with the N-terminal helix in the LAP domain will be affected by the substitution with threonine (hydrophilic). Substitution from Leu401 to proline is predicted to change the hydrophobic interactions with residues of both the LAP and TGFB3 domain.

The clinical phenotypes in the 10 additional families demonstrate significant overlap with Loeys-Dietz syndrome (Supplementary Tables 2.3, 2.4, 2.5, 2.6). Vascular involvement ranges from no cardiovascular abnormalities at age 64 (3-II:2) to type A (median age of 51 years, range 40 to 80 years) or type B aortic dissection (median age of 44.5 years, range 30 to 57), abdominal aortic dissection and death as a result of cerebral aneurysm dissection at age 55 (2-II:1) (Table 2.1). So far, no examples of early arterial dissection or dissection at small aortic dimension were observed. Other cardiovascular features include mitral valve disease, ranging from mild insufficiency to chorda rupture necessitating surgery, and persistent foramen ovale and atrial or ventricular septal defects. Disease beyond
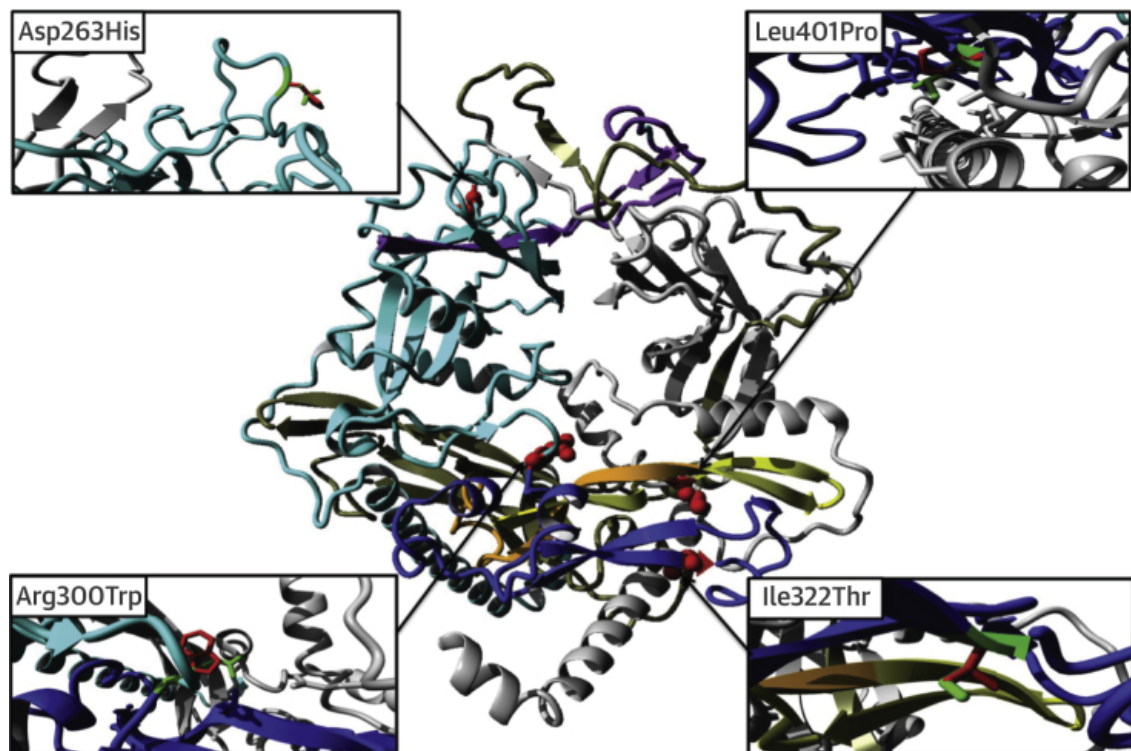
Figure 2.5: Overview of the TGFB3 dimer model and mutations. One monomer is shown in **grey**, with the other monomer in **cyan** (LAP domain) and *blue* (TGFB3 domain). Residues deleted by the p.Glu216_Lys251del mutation are in **purple**. Residues affected by the p.Leu386Argfs21* mutation are in **yellow** (note that this mutation also adds 21 different residues that cannot be modeled). Residues deleted by the p.Tyr365* mutation are shown in **orange** and **yellow** (note that this mutation deletes all residues following Tyr365). Residues deleted by mutation p.Asn235Metfs*11 are shown in **grey-olive** in the second monomer (note that this mutation also adds 11 different new residues, which cannot be modeled). The point mutations p.Asp263His, p.Arg300Trp, p.Ile322Thr, and p.Leu401Pro are shown in **red** with their side chains visible as **red spheres**. A detailed close-up of these mutations is shown in 4 extra panels. In these panels, the wild-type residue side chain is in **green**, whereas the mutant side chain is in **red**. For the p.Arg300Trp mutation, side chains of nearby negative residues are also shown. For the p.Leu401Pro mutation, nearby hydrophobic residues are shown.

the aorta, with iliac and subclavian artery aneurysms, was only identified in 2 patients (1-II:12 and 1-III:13). No striking aortic or arterial tortuosity was observed.

Typical LDS findings such as hypertelorism, bifid uvula and cleft palate, cervical spine instability, and club foot deformity are commonly observed (Figure 2.3, Tables 2.1, 2.2, Supplementary Tables 2.3, 2.4, 2.5, 2.6). Other recurrent features include

dolichocephaly, high-arched palate, retrognathia (with surgery in case 3-III:1), tall stature, joint hypermobility, arachnodactyly, pectus deformity, and inguinal hernia (Table 2.1, Figure 2.3). No evidence for ectopia lentis was found in the medical records. Early-onset osteoarthritis was only reported in 2 individuals (10-II:1 and 11-II:1). The clinical features from 43 identified patients belonging to 11 families are summarized in Table 2.1. We observed a striking intrafamilial and interfamilial clinical variability with typical LDS features in some, but complete absence in others.

We subsequently investigated the effect of the p.Asp263His mutation on aortic wall architecture and TGF-β signaling. Microscopic examination of the dissected aortic wall, obtained at the time of surgery (3-III:1), showed elastic fiber fragmentation with higher collagen and proteoglycan deposition (Figure 2.6A-C). These histopathological findings are highly reminiscent of both MFS and LDS[8]. Retrieved pathology reports from 2 patients (1-II:4 and II:5) carrying the p.Glu216_Lys251del mutation (family 1) also described extensive elastic fiber fragmentation with "pseudo cyst formation" in the medial layer of the dissected aorta and "aortic medial degeneration." In families 9 and 10, only mild elastic fiber fragmentation was observed.

To investigate TGF-β signaling in the aortic wall of a patient carrying a *TGFB3* mutation (p.Asp263His), we performed immunohistochemical analysis of aortic tissue (Figure 2.6D-F). Very similar to what has been detected in TGFB2-deficient aortic walls of humans and mice[8], we observed evidence of paradoxically enhanced TGF-β signaling in the aortic wall of a *TGFB3* mutant patient, as shown by increased pSMAD2 (canonical TGF-β signaling), pERK (noncanonical TGF-β signaling), and elevated *TGFB1* messenger RNA (Figures 2.6D-F).

Table 2.1: Patient Characteristics

	Affected Individuals (n = 43)*
Sex, M/F	23/20
Age, yrs	34 (3–74)
Age at death, yrs	56 (40–80)
Age at dissection, yrs	47.5 (30–80)
Cardiovascular findings	
- Type A dissections, age, yrs	4 (51; 40–80)
- Type B dissections, age, yrs	6 (44.5; 30–57)
- Aortic aneurysm†, age, yrs	6 (34; 3–68)
- Abdominal aortic surgery‡	2
Disease beyond aorta§ §	3
- Skeletal findings	
- Tall stature	12
- Arachnodactyly	16
- Pectus deformity	8
- Kyphoscoliosis	11
- Joint hypermobility	9
Loeys-Dietz features	
- Hypertelorism	14
- Bifid uvula	11
- Cleft palate	5

Values are n, median (range), or n (median; range). *Not all patients were evaluated for all features. †Four aneurysms affected the sinuses of Valsalva, and 2 only affected the ascending aorta. ‡Surgery was performed on 1 patient at age 43 years and 1 at 50 years. §Cerebral, iliac, or subclavian arteries (n = 1 for each location)

Table 2.2:   Comparison of phenotypical characteristics of patients with *TGFBR1/2*,*SMAD3*,*TGFB2*, and *TGFB3* mutations

Phenotype	TGFBR1/2	SMAD3	TGFB2	TGFB3
Hypertelorism	v	v	v	v
Bifid uvula/cleft palate	v	v	v	v
Exotropia	v	v	v	v
Craniosynostosis	v	v	x	x
Cervical spine instability	v	v	x	v
Retrognathia surgery	v	v	v	v
Scoliosis/spondylolisthesis	v	v	v	v
Clubfoot	v	v	v	v
Osteoarthritis	v	v	x	v
Dural ectasia	v	v	v	?
Pneumothorax	v	v	v	x
Hernia	v	v	v	v
Dissection at young age	v	v	v	?
Disease beyond root	v	v	v	v
Cerebral hemorrhage	v	v	v	v
Arterial tortuosity	v	v	v	x
Autoimmune findings	v	v	v	v

A check mark indicates presence of the clinical feature, an X indicates absence of the clinical feature, and a question mark indicates presence of a clinical feature is unknown.
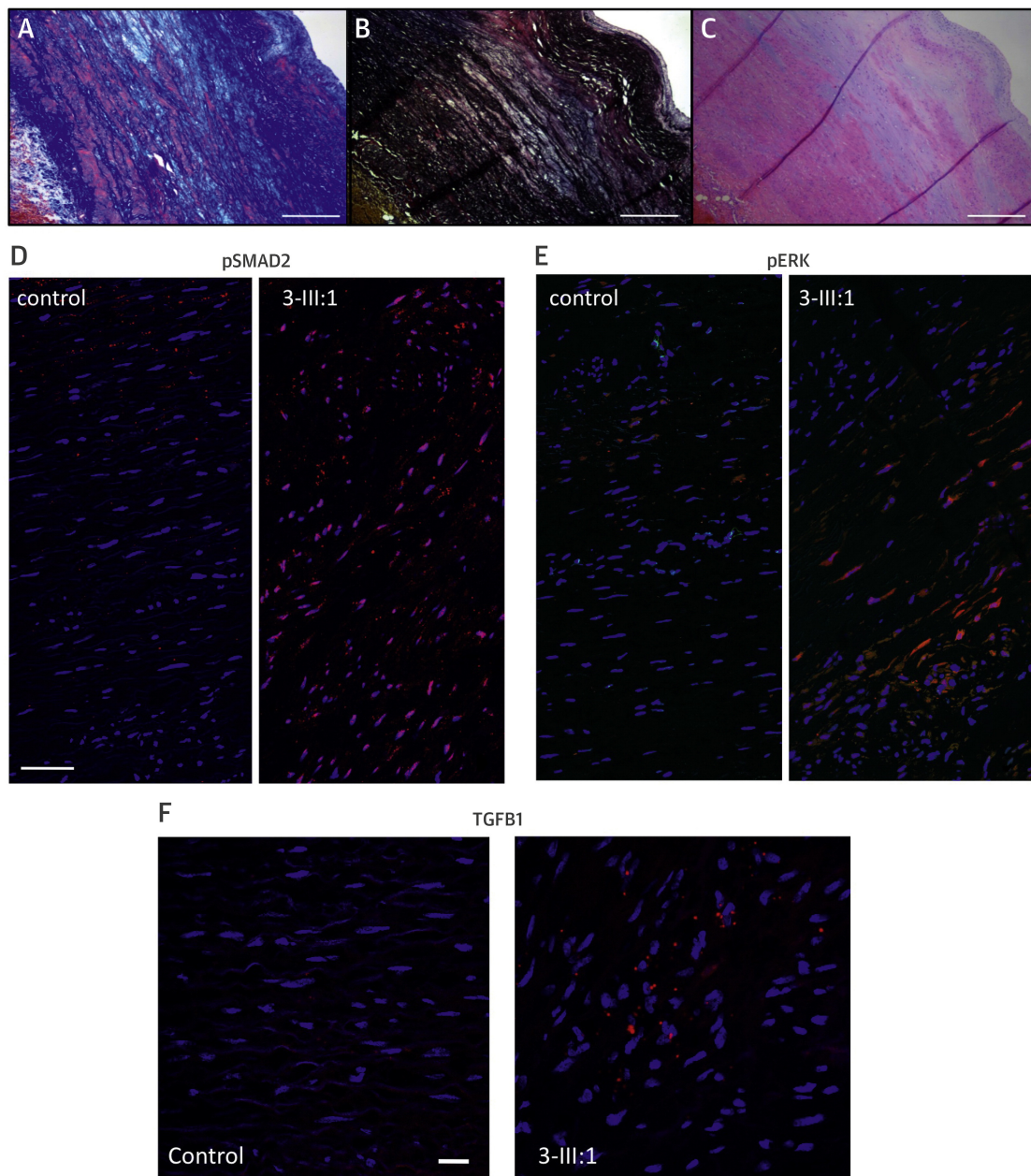
Figure 2.6: **(A)** Masson trichrome staining shows increased deposition of collagen **(dark blue)** and loss of smooth muscle fibers **(red)** in the media. **(B)** Elastin stain (Elastica van Gieson) shows loss of elastin fibers **(black)**. **(C)** Hematoxylin-eosin staining shows deposition of proteoglycan **(light blue)** in the media. **(A–C)** Scale bar indicates 2 mm. **(D–F)** Cross sections of the media of the aortic wall of patient 3-III:1 and a matched control. Red staining corresponds to pSmad2 **(D)**; pERK **(E)**; and TGFB1 **(F)**. Scale bars indicate 50 mm **(D–E)**,20 μm **(F)**. **Blue** staining shows cell nuclei (DAPI), colocalization is **purple**. **Red** staining not colocalized with DAPI is nonspecific.

2.5   Discussion

During mouse embryonic development, *Tgfb3* is expressed in several tissues, including cardiovascular, pulmonary, skin, and craniofacial structures. Although *Tgfb3* is expressed in overlapping fashion with *Tgfb2* in the cardiovascular system, most attention has been paid to its role in palatogenesis, as *Tgfb3* knockout mice die at birth because of cleft palate [38, 39]. No major cardiac developmental defects have been reported in *Tgfb3*-deficient mice [38, 40, 41]. Although minor abnormalities at the aortic arch level, as well as in position and curvature of the aortic arches and myocardial architecture, were described in the *Tgfb3* knockout mice, no data are available on the aortic sizes of conditional knockout or haploinsufficient animals [39, 40]. Of interest, the presence of aortic aneurysms and ruptures recapitulating the human phenotype were previously overlooked upon the initial phenotypic description of *Tgfb2* haploinsufficient and *Smad3* knockout mouse models[7, 8].

Because we observed 3 truncating mutations and an in-frame splice site mutation, we hypothesize that the *TGFB3* mutations lead to loss of function (LOF) of TGFB3. In addition, 2 missense mutations, located in the LAP domain, alter critical residues that are relevant for TGFB3 activation by integrins and TGFB3 processing [35, 42]. Mice carrying a missense mutation affecting the RGD integrin-binding motif of Tgfb1 recapitulate the phenotype of *Tgfb1* knockout mice [43], suggesting that the *TGFB3* mutation disrupting the RGD (p.Arg263His) might also lead to LOF. Similarly, molecular analyses and predictions based on the TGFB3 dimer model confirm that most *TGFB3* mutations reported here cause LOF. Although it was previously hypothesized that patients with LOF mutations in *TGFB3* lack cardiovascular phenotypes [16],we clearly demonstrate that *TGFB3* LOF mutations associate with aortic and other arterial aneurysms/dissections and mitral valve disease, and recognize an extremely variable cardiovascular phenotype in the *TGFB3* cohort described here. The relatively young age of previously reported patients with *TGFB3* mutations (8 [16] and 10.5 years of age [17]) might explain the lack of obvious cardiovascular disease. On the basis of expression studies of the mutant TGFB3 protein in a Xenopus model, Rienhoff et al.[16] hypothesized that the mutated, inactivated allele (p.Cys409Tyr) leads to a nonfunctional protein, decreasing both canonical and noncanonical TGF-β signaling. By contrast, our

experiments on human aortic tissue reveal a signature of increased TGF-β signaling. These findings confirm our prior experience that mutational hits in the TGFBR1/2 receptors, the SMAD3 signal transducer, or the TGFB2 ligand lead to a paradoxical increase in TGF-β signaling, as evidenced here by increased immunohistochemical signals for pSMAD2, pERK, and TGFB1 [5, 7, 8]. Shifts in balances between canonical (pSMAD2) and non-canonical (pERK) cascades, classic, and alternative (BMP-driven) TGF-β superfamily cascades, as well as shifts in ligand expression (TGFB1 vs. TGFB2 or TGFB3) seem likely to be important contributing factors [44, 45].

TGFB3 mutations also appear to have opposing effects on height, as 1 patient in this study (3-III:1, p.Asp263His) has short stature and received growth hormone therapy during puberty, and the patient reported by Rienhoff et al.[16] (p.Cys409Tyr) presented with short stature (5th percentile), whereas others (several patients in this study and the patient reported by Matyas et al.[17]) presented with tall stature. *TGFB3* mutations affecting residue Arg300 are associated with cleft palate and/or bifid uvula in our patients (Supplementary Tables 2.3, 2.4 and 2.6) and in the patient reported by Matyas et al.[17]. Our study confirms the association of *TGFB3* mutations with overt cleft palate in humans and endorses its important role in palatogenesis.

Although our experience is limited to 43 patients in 11 families, our findings warrant comprehensive cardiovascular imaging of the patients. Thus far, no strong evidence has emerged for early aortic dissection in *TGFB3* mutant patients, but as the phenotypical spectrum associated with *TGFBR1/2*, *SMAD3*, and *TGFB2* has now been demonstrated to be extremely wide, we cannot rule out the occurrence of early catastrophic events. We recommend yearly echocardiographic evaluation of the aortic root in all mutation carriers, complemented with at least 1 baseline imaging of the complete aorta and side branches. Frequency of follow-up should be guided by initial findings, family history, and experience still to be gained. Depending on family history and future knowledge, additional imaging of the brain vessels might be indicated. Furthermore, the true incidence and full spectrum of autoimmune manifestations in *TGFB3* mutation carriers should be determined in follow-up studies.

2.5.1 Study limitations

Not all clinical features are acquired in all patients. Further studies are needed to fully characterize the phenotypical spectrum we identified here. The predicted effects of the mutations in the homology model of TGFB3 are theoretical and should be complemented with additional protein studies, and the immunohistochemistry studies are hampered by limited availability of patients' aortic wall tissues.

2.6 Conclusions

We demonstrate that mutations in the TGFB3 ligand are responsible for a syndromic form of aortic aneurysmal disease. Consistent with our previous findings in *TGFBR1/2*, *SMAD3*, and *TGFB2* mutation carriers, our study also provides evidence for a paradoxical increase in TGF-β signaling in the aorta. The clinical histories of the patients in our cohort warrant life-long and widespread cardiovascular surveillance in patients with *TGFB3* mutations (Figure 2.1). Further research explaining the wide clinical variability is strongly indicated.

2.7 Supplementary material
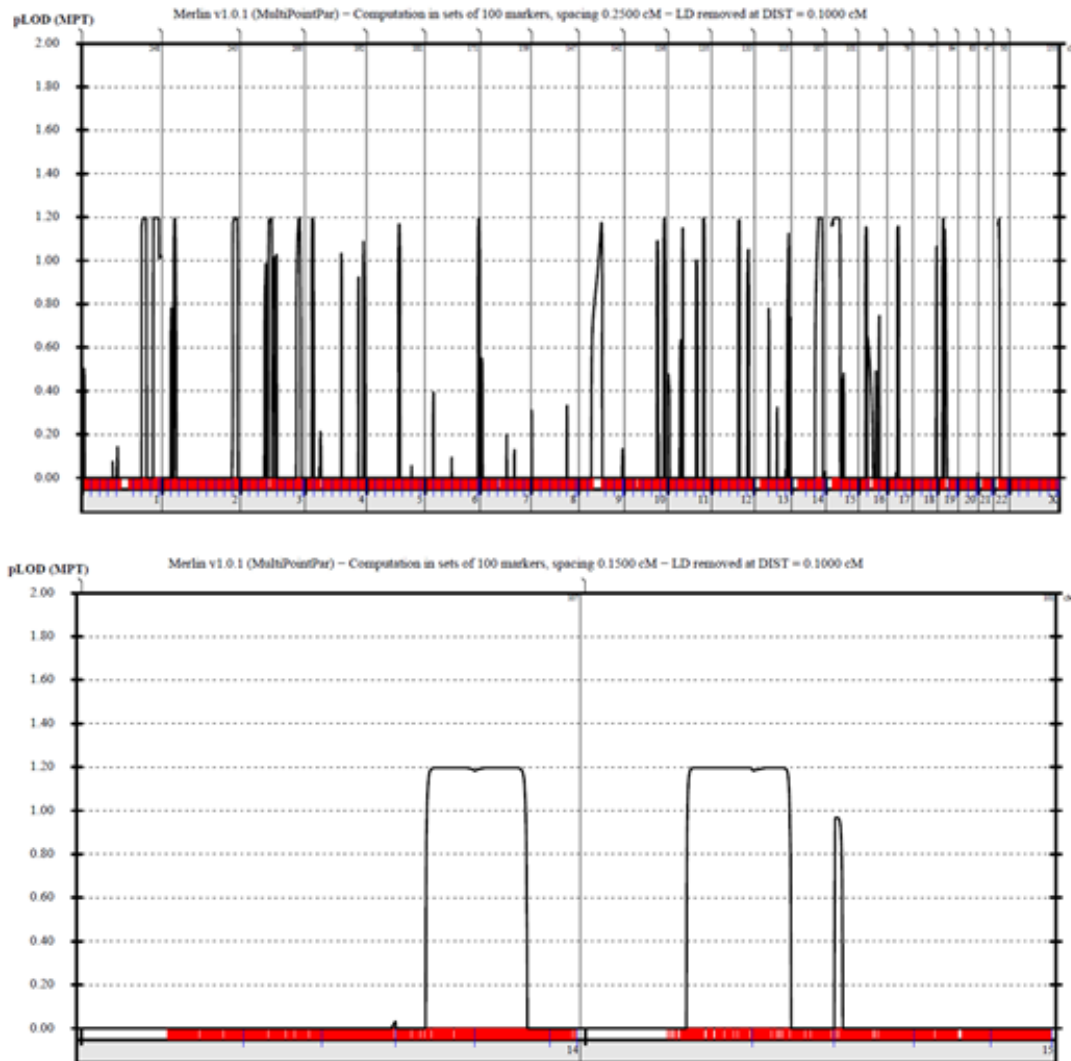
Supplementary Figure 2.1: Plots of the genome wide linkage analysis (upper graph) and chromosome 14 and 15 (lower graph) displaying the largest genomic regions identified. LOD scores appear in the Y-axis and chromosome numbers are on the X-axis. Vertical red lines indicate SNP coverage.
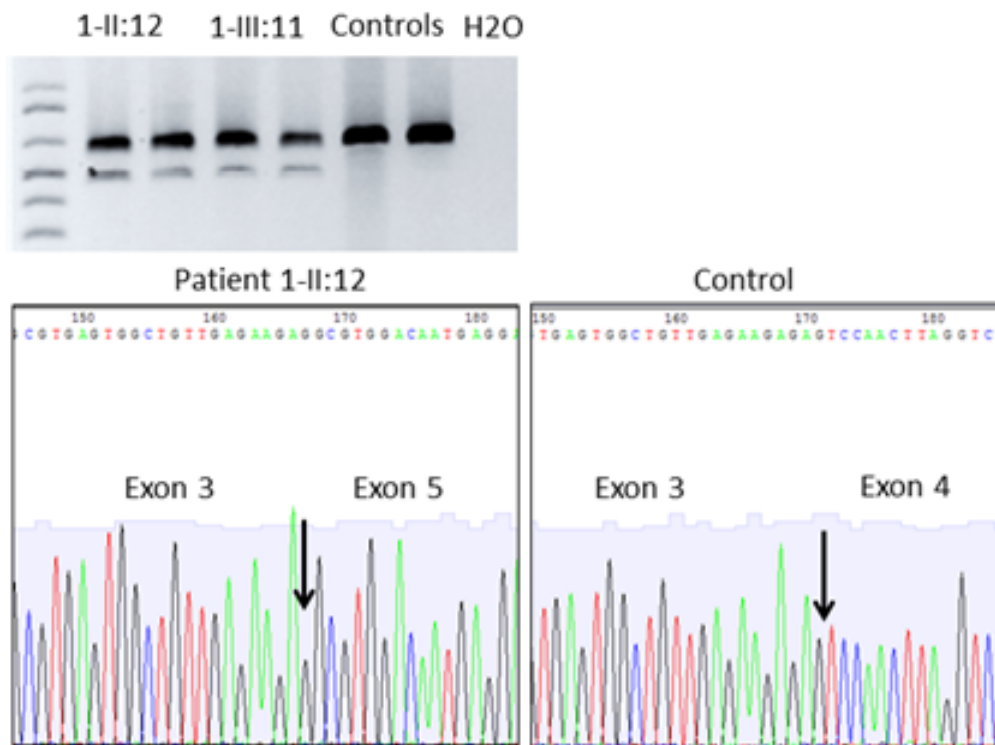
Supplementary Figure 2.2: To investigate the effect of the *TGFB3* c.754+2T>C variant on splicing, we designed three different PCR experiments using blood complementary DNA (cDNA) from two patients from family 1 (II:12 and III:11). The investigated fragments covered *TGFB3* exons 2-5, 3-6 and 2-6. PCR fragments corresponding to exons 2 to 5 are shown in the gel picture (in duplicate, patients in lanes 2 to 5 and normal controls in lanes 6-7). Normal expected size was 466 bp. An abnormal, smaller fragment, probably with a deletion of exon 4 was observed in the patients. Sanger sequencing using the smaller PCR band as template confirmed that the *TGFB3* c.754+2T>C mutation is leading to a deletion of exon 4 with an in-frame deletion of 108 nucleotides.

Supplementary Table 2.1: List of *TGFB3* PCR primers used for Sanger sequencing

Name	Sense primer	Antisense primer	Amplicon size
TGFB3 ex1	5'-CCCTCCTTCTGCACGTCTGC-3'	5'-TCCCAGCTCCAGTTCAGACC-3'	487
TGFB3 ex2	5'-GAGGCCACACTGCTCCTTGC-3'	5'-AAACCCAGGTCTGCCAAACG-3'	469
TGFB3 ex3	5'-GAGGGCCATGGCATTCAGG-3'	5'-TGGAGGATACTCAGTGGCAAAGC-3'	391
TGFB3 ex4	5'-GCAACGTGCGCTTGAAGG-3'	5'-GGAGCTTGGTTTCTTTTCTTGAGG-3'	402
TGFB3 ex5	5'-CACGGGGCATCTTTCAGTGG-3'	5'-TGAGTGTGGCTTGGCTCTGG-3'	502
TGFB3 ex6	5'-TGGCATGAAAGGACTCCAAGG-3'	5'-TCACCCCAGACCATCATTTGC-3'	365
TGFB3 ex7	5'-GGACTGCCCCTGGAACTGG-3'	5'-TCCCTTTCCTCTATCCCCATCC-3'	532

Supplementary Table 2.2: Clinical characteristics of family 1 (c.754+2T>C, p.Glu216_Lys251del).

Person	1-II:4	1-II:5*	1-II:7	1-II:10	1-III:6*	1-III:8	1-IV:1*	1-IV:2*	1-II:12*	1-II:14*	1-III:11*	1-II:16*	-III:13*
Age	57†	56†	40†	74	51	49	17	24	72	72	47	69	44
Sex	M	M	M	F	M	M	F	M	F	F	M	F	M
Height	-	-	-	168 cm	183 cm	190 cm	181 cm	198 cm	162 cm	?	185 cm	168 cm	187 cm
Vascular	Ruptured descending TAA at age 57 AAD at age 57	arotid artery surgery Descending TAA at age 50 Infrarenal AA at age 52	Aortic rupture at age 40	No imaging	Aortic sinus: 38 mm	Aortic sinus: 36 mm Stroke at age 48	Aortic sinus: 32 mm	No imaging	Dissection aortic arch at age 45 Aneurysm left subclavian artery at age 45	Infrarenal AA at age 68	TAA	Aortic sinus: 32 mm Ascending aorta: 35 mm	Aortic sinus: 39 mm Aneurysm right common iliac artery at age 44
Mitral valve					Mild MVP	MI with chorda rupture surgery at age 49					MVP with MI grade 3 TI grade 3		Mild MVP

Person	1-II:4	1-II:5*	1-II:7	1-II:10	1-III:6*	1-III:8	1-IV:1*	1-IV:2*	1-II:12*	1-II:14*	1-III:11*	1-II:16*	-III:13*
Skeletal		Long face			Pectus excavatum High-arched palate Retrognathia		Mild scoliosis Mild joint laxity	Pectus carinatum surgery at age 14 High-arched palate Retrognathia	Long face		Long face Pes plani	Mild scoliosis Total hip replacement	Severe scoliosis Spondylodesis Th4-L1 Long face Retrognathia
LDS features							Soft skin Easy bruising		Thin skin Easy bruising				
Other					Varices			Varices		Hiatal hernia	Hiatal hernia	Pelvic organ prolapse Hiatal hernia Varices	

A check mark indicates presence of the clinical feature, an X indicates absence of the clinical feature, and a question mark indicates presence of a clinical feature is unknown.

Supplementary Table 2.3: Clinical characteristics of family 2 (c.898C>T, p.Arg300Trp)

Person	2-II:1	2-II:4	2-III:3	2-IV:1	2-III:7*	2-IV:2*	2-IV:3
Age	55†	60	26	6	31	7	6
Sex	M	F	F	M	F	F	M
Aorta	Cerebral aneurysm dissection	Normal echo	Normal echo	Aortic dilatation	Aortic sinus: 28 mm at age 29 years (Z score = -0.25)	Normal echo at age 4 years	Normal echo at age 5 years
Skeletal	Arachnodactyly Pectus excavatum	Joint hypermobility	Arm-span to height ratio >1.05		Pectus carinatum Cervical rib	Tall stature Cervical spine instability C2-C4 Club feet Joint hypermobility Hip dysplasia	Arachnodactyly Joint hypermobility
LDS features		Bifid uvula	Bifid uvula Hypertelorism Blue sclerae	Cleft palate Hypertelorism	Bifid uvula Hypertelorism Translucent skin	Bifid uvula Hypertelorism	Bifid uvula Hypertelorism

Person	2-II:1	2-II:4	2-III:3	2-IV:1	2-III:7*	2-IV:2*	2-IV:3
Other						Hemiparesis – cause unknown Learning difficulties	

* Mutation present. No DNA was available from the other patients; C: cervical vertebra; †: deceased

Supplementary Table 2.4: Clinical characteristics of families 3-6 (c.787G>C, p.Asp263His in family 3, c.898C>T, p.Arg300Trp in families 4 and 5, c.1095C>A, p.Tyr365* in family 6).

Person	3-II:2*	3-II:3*	3-III:1*	3-III:2*	4-II:2*	4-III:1	4-III:2	5-II:1*	6-II:1*
Age	64	70	31	34	42	13	10	24	42
Sex	F	F	M	M	M	F	F	M	F
Aorta	Aortic sinus: 34 mm, Mild MI	Aortic sinus: 38 mm, Mild MI	TAAD, at age 30 with root = 70 mm	Aortic sinus: 32 mm	Aortic sinus: 42 mm	Normal echo	Normal echo	Aortic sinus: 40 mm (Z=3.6), MVP, PFO	Normal echo
Skeletal			Dolichocephaly, High-arched palate		Arachnodactyly, Increased arm-span to height ratio, Retrognathia, Scoliosis, Pes plani	Arachnodactyly, Asymmetric chest, Narrow palate with dental crowding		Pectus carinatum, Pes plani	Arachnodactyly, Joint hyperlaxity, Camptodactyly toes, Pes plani
LDS features			Retrognathia with surgery at age 22		Bifid uvula, Hypertelorism, Soft skin	Cleft palate	Cleft palate	Bifid uvula, Cleft palate, Hypertelorism, Club foot	Bifid uvula, Hypertelorism, Easy bruising
Other			Delayed puberty, Short stature: growth hormone therapy		Inguinal hernia surgery at age 6 years	Inguinal hernia			Delayed motor development, Varices, Cataract

MI: mitral insufficiency; MVP: mitral valve prolapse; PFO: patent foramen ovale; *Mutation present. No DNA was available from the other patients

Supplementary Table 2.5: Clinical characteristics of families 7-8 (c.1157delT, p.Leu386Argfs*21 in family 7; c.1202T>C, p.Leu401Pro in family 8).

Person	7-I:1	7-II:1*	7-II:4	7-III:4	8-II:1*	8-III:1*
Age	70†	43	?	14	50†	30
Sex	M	M	F	F	M	F
Aorta	TAA at age 61 with TAAD at age 70	No aneurysm, MVP		Normal echocardiography	Age 42: ascending aorta of 60 mm, At age 43: Type A dissection with supracoronary replacement, At age 44: TEVAR for type B dissection, Age 50: abdominal aortic dissection	Normal echocardiography
Skeletal	Tall stature	Dolichocephaly, Tall stature, Arachnodactyly, Scoliosis, Pes plani	Tall stature, Arachnodactyly	Tall stature, High arched palate, Arachnodactyly, Scoliosis	Enlarged arm span, Arachnodactyly, Dolichocephaly, Mild scoliosis	Enlarged, arm span, Arachnodactyly, Scoliosis, Joint hypermobility, Metatarsus adductus, Camptodactyly of 4th/5th toes
LDS features	Cleft palate and bifid uvula	Bifid uvula, Hypertelorism			Hypertelorism, Spondylosis C3-C4, C5-C6 and C6-C7	
Other					Bilateral inguinal hernia surgery at age 39	

TAA(D): thoracic aortic aneurysm and (dissection); MVP: mitral valve prolapse; PFO: patent foramen ovale; C: cervical vertebra; TEVAR: Thoracic EndoVascular Aortic Repair; *Mutation present. No DNA was available from the other patients; †: deceased

Supplementary Table 2.6: Clinical characteristics of families 9-11 (c.704delA, p.Asn235Metfs*11 in family 9; c.965T>C, p.Ile322Thr in family 10; c.898C>T,p.Arg300Trp in family 11).

Person	9-I:1	9-II:2*	9-III:1*	10-II:1*	10-III:1*	10-III:2*	11-I:1*	11-II:1*
Age	80†	67	43	56	24	22	27	3
Sex	M	F	M	M	M	F	M	F
Aorta	TAAD at age 80	TAAD type A at age 59	TAAD type A at age 40	AAA with Y-graft at age 43, TAA (47 mm) with severe AR: Bentall surgery	Aortic root 32 mm	Aortic root 34 mm		VSD+ASD, Aortic root aneurysm: 19.5 mm (Z¿2)
Skeletal		Thin and tall habitus, Arachnodactyly	Tall stature, Kyphoscoliosis, Pectus deformity, Retrognathia, Flat occiput	Tall stature, Arachnodactyly, Kyphoscoliosis, Pectus deformity, Retrognathia, Down-slanting palp fissures	Tall stature, Arachnodactyly, Scoliosis	Tall stature, Arachnodactyly, Joint hypermobility, Kyphoscoliosis, Pes plani, Retrognathia, Down-slanting palp fissures	Tall stature, Arachnodactyly, Joint hypermobility, High arched palate, Kyphosis, Pes plani	Tall stature, Arachnodactyly, Joint hypermobility, Retrognathia, Down-slanting palpebral fissures
LDS features				Hypertelorism, Osteoarthritis		Hypertelorism, Bifid uvula	Hypertelorism, Bifid uvula, Spondylolisthesis	Hypertelorism, Bifid uvula, Osteoarthritis, Translucent, skin, Easy bruising
Other		Inguinal hernia, Myopia			Striae			

TAA(D): thoracic aortic aneurysm and (dissection); AAA: abdominal aortic aneurysm; ASD, atrial septal defect; VSD, ventricular septal defect; *Mutation present, No DNA available on other patients; †: deceased

Detailed Methods

Immunohistochemistry: Protocol for staining of FFPE sections was adapted from Baschong et al.[31] with the following modifications. Slides were stained overnight at 4° with anti-pSmad2 antibody (clone A5S, Millipore, Cat. 04-953, 1:100) and anti-pERK1/2 (clone D13.14.4E, Cell Signaling, Cat. 4370, 1:100) in 0.1% Triton/TBS buffer, washed 3x10min in Perm/Staining buffer, and then stained with anti-rabbit Alexa594 (Molecular Probes) at 1:200 for 1h at room temperature (RT). Slides were then washed 3x10min in Perm/Staining buffer and mounted with Hard Set VECTASHIELD Mounting Media with DAPI. Images were acquired on Zeiss AxioExaminer with 710NLO-Meta multiphoton confocal microscope at a 25x magnification.

For removal of paraffin, slides were immersed in xylene (3x5 min), followed by graded ethanol treatment (3x5' 100%, 3x5' 95%, 3x5' 80%, 3x5' 70%), rinsed in water and immersed in Tris buffered saline (TBS) buffer (50 mM Tris-Cl, pH 7.6, 150 mM NaCl). Antigen retrieval was performed in a rice steamer using 1M Sodium Citrate Buffer/0.1% Tween for 30 min. Slides were then cooled to RT for 20 min, rinsed in water, and transferred to TBS buffer. In order to minimize autofluorescence background, slides were then treated with freshly prepared "bubbling" 10mg/ml of sodium borohydride in TBS for 30 minutes and then rinsed 3 times in TBS. Slides were then permeabilized with Perm/Staining buffer (0.1% Triton in TBS buffer) for 20 min, followed by a 20 min treatment with Fc block Reagent (Innovex Biosciences) and a 20 min treatment with Background Buster Reagent (Innovex Biosciences).

In situ RNA with ACD RNAscope probes: The ACD RNAscope probe Hs-TGFB1 probe (cat 400881) was used to detect human TGFB1 transcript in conjunction with the RNAscope 2.0 HD Reagent Kit (RED) from ACD. FFPE sections were stained following the manufacturer recommended protocol, except that slides were counterstained with DAPI and not with hematoxylin. Red fluorescent signal was detected on Zeiss AxioExaminer with 710NLO-Meta multiphoton confocal microscope at a 25x magnification.

References

1. Massagué, J. TGFβ signalling in context. *Nature reviews. Molecular cell biology* **13,** 616–30. ISSN: 1471-0080 (Oct. 2012).

2. Neptune, E. R. *et al.* Dysregulation of TGF-beta activation contributes to pathogenesis in Marfan syndrome. *Nat Genet* **33,** 407–11. ISSN: 1061-4036 (Mar. 2003).

3. Habashi, J. P. *et al.* Losartan, an AT1 antagonist, prevents aortic aneurysm in a mouse model of Marfan syndrome. *Science* **312,** 117–121. ISSN: 1095-9203 (Apr. 2006).

4. Dietz, H. C. *et al.* Marfan syndrome caused by a recurrent de novo missense mutation in the fibrillin gene. *Nature* **352,** 337–9. ISSN: 0028-0836 (July 1991).

5. Loeys, B. L. *et al.* A syndrome of altered cardiovascular, craniofacial, neurocognitive and skeletal development caused by mutations in TGFBR1 or TGFBR2. *Nat Genet* **37,** 275–81. ISSN: 1061-4036 (Mar. 2005).

6. Mizuguchi, T. *et al.* Heterozygous TGFBR2 mutations in Marfan syndrome. *Nat Genet* **36,** 855–60. ISSN: 1061-4036 (Aug. 2004).

7. Van de Laar, I. M. B. H. *et al.* Mutations in SMAD3 cause a syndromic form of aortic aneurysms and dissections with early-onset osteoarthritis. *Nature genetics* **43,** 121–126. ISSN: 1061-4036 (Feb. 2011).

8. Lindsay, M. E. *et al.* Loss-of-function mutations in TGFB2 cause a syndromic presentation of thoracic aortic aneurysm. *Nat Genet* **44,** 922–7. ISSN: 1546-1718 (Aug. 2012).

9. Boileau, C. *et al.* TGFB2 mutations cause familial thoracic aortic aneurysms and dissections associated with mild systemic features of Marfan syndrome. *Nat Genet* **44,** 916–21. ISSN: 1546-1718 (Aug. 2012).

10. Doyle, A. J. *et al.* Mutations in the TGF-β repressor SKI cause Shprintzen-Goldberg syndrome with aortic aneurysm. *Nat Genet* **44,** 1249–54. ISSN: 1546-1718 (Sept. 2012).

11. Loeys, B. L. *et al.* Aneurysm syndromes caused by mutations in the TGF-beta receptor. *N Engl J Med* **355,** 788–98. ISSN: 1533-4406 (Aug. 2006).

12. Van de Laar, I. M. B. H. *et al.* Phenotypic spectrum of the SMAD3-related aneurysms-osteoarthritis syndrome. *Journal of Medical Genetics* **49,** 47–57. ISSN: 0022-2593 (Jan. 2012).

13. Van der Linde, D. *et al.* Aggressive cardiovascular phenotype of aneurysms-osteoarthritis syndrome caused by pathogenic SMAD3 variants. *Journal of the American College of Cardiology* **60,** 397–403. ISSN: 1558-3597 (July 2012).

14. Shprintzen, R. J. & Goldberg, R. B. A recurrent pattern syndrome of craniosynostosis associated with arachnodactyly and abdominal hernias. en. *J Craniofac Genet Dev Biol* **2,** 65–74. ISSN: 0270-4145 (Jan. 1982).

15. Rienhoff, H. Y. Response to "De novo mutation of the TGFB3 latency-associated peptide domain in a patient with overgrowth and Loeys-Dietz syndrome features". *American journal of medical genetics. Part A* **164A,** 2144–5. ISSN: 1552-4833 (Aug. 2014).

16. Rienhoff, H. Y. *et al.* A mutation in TGFB3 associated with a syndrome of low muscle mass, growth retardation, distal arthrogryposis and clinical features overlapping with Marfan and Loeys-Dietz syndrome. *American journal of medical genetics. Part A* **161A,** 2040–6. ISSN: 1552-4833 (Aug. 2013).

17. Matyas, G., Naef, P., Tollens, M. & Oexle, K. De novo mutation of the latency-associated peptide domain of TGFB3 in a patient with overgrowth and Loeys-Dietz syndrome features. *American journal of medical genetics. Part A* **164A,** 2141–3. ISSN: 1552-4833 (Aug. 2014).

18. Campens, L. *et al.* Reference values for echocardiographic assessment of the diameter of the aortic root and ascending aorta spanning all age categories. English. *The American journal of cardiology* **114,** 914–20. ISSN: 1879-1913 (Sept. 2014).

19. Rogers, I. S. *et al.* Distribution, determinants, and normal reference values of thoracic and abdominal aortic diameters by computed tomography (from the Framingham Heart Study). English. *The American journal of cardiology* **111,** 1510–6. ISSN: 1879-1913 (May 2013).

20. Hoffmann, K. & Lindner, T. H. easyLINKAGE-Plus–automated linkage analyses using large-scale SNP data. *Bioinformatics (Oxford, England)* **21,** 3565–7. ISSN: 1367-4803 (Sept. 2005).

21. Van de Laar, I. *et al.* First locus for primary pulmonary vein stenosis maps to chromosome 2q. *European heart journal* **30,** 2485–92. ISSN: 1522-9645 (Oct. 2009).

22. Thiele, H. & Nürnberg, P. HaploPainter: a tool for drawing pedigrees with complex haplotypes. *Bioinformatics (Oxford, England)* **21,** 1730–2. ISSN: 1367-4803 (Apr. 2005).

23. Den Dunnen, J. T. & Antonarakis, S. E. Mutation nomenclature extensions and suggestions to describe complex mutations: A discussion. *Human Mutation* **15,** 7–12. ISSN: 10597794 (2000).

24. Exome Variant Server, NHLBI GO Exome Sequencing Project (ESP) NHLBI GO Exome Sequencing Project (ESP), Seattle, Washington. Accessed January 27, 2015.

25. Abecasis, G. R. *et al.* An integrated map of genetic variation from 1,092 human genomes. *Nature* **491,** 56–65. ISSN: 1476-4687 (Nov. 2012).

26. Swertz, M. A. *et al.* The MOLGENIS toolkit: rapid prototyping of biosoftware at the push of a button. En. *BMC bioinformatics* **11 Suppl 1,** S12. ISSN: 1471-2105 (Jan. 2010).

27. Reese, M. G., Eeckman, F. H., Kulp, D. & Haussler, D. Improved Splice Site Detection in Genie. EN. *Journal of Computational Biology* **4,** 311–323. ISSN: 1066-5277 (Jan. 1997).

28. Brunak, S., Engelbrecht, J. & Knudsen, S. Prediction of human mRNA donor and acceptor sites from the DNA sequence. *Journal of Molecular Biology* **220,** 49–65. ISSN: 00222836 (July 1991).

29. Shi, M. *et al.* Latent TGF-β structure and activation. *Nature* **474,** 343–9. ISSN: 1476-4687 (June 2011).

30. Krieger, E. & Vriend, G. YASARA View - molecular graphics for all devices - from smartphones to workstations. *Bioinformatics (Oxford, England)* **30,** 2981–2. ISSN: 1367-4811 (Oct. 2014).

31. Baschong, W., Suetterlin, R. & Laeng, R. H. Control of Autofluorescence of Archival Formaldehyde-fixed, Paraffin-embedded Tissue in Confocal Laser Scanning Microscopy (CLSM). *Journal of Histochemistry & Cytochemistry* **49,** 1565–1571. ISSN: 0022-1554 (Dec. 2001).

32. Ng, P. C. & Henikoff, S. Predicting deleterious amino acid substitutions. *Genome research* **11,** 863–74. ISSN: 1088-9051 (May 2001).

33. Schwarz, J. M., Cooper, D. N., Schuelke, M. & Seelow, D. MutationTaster2: mutation prediction for the deep-sequencing age. *Nature methods* **11,** 361–2. ISSN: 1548-7105 (Apr. 2014).

34. Munger, J. S., Harpel, J. G., Giancotti, F. G. & Rifkin, D. B. Interactions between Growth Factors and Integrins: Latent Forms of Transforming Growth Factor-beta Are Ligands for the Integrin alpha vbeta 1. *Molecular Biology of the Cell* **9,** 2627–2638. ISSN: 1059-1524 (Sept. 1998).

35. Annes, J. P., Rifkin, D. B. & Munger, J. S. The integrin α V β 6 binds and activates latent TGFβ3. *FEBS Letters* **511,** 65–68. ISSN: 00145793 (Jan. 2002).

36. Ludbrook, S. B., Barry, S. T., Delves, C. J. & Horgan, C. M. T. The integrin alphavbeta3 is a receptor for the latency-associated peptides of transforming growth factors beta1 and beta3. en. *The Biochemical journal* **369,** 311–8. ISSN: 0264-6021 (Jan. 2003).

37. Constam, D. B. Regulation of TGFβ and related signals by precursor processing. *Seminars in cell & developmental biology* **32,** 85–97. ISSN: 1096-3634 (Aug. 2014).

38. Kaartinen, V. *et al.* Abnormal lung development and cleft palate in mice lacking TGF-beta 3 indicates defects of epithelial-mesenchymal interaction. *Nature genetics* **11,** 415–21. ISSN: 1061-4036 (Dec. 1995).

39. Azhar, M. *et al.* Transforming growth factor beta in cardiovascular development and function. *Cytokine Growth Factor Rev* **14,** 391–407. ISSN: 1359-6101 (Oct. 2003).

40. Doetschman, T. *et al.* Generation of mice with a conditional allele for the transforming growth factor beta3 gene. *Genesis (New York, N.Y. : 2000)* **50,** 59–66. ISSN: 1526-968X (Jan. 2012).

41. Azhar, M. *et al.* Ligand-specific function of transforming growth factor beta in epithelial-mesenchymal transition in heart development. *Developmental dynamics : an official publication of the American Association of Anatomists* **238,** 431–42. ISSN: 1058-8388 (Feb. 2009).

42. Worthington, J. J., Klementowicz, J. E. & Travis, M. A. TGFβ: a sleeping giant awoken by integrins. English. *Trends in biochemical sciences* **36,** 47–54. ISSN: 0968-0004 (Jan. 2011).

43. Yang, Z. *et al.* Absence of integrin-mediated TGFbeta1 activation in vivo recapitulates the phenotype of TGFbeta1-null mice. *The Journal of cell biology* **176,** 787–93. ISSN: 0021-9525 (Mar. 2007).

44. Lindsay, M. E. & Dietz, H. C. Lessons on the pathogenesis of aneurysm from heritable conditions. *Nature* **473,** 308–16. ISSN: 1476-4687 (May 2011).

45. Gallo, E. M. *et al.* Angiotensin II-dependent TGF-beta signaling contributes to Loeys-Dietz syndrome vascular pathogenesis. *Journal of Clinical Investigation* **124,** 448–460. ISSN: 00219738 (2014).

Chapter 3

Candidate gene resequencing in a large bicuspid aortic valve-associated thoracic aortic aneurysm cohort: *SMAD6* as an important contributor

Elisabeth Gillis[1], Ajay Anand Kumar[1], Ilse Luyckx[1], Christoph Preuss[2], Elyssa Cannaerts[1], Gerarda van de Beek[1], Björn Wieschendorf[1,3], Maaike Alaerts[1], Nikhita Ajit Bolar[1], Geert Vandeweyer[1], Josephina Meester[1], Florian Wünnemann[2], Russell A. Gould[4], Rustam Zhurayev[5], Dmytro Zerbino[5], Salah A Mohamed[3], Seema Mittal[6], Luc Mertens[6], Hanna M. Björck[7], Anders Franco-Cereceda[8], Andrew S. McCallion[4], Lut Van Laer[1], Judith M. A. Verhagen[9], Ingrid M. B. H. van de Laar[9], Marja W. Wessels[9], Emmanuel Messas[10], Guillaume Goudot[10], Michaela Nemcikova[11], Alice Krebsova[12], Marlies Kempers[13], Simone Salemink[13], Toon Duijnhouwer[13], Xavier Jeunemaitre[10], Juliette Albuisson[10], Per Eriksson[7], Gregor Andelfinger[2], Harry C. Dietz[4,14], Aline Verstraeten[1], Bart L. Loeys[1,13,*], and Mibava Leducq Consortium

1 Faculty of Medicine and Health Sciences, Center of Medical Genetics, University of Antwerp and Antwerp University Hospital, Antwerp, Belgium

2 Cardiovascular Genetics, Department of Pediatrics, CHU Sainte-Justine, Université de Montreal, Montreal, QC, Canada

3 Department of Cardiac and Thoracic Vascular Surgery, University Hospital Schleswig-Holstein, Lübeck, Germany

4 McKusick-Nathans Institute of Genetic Medicine, Johns Hopkins University School of Medicine, Baltimore, MD, United States

5 Department of Clinical pathology, Lviv National Medical University after Danylo Halytsky, Lviv, Ukraine

6 Cardiovascular Research, SickKids University Hospital, Toronto, ON, Canada

7 Cardiovascular Medicine Unit, Department of Medicine, Karolinska Institute, Stockholm, Sweden

8 Cardiothoracic Surgery Unit, Department of Molecular Medicine and Surgery, Karolinska Institute, Stockholm, Sweden

9 Department of Clinical Genetics, Erasmus University Medical Center, Rotterdam, Netherlands

10 Assistance Publique–Hôpitaux de Paris, Hôpital Européen Georges Pompidou; Université Paris Descartes, Paris Sorbonne Cité; Institut National de la Santé et de la Recherche Médicale, UMRS, Paris, France

11 Department of Biology and Medical Genetics, 2nd Faculty of Medicine-Charles University and Motol University Hospital, Prague, Czechia

12 Institute of Clinical and Experimental Medicine, Prague, Czechia

13 Department of Human Genetics, Radboud University Medical Centre, Nijmegen, Netherlands

14 Howard Hughes Medical Institute, Baltimore, MD, United States

Contribution: Targeted resequencing, data analysis and filtering, validation by Sanger sequencing, segregation analysis

3.1 Abstract

Bicuspid aortic valve (BAV) is the most common congenital heart defect. Although many BAV patients remain asymptomatic, at least 20% develop thoracic aortic aneurysm (TAA). Historically, BAV-related TAA was considered as a hemodynamic consequence of the valve defect. Multiple lines of evidence currently suggest that genetic determinants contribute to the pathogenesis of both BAV and TAA in affected individuals. Despite high heritability, only very few genes have been linked to BAV or BAV/TAA, such as *NOTCH1*, *SMAD6*, and *MAT2A*. Moreover, they only explain a minority of patients. Other candidate genes have been suggested based on the presence of BAV in knockout mouse models (e.g.,*GATA5*, *NOS3*) or in syndromic (e.g., *TGFBR1/2*, *TGFB2/3*) or non-syndromic (e.g., *ACTA2*) TAA forms. We hypothesized that rare genetic variants in these genes may be enriched in patients presenting with both BAV and TAA. We performed targeted resequencing of 22 candidate genes using Haloplex target enrichment in a strictly defined BAV/TAA cohort (n = 441; BAV in addition to an aortic root or ascendens diameter ≥ 4.0 cm in adults, or a Z-score ≥ 3 in children) and in a collection of healthy controls with normal echocardiographic evaluation (n = 183). After additional burden analysis against the Exome Aggregation Consortium database, the strongest candidate susceptibility gene was *SMAD6* (p = 0.002), with 2.5% (n = 11) of BAV/TAA patients harboring causal variants, including two nonsense, one in-frame deletion and two frameshift mutations. All six missense mutations were located in the functionally important MH1 and MH2 domains. In conclusion, we report a significant contribution of *SMAD6* mutations to the etiology of the BAV/TAA phenotype.

3.2   Introduction

With a prevalence of 1–2% in the general population, bicuspid aortic valve (BAV) is the most common congenital heart defect. It has a 3:1 male preponderance and is characterized by an aortic valve with two cusps instead of the normal three. BAV often coincides with aortic manifestations such as coarctation of the aorta and thoracic aortic aneurysm (TAA)[1]. The latter can lead to lethal dissections if left untreated. Although first described over 400 years ago and high heritability (89%)[2], the genetic etiology of BAV, with or without TAA, remains largely elusive. It was initially suggested that TAA results from altered blood flow dynamics imposed by the abnormal bicuspid valve. Changes in shear stress were presumed to weaken the aortic wall, resulting in dilatation and rupture. At present, common genetic risk factors for BAV and TAA are proposed[3], based on the following observations: (i) the aortic valve and the aorta share common embryologic origins (i.e., the cardiac neural crest (CNC) and the second heart field)[4] (ii) family members of BAV/TAA probands show TAA without valve abnormalities and/or BAV without aneurysmal disease[5], and (iii) TAA formation in BAV probands that previously underwent valve replacement has been reported[6].

Transmission of BAV/TAA mostly complies with an autosomal dominant inheritance pattern, displaying reduced penetrance and variable expressivity[7, 8]. Few genes have been robustly linked to the BAV phenotype to date. *NOTCH1* is often considered the sole established BAV gene, either as an isolated finding or in association with early onset valve calcification, TAA, or other left-sided heart defects[9–16]. *SMAD6*[17] and *MAT2A*[18] have also been implicated in BAV, but only in a very limited number of patients. A dozen candidate genes emanated from knockout mouse models with increased BAV occurrence[19–25]. The prevalence of BAV in these knockoutmodels is often low (range: 2–42% in single knockouts) (Table 3.1), probably due to reduced penetrance and/or activation of compensatory mechanisms. Mutations in some syndromic[26–31] or non-syndromic[32] TAA genes also associate with increased BAV occurrence (Table 3.1).

To date, no major BAV/TAA gene has emerged. The described genes have been

associated with BAV, but their contribution to the etiology of BAV/TAA has never been examined systematically. Here, we evaluate this contribution in 22 BAV-associated genes (Table 3.1) using a targeted gene panel and and variant burden approach.

Table 3.1: Genes included in the targeted gene panel and criteria on which their selection was based.

Context	Genes	Incidence	References
BAV in humans	NOTCH1	Mutations found in 27 BAV patients	[9–16]
	SMAD6	Mutations found in 2 BAV patients	[17]
	MAT2A	Mutations found in 1 BAV patient	[18]
BAV in mice	ACVR1	BAV in 78-83% of $\text{Alk2}^{FXKO}/\text{Gata5}^{-Cre+}$ mice	[23]
	GATA4	BAV in 43% of $\text{Gata4}^{+/-};\text{Gata5}^{+/-}$ mice	[21]
	GATA5	BAV in 25% of $\text{Gata5}^{-/-}$ mice	[22]
	GATA6	BAV in 25% $\text{Gata5}^{+/-};\text{Gata6}^{+/-}$ mice	[21]
	MATR3	BAV in 12% in $\text{Matr3}^{+/-}$ mice	[25]
	NKX2-5	BAV in 2–20% of $\text{Nkx2-5}^{+/-}$ mice	[19]
	NOS3	BAV in 42% of $\text{Nos3}^{-/-}$ mice	[20]
	ROBO1	BAV in 100% of $\text{Robo1}^{-/-};\text{Robo2}^{-/-}$ mice	[24]
	ROBO2	BAV in 100% of $\text{Robo1}^{-/-};\text{Robo2}^{-/-}$ mice	[24]
BAV in (non)syndromic TAA cases	FBN1	Occasional BAV in Marfan syndrome	[26, 29, 31]
	ACTA2	7% BAV in non-syndromic TAA	[32]
	ELN	Occasional BAV in cutis laxa	[27]
	FLNA	Occasional BAV in X-linked valve disease	[33]

Context	Genes	Incidence	References
	MYH11	Occasional BAV in non-syndromic TAA	Personal observation
	SMAD3	3–11% BAV in Loeys-Dietz syndrome	[30]
	TGFB2	8–13% BAV in Loeys-Dietz syndrome	[28]
	TGFB3	4% BAV in Loeys-Dietz syndrome	Personal observation
	TGFBR1	8–12% BAV in Loeys-Dietz syndrome	Personal observation
	TGFBR2	8–12% BAV in Loeys-Dietz syndrom	Personal observation

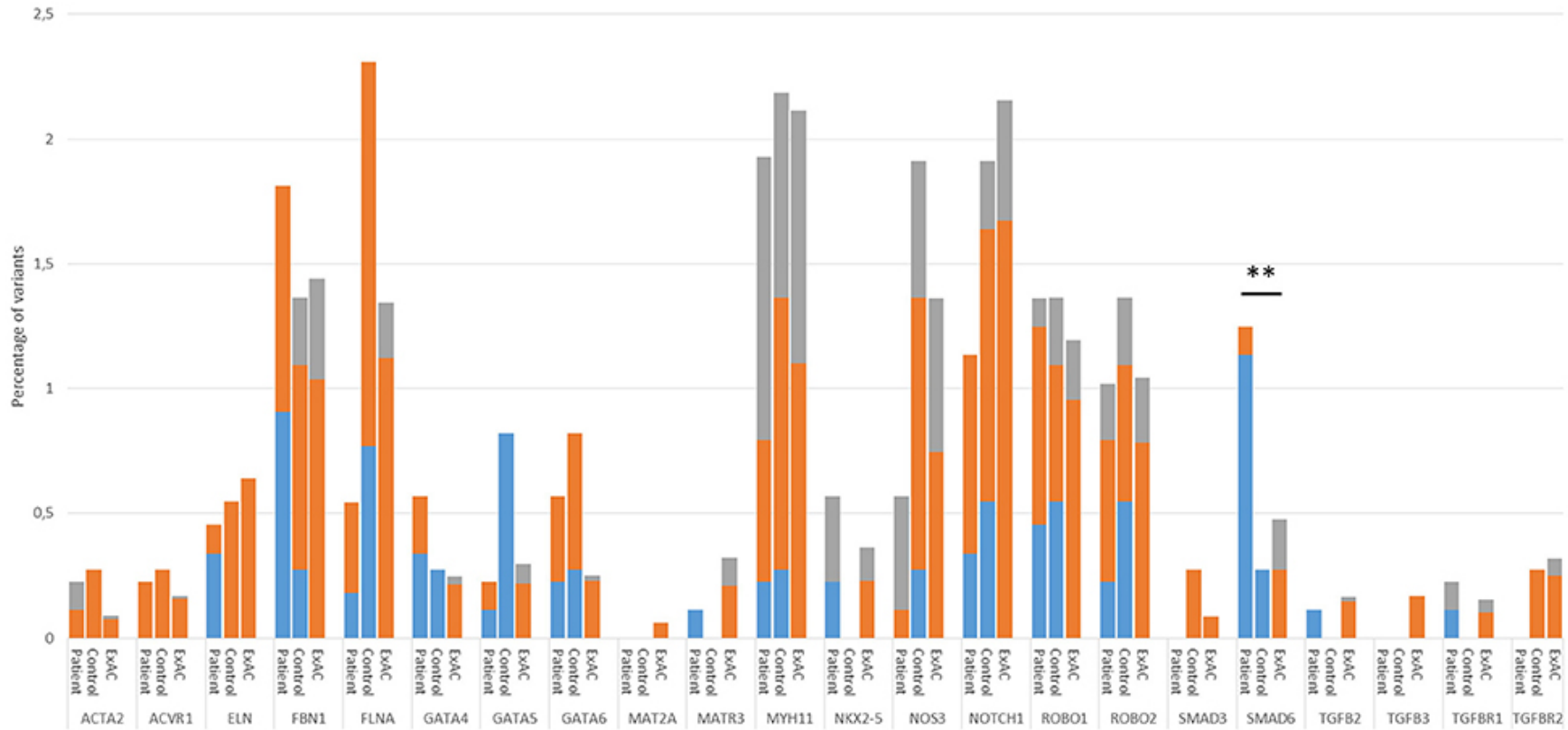BAV Bicuspid aortic valve; TAA Thoracic aortic aneurysm.

Figure 3.1: Proportion of variant alleles per gene in the patient group, control group and ExAC cohort. Variants were selected as follows: First, we selected heterozygous coding or splice site variants with an allelic balance between 0.25 and 0.85 (FLNA in males: 0.75-1) and a minimum coverage of 10×. Next, we made three variant groups based on their frequency in the ExAC database; that is, variants that are absent from the ExAC control dataset (blue), variants with an ExAC MAF lower than 0.01% (orange) and variants with an ExAC MAF between 0.01% and 0.1% that had a CADD score above 20 (gray). Only statistics of the patient-ExAC comparison are shown (∗∗ p ≤ 0.01). No statistically significant differences in allele frequencies were observed between our control cohort and the ExAC controls. Abbreviations: ExAC, Exome Aggregation Consortium; MAF, Minor Allele frequency; CADD, Combined Annotation Dependent Depletion.

3.3 Materials and methods

3.3.1 Study cohort

Genomic DNA (gDNA) of 441 BAV/TAA patients was collected through a collaborative effort involving 8 different centers (Supplementary Table 3.1). Patients were selected based on the presence of BAV and either an aortic diameter at the sinus of Valsalva or the ascending aorta of at least 4.0 cm in adults, or a Z-score exceeding 3 in children. Aortic diameter dimensions were determined using echocardiography, computed tomography or magnetic resonance imaging. A positive family history was defined as having at least one first- or second-degree relative with BAV and/or TAA. Control gDNA was obtained from 183 cancer patients who presented at the SickKids Hospital, Toronto, Canada. None of the controls showed structural heart disease upon examination with echocardiography. All study participants or their legal guardians gave informed consent at the respective sample-contributing centers.

3.3.2 Targeted enrichment

Genes (n = 22) were selected for targeted resequencing based on the following criteria: (i) mutations occur in human BAV cases (n = 3), (ii) knockout mouse models present with incomplete penetrance of BAV (n = 9), and (iii) occasional or increased BAV manifestation occurs in patients with mutations in known TAA genes (n = 10) (Table 3.1). Enrichment of all exons of these candidate genes, including ± 10 nucleotides of adjacent intronic sequence, was performed with a custom Haloplex target enrichment kit per instructions of the manufacturer (Agilent Technologies, USA). Probe design covered a theoretical 99.7% of the complete target region (560 kb). Pooled samples were sequenced either on a HiSeq 2500 (Illumina, USA) with $2 \times$ 150 bp reads or on a HiSeq 1500 (Illumina, USA) with 2×100 bp reads.

3.3.3 Data analysis and filtering

The raw data were processed using an in-house-developed Galaxy-based pipeline, followed by variant calling with the Genome Analysis Toolkit Unified Genotyper[34].

Variants were subsequently annotated and filtered with the in-house developed database VariantDB[35],which uses ANNOVAR. Heterozygous coding or splice site (±2 bp from exon-intron boundaries for nucleotide substitution, and ±5 bp for multi-bp deletions or insertions) variants with an allelic balance between 0.25 and 0.85 (*FLNA* in males: 0.75–1) and a minimum coverage of 10 reads were selected. Finally, we included variants that fitted within at least one of the following three categories; unique variants [absent in the Exome Aggregation Consortium (ExAC) database[36]], variants with an ExAC Minor Allele Frequency (MAF) lower than 0.01% or variants with an ExAC MAF between 0.01% and 0.1% that had a Combined Annotation Dependent Depletion (CADD)[37] score above 20. All splice region variants underwent splice site effect prediction using ALAMUT (Interactive Biosoftware, France). Synonymous variants outside of splicing regions were not taken into account.

The ExAC database was used as an independent control dataset. The raw data of variants (∼all ExAC datasets) fulfilling ExAC's quality control parameters ("PASS") were extracted from the offline version of ExAC v0.3.1. Since the ExAC variants were annotated using VEP, whereas our patient variant annotation was ANNOVAR-based, we re-annotated the ExAC variants with ANNOVAR. The same variant filtering strategy as described for the patient cohort was subsequently applied. For each selected ExAC variant, the allele frequency was determined by computing the ratio of the Mutant Allele Count (mAC) and Total Allele Count (tAC). Next, we re-scaled each variant's mAC by multiplying its computed allele frequency by its respective tAC Adj, i.e., the tAC average of all variants in that specific gene. Finally, the variant counts for each panel gene were obtained by summing up the re-scaled mACs.

3.3.4   Validation by Sanger Sequencing

Variants discussed in the results section were confirmed with Sanger sequencing. Primers were designed using Primer3 software[38] v4.0.0 and polymerase chain reaction (PCR) products were purified with Calf Intestinal Alkaline Phosphatase (Sigma-Aldrich, USA). Sequencing reactions were performed using the BigDye Terminator Cycle Sequencing kit (Applied Biosystems, Life Technologies, USA), followed by

capillary electrophoresis on an ABI3130XL (Applied Biosystems, Life Technologies, USA). The obtained sequences were analyzed with CLC DNA Workbench v5.0.2 (CLC bio, Denmark).

3.3.5 Segregation Analysis

When family members were available, Sanger sequencing of the *SMAD6* variants identified in the proband was performed in additional relatives to check if the phenotype segregated with the variant.

3.3.6 Statistical Analysis

We performed burden analyses comparing frequencies of the variants fulfilling the three criteria that were mentioned in "Section Data Analysis and Filtering" between patients and controls. Whereas the Fisher's Exact Test was used to statistically compare variant frequencies in the patient cohort to those in the study control cohort, the Chi-Square Test with Yates' correction was used for the patient-ExAC comparison. No p-values were calculated if the number of variants in patients and/or controls was zero. Fisher's Exact statistics were also used to determine if significant variant type enrichment and/or domain clustering of variants occurs in patients. Statistical significance was considered when $p < 0.05$.

3.4 Results

The patient cohort consisted of 441 BAV/TAA patients (75% males and 25% females) with an average age at inclusion of 63.5 ± 14.4 years. For these patients, the most common associated feature was coarctation of the aorta (2.9%, n = 13). About 3% (n = 14) had other additional findings such as mitral valve prolaps, aortic stenosis, dilated cardiomyopathy, aortic insufficiency, patent ductus arteriosus or intracranial aneurysm. 46.7% (n = 206) had a left-right leaflet BAV orientation, 15.9% (n = 70) had a right-non-coronary leaflet BAV orientation and for 37.4% (n = 165) of the patients the subtype of valve leaflet morphology was not specified. A positive family history was known for 9.3% of the patients, whereas for the

remainder the family history was negative or unknown. The study control cohort (n = 183) consisted of 58% males and 42% females. The average age at inclusion of this control cohort was 13.1 ± 5.1 years.

Targeted gene panel sequencing reached an overall coverage at 10x of 99.13% of the targeted regions. In total, 169 variants passed our selection criteria in our patient and control group (Supplementary Table 3.2). Of these, 112 variants were identified in 441 patients. They included 101 missense, 2 nonsense, 2 splice-site, 5 in-frame indel, and 2 frameshift varian ts. The 183 study controls contained 57 variants including 53 missense, 1 nonsense, 2 splice-site, and 1 frameshift variant. After applying the identical filtering criteria to the ExAC control cohort, 15 660 variants were retained in on average 54 940 individuals: i.e., 14 931 missense, 190 splice-site, 72 nonsense, 10 no-stop, 204 frameshift, and 253 in-frame indel variants.

To validate our control cohort, we compared its variant frequencies for the 22 selected candidate genes to those of the ExAC cohort. No significant differences were observed (Figure 1). We then performed a variant burden analysis equating the numbers of patient variants per gene to the numbers found in the control cohort (Table 2). Results are graphically presented in Figure 1, showing the proportion of variants per gene in the three different cohorts. Although a few genes (e.g., *FLNA*) showed trends toward significance when comparing our study patient and control cohort, we decided to focus on the patient-ExAC comparison because of the larger number of controls in the ExAC cohort and hence, higher power. Only *SMAD6* reached significance (p = 0.002) in the patient-ExAC comparison. Remarkably, a protective effect for *NOS3* and *NOTCH1* variants was suggested (p = 0.06 and p = 0.05, respectively).

We identified 11 *SMAD6* variants in 441 patients (2.5%). These included two frameshift deletions, two nonsense mutations, one in-frame deletion, and six missense variants (Figure 3.2). Only a single individual (0.55%) in the study control cohort harbored a *SMAD6* missense variant. The ExAC database harbored 450 *SMAD6* variants in 47,389 individuals (0.9%). Whereas 36.4% (n = 4/11) of the *SMAD6* mutations in the patient cohort were loss of function (LOF; frameshift,

nonsense or splice site) mutations, truncating *SMAD6* mutations were found in only 4.0% (n = 18/450) of the ExAC individuals, demonstrating a clear enrichment in BAV/TAA patients compared to controls (p=0.001).

The *SMAD6* c.726del variant leads to a frameshift (p.Lys242Asnfs*300) and a predicted protein with a C-terminal extension due to loss of the intended stop codon. The c.455_461del frameshift variant (p.Pro152Profs*27) causes the introduction of a premature stop codon, most likely resulting in haploinsufficiency due to nonsense-mediated mRNA decay (NMD). Also the two nonsense variants (p.Tyr279* and p.Tyr288*) are predicted to lead to NMD. All of the missense variants cluster in the functionally important MH1 and MH2 domains[39] (amino acids 148–275 and 331–496, respectively), which is not the case for the sole missense variant (p.Ser130Leu) found in a control individual (Figure 3.2). All but one (p.Arg443His) of the identified variants were absent in the ExAC control cohort (v0.3.1; Supplementary Table 3.2). Moreover, the missense variants in the patient cohort (7/7) are enriched in the MH1 and MH2 domains when compared to ExAC controls (n=228/430; p=0.02).

For two *SMAD6* mutation carriers (P89, p.Gly271Glu; P99, p.Pro152Profs*27), gDNA of family members was available for segregation analysis (Supplementary Figure 3.1). Although neither of these probands had a documented family history of BAV/TAA, a brother of P89 has been diagnosed with a sinus of Valsalva aneurysm (45 mm) and carried the *SMAD6* mutation. The mutation was also observed in an unaffected daughter (age 28) of the proband (Supplementary Figure 3.1). Three unaffected siblings at ages 54, 58, and 64 did not carry the mutation. No gDNA was available from a sister of P99 with unspecified aortic valve problems. The p.Pro152Profs*27 mutation was found in an unaffected daughter (age 39) of P99 but was absent in his 39 year-old unaffected son (Supplementary Figure 3.1).

Intriguingly, two genes (*NOTCH1* and *NOS3*) that previously had been associated with increased BAV risk in humans[9–12] and/or mice[20, 40] revealed borderline significance for protection from BAV/TAA (p = 0.05 and p = 0.06, respectively). Analysis of *NOTCH1* identified 10 variants in patients (2.3%), including two

splice-site variants, vs. seven variants (all missense) in controls (3.8%) and 2,181 (4.3%) variants in ExAC. One variant in the patient cohort (c.5167+3_5167+6del) leads to complete loss of the 5' donor splice site of intron 27, predicted to result in skipping of exon 27 (149 bp) and hence a frameshift. For the second variant (p.S784S), the predicted effect on splicing is more ambiguous. If loss of the 5' donor splice site of intron 14 would occur, skipping of exon 14 (146 bp) would again lead to a frameshift event. Unfortunately, cDNA to reliably determine the precise effect of these mutations on splicing is not available. None of the *NOTCH1* variants that we identified in BAV/TAA patients has previously been reported in the literature. We did not observe any variant-domain clustering or significant differences in CADD scores when comparing the patient and control NOTCH1 variants. Similarly, for *NOS3* a total of five missense variants (1.1%) was found in patients, whereas the control cohort harbored seven variants (3.8%), including one out-of-frame mutation (p.Leu927Hisfs*32). In the ExAC control cohort, 1390 NOS3 variants (2.7%) were found in 51 035 individuals.

Based on statistical analyses of BAV/TAA heritability and the fact that BAV/TAA shows prominent gender bias, oligogenic inheritance of BAV/TAA is an emerging concept[1, 41]. To test for such oligogenic patterns, we determined the number of patients and controls in our study cohort with variants in at least two out of the 22 analyzed genes. In the patient cohort, 10 patients presented with two variants (2.3%), while the control group harbored 7 individuals that carried two variants (3.8%). Based on these data, there is no evidence for a digenic or multigenic model in the analyzed genes (p=0.29).

Table 3.2: Results summary of all genes and number of identified variants

Gene	Number of variants in 882 patient alleles	Number of variants in 366 control alleles	Number) of variants in ExAC alleles	p-value patients-controls	p-value patients-ExAC
ACTA2	2	1	109 in 120631	1.00	0.44
ACVR1	2	1	202 in 120994	1.00	0.98
ELN	4	2	728 in 113954	1.00	0.63

Gene	Number of variants in 882 patient alleles	Number of variants in 366 control alleles	Number) of variants in ExAC alleles	p-value patients-controls	p-value patients-ExAC
FBN1	16	5	1740 in 120988	0.81	0.43
FLNA	3*	6*	1133 in 84359*	**0.03**	0.15
GATA4	5	1	260 in 105980	0.68	0.11
GATA5	2	3	259 in 86819	0.15	0.94
GATA6	5	3	240 in 95775	0.70	0.13
MAT2A	0	0	74 in 116667	/	/
MATR3	1	0	382 in 119089	/	0.43
MYH11	17	8	2513 in 119001	0.82	0.79
NKX2-5	5	0	360 in 98978	/	0.47
NOS3	5	7	1390 in 102070	0.05	0.06
NOTCH1	10	7	2181 in 101245	0.29	0.05
ROBO1	12	5	1354 in 113390	1.00	0.77
ROBO2	9	5	1245 in 119282	0.57	0.95
SMAD3	0	1	95 in 111500	/	/
SMAD6	11	1	450 in 94779	0.20	**0.002**
TGFB2	1	0	192 in 117070	/	0.71
TGFB3	0	0	205 in 121315	/	/
TGFBR1	2	0	181 in 118320	/	0.90
TGFBR2	0	1	366 in 115147	/	/

Variant burden analyses were performed comparing frequencies of the variants fulfilling the three criteria that were mentioned in "Section Data Analysis and Filtering" between patients and controls. Whereas, the Fisher's Exact Test was used to statistically compare variant frequencies in the patient cohort to those in the study control cohort, the Chi-Square Test with Yates' correction was used for the patient-ExAC comparison. No p-values were calculated if the number of variants in patients and/or controls was zero. Statistical significance was considered when $p < 0.05$. The asterisks denote that in these cases the number of alleles is consistent with the number of X-chromosomes, i.e., 553 patient alleles and 260 control alleles were checked for variants. Statistically significant p-values are represented in bold.
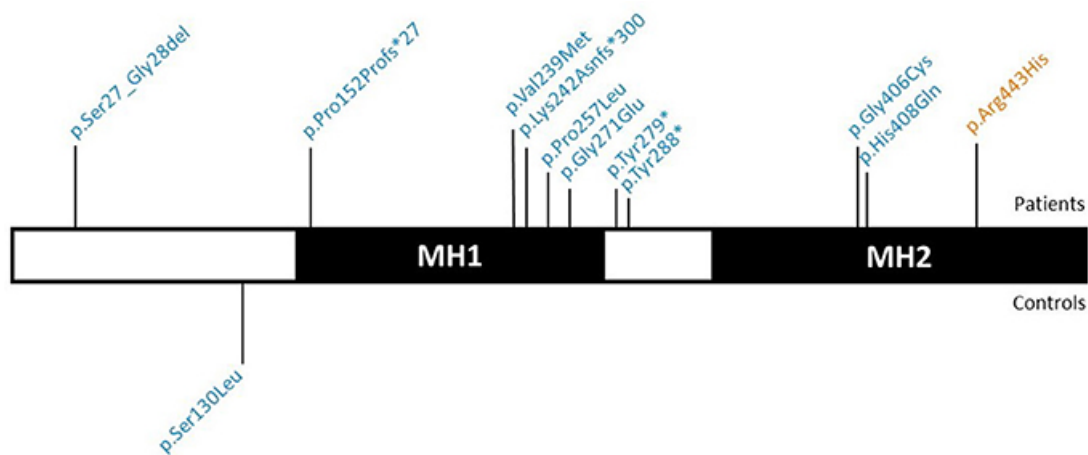
Figure 3.2: Graphical representation of the identified *SMAD6* variants. SMAD6 has two major protein domains, a DNA-binding MH1 domain and a MH2 domain that interacts with components of the TGF-β and BMP signaling pathways. Variants above the protein have been found in patients, while those below the protein occurred in control individuals. Variants in blue are absent from the ExAC database, variants in orange have an ExAC MAF below 0.01%. Abbreviations: TGF-β, Transforming growth factor-β; BMP, Bone morphogenetic protein; ExAC, Exome Aggregation Consortium; MAF, Minor Allele frequency.

3.5 Discussion

So far, no gene with a contribution of more than 1% to BAV or BAV/TAA has been identified in humans. Gene identification has been hampered by low penetrance, variable clinical expressivity, the likelihood of BAV-phenocopies within individual families and, most likely, substantial locus heterogeneity[1]. *NOTCH1* has been suggested as a BAV(/TAA) gene, but does not contribute greatly to disease etiology. About 20 other genes have been associated with BAV in humans and mice (Table 3.1), but few of them also showed association with TAA. This suggests that whereas some disease genes might be linked to both BAV and TAA, others increase risk for only one of the component phenotypes. In this study, we used a targeted gene panel approach to study the prevalence of mutations in genes that previously have been associated with BAV and/or TAA in people or mice in a cohort of BAV/TAA patients. In total, 22 genes were sequenced in 441 BAV/TAA patients and 183 controls. *SMAD6* was identified as the most important known gene in the etiology of BAV with associated TAA. With 11 mutation-carrying probands, *SMAD6* offers a molecular explanation for 2.5% of

our study population. For two of the variants segregation analysis in relatives could be performed, revealing the presence of one of the respective *SMAD6* mutations in a TAA patient and two rather young individuals (age 28 & 39) that might still develop TAA later in life. Four unaffected individuals (age 37, 54, 58, 64) did not carry a *SMAD6* mutation. As two nonsense and two frameshift *SMAD6* variants in our cohort are predicted to lead to haploinsufficiency, LOF is the most likely mechanism. All the patient-specific missense variants (n = 7) are in the functionally important MH1 and MH2 domains of SMAD6[39]. LOF missense mutations in *SMAD2* and *SMAD3* causing Loeys-Dietz syndrome, another syndromic TAA form, are also located in the MH1 and MH2 domains[42, 43]. The MH1 domain of SMAD6 binds DNA[44], while the MH2 domain interacts with key components of the transforming growth factor (TGF-β) and bone morphogenetic protein (BMP) signaling cascades[45–47]. In 2012, two missense variants in the MH2 domain of SMAD6 were identified in two patients with BAV in association with mild to moderate aortic stenosis[17]. Interestingly, in our cohort one *SMAD6* patient (p.Tyr288*) presented with coarctation in addition to BAV and TAA. Moreover, mice lacking expression of the murine orthologue of *SMAD6*, i.e., *Madh6*$^{-/-}$ mice, also present with cardiovascular pathologies, including abnormal vascular smooth muscle cell relaxation, thickening of the cardiac valves and misplaced septation and ossification of the outflow tract (OFT)[48]. As such, our findings confirm a role for *SMAD6* mutations in the etiology of BAV and expand the spectrum of *SMAD6*-related cardiovascular manifestations with BAV-related TAA.

SMAD6 is highly expressed in the cardiac valves and OFT of the embryonic heart, in the late-embryonic, and adult vascular endothelium as well as in the vascular smooth muscle cells of the adult aortic root[48, 49]. Upregulation in response to laminar shear stress has been reported[50]. *SMAD6* encodes an inhibitory SMAD protein which negatively regulates BMP signaling by binding to BMP type I receptors or by establishing competitive interactions for SMAD4[51, 52]. In doing so, SMAD1/5/8 phosphorylation and/or nuclear translocation are prevented. Additionally, SMAD6 cooperates with SMURF E3 ubiquitin ligases to prime ubiquitin-mediated proteasomal degradation of BMP receptors and SMAD effector proteins[53], including SMAD1 and 5. BMP signaling has previously been independently implicated in BAV- and TAA-related processes[54, 55]. In addition

to mediating CNC cell migration into the cardiac cushions and differentiation to smooth muscle cells, BMP signaling promotes endothelial-to-mesenchymal transition and instigates mesenchymal cell invasion[55, 56]. While SMAD6 and SMAD7 are thought to have a predominant negative regulatory effect on BMP and TGF-β signaling, respectively, there is strong evidence that this specificity is not absolute and that SMAD6 can directly suppress the TGF-β signaling cascade. Important crosstalk between BMP, TGF-β and NOTCH signaling has been reported[55]. Many syndromic forms of TAA are caused by mutations in genes encoding effectors or regulators of the TGF-β signaling pathway (including *TGFB2/3*, *TGFBR1/2*, *SMAD2/3*, *SKI*)[28, 42, 43, 57–61], with increased activity observed in aortic specimens from people and mice with these conditions. An increased prevalence of BAV has been observed in patients carrying mutations in these genes (Table 3.1). Overall, these results imply that mutations in *SMAD6* likely cause BAV/TAA through impaired negative regulation of BMP and/or TGF-β signaling.

Multiple studies have previously reported a link between *NOTCH1* mutations and BAV[9–12]. In 2005, a nonsense and a frameshift *NOTCH1* mutation were found to segregate with BAV associated with early onset valve calcification in the respective families[10]. Since the initial report, multiple *NOTCH1*, mostly missense, variants have been associated with BAV, BAV/TAA, aortic valve stenosis, coarctation, and hypoplastic left heart[9, 11, 12, 15, 62–64]. In addition to these mutations in association with left-sided heart defects, frameshift and nonsense mutations were also identified in patients with right-sided heart defects affecting the pulmonary valve and conotruncal disease including pulmonary atresia with intact ventricular septum, tetralogy of Fallot, and truncus arteriosus, and other congenital heart diseases, such as anomalous pulmonary venous return, atrial septal defect, and ventricular septal defect[16]. Mouse models have confirmed a role for Notch1 in the development of the aortic valve and the cardiac OFT[65]. Unexpectedly, in our dataset *NOTCH1* did not stand out as a prominent BAV/TAA gene, with the suggestion that *NOTCH1* variants might even be protective. Sample selection bias might contribute to this observation as *NOTCH1* variants appear to associate with early and severe valve calcification and seem to be enriched in families with highly penetrant BAV but far lower penetrance of TAA[13]. Given that our study did not select for valve calcification and prioritized the BAV/TAA phenotype, it is understandable

that *NOTCH1* variants would be underrepresented. It also seems notable that only missense variants were seen in controls, while multiple variants in the patient cohort are predicted to have a more overt impact on protein expression and function.

Similarly, our variant burden test suggested that *NOS3* variants might be protective for BAV/TAA development. NOS3, the endothelial specific nitric oxide (NO) synthase, is important in balancing NO production and in the reduction of oxidative stress[66]. Its role in cardiac development is demonstrated by the formation of BAV in *Nos3*-targeted mice (Table 3.1). Furthermore, it has already been shown that specific *NOS3* polymorphisms can affect NO production[67], and increased NO levels have been found in a MFS mouse model and in *Adamts1*-deficient mice that develop TAA[68]. Pharmacological inhibition of NOS2 in mice led to a protective effect in aortic aneurysm development[68]. This supports the importance of NO levels and nitric oxide synthases in aneurysm pathology. The variants in *NOS3* identified in the current study may lead to less active NOS3 and as such may protect against development of aortic aneurysm.

Our study has several methodological limitations: (i) The small number of genes included in our study, as well as the patient cohort size, precludes the ability to detect oligogenic inheritance or gene-gene interactions involved in BAV/TAA. An extended experiment in a larger BAV/TAA cohort, including BAV-related pathways instead of selected genes, could give us more insight regarding how genes work together in BAV and/or TAA development; (ii) The size of the patient and study/ExAC control cohort only allows us to detect BAV/TAA genes with a fairly large contribution (variant burden in patients: $\geq 3\%$ & $\geq 2\%$, respectively); (iii) The control cohort consists of younger, adolescent patients that did not show cardiac complications at the time of investigation but may still develop complications such as TAA later-on in life. Therefore, the ExAC database was used as an additional dataset for allele frequencies in a cohort without gross developmental defects.

Our study specifically assesses the presence of pathogenic variants in BAV-associated genes in a large BAV/TAA cohort. We conclude that *SMAD6* is currently the most important contributor to the genetic architecture of BAV/TAA. More research

and larger cohorts will be needed to fully elucidate the genetic architecture of this common but complex cardiovascular pathology.

3.6   Supplementary material
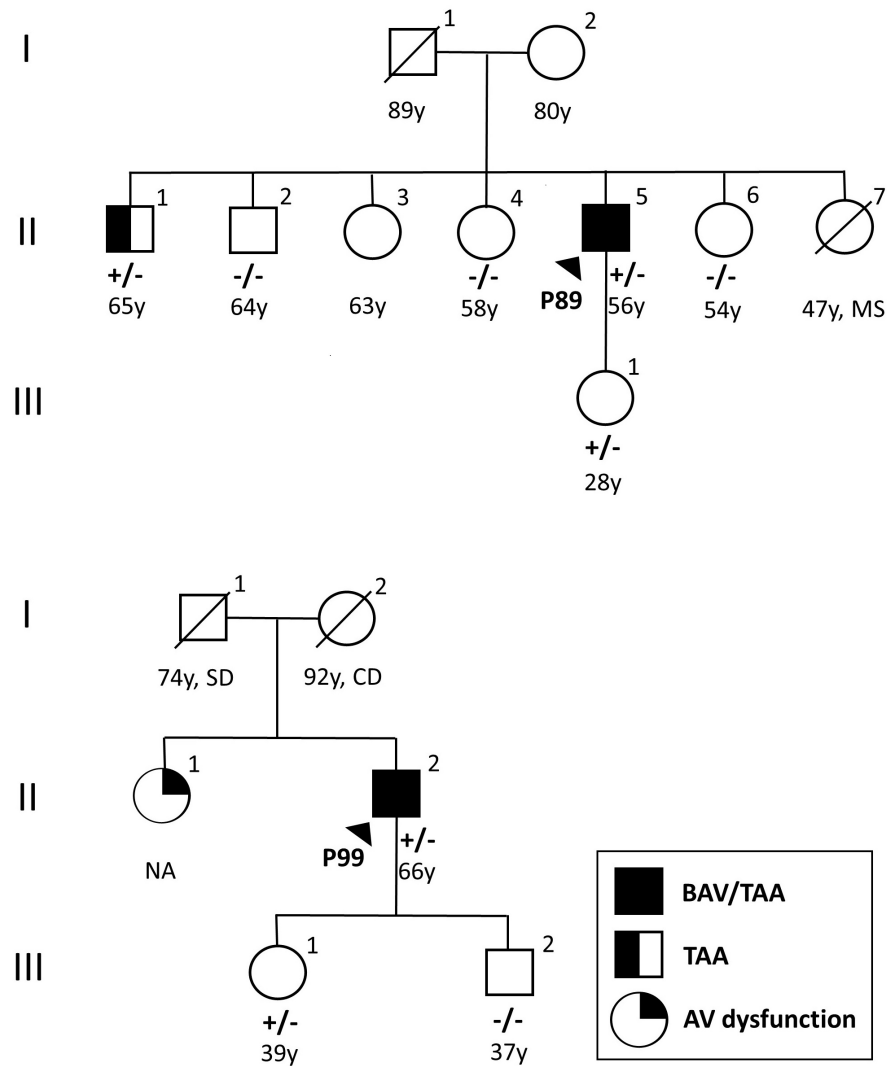
Supplementary Figure 3.1: Family pedigrees for the two *SMAD6* mutation carriers (P89, p.Gly271Glu; P99, p.Pro152Profs*27)

Supplementary Table 3.1: Patient cohort overview

Centre	City, Country	#
Radboud University Medical Centre	Nijmegen, the Netherlands	27
APHP-Hôpital Européen Georges Pompidou	Paris, France	59
Erasmus University Medical Center	Rotterdam, the Netherlands	30
University of Luebeck	Luebeck, Germany	87
Institute for Clinical and Experimental Medicine	Prague, Czech Republic	16
Sickkids Hospital	Toronto, Canada	62
Karolinska University Hospital, Karolinska Institutet	Stockholm, Sweden	156
Lviv National Medical University after Danylo Halytsky	Lviv, Ukraine	4
Total		441

Supplementary Table 3.2: Overview of the identified variants in the genes from the targeted gene panel and their phenotypic data.

Gene	ID	Sex	BAV type	Nucleotide change	Protein change	Classification	MAF ExAC	CADD score
ACTA2	P11	M	NA	c.678A>C	p.Glu226Asp	Missense	1/121150	15.8
	P281	M	L-R	c.977C>A	p.Thr326Asn	Missense	16/121284	21.2
	C102	F	TAV	c.959C>T	p.Thr320Met	Missense	7/121328	19.1
ACVR1	P25	F	NA	c.636G>C	p.Glu212Asp	Missense	5/121074	18.7
	P286	M	R-N	c.718C>T	p.Arg240Cys	Missense	1/121392	19.8
	C172	M	TAV	c.1394C>T	p.Pro465Leu	Missense	7/121410	23.9
ELN	P311	F	L-R	c.1114_1125del	p.Ala372_Lys375del	In-frame deletion	Absent	/
	P349	M	NA	c.1114_1125del	p.Ala372_Lys375del	In-frame deletion	Absent	/
	P179	F	R-N	c.1421_1422insTC CTGGTGTCG GCGTGGC	p.Pro475_Ala480dup	In-frame duplication	Absent	/
	P381	F	L-R	c.1909G>A	p.Ala637Thr	Missense	1/17222	12.2
	C165	M	TAV	c.1021G>A	p.Val341Ile	Missense	4/121176	0
	C95	F	TAV	c.1883G>C†	p.Gly628Ala	Missense	6/111550	11.8
FBN1	P117	F	NA	c.1158C>G	p.Asn386Lys	Missense	8/119050	13.8
	P126	M	NA	c.1472T>C	p.Val491Ala	Missense	Absent	16
	P227	F	L-R	c.1651G>A	p.Gly551Ser	Missense	1/121162	36

Gene	ID	Sex	BAV type	Nucleotide change	Protein change	Classification	MAF ExAC	CADD score
	P431	M	L-R	c.2115G>A	p.Ala705Ala	Splice site	Absent	11.5
	P287	M	R-N	c.2315A>G	p.Asn772Ser	Missense	Absent	23.7
	P174	M	R-N	c.3142A>G	p.Ile1048Val	Missense	Absent	18.8
	P28	M	NA	c.3382G>A	p.Val1128Ile	Missense	Absent	8.4
	P132	M	NA	c.3797A>T	p.Tyr1266Phe	Missense	12/121316	12.5
	P137	F	NA	c.4340T>C	p.Ile1447Thr	Missense	Absent	19
	P196	M	NA	c.4609G>T	p.Asp1537Tyr	Missense	Absent	22.1
	P426	M	NA	c.4727T>C	p.Met1576Thr	Missense	10/121398	6.5
	P117	F	NA	c.5123G>A	p.Gly1708Glu	Missense	1/121388	23.7
	P85	F	NA	c.6595G>A	p.Gly2199Ser	Missense	1/121280	36
	P332	M	L-R	c.6783A>C	p.Lys2261Asn	Missense	4/121108	16
	P150	F	R-N	c.7846A>G	p.Ile2616Val	Missense	8/121320	3
	P41	M	NA	c.8232G>C	p.Gln2744His	Missense	Absent	8.4
	C32	M	TAV	c.185G>A	p.Arg62His	Missense	7/119890	17
	C28	M	TAV	c.716T>C	p.Ile239Thr	Missense	2/121008	13.8
	C55	F	TAV	c.1118C>T	p.Ala373Val	Missense	1/121226	9.2
	C29	M	TAV	c.6163+2dupT	/	Splice site	Absent	/
	C167	M	TAV	c.6832C>G	p.Pro2278Ala	Missense	19/121266	25.7
FLNA	P209	F	L-R	c.2906T>C	p.Leu969Pro	Missense	4/86745	20.3
	P434	M	R-N	c.5908G>A	p.Asp1970Asn	Missense	Absent	23.5
	P51	M	NA	c.7172G>A	p.Arg2391His	Missense	7/86932	18.2
	C160	F	TAV	c.C901C>T	p.Arg301Trp	Missense	6/85694	11.6
	C132	F	TAV	c.1270A>G	p.Met424Val	Missense	2/85774	0.1

Gene	ID	Sex	BAV type	Nucleotide change	Protein change	Classification	MAF ExAC	CADD score
	C136	F	TAV	c.2738G>C	p.Gly913Ala	Missense	2/86788	11.8
	C55	F	TAV	c.3346G>C	p.Asp1116His	Missense	Absent	19.4
	C81	M	TAV	c.4520A>G	p.Gln1507Arg	Missense	Absent	18.2
	C167	M	TAV	c.4711G>A	p.Asp1571Asn	Missense	2/82272	35
GATA4	P339	M	L-R	c.142G>T	p.Val48Leu	Missense	Absent	0.2
	P370	M	NA	c.173G>T	p.Gly58Val	Missense	Absent	10.2
	P177	M	L-R	c.611A>G	p.Asn204Ser	Missense	Absent	5
	P29	M	NA	c.939G>T	p.Glu313Asp	Missense	8/120012	16.5
	P30	M	NA	c.939G>T	p.Glu313Asp	Missense	8/120012	16.5
	C155	M	TAV	c.175G>T	p.Ala59Ser	Missense	Absent	0
GATA5	P438	M	L-R	c.472C>T	p.Pro158Ser	Missense	Absent	15.4
	P98	F	NA	c.616G>A	p.Gly206Ser	Missense	0.00003	36
	C161	F	TAV	c.287C>G	p.Ala96Gly	Missense	Absent	3.9
	C104	M	TAV	c.395G>A	p.Arg132Gln	Missense	Absent	16.1
	C152	F	TAV	c.1153G>T	p.Ala385Ser	Missense	Absent	0
GATA6	P138	M	NA	c.148G>A	p.Gly50Arg	Missense	1/95966	18.8
	P395	F	NA	c.271C>T	p.Pro91Ser	Missense	6/73362	12
	P133	M	NA	c.706G>T	p.Gly236Cys	Missense	Absent	11.5
	P289	M	L-R	c.968_976delACCACCACC	p.His324_His326del	In-frame deletion	Absent	0
	P98	F	NA	c.1555A>G	p.Thr519Ala	Missense	3/121370	12.4
	C166	M	TAV	c.89G>A	p.Arg30Gln	Missense	1/106184	16.4
	C94	M	TAV	c.352C>T	p.Leu118Phe	Missense	6/103504	14.7

Gene	ID	Sex	BAV type	Nucleotide change	Protein change	Classification	MAF ExAC	CADD score
	C130	F	TAV	c.727G>T	p.Gly243Cys	Missense	Absent	9.1
MATR3	P255	M	L-R	c.35G>A	p.Arg12Lys	Missense	Absent	16.4
MYH11	P377	F	L-R	c.2026C>T	p.Arg676Cys	Missense	70/121144	21.5
	P167	F	R-N	c.2026C>T	p.Arg676Cys	Missense	70/121144	21.5
	P181	M	R-N	c.2026C>T	p.Arg676Cys	Missense	70/121144	21.5
	P252	M	L-R	c.2026C>T	p.Arg676Cys	Missense	70/121144	21.5
	P372	M	L-R	c.2981T>A	p.Ile994Asn	Missense	Absent	12.4
	P153	M	L-R	c.3784A>G	p.Lys1262Glu	Missense	1/121400	29.4
	P252	M	L-R	c.3826A>G	p.Ser1276Gly	Missense	6/121368	15.4
	P160	M	L-R	c.3848C>T	p.Ala1283Val	Missense	6/121224	7.2
	P7	F	NA	c.3917C>A	p.Ala1306Asp	Missense	Absent	19.3
	P314	F	L-R	c.4531C>T	p.Arg1511Trp	Missense	7/121404	19.6
	P79	F	L-R	c.4624C>T	p.Arg1542Trp	Missense	15/121346	21.1
	P57	F	NA	c.4694C>T	p.Thr1565Met	Missense	90/121408	23.2
	P223	M	R-N	c.4694C>T	p.Thr1565Met	Missense	90/121408	23.2
	P88	M	NA	c.4681G>A	p.Ala1568Thr	Missense	15/121408	34
	P64	M	L-R	c.5247G>C	p.Glu1749Asp	Missense	66/90680	21.3
	P341	M	L-R	c.5294G>A	p.Arg1765Gln	Missense	25/116672	33
	P391	M	L-R	c.5687C>T	p.Ala1896Val	Missense	6/121208	25.9
	C110	F	TAV	c.33G>T	p.Glu11Asp	Missense	7/121350	11.6
	C23	F	TAV	c.1223T>C	p.Ile408Thr	Missense	1/121412	21
	C40	F	TAV	c.1934C>T	p.Ser645Leu	Missense	17/106978	24.8
	C81	M	TAV	c.1934C>T	p.Ser645Leu	Missense	17/106978	24.8
	C173	M	TAV	c.3430G>T	p.Ala1144Ser	Missense	1/121412	18.6

Gene	ID	Sex	BAV type	Nucleotide change	Protein change	Classification	MAF ExAC	CADD score
	C95	F	TAV	c.3583C>T	p.Arg1195Trp	Missense	20/121406	24.1
	C34	F	TAV	c.4599C>T	p.Asn1533Asn	Splice site	Absent	8.5
	C143	M	TAV	c.5687C>T	p.Ala1896Val	Missense	6/121208	25.9
NKX2-5	P30	M	NA	c.61G>C	p.Glu21Gln	Missense	92/114290	22.9
	P352	M	L-R	c.61G>C	p.Glu21Gln	Missense	92/114290	22.9
	P273	M	L-R	c.89C>A	p.Ala30Asp	Missense	Absent	16.1
	P157	F	R-N	c.358G>T	p.Val120Leu	Missense	Absent	4.8
	P257	F	NA	c.650G>A	p.Arg217Lys	Missense	21/92066	24.6
NOS3	P343	M	L-R	c.466G>A	p.Glu156Lys	Missense	26/94176	36
	P336	M	R-N	c.668A>G	p.Asn223Ser	Missense	2/112186	22.6
	P65	M	L-R	c.1267G>A	p.Ala423Thr	Missense	73/120868	25.1
	P175	F	R-N	c.2457C>G	p.Asp819Glu	Missense	5/11892	23.7
	P382	M	NA	c.2642C>T	p.Ala881Val	Missense	14/119328	22.4
	C19	M	TAV	c.466G>A	p.Glu156Lys	Missense	26/94176	36
	C6	M	TAV	c.638A>G	p.Asn213Ser	Missense	Absent	13.7
	C68	M	TAV	c.1267G>A	p.Ala423Thr	Missense	73/120868	25.1
	C85	M	TAV	c.2471C>T	p.Thr824Ile	Missense	1/11184	12.7
	C152	F	TAV	c.2546G>A	p.Arg849Gln	Missense	1/115870	36
	C151	M	TAV	c.2776_2776delinsCCA	p.Leu927Hisfs*32	Frameshift	1/84330	/
	C182	F	TAV	c.3589G>A	p.Gly1197Ser	Missense	3/110874	7.3
NOTCH1	P113	M	NA	c.983C>G	p.Thr328Ser	Missense	1/119274	18.3
	P373	F	L-R	c.1951G>A	p.Asp651Asn	Missense	Absent	14.7

Gene	ID	Sex	BAV type	Nucleotide change	Protein change	Classification	MAF ExAC	CADD score
	P344	F	L-R	c.2352C>T	p.Ser784Ser	Splice site	7/118434	9.1
	P423	M	L-R	c.4013C>T	p.Ala1338Val	Missense	Absent	19.1
	P155	M	R-N	c.4021G>A	p.Glu1341Lys	Missense	3/66948	7.7
	P128	M	NA	c.5047C>T	p.Arg1683Trp	Missense	1/119254	29.4
	P202	F	L-R	c.5167+3_5167+6del		Splice site	Absent	/
	P134	M	NA	c.5248G>A	p.Val1750Met	Missense	3/100758	17.3
	P420	M	L-R	c.5414T>C	p.Leu1805Pro	Missense	3/119106	22.1
	P106	M	NA	c.6413C>T	p.Pro2138Leu	Missense	1/114110	3.6
	C103	M	TAV	c.121A>G	p.Asn41Asp	Missense	Absent	12.8
	C45	M	TAV	c.800A>G	p.Lys267Arg	Missense	1/119480	11.1
	C162	M	TAV	c.2003C>T	p.Pro668Leu	Missense	4/118872	17.7
	C158	M	TAV	c.2003C>T	p.Pro668Leu	Missense	4/118872	17.7
	C54	M	TAV	c.5273G>A	p.Arg1758His	Missense	13/107714	27.1
	C101	M	TAV	c.7361A>G	p.His2454Arg	Missense	Absent	11.9
	C49	F	TAV	c.7372C>A	p.Pro2458Thr	Missense	2/78680	12.9
ROBO1	P344	F	L-R	c.153C>A	p.Asp51Glu	Missense	Absent	22
	P252	M	L-R	c.497C>G	p.Ala166Gly	Missense	Absent	21.9
	P5	M	NA	c.703G>A	p.Ala235Thr	Missense	5/118284	34
	P432	M	L-R	c.818T>C	p.Val273Ala	Missense	15/120622	23.1
	P374	M	R-N	c.979T>C	p.Ser327Pro	Missense	23/120206	21.2
	P328	M	NA	c.979T>C	p.Ser327Pro	Missense	23/120206	21.2
	P69	F	R-N	c.1432G>C	p.Ala478Pro	Missense	Absent	33
	P5	M	NA	c.1616A>G	p.Tyr539Cys	Missense	5/120482	15.9

Gene	ID	Sex	BAV type	Nucleotide change	Protein change	Classification	MAF ExAC	CADD score
	P191	M	NA	c.3007G>A	p.Asp1003Asn	Missense	3/120414	19
	P384	M	L-R	c.3259A>C	p.Met1087Leu	Missense	8/120756	7.1
	P348	M	NA	c.3472A>G	p.Ser1158Gly	Missense	Absent	16.1
	P34	M	NA	c.4821G>A	p.Met1607Ile	Missense	2/120590	19.4
	C99	M	TAV	c.394A>G	p.Ile132Val	Missense	Absent	18.9
	C105	M	TAV	c.508G>A	p.Asp170Asn	Missense	Absent	24.3
	C145	M	TAV	c.818T>C	p.Val273Ala	Missense	15/120622	23.1
	C60	M	TAV	c.2987C>T	p.Thr996Met	Missense	2/120118	17.8
	C158	M	TAV	c.3259A>C	p.Met1087Leu	Missense	8/120756	7.1
ROBO2	P48	F	NA	c.1238C>T	p.Thr413Ile	Missense	10/120348	14.2
	P423	M	L-R	c.1859C>T	p.Pro620Leu	Missense	Absent	21.4
	P364	F	NA	c.2018G>T	p.Arg673Leu	Missense	Absent	31
	P432	M	L-R	c.2897C>T	p.Thr966Met	Missense	5/120752	21.3
	P164	M	L-R	c.3229C>G	p.Pro1077Ala	Missense	6/120516	13.1
	P29	M	NA	c.3230C>A	p.Pro1077His	Missense	2/120524	17.2
	P180	F	L-R	c.3857G>T	p.Arg1286Leu	Missense	67/120712	27
	P250	F	L-R	c.3857G>T	p.Arg1286Leu	Missense	67/120712	27
	P168	M	R-N	c.4063C>T	p.Arg1355Cys	Missense	3/120728	15
	C90	F	TAV	c.406C>T	p.Arg136*	Nonsense	Absent	37
	C20	M	TAV	c.2018G>A	p.Arg673His	Missense	16/120314	32
	C125	F	TAV	c.2390G>A	p.Arg797Gln	Missense	6/120660	21
	C74	M	TAV	c.2902C>G	p.Leu968Val	Missense	Absent	17.7
	C5	F	TAV	c.3230C>A	p.Pro1077His	Missense	2/120524	17.2
SMAD3	C72	M	TAV	c.448T>C	p.Phe150Leu	Missense	2/121372	11.9

Gene	ID	Sex	BAV type	Nucleotide change	Protein change	Classification	MAF ExAC	CADD score
SMAD6	P128	M	NA	c.74_79del	p.Ser27_Gly2827del	In-frame deletion	Absent	/
	P99	M	NA	c.455_461del	p.Pro152Profs*27	Frameshift deletion	Absent	/
	P94	M	NA	c.715G>A	p.Val239Met	Missense	Absent	24.4
	P231	M	L-R	c.726del	p.Lys242Asnfs*300	Frameshift deletion	Absent	/
	P12	F	NA	c.770C>T	p.Pro257Leu	Missense	Absent	16
	P89	M	NA	c.812G>A	p.Gly271Glu	Missense	Absent	23.6
	P308	F	L-R	c.837C>A	p.Tyr279*	Nonsense	Absent	38
	P180	F	L-R	c.864C>G	p.Tyr288*	Nonsense	Absent	38
	P367	M	R-N	c.1216G>T	p.Gly406Cys	Missense	Absent	19.6
	P67	F	R-N	c.1224C>G	p.His408Gln	Missense	Absent	18.3
	P201	M	NA	c.1328G>A	p.Arg443His	Missense	1/106314	23.7
	C148	M	TAV	c.389C>T	p.Ser130Leu	Missense	Absent	12.8
TGFB2	P133	M	NA	c.1048C>T	p.Leu350Phe	Missense	Absent	18.8
TGFBR1	P334	M	L-R	c.119T>A	p.Leu40His	Missense	Absent	9.5
	P105	M	NA	c.926C>T	p.Thr309Met	Missense	2/121364	24.9
TGFBR2	C72	M	TAV	c.1090C>T	p.Arg364Trp	Missense	6/120734	14.7

Gene	ID	Sex	BAV type	Nucleotide change	Protein change	Classification	MAF ExAC	CADD score

The patient ID prefix denotes variants identified in patients (P) and controls (C). Bicuspid aortic valve (BAV) subtypes can be left-right (L-R), right-non-coronary (R-N), or unknown (NA). Controls have a tricuspid aortic valve (TAV). Used RefSeq transcripts (except † NM_001278939): NM_001613 (*ACTA2*), NM_001105 (*ACVR1*), NM_000501 (*ELN*), NM_000138 (*FBN1*), NM_212482 (*FN1*), NM_002052 (*GATA4*), NM_080473 (*GATA5*), NM_005257 (*GATA6*), NM_018834 (*MATR3*), NM_001040113 (*MYH11*), NM_172387 (*NFTAC1*), NM_004387 (*NKX2-5*), NM_000603 (*NOS3*), NM_017617 (*NOTCH1*), NM_002941 (*ROBO1*), NM_002942 (*ROBO2*), NM_005902 (*SMAD3*), NM_005585 (*SMAD6*), NM_001135599 (*TGFB2*), NM_004612 (*TGFBR1*), NM_001024847 (*TGFBR2*).

References

1. Verstraeten, A., Roos-Hesselink, J. & Loeys, B. in *Clinical Cardiogenetics* 295–308 (Springer International Publishing, Cham, 2016). doi:10.1007/978-3-319-44203-7_18.

2. Cripe, L., Andelfinger, G., Martin, L. J., Shooner, K. & Benson, D. W. Bicuspid aortic valve is heritable. *J Am Coll Cardiol* **44,** 138–43. ISSN: 0735-1097 (July 2004).

3. Hinton, R. B. Bicuspid aortic valve and thoracic aortic aneurysm: three patient populations, two disease phenotypes, and one shared genotype. *Cardiology research and practice* **2012,** 926975. ISSN: 2090-0597 (Jan. 2012).

4. Martin, P. S. *et al.* Embryonic Development of the Bicuspid Aortic Valve, 248–272. ISSN: 2308-3425 (2015).

5. Loscalzo, M. L. *et al.* Familial thoracic aortic dilation and bicommissural aortic valve: a prospective analysis of natural history and inheritance. *Am J Med Genet* **143A,** 1960–7. ISSN: 1552-4825 (Sept. 2007).

6. Braverman, A. C. *et al.* The bicuspid aortic valve. *Curr Probl in Cardiol* **30,** 470–522. ISSN: 0146-2806 (Sept. 2005).

7. Clementi, M., Notari, L., Borghi, A. & Tenconi, R. Familial congenital bicuspid aortic valve: a disorder of uncertain inheritance. *American journal of medical genetics* **62,** 336–8. ISSN: 0148-7299 (Apr. 1996).

8. Huntington, K., Hunter, A. G. & Chan, K. L. A prospective study to assess the frequency of familial clustering of congenital bicuspid aortic valve. *Journal of the American College of Cardiology* **30,** 1809–12. ISSN: 0735-1097 (Dec. 1997).

9. Mohamed, S. A. *et al.* Novel missense mutations (p.T596M and p.P1797H) in NOTCH1 in patients with bicuspid aortic valve. *Biochemical and biophysical research communications* **345,** 1460–5. ISSN: 0006-291X (July 2006).

10. Garg, V. *et al.* Mutations in NOTCH1 cause aortic valve disease. *Nature* **437,** 270–4. ISSN: 1476-4687 (Sept. 2005).

11. McKellar, S. H. *et al.* Novel NOTCH1 mutations in patients with bicuspid aortic valve disease and thoracic aortic aneurysms. *The Journal of thoracic and cardiovascular surgery* **134,** 290–296. ISSN: 1097-685X (2007).

12. Foffa, I. *et al.* Sequencing of NOTCH1, GATA5, TGFBR1 and TGFBR2 genes in familial cases of bicuspid aortic valve. En. *BMC medical genetics* **14,** 44. ISSN: 1471-2350 (Jan. 2013).

13. Kent, K. C., Crenshaw, M. L., Goh, D. L. M. & Dietz, H. C. Genotype–phenotype correlation in patients with bicuspid aortic valve and aneurysm. *The Journal of thoracic and cardiovascular surgery* **146,** 158 (2013).

14. Bonachea, E. M. *et al.* Rare GATA5 sequence variants identified in individuals with bicuspid aortic valve. *Pediatric research* **76,** 211–216. ISSN: 1530-0447 (2014).

15. Freylikhman, O. *et al.* Variants in the NOTCH1 gene in patients with aortic coarctation. *Congenital heart disease* **9,** 391–6. ISSN: 1747-0803 (Sept. 2014).

16. Kerstjens-Frederikse, W. S. *et al.* Cardiovascular malformations caused by NOTCH1 mutations do not keep left: data on 428 probands with left-sided CHD and their families. *Genetics in Medicine.* ISSN: 1098-3600. doi:`10.1038/gim.2015.193` (2016).

17. Tan, H. L. *et al.* Nonsynonymous variants in the SMAD6 gene predispose to congenital cardiovascular malformation. *Human mutation* **33,** 720–7. ISSN: 1098-1004 (Apr. 2012).

18. Guo, D.-c. *et al.* MAT2A Mutations Predispose Individuals to Thoracic Aortic Aneurysms. *The American Journal of Human Genetics* **96,** 170–177. ISSN: 00029297 (Jan. 2015).

19. Biben, C. *et al.* Cardiac septal and valvular dysmorphogenesis in mice heterozygous for mutations in the homeobox gene Nkx2-5. *Circulation research* **87,** 888–895. ISSN: 0009-7330 (2000).

20. Lee, T. C., Zhao, Y. D., Courtman, D. W. & Stewart, D. J. Abnormal aortic valve development in mice lacking endothelial nitric oxide synthase. *Circulation* **101,** 2345–8. ISSN: 1524-4539 (May 2000).

21. Laforest, B. & Nemer, M. GATA5 interacts with GATA4 and GATA6 in outflow tract development. *Developmental Biology* **358,** 368–378. ISSN: 00121606 (2011).

22. Laforest, B., Andelfinger, G. & Nemer, M. Loss of Gata5 in mice leads to bicuspid aortic valve. *J Clin Invest* **121,** 2876–87. ISSN: 1558-8238 (July 2011).

23. Thomas, P. S., Sridurongrit, S., Ruiz-Lozano, P. & Kaartinen, V. Deficient signaling via Alk2 (Acvr1) leads to bicuspid aortic valve development. *PloS one* **7,** e35539. ISSN: 1932-6203 (2012).

24. Mommersteeg, M. T. M., Yeh, M. L., Parnavelas, J. G. & Andrews, W. D. Disrupted Slit-Robo signalling results in membranous ventricular septum defects and bicuspid aortic valves. *Cardiovascular Research* **106,** 55–66. ISSN: 17553245 (2015).

25. Quintero-Rivera, F. *et al.* MATR3 disruption in human and mouse associated with bicuspid aortic valve, aortic coarctation and patent ductus arteriosus. *Human Molecular Genetics* **24,** 2375–2389. ISSN: 0964-6906 (2015).

26. Attias, D. *et al.* Comparison of clinical presentations and outcomes between patients with TGFBR2 and FBN1 mutations in Marfan syndrome and related disorders. *Circulation* **120,** 2541–9. ISSN: 1524-4539 (Dec. 2009).

27. Callewaert, B. *et al.* New insights into the pathogenesis of autosomal-dominant cutis laxa with report of five ELN mutations. *Human mutation* **32,** 445–55. ISSN: 1098-1004 (Apr. 2011).

28. Lindsay, M. E. *et al.* Loss-of-function mutations in TGFB2 cause a syndromic presentation of thoracic aortic aneurysm. *Nat Genet* **44,** 922–7. ISSN: 1546-1718 (Aug. 2012).

29. Nistri, S. *et al.* Association of Marfan syndrome and bicuspid aortic valve: Frequency and outcome. *International Journal of Cardiology* **155,** 324–325. ISSN: 01675273 (Mar. 2012).

30. Van de Laar, I. M. B. H. *et al.* Phenotypic spectrum of the SMAD3-related aneurysms-osteoarthritis syndrome. *Journal of Medical Genetics* **49,** 47–57. ISSN: 0022-2593 (Jan. 2012).

31. Pepe, G. *et al.* Identification of fibrillin 1 gene mutations in patients with bicuspid aortic valve (BAV) without Marfan syndrome. *BMC medical genetics* **15,** 23. ISSN: 1471-2350 (Jan. 2014).

32. Guo, D.-C. *et al.* Mutations in smooth muscle α-actin (ACTA2) lead to thoracic aortic aneurysms and dissections. *Nature Genetics* **39,** 1488–1493. ISSN: 1061-4036 (Dec. 2007).

33. Jefferies, J. L., Taylor, M. D., Rossano, J., Belmont, J. W. & Craigen, W. J. Novel cardiac findings in periventricular nodular heterotopia. *American journal of medical genetics. Part A* **152A,** 165–8. ISSN: 1552-4833 (Jan. 2010).

34. DePristo, M. A. *et al.* A framework for variation discovery and genotyping using next-generation DNA sequencing data. *Nature genetics* **43,** 491–8. ISSN: 1546-1718 (May 2011).

35. Vandeweyer, G., Loeys, B. L. & Van den Bulcke, T. VariantDB: A flexible annotation and filtering portal for NGS data. *Genome Med,* in press (2014).

36. Lek, M. *et al.* Analysis of protein-coding genetic variation in 60,706 humans. *Nature* **536,** 285–91. ISSN: 1476-4687 (Aug. 2016).

37. Kircher, M. *et al.* A general framework for estimating the relative pathogenicity of human genetic variants. *Nature genetics* **46,** 310–5. ISSN: 1546-1718 (Mar. 2014).

38. Untergasser, A. *et al.* Primer3-new capabilities and interfaces. *Nucleic Acids Research* **40,** e115. ISSN: 03051048 (Aug. 2012).

39. Makkar, P., Metpally, R. P. R., Sangadala, S. & Reddy, B. V. B. Modeling and analysis of MH1 domain of Smads and their interaction with promoter DNA sequence motif. *Journal of molecular graphics & modelling* **27,** 803–12. ISSN: 1873-4243 (Apr. 2009).

40. Bosse, K. *et al.* Endothelial nitric oxide signaling regulates Notch1 in aortic valve disease. *Journal of molecular and cellular cardiology* **60,** 27–35. ISSN: 1095-8584 (July 2013).

41. Andelfinger, G., Loeys, B. & Dietz, H. A Decade of Discovery in the Genetic Understanding of Thoracic Aortic Disease. *The Canadian journal of cardiology* **32,** 13–25. ISSN: 1916-7075 (Jan. 2016).

42. Van de Laar, I. M. B. H. *et al.* Mutations in SMAD3 cause a syndromic form of aortic aneurysms and dissections with early-onset osteoarthritis. *Nature genetics* **43,** 121–126. ISSN: 1061-4036 (Feb. 2011).

43. Micha, D. *et al.* SMAD2 Mutations Are Associated with Arterial Aneurysms and Dissections. *Human Mutation* **36,** 1145–1149. ISSN: 10597794 (Dec. 2015).

44. Bai, S. & Cao, X. A Nuclear Antagonistic Mechanism of Inhibitory Smads in Transforming Growth Factor- Signaling. *Journal of Biological Chemistry* **277,** 4176–4182. ISSN: 0021-9258 (Feb. 2002).

45. Hanyu, A. *et al.* The N domain of Smad7 is essential for specific inhibition of transforming growth factor-beta signaling. *The Journal of cell biology* **155,** 1017–27. ISSN: 0021-9525 (Dec. 2001).

46. Lin, X. *et al.* Smad6 recruits transcription corepressor CtBP to repress bone morphogenetic protein-induced transcription. *Molecular and cellular biology* **23,** 9081–93. ISSN: 0270-7306 (Dec. 2003).

47. Jung, S. M. *et al.* Smad6 inhibits non-canonical TGF-β1 signalling by recruiting the deubiquitinase A20 to TRAF6. *Nature Communications* **4,** 2562. ISSN: 2041-1723 (2013).

48. Galvin, K. M. *et al.* A role for smad6 in development and homeostasis of the cardiovascular system. *Nature genetics* **24,** 171–174. ISSN: 1061-4036 (2000).

49. Dickel, D. E. *et al.* Genome-wide compendium and functional assessment of in vivo heart enhancers. *Nature communications* **7,** 12923. ISSN: 2041-1723 (Oct. 2016).

50. Topper, J. N. *et al.* Vascular MADs: two novel MAD-related genes selectively inducible by flow in human vascular endothelium. *Proceedings of the National Academy of Sciences of the United States of America* **94,** 9314–9. ISSN: 0027-8424 (Aug. 1997).

51. Imamura, T. *et al.* Smad6 inhibits signalling by the TGF-beta superfamily. *Nature* **389,** 622–626. ISSN: 00280836 (Oct. 1997).

52. Hata, A., Lagna, G., Massagué, J. & Hemmati-Brivanlou, A. Smad6 inhibits BMP/Smad1 signaling by specifically competing with the Smad4 tumor suppressor. *Genes & development* **12,** 186–97. ISSN: 0890-9369 (Jan. 1998).

53. Murakami, G., Watabe, T., Takaoka, K., Miyazono, K. & Imamura, T. Cooperative inhibition of bone morphogenetic protein signaling by Smurf1 and inhibitory Smads. *Molecular biology of the cell* **14,** 2809–17. ISSN: 1059-1524 (July 2003).

54. Cai, J., Pardali, E., Sánchez-Duffhues, G. & ten Dijke, P. BMP signaling in vascular diseases. *FEBS letters* **586,** 1993–2002. ISSN: 1873-3468 (July 2012).

55. Garside, V. C., Chang, A. C., Karsan, A. & Hoodless, P. A. Co-ordinating Notch, BMP, and TGF-β signaling during heart valve development. *Cellular and molecular life sciences : CMLS* **70,** 2899–917. ISSN: 1420-9071 (Aug. 2013).

56. Kaartinen, V. *et al.* Cardiac outflow tract defects in mice lacking ALK2 in neural crest cells. *Development (Cambridge, England)* **131,** 3481–90. ISSN: 0950-1991 (July 2004).

57. Loeys, B. L. *et al.* A syndrome of altered cardiovascular, craniofacial, neurocognitive and skeletal development caused by mutations in TGFBR1 or TGFBR2. *Nat Genet* **37,** 275–81. ISSN: 1061-4036 (Mar. 2005).

58. Boileau, C. *et al.* TGFB2 mutations cause familial thoracic aortic aneurysms and dissections associated with mild systemic features of Marfan syndrome. *Nat Genet* **44,** 916–21. ISSN: 1546-1718 (Aug. 2012).

59. Carmignac, V. *et al.* In-frame mutations in exon 1 of SKI cause dominant Shprintzen-Goldberg syndrome. *Am J Hum Genet* **91,** 950–957. ISSN: 1537-6605 (Nov. 2012).

60. Doyle, A. J. *et al.* Mutations in the TGF-β repressor SKI cause Shprintzen-Goldberg syndrome with aortic aneurysm. *Nat Genet* **44,** 1249–54. ISSN: 1546-1718 (Sept. 2012).

61. Bertoli-Avella, A. M. *et al.* Mutations in a TGF-β Ligand, TGFB3, Cause Syndromic Aortic Aneurysms and Dissections. *Journal of the American College of Cardiology* **65,** 1324–36. ISSN: 1558-3597 (Apr. 2015).

62. Iascone, M. *et al.* Identification of de novo mutations and rare variants in hypoplastic left heart syndrome. *Clinical genetics* **81,** 542–54. ISSN: 1399-0004 (June 2012).

63. Preuss, C. *et al.* Family Based Whole Exome Sequencing Reveals the Multifaceted Role of Notch Signaling in Congenital Heart Disease. *PLoS genetics* **12** (ed Gibson, G.) e1006335. ISSN: 1553-7404 (Oct. 2016).

64. Irtyuga, O. *et al.* NOTCH1 Mutations in Aortic Stenosis: Association with Osteoprotegerin/RANK/RANKL. *BioMed research international* **2017,** 6917907. ISSN: 2314-6141 (2017).

65. Koenig, S. N. *et al.* Endothelial Notch1 Is Required for Proper Development of the Semilunar Valves and Cardiac Outflow Tract. *Journal of the American Heart Association* **5.** ISSN: 2047-9980. doi:`10.1161/JAHA.115.003075` (Jan. 2016).

66. Forstermann, U. & Münzel, T. Endothelial Nitric Oxide Synthase in Vascular Disease: From Marvel to Menace. *Circulation* **113,** 1708–1714. ISSN: 0009-7322 (Apr. 2006).

67. Oliveira-Paula, G. H., Lacchini, R. & Tanus-Santos, J. E. Endothelial nitric oxide synthase: From biochemistry and gene structure to clinical implications of NOS3 polymorphisms. *Gene* **575,** 584–99. ISSN: 1879-0038 (Jan. 2016).

68. Oller, J. *et al.* Nitric oxide mediates aortic disease in mice deficient in the metalloprotease Adamts1 and in a mouse model of Marfan syndrome. *Nature Medicine* **23,** 200–212. ISSN: 1078-8956 (Jan. 2017).

Chapter 4

Mutations in the transcriptional regulator, *KLF15*, are associated with thoracic aortic aneurysms

Elisabeth Gillis[1], Jefferson J. Doyle[2], Ilse Luyckx[1], Elyssa Cannaerts[1], Isabel Pintelon[3], Nikhita Ajit Bolar[1], Yuan Lu[4], Gerarda van de Beek[1], Mukesh Jain[4], Harry C. Dietz[2,5,6], Seema Mittal[7], Marlies Kempers[8], Aline Verstraeten[1], Lut Van Laer[1], Bart L Loeys[1,8], the MIBAVA-Leducq Consortium

1 Center for Medical Genetics, Faculty of Medicine and Health Sciences, University of Antwerp and Antwerp University Hospital, Antwerp, Belgium
2 McKusick-Nathans Institute of Genetic Medicine, Johns Hopkins University School of Medicine, Baltimore, Maryland, USA
3 Department of Cell Biology and Histology, University of Antwerp, Antwerp, Belgium
4 Cardiovascular Research Institute, Case Western Reserve University, Cleveland, Ohio, USA
5 Howard Hughes Medical Institute, Baltimore, Maryland, USA
6 Department of Pediatrics, Division of Pediatric Cardiology, Johns Hopkins University School of Medicine, Baltimore, Maryland, USA
7 Cardiovascular Research, SickKids University Hospital, Toronto, ON, Canada
8 Department of Human Genetics, Radboud University Nijmegen Medical Centre, Nijmegen, The Netherlands

Research in progress

Contribution: Whole genome sequencing analysis, variant phase determination, promoter luciferase assays, histology, immunohistochemistry, immunocytochemistry

4.1 Abstract

Thoracic aortic aneurysms (TAA) have an incidence of roughly 10.4 per 100 000 person-years. TAAs are associated with high mortality when dissections occur. Recent studies on syndromic forms of TAA, such as Marfan syndrome and Loeys-Dietz syndrome, have increased our understanding of TAA pathogenesis. For non-syndromic forms of TAA, the current genetic knowledge explains only 20-30% of patients with a positive family history. As such, new TAA genes await their discovery. Whole exome sequencing (WES) in a non-syndromic TAA family revealed a possible pathogenic variant (p.Arg343Cys) in the *KLF15* gene, which encodes a transcriptional regulator. A WES cohort consisting of bicuspid aortic valve (BAV)/TAA patients (n=196) unveiled another interesting rare variant in *KLF15* (p.Ser335Asn), whereas resequencing of 458 TAA patients could not identify additional pathogenic variants. Both p.Arg343Cys and p.Ser335Asn are located in the first of three highly conserved Zn-Finger domains of the KLF15 protein. Promoter luciferase assays demonstrated that both p.Arg343Cys and p.Ser335Asn affect the activator function of KLF15. Moreover, p.Arg343Cys may affect the interaction of KLF15 with other transcriptional cofactors as well. In line with previous studies demonstrating that altered TGF-β signaling is a key mechanism in (non-)syndromic forms of TAA, we show that variation in KLF15 likewise dysregulates non-canonical TGF-β signaling, as we observed increased levels of pERK in aortic tissue of the p.Arg343Cys patient. Finally, in vivo experiments confirmed the involvement of *KLF15* in TAA as *KLF15* knockout mice developed TAA. TAA development was even more severe in *KLF15* knockout mice on a Marfan syndrome background (Fbn1$^{C1039G/+}$), suggesting a genetic interaction between *KLF15* and *FBN1*, and possibly linking KLF15 and the TGF-β signaling pathway. Taken together, we propose *KLF15* as a new TAA candidate gene.

4.2 Introduction

Thoracic aortic aneurysms (TAA) are dilations of the thoracic aorta with an incidence of roughly 10.4 per 100 000 person-years[1]. When left untreated, they can lead to lethal dissections. TAAs appear isolated or as part of a syndrome, e.g. Mar-

fan syndrome (MFS) or Loeys-Dietz syndrome. Both syndromic and non-syndromic forms of TAA are caused by genetic defects, with up to 20% of patients having a positive family history[2, 3]. Gene identification studies on syndromic forms of TAA have identified loss-of-function mutations in several members of the TGF-β (transforming growth factor beta) signaling pathway, including TGFBR1/2[4], TGFB2/3[5, 6] and SMAD2/3[7, 8] as disease culprits. Paradoxically, loss-of-function mutations in these genes cause upregulation of TGF-β signaling in patient aortic wall tissue, as evidenced by increased pSMAD2 and pERK[5–7]. For non-syndromic TAA genes, the encoded proteins are mainly involved in smooth muscle cell contraction, e.g. ACTA2[9, 10], MYH11[10], MYLK[11] and PRKG1[12]. Interestingly, mutations in MYH11 have also been linked to an increase in TGF-β signaling[10], which further emphasizes the importance of the TGF-β pathway in TAA development.

KLF15 is a member of the Krüppel-like factors (KLF), a family of DNA-binding transcriptional regulators. KLF proteins typically contain three C2H2 zinc finger domains[13]. These mediate KLF binding to specific DNA motifs within promoters of target genes and are thus key in regulating these genes' expression[13]. KLF15 is a multifunctional transcriptional regulator which is able to operate both as a transcriptional activator and repressor[14], as well as a transcriptional cofactor by affecting recruitment of other coregulators[15]. KLF15 plays a role in amino acid, lipid and glucose metabolism[16–18] and in cardiac fibrosis. The latter function of KLF15 involves repression of CTGF[15], which normally promotes fibroblast proliferation and collagen deposition[19]. After TGFB1 treatment of rat fibroblasts, *KLF15* expression is downregulated, which causes an increase in CTGF[15]. In renal fibroblasts, it was shown that the extracellular-regulated kinase (ERK)/mitogen-activated protein kinase (MAPK) and Jun N-terminal kinase (JNK)/MAPK pathways, which are also regulated by TGFB1, have an inhibitory effect on *KLF15* expression[20]. Interestingly, heart failure and TAA are observed in *Klf15*$^{-/-}$ mice[21] challenged with angiotensin II, which simulates stress on the heart and arterial vessels.

Only 20-30% of the familial non-syndromic TAA cases are explained by mutations in known causal genes, suggesting that additional TAA genes remain to be identified[22]. In this study, we propose *KLF15* as a possible candidate gene for familial TAA. Mechanistic insights are derived from promoter luciferase assays, human aortic wall immunohistochemistry as well as from the generation and cardiovascular phenotyping of *KLF15* knockout mice.
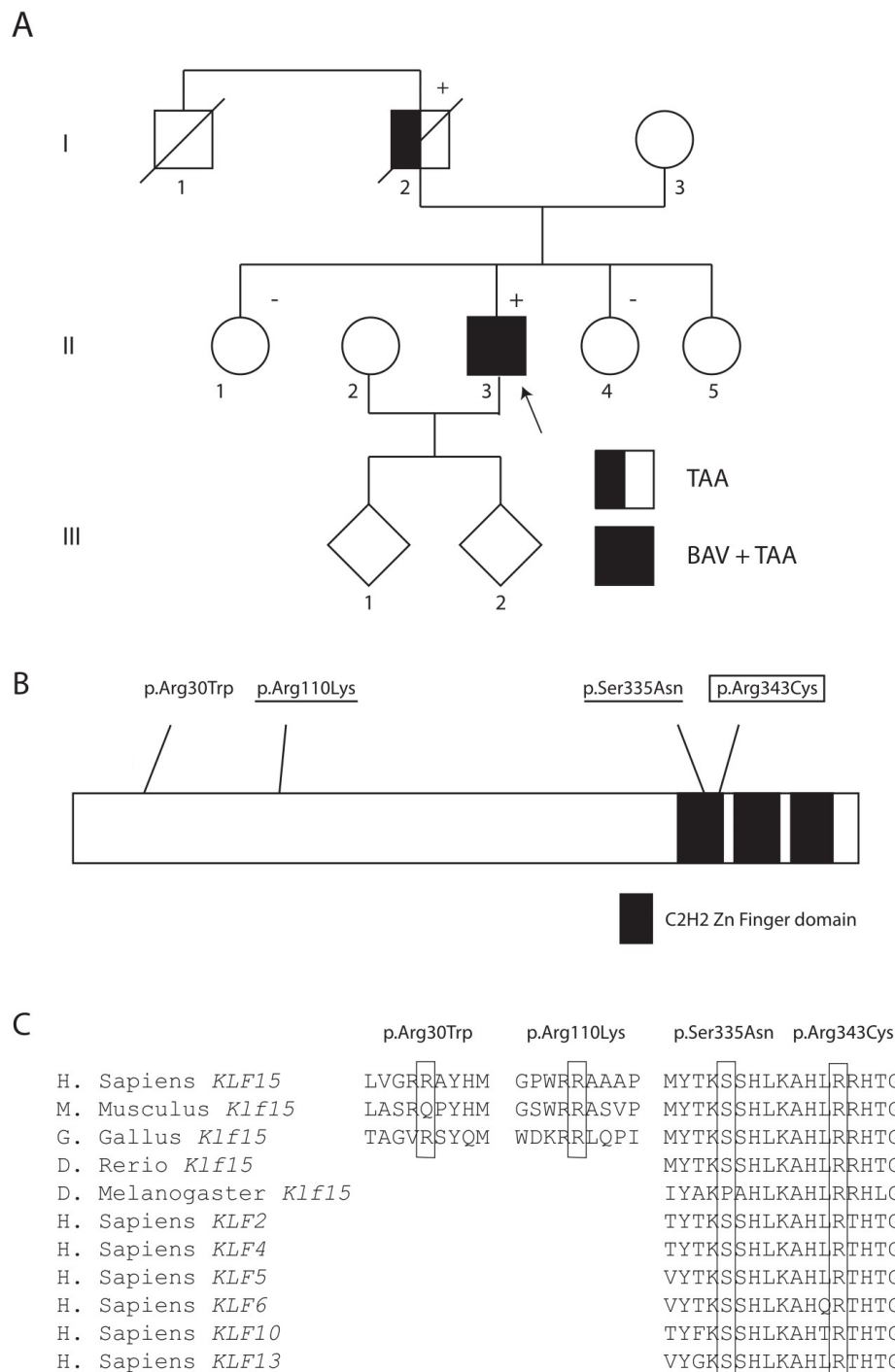
A

III:1   III:2

| | TAA |
| | BAV + TAA |

B

C

	p.Arg30Trp	p.Arg110Lys	p.Ser335Asn	p.Arg343Cys
H. Sapiens *KLF15*	LVGR**R**AYHM	GPWR**R**AAAP	MYTK**S**SHLKAHL**R**RHTG
M. Musculus *Klf15*	LASR**Q**PYHM	GSWR**R**ASVP	MYTK**S**SHLKAHL**R**RHTG
G. Gallus *Klf15*	TAGV**R**SYQM	WDKR**R**LQPI	MYTK**S**SHLKAHL**R**RHTG
D. Rerio *Klf15*			MYTK**S**SHLKAHL**R**RHTG
D. Melanogaster *Klf15*			IYAK**P**AHLKAHL**R**RHLG
H. Sapiens *KLF2*			TYTK**S**SHLKAHL**R**THTG
H. Sapiens *KLF4*			TYTK**S**SHLKAHL**R**THTG
H. Sapiens *KLF5*			VYTK**S**SHLKAHL**R**THTG
H. Sapiens *KLF6*			VYTK**S**SHLKAHQ**R**THTG
H. Sapiens *KLF10*			TYFK**S**SHLKAHT**R**THTG
H. Sapiens *KLF13*			VYGK**S**SHLKAHL**R**THTG

Figure 4.1: **A**: Pedigree of family 1 (p.Arg343Cys) with II:3 as the proband. + this person carries the mutation; - this person does not carry the mutation. I:1 died at age 50 from cardiomyopathy. III:1 and III:2 had tricuspid aortic valves. **B**: KLF15 mutation overview. The boxed mutation (p.Arg343Cys) was found in family 1. The underlined mutations (p.Arg110Lys and p.Ser335Asn) are present in the same patient from family 2. The p.Arg30Trp mutation was identified in family 3. **C**: Evolutionary conservation in KLF15 and its related proteins is given for p.Arg30Trp, p.Arg110Lys, p.Ser335Asn and p.Arg343Cys.

4.3 Materials and methods

4.3.1 Patients

Peripheral blood samples of the proband and available family members of family 1 were collected at the Radboud university medical center, the Netherlands. DNA isolation was carried out following standard procedures. DNA from the proband was analyzed with a next generation sequencing panel containing 147 TAA genes, based on Haloplex technology (Agilent). The proband of family 2 was part of an in-house bicuspid aortic valve (BAV)/TAA whole exome sequencing cohort (n=196), which came from a collaborative effort of the MIBAVA Leducq Consortium. Blood sample collection and DNA extraction of the proband of family 2 was performed at the SickKids Hospital, Toronto, Canada. All patients and their relatives gave informed consent for participation.

4.3.2 Whole exome sequencing and data analysis

Whole exome sequencing of the proband of family 1 was performed on a HiSeq 1500 (Illumina, CA, USA) using the TruSeq Sample Preparation Enrichment kit (Illumina). The raw data were processed using an in-house-developed Galaxy-based pipeline[23]. Variants were called with the Genome Analysis Toolkit (GATK) Unified Genotyper[24] and annotated using an in-house-developed database, VariantDB[25]. Quality-based variant filtering involved the following parameters: Mapping Quality $\geqslant$ 50; Quality by Depth $\geqslant$ 4.8; -3 $\leqslant$ MappingQualityRankSum $\leqslant$ 3; Fisher Scaled StrandBias $\leqslant$ 20; total depth $\geqslant$ 6; 0.23 $\leqslant$ Allelic ratio $\leqslant$ 0.8. Variants present in our in-house control database or variants having an ExAC v03 minor allele frequency (MAF)>0.1% were excluded. Additionally, synonymous, intergenic and UTR variants were not taken into account. All variants selected for follow-up were validated with Sanger Sequencing. Primers were designed using Primer3 software V4.0.0[26, 27] and polymerase chain reaction (PCR) products were purified with Calf Intestinal Alkaline Phosphatase (Sigma-Aldrich, MO, USA). Sequencing reactions were performed using the BigDye Terminator Cycle Sequencing kit (Applied Biosystems, Life Technologies, MA, USA), followed by capillary electrophoresis on an ABI3130XL (Applied Biosystems, Life Technologies). The obtained sequences

were analyzed with CLC DNA Workbench 5.0.2 (CLC bio, Denmark). Combined Annotation Dependent Depletion (CADD) scores were used to aid interpretation of variant pathogenicity28. Conservation was examined using Uniprot's alignment tool[28], used protein ID's were gi—20138787 (Q9UIH9.1), gi—7387592 (Q99612.3), gi—223590252 (O43474.3), gi—17369913 (Q9Y2Y9.1), gi—11387050 (Q13118.1), gi—20141620 (Q9Y5W3.2), GI—12644412 (Q13887.2), gi—20138727 (Q9EPW2.1), E1BYR7, Q6YLV7 and Q0IGQ2.

4.3.3   smMIPS resequencing of TAA samples

In search for additional genetic evidence, we selected 458 unrelated non-syndromic and syndromic TAA patients with an unresolved genetic defect. The small molecule Molecular Inversion Probes (smMIPs) technology, as described by Hiatt et al, 2013[29], was used to enrich all coding exons and intron-exon boundaries $(+/-10$ bp) of *KLF15* (NM_014079). Sequence capture and library preparation was performed for all samples using unique barcodes per sample. The targeted fragments were sequenced on an Illumina NextSeq 500 system (Illumina, USA), using NextSeq 500/550 Mid Output Kit v2 (300 cycles) (Illumina). Data-analysis was performed with an in-house developed automated Galaxy-based pipeline[23, 24] and a variant interpretation tool, VariantDB[25]. After a quality check, we selected for rare deleterious non-synonymous exonic variants and splice site variants using the frequency database of ExAC v0.3.1. (MAF<1%) and prediction programs (CADD, PolyPhen-2 and SIFT).

4.3.4   Variant phase determination

In the proband of family 2, we identified two rare coding *KLF15* variants, urging variant phase determination. The proband's gDNA sequence, encompassing the two *KLF15* variants, was PCR amplified. A TOPO TA Cloning Kit for Sequencing, with One-Shot TOP10 Chemically Competent E. coli cells (Invitrogen, Life Technologies) was used to transform and clone the sequence. The manufacturer's protocol was followed. Colony PCR was performed on 17 randomly chosen colonies, followed by Sanger sequencing as described above.

4.3.5 Promoter luciferase assays

Functional difference between wild-type (WT) and mutant *KLF15* was assessed using overexpression of co-transfected *KLF15* expression vectors (either WT or Mutant: p.Arg110Lys, p.Ser335Asn, p.Arg343Cys) and luciferase constructs containing promoter regions of genes known to be affected by KLF15 (i.e. *BNP*, *ANF*, *PDK4*, *FATP* and *COL3A1*). The Dual Luciferase Reporter Assay System (Promega, WI, USA) was used. The KLF15-3'Flag expression plasmid was kindly provided by Prof. Dr. Jain (Case Western Reserve University, USA)[30]. The QuikChange Site-Directed Mutagenesis Kit (Stratagene, CA, USA) was used to create the following mutant KLF15-3'Flag expression plasmids; p.Arg343Cys, p.Arg110Lys, p.Ser335Asn and p.Arg110Lys-p.Ser335Asn. Co-transfections include: ANF-638-luc (25ng) (courtesy of Prof. Dr. Glembotski, San Diego State University, USA[30]) and KLF15-3'Flag WT or mutant plasmids (2.5ng); BNP-116-luc (25ng) (courtesy of Prof. Dr. Glembotski[30]) and KLF15-3'Flag WT or mutant plasmids (1ng) and GATA4 (1ng) (Prof. Dr. Huggins, Tufts Medical Center, Boston Hospital and Academic Medical Center, USA[31]); PDK4-luc (25ng) (courtesy of Prof. Dr. Jain[32]) and KLF15-3'Flag WT or mutant plasmids (0.75ng); FATP-luc (25ng) (courtesy of Prof. Dr. Jain[32]) and KLF15-3'Flag WT or mutant plasmids (5ng); COL3A1-luc (25ng)(-1.08kB promoter in pGL3 vector, custom order at Genscript, NJ, USA) and KLF15-3'Flag WT or mutant plasmids (2.5ng). The renilla luciferase pRL-TK (2.5 ng) was co-transfected in all experiments as a normalization control. Empty pcDNA3.1 vector was co-transfected to equalize total DNA amounts in each experiment.

All promoter luciferase assays were performed in human embryonic kidney (HEK) 293T cells. Cells were grown in Dulbecco's Modified Eagle Medium (DMEM) medium (Invitrogen, Life Technologies), supplemented with fetal bovine serum (FBS, 10% v/v, Invitrogen, Life Technologies) and Penicillin-Streptomycin (Gibco, Life Technologies). Cells were counted, plated out at $0.3*10^5$ cells/well in 96-well plates and grown for 24h prior to being transfected with Fugene 6 (6:1 Fugene:DNA ratio, Promega). After 24h, cells were lysed and chemiluminiscence of the Firefly and Renilla luciferases was measured with the Glomax Multi Luminometer (Turner Designs, CA, USA). Statistics were performed using a mixed model in JMP Pro software (Version 12.0.1, SAS Institute Inc., Cary, NC, 1989-2007).

4.3.6 Histology and immunohistochemistry

Formalin-Fixed, Paraffin-Embedded (FFPE) aortic tissue was available of patient I-2 of family 1 (Figure 4.1). Verhoeff-Van Gieson (VVG) staining with the Elastic Stain Kit (Sigma-Aldrich) and collagen staining with the Trichrome Stain (Masson) Kit (Sigma-Aldrich) were carried out according to the manufacturer's protocol. Immunofluorescence involved deparaffinization with xylene and graded ethanol treatment, followed by antigen retrieval in 10mM Sodium citrate (0.05% Tween, pH6) in a steam cooker. Slides were incubated in 100mg/ml sodium borohydrate before permeabilization in 300mM glycine. All slides were blocked overnight in 5% normal goat serum in TBST (1x Tris buffered saline (TBS) buffer, 0.1% Triton-X), except for KLF15 stained slides. These were incubated with Fc-Receptor Blocking (Innovex Biosciences, USA) for 30min, followed by 20min blocking in Background Buster (Innovex Biosciences). Primary antibody incubation (pERK (Cat # 4370, Cell Signaling Technology, 1/100); pSMAD2 (Cat # 04-953, Merck Millipore, USA, 1/200), Collagen III (Cat # ab7778, Abcam, UK; 1/100), KLF15 (Cat # sc-34827, Santa Cruz Biotechnology, USA; 1/100)) was done overnight at 4°C. As secondary antibodies we used anti-rabbit IgG, TRITC (Cat # T-2769, Invitrogen, USA; 1/200) and anti-Goat Alexa 488 (Cat # A-11055, Invitrogen; 1/200), these incubations were performed for 2h at room temperature. Slides were mounted using Vectashield with DAPI (Vector Laboratories, CA, USA). Finally, confocal microscopy images were acquired with 40x and 20x objectives on the UltraView imaging analysis system (PerkinElmer, Waltham, MA, USA) or the Zeiss LSM780-FCS (Zeiss, Germany).

Statistical analysis on the pERK-stained images was performed by measuring the mean gray value with ImageJ[33] and performing an unpaired student t-test.

4.3.7 Immunocytochemistry

Human Aortic Endothelial Cells were grown in Endothelial Cell Growth (EGM)-2 medium (PromoCell, Heidelberg, Germany) in the Nunc Lab-Tek II Chamber Slide System (Thermo Scientific, Massachusetts, USA). Cells were fixed for 1h in 4% paraformaldehyde, permeabilized for 10 min in 0.2% Triton X-100 in D-PBS (Dubelcco's-PBS, Gibco, Thermo Scientic) and blocked for 30min in 1% Bovine Serum Albumine (BSA). Incubation with the KLF15 primary antibody (Cat # sc-

34827, Santa Cruz Biotechnology, USA; 1/00) was done overnight at 4°C. Cells were incubated with the secondary antibody, anti-goat Alexa 488 (Cat # ab150129, Invitrogen, Life Technologies; 1/200), for 1h at room temperature. Slides were mounted using Vectashield Hardset mounting medium with DAPI (Vector Laboratories). Confocal images were acquired on a Zeiss LSM780-FCS (Zeiss, Germany) at 63x magnification.

4.3.8 Mice

All mice were bred in compliance with the Animal Care and Use Committee of the Johns Hopkins University School of Medicine or the Ethical Committee for Animal Testing at the University of Antwerp. The B6.129X1-*Klf15^{tm1Jain}* mice[21] (from here on named *Klf15$^{-/-}$*), which were kindly provided by MJ, were crossed with the *Fbn1$^{C1039G/+}$* mice to create combined transgenic knock-out mice. All experimental mice were maintained on a C57Bl/6J background. Echocardiograms were performed according to Doyle et al[5].

Nair hair removal cream was used on all mice the day prior to echocardiograms. All echocardiograms were performed on awake, unsedated mice using the Visualsonics Vevo660 imaging system and a 30 MHz transducer. The aorta was imaged at 2 and 6 months of age using a standard parasternal long axis view. One of several cardiologists blinded to genotype performed all imaging and measurements.

4.4 Results

We report on a family (Figure 4.1A, Table 4.1: Family 1), in which the proband (II:3) presented with TAA in the ascending aorta associated with right/non-coronary fused bicuspid aortic valve (BAV). The proband's father died from aortic dissection at age 50 years and the proband's uncle died from heart failure at an unknown age. Because no mutation in the known TAA genes was identified, whole exome sequencing (WES) was performed. After filtering, 150 variants passed our criteria. Among these, we identified three interesting candidates: p.Pro149Leu in *COL5A1*, p.Thr365Met in *RXRA* and p.Arg343Cys in *KLF15*. Of the three variants, only the *KLF15* variant was inherited from the affected father. Several lines of evidence

support pathogenicity of the identified *KLF15* p.Arg343Cys substitution in this family. First, the variant is absent from the largest control database currently available (gnoMAD has 245358 alleles at this genomic position)[34]. Second, the variant is located in the first of three DNA-binding Zn-Finger domains (Figure 4.1B), functionally important domains in KLF15. Third, the arginine at that position is highly conserved among KLF15 orthologues and other human members of the KLF superfamily (Figure 4.1C). Fourth, additional segregation analysis in the family demonstrated the absence of the variant in the healthy sisters (Figure 4.1A). No DNA of the paternal uncle was available. Finally, KLF15 is causally linked to TAA-development in angiotensin II-challenged *Klf15*$^{-/-}$ mice[21].

We next searched for additional genetic evidence supporting the role of KLF15 in (BAV)/TAA pathogenesis. Taking advantage of an in-house available WES dataset of 196 BAV/TAA patients that was analyzed with the same filtering parameters, we identified two additional *KLF15* mutation carriers. Two patients harbored three rare *KLF15* variants; p.Arg30Trp, p.Arg110Lys and p.Ser335Asn (Table 4.2: Families 2-3 and Figure 4.1B), of which the latter two were shown to be in cis in the proband of family 2 after PCR fragment cloning. The CADD score of the p.Arg30Trp is rather low (6) but the score of p.Ser335Asn is 27.3 indicating this substitution belongs to the 1% most deleterious substitutions possible in the human genome. Moreover, the p.Ser335Asn variant was also located in the first Zn-Finger domain at a highly conserved amino acid position (Figure 4.1C). Unfortunately, no family members were available for further segregation analysis of this variant. Secondly, we also resequenced an additional cohort of 458 TAA patients using MIPS but failed to identify additional pathogenic variants.

Table 4.1: Clinical characteristics *KLF15* probands and their relatives

Family	Ped ID	Current age or age of death	Sex	Phenotype
Family 1 p.Arg343Cys	I:1		M	Died from heart failure
	I:2*	50†	M	Died from aortic dissection
	II:1	38	F	Aorta ascendens 27mm
	II:3* (proband)	36	M	TAA - aorta root 43mm, aorta ascendens 42mm, BAV (R-N)
	II:4	32	F	Aorta root 30mm, TAV
Family 2 p.Arg110Lys, p.Ser335Asn	Proband		F	TAA, BAV(R-L)
Family 3 p.Arg30Trp	Proband		/	TAA, BAV

Ped ID Pedigree identifier; TAA Thoracic aortic aneurysm; BAV Bicuspid aortic valve; R-N Right- non- coronary leaflet fusion; R-L Right- left coronary leaflet fusion; * mutation present.

For further testing of the repressor and activator function of the mutant KLF15 protein, we selected the variants that are most likely to be damaging (p.Ser335Asn and p.Arg343Cys). Both are located in the same well-conserved first Zn-Finger domain of KLF15 and could thus affect KLF15 protein function. The p.Arg110Lys variant, which was identified on the same allele as p.Ser335Asn, was included to study a possible additive effect. First, we aimed at determining the difference in transcription repressing potential between wildtype (WT) and mutant (p.Arg343Cys, p.Ser335Asn and p.Arg110Lys) KLF15 on two known downstream targets[29], i.e. ANF/Nppa and BNP/Nppb, using luciferase reporter experiments. In addition, because of the suggested role in cardiac fibrosis, we also studied the effect on the *COL3A1* gene

Table 4.2: *KLF15* variants identified by whole exome sequencing

	Nucleotide change	Protein change	MAF ExAC	MAF gnomAD	CADD score
Family 1	c.C1027T	p.Arg343Cys	1/117626	0/245358	17.5
Family 2	c.G329A	p.Arg110Lys	4/96960	6/237086	10.7
	c.G1004A	p.Ser335Asn	4/113484	5/245002	27.3
Family 3	c.C88T	p.Arg30Trp	16/73724	67/267284	6.0

expression. None of the mutations appeared to affect KLF15-dependent *ANF*, *BNP* or *COL3A1* expression (Figure 4.2A). As it was known that KLF15 can affect competitor transcription factors (for eg. KLF15 inhibits recruitment of the coactivator P/CAF to the CTGF promoter[15]) and in order to create a more biologically relevant setting, we added GATA4, a known transcriptional activator of BNP and competitor of KLF15[29]. Interestingly, in the presence of the same amount of GATA4, the p.Arg343Cys KLF15 significantly augmented BNP expression compared to WT KLF15, suggesting this mutation might affect the KLF15 repressor function through its competitive function towards other competitors. The other mutations (p.Ser335Asn with or without p.Arg110Lys) did not show statistically significant differences. Second, the activating role of KLF15 was studied by testing the effect on transcription of *PDK4* and *FATP* (Figure 4.2B), both upregulated by KLF15[35]. The p.Arg343Cys mutation had a significantly increased effect on the activator function for both PDK4 and FATP, whereas the p.Ser335Asn only affected FATP activation. The double mutant p.Ser335Asn/p.Arg110Lys has the same significant effect as p.Ser335Asn by itself, suggesting that the p.Arg110Lys variant does not influence KLF15 function, nor do we see a synergistic effect. Taken together, both mutations located in the Zn-Finger domain are able to alter the KLF15 repressor and/or activation functions.

Subsequently, we investigated whether *Klf15* is expressed in the aortic valve and aortic wall of wild type mouse at the age of 3 weeks. Immunohistochemistry indeed confirms the expression of *Klf15* in aortic wall and aortic valve tissue (Figure 4.3) of mice. Particularly the endothelial cells showed *Klf15* expression.
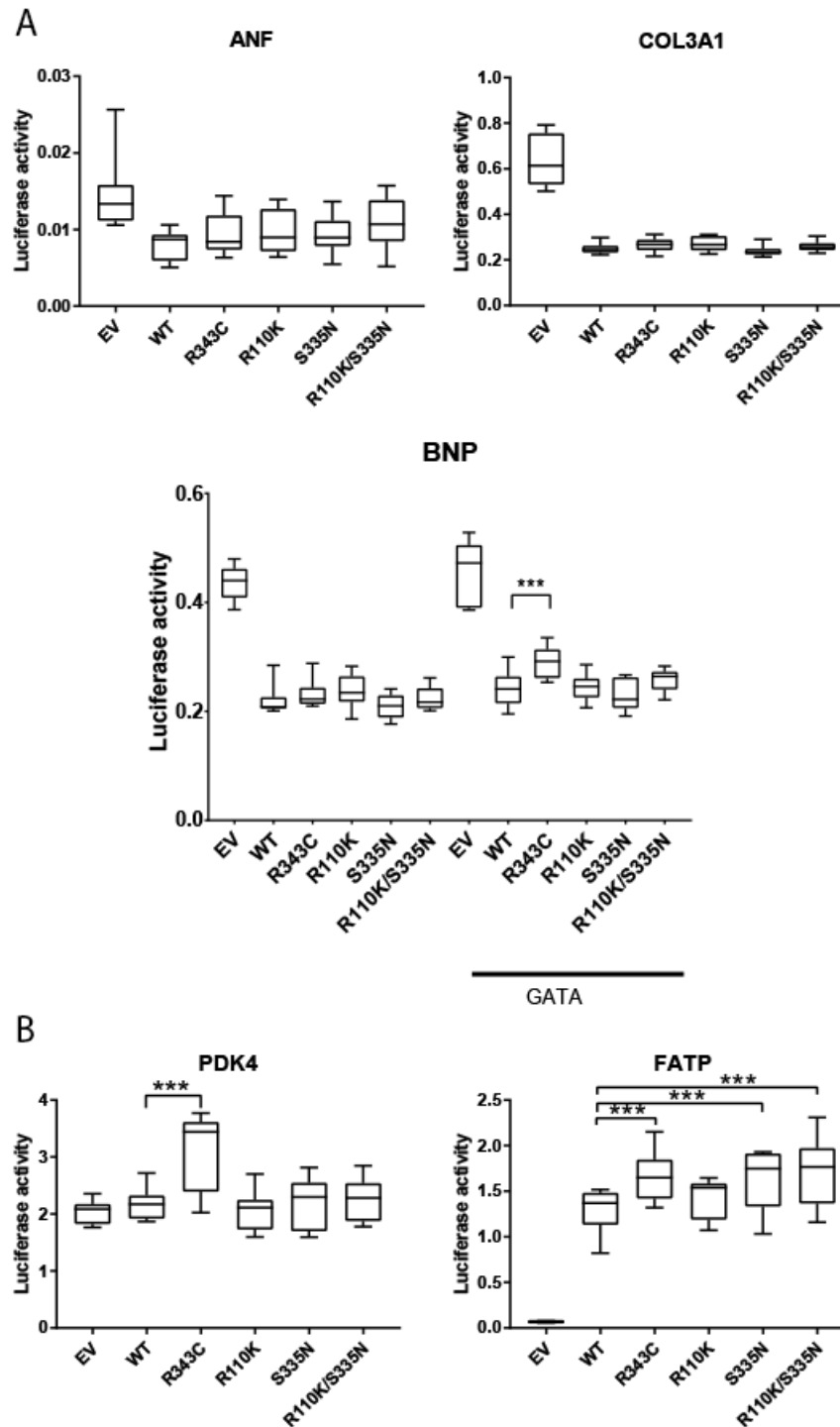
Figure 4.2: Luciferase assay results. **A**: Analysis of the repressor function of KLF15, using downstream genes *ANF*, *BNP* and *COL3A1*. GATA presents the addition of the transcriptional activator GATA4. **B**: Analysis of the activator function of KLF15, using downstream genes *FATP* and *PDK4*. ***p<0.001. EV Empty vector. WT Wild-type.

To study the effect of loss-of-function of *Klf15 in vivo*, we examined for the first time the aortic phenotype of *Klf15*$^{-/-}$ mice without angiotensin II infusion. By echocardiography, we observed significantly increased aortic growth between age 2 and 6 months, resulting in larger aortic root and ascending aortic diameters in *Klf15*$^{-/-}$ mice at 6 months of age (Figure 4.4). Next, we assessed a possible genetic interaction between *KLF15* and *FBN1*. When *Klf15*$^{-/-}$ mice were crossed onto a Marfan background (*Fbn1*$^{C1039G/+}$), a synergistic effect as to aortopathy was observed. Again the aortic growth between 2 and 6 months of age and the resulting aortic root and ascending aorta diameters were significantly increased in *Klf15*$^{-/-}$;*Fbn1*$^{C1039G/+}$ mice compared to age-matched *Klf15*$^{-/-}$ or *Fbn1*$^{C1039G/+}$ mice. Finally, the aortic valves of 30 *Klf15*$^{-/-}$ mice were examined. All mice had normal tricuspid aortic valves.

Because KLF15 has been linked to the TGF-β pathway before[15], and altered TGF-β signaling is a known pathomechanism in syndromic and non-syndromic forms of TAA[10], we investigated the effect of the *KLF15* mutations on TGF-β signaling in aortic wall of a *KLF15* mutant patient. Aortic wall tissue was only available for one of the p.Arg343Cys mutation carriers, namely the proband's affected father (I:2). Verhoeff-Van Gieson staining showed little difference in elastin content and structure between control and p.Arg343Cys patient tissue (Figure 4.5A-C). Trichrome staining suggested that the patient had low to normal collagen levels (Figure 4.5D-F). Immunohistochemistry showed that canonical TGF-β signaling as evidenced by normal pSMAD2 staining was not affected (Figure 4.5G-I), while the non-canonical pathway was strongly altered. There is a statistically significant (p<0.0001) difference in pERK staining between patient and control tissue, especially in the intima (Figure 4.5J-L).
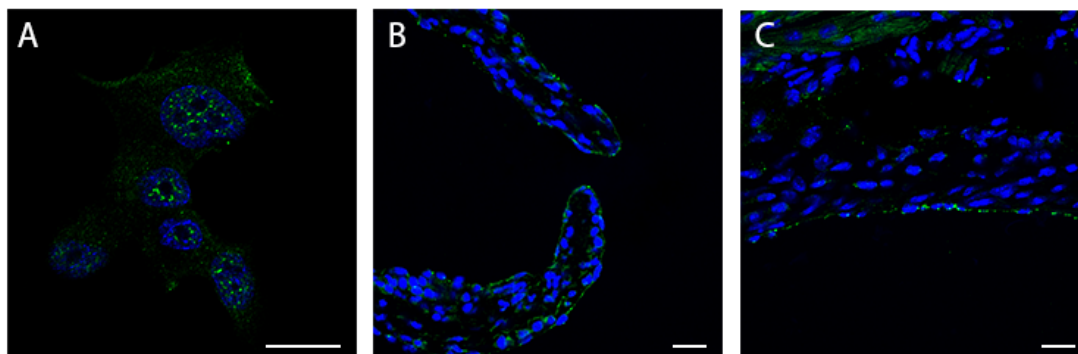
Figure 4.3: **A**: Immunocytochemistry of KLF15 staining in Human aortic endothelial cells. **B**: Endothelial staining of KLF15 in aortic valves of 3 wk old mice. **C**: Endothelial staining of KLF15 in sinus of valsalva of 3 wk old mice. Scale bars are 20μm

4.5 Discussion

After application of WES, we identified *KLF15* as new candidate gene for TAA. KLF15, a transcriptional regulator, was first linked to TAA in 2010[21]. Angiotensin II-challenged $Klf15^{-/-}$ mice showed an increased frequency of aneurysm formation. Based on this observation, we hypothesized that human *KLF15* mutations also contribute to TAA development. We present three rare *KLF15* variants that were all identified in BAV/TAA patients. The p.Arg343Cys and p.Ser335Asn mutations are most interesting because of their location within the first Zn-Finger domain, a highly conserved motif in the KLF transcription factor family. This domain is important for KLF15's DNA-binding function, which led to the hypothesis that the identified *KLF15* mutations could affect downstream gene transcription. The luciferase reporter assays confirmed that p.Arg343Cys and to a lesser extent p.Ser335Asn affect the activator function, but not the repressor function of KLF15. In addition, for p.Arg343Cys we detected a significant difference in repressing BNP in the presence of the activator GATA4. As such, the mutation could affect the competition between transcription factors and thus disturb the normal balance of the transcriptional machinery, a mechanism previously described[15]. This implies that KLF15 has different mechanisms to act as a regulator. Further studies are required to discover the whole range of transcriptional regulators (for different target genes) that

are affected by *KLF15* mutations.

In 2015, Zhan et al demonstrated decreased KLF15 mRNA and protein expression in the aortic wall of aortic dissection patients[36]. In addition, overexpression of Klf15 protects β-aminopropionitrile- (BAPN-) induced aortic rupture in a rat model through the inhibition of CTGF and its target collagens I and III. BAPN is a lysyl oxidase inhibitor that disrupts collagen and elastin-cross links and mimics TGF-β-mediated disruptions of the aorta histology as observed in human aortic dissection pathology. Dysregulation of TGF-β is an important mechanism in the pathogenesis of thoracic aortic dissection[37]. For example, it was previously shown that in Marfan mouse models the physiological function of fibrillins to regulate the activation and bio-availability of TGF-β[38] is disturbed, leading to dysregulation of both canonical and non-canonical TGF-β signaling[39]. It has been reported by several independent groups that aortic dissection is accompanied by significantly increased CTGF and collagen deposition[40, 41]. KLF15 has been shown to regulate CTGF expression in renal[20] and cardiac fibroblasts[15]. The precise mechanism by which KLF15 regulates CTGF and other extracellular matrix target genes, remains unknown but an effect on TGF-β has also been suggested[42]. Whether this is a direct or indirect effect remains to be elucidated. In our study, we demonstrated that the p.Arg343Cys mutation affects TGF-β signaling in the aortic wall of a KLF15 mutant patient, in particular the non-canonical pathway, as we observed a difference for pERK staining between control and disease tissue but not for pSMAD2. Based on our observations, we hypothesize that mutations in *KLF15* disrupt its transcriptional regulatory capabilities and lead to altered production of downstream extracellular matrix proteins and TGF-β signaling components. This dysregulation and its potential feedback loops set the stage for aortic aneurysm development. Further evidence for this hypothesis is provided by the observation of a synergistic effect between mutant *KLF15* and deficient *FBN1* in $Klf15^{-/-};Fbn1^{C1039G/+}$ mice, which indicates a deleterious genetic interaction between *KLF15* and *FBN1*. Possibly, this could happen by affecting transcription or coregulatory recruitment of certain members of the TGF-β pathway. Finally, for the first time we were able to show that $Klf15^{-/-}$ mice develop aortic aneurysm in the root and ascending aorta, not only when induced via angiotensin[21]. Even though we do not yet understand the mechanism of how KLF15 influences aortic diameter growth, the presented human genetic evidence and the mouse model confirm that abnormal *KLF15* plays a sig-

nificant role in aneurysm development. Finally, because the *KLF15* variants were identified in patients with both TAA and BAV and because *KLF15* is expressed in the aortic valve leaflets, a role for *KLF15* in BAV was also examined. All 30 *Klf15*$^{-/-}$ mice had normal tricuspid aortic valves, suggesting that it is unlikely that the BAV phenotype in these patients is caused by *KLF15*.

In conclusion, we identified two *KLF15* variants in BAV/TAA patients and present *KLF15* as a new TAA candidate gene. We performed functional studies focusing on the identified variants, demonstrating their effect on the repressor and activator role of KLF15's function. In addition, we showed the first results of aortic phenotyping in *Klf15*$^{-/-}$ mice which develop TAA spontaneously.
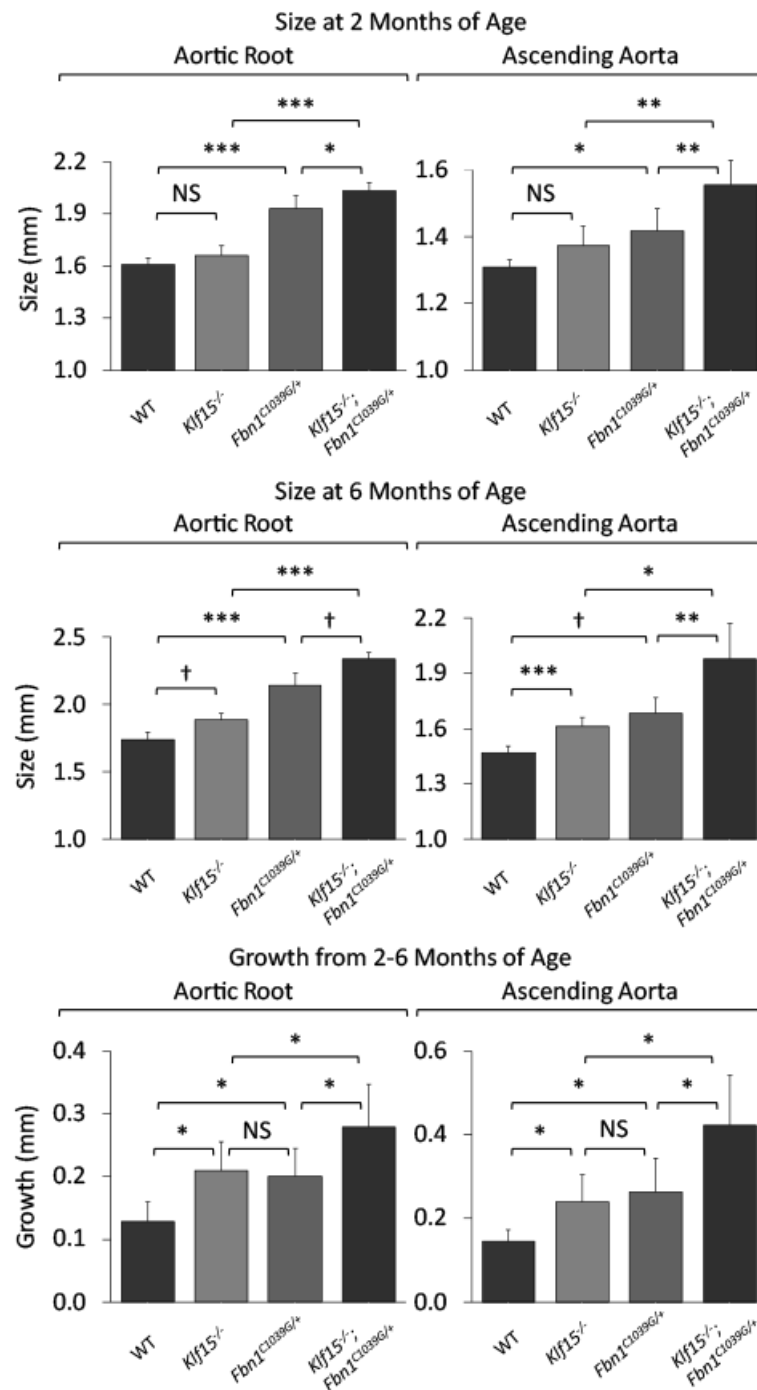
Figure 4.4: *Klf15*$^{-/-}$ mice developing TAA. The upper panel shows results at 2 months of age, while the middle panel depicts results at 6 months of age. The growth between 2 and 6 months is shown in de lower panel. *p<0.05; **p<0.01; †p<0.005; ***p<0.001

4.6   Future perspectives

More research is needed to confirm and elucidate the specific role of KLF15 in TAA development. First of all, additional screening of a larger cohort of BAV/TAA or TAA patients is needed to identify more *KLF15* variants to confirm our genetic findings. Secondly, we propose to confirm our promoter luciferase assays in additional cell lines, for example the NIH 3T3 cells, a mouse fibroblast cell line. The NIH 3T3 cells have the advantage that they have no endogenous KLF15[43] that could possibly influence the results. Human Aortic Endothelial Cells on the other hand would be more biologically relevant. Thirdly, to confirm the effect on the TGF-β signaling pathway, we would ideally use patient fibroblasts to measure expression of ECM proteins and compare with control fibroblast to study the mutations' effects. If these are not available, we suggest to knock-in the p.Arg343Cys and p.Ser335Asn mutations in a cell line (HEK, NIH3T3 or Human Aortic Endothelial Cells). Immunocytochemistry needs to be performed to look at the effect on pSMAD2/pERK signaling and some of the downstream ECM proteins, such as COL3A1 and CTGF. We would also like to perform additional IHC-stainings on the aortic walls of the $Klf15^{-/-}$ mice to investigate effect on TGF-β signaling (eg. pSMAD2, pERK1/2, CTGF). Finally, another interesting experiment would be to develop a CRISPR knock-in mouse model with either the p.Arg343Cys or the p.Ser335Asn mutation. Through cardiovascular phenotyping of the mice and performing immunofluorescence experiments on aortic tissue to evaluate effects on the TGF-β pathway, we would be able to learn more about the *in vivo* downstream effects of the identified mutations and the role of *KLF15* in TAA.
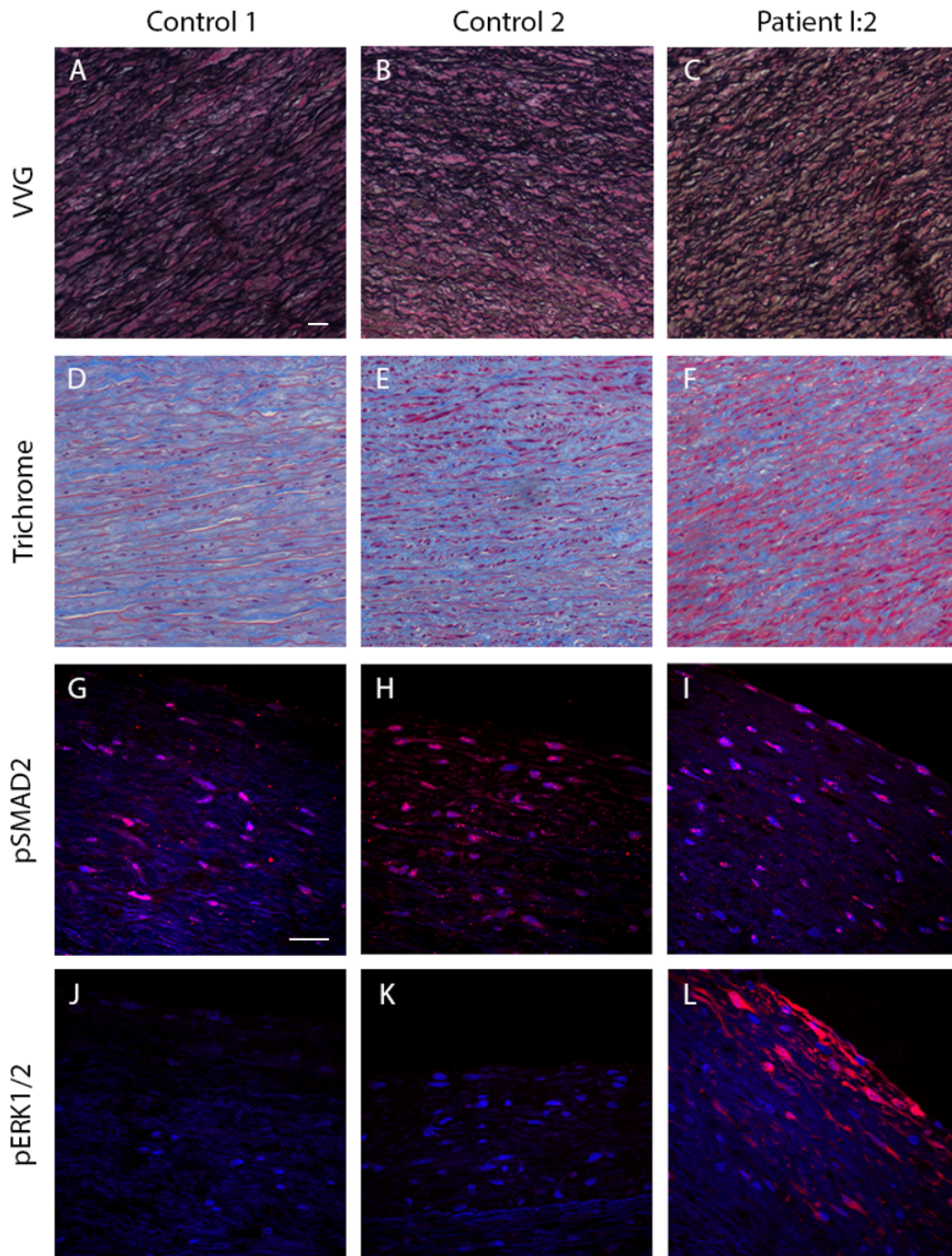
Figure 4.5: **A-C**: Verhoeff–Van Gieson staining visualising elastin fibers in black. **D-F**: Trichrome staining visualising collagen in blue. **G-I**: pSMAD2 staining in red, DAPI staining in blue. **J-L**: pERK1/2 staining in red, DAPI in blue. Scale bar is 23 μm

References

1. Ramanath, V. S., Oh, J. K., Sundt, T. M. & Eagle, K. A. Acute aortic syndromes and thoracic aortic aneurysm. *Mayo Clin Proc* **84,** 465–81. ISSN: 1942-5546 (May 2009).

2. Biddinger, A., Rocklin, M., Coselli, J. & Milewicz, D. M. Familial thoracic aortic dilatations and dissections: A case control study. *J Vasc Surg* **25,** 506–511. ISSN: 07415214 (Mar. 1997).

3. Albornoz, G. *et al.* Familial thoracic aortic aneurysms and dissections–incidence, modes of inheritance, and phenotypic patterns. *Ann Thorac Surg* **82,** 1400–5. ISSN: 1552-6259 (Oct. 2006).

4. Loeys, B. L. *et al.* A syndrome of altered cardiovascular, craniofacial, neurocognitive and skeletal development caused by mutations in TGFBR1 or TGFBR2. *Nat Genet* **37,** 275–81. ISSN: 1061-4036 (Mar. 2005).

5. Lindsay, M. E. *et al.* Loss-of-function mutations in TGFB2 cause a syndromic presentation of thoracic aortic aneurysm. *Nat Genet* **44,** 922–7. ISSN: 1546-1718 (Aug. 2012).

6. Bertoli-Avella, A. M. *et al.* Mutations in a TGF-β Ligand, TGFB3, Cause Syndromic Aortic Aneurysms and Dissections. *Journal of the American College of Cardiology* **65,** 1324–36. ISSN: 1558-3597 (Apr. 2015).

7. Micha, D. *et al.* SMAD2 Mutations Are Associated with Arterial Aneurysms and Dissections. *Human Mutation* **36,** 1145–1149. ISSN: 10597794 (Dec. 2015).

8. Van de Laar, I. M. B. H. *et al.* Mutations in SMAD3 cause a syndromic form of aortic aneurysms and dissections with early-onset osteoarthritis. *Nature genetics* **43,** 121–126. ISSN: 1061-4036 (Feb. 2011).

9. Guo, D.-C. *et al.* Mutations in smooth muscle α-actin (ACTA2) lead to thoracic aortic aneurysms and dissections. *Nature Genetics* **39,** 1488–1493. ISSN: 1061-4036 (Dec. 2007).

10. Renard, M. *et al.* Novel MYH11 and ACTA2 mutations reveal a role for enhanced TGFβ signaling in FTAAD. *Int J Cardiol* **165,** 314–21. ISSN: 1874-1754 (Sept. 2013).

11. Wang, L. *et al.* Mutations in myosin light chain kinase cause familial aortic dissections. *Am J Hum Genet* **87,** 701–7. ISSN: 1537-6605 (Nov. 2010).

12. Guo, D.-c. *et al.* Recurrent gain-of-function mutation in PRKG1 causes thoracic aortic aneurysms and acute aortic dissections. *American journal of human genetics* **93,** 398–404. ISSN: 1537-6605 (Aug. 2013).

13. Pearson, R., Fleetwood, J., Eaton, S., Crossley, M. & Bao, S. Krüppel-like transcription factors: a functional family. *The international journal of biochemistry & cell biology* **40,** 1996–2001. ISSN: 1357-2725 (Jan. 2008).

14. Otteson, D. C., Lai, H., Liu, Y. & Zack, D. J. Zinc-finger domains of the transcriptional repressor KLF15 bind multiple sites in rhodopsin and IRBP promoters including the CRS-1 and G-rich repressor elements. *BMC molecular biology* **6,** 15. ISSN: 1471-2199 (Jan. 2005).

15. Wang, B. *et al.* The Kruppel-like factor KLF15 inhibits connective tissue growth factor (CTGF) expression in cardiac fibroblasts. *Journal of molecular and cellular cardiology* **45,** 193–7. ISSN: 1095-8584 (Aug. 2008).

16. Haldar, S. M. *et al.* Kruppel-like factor 15 regulates skeletal muscle lipid flux and exercise adaptation. *Proceedings of the National Academy of Sciences of the United States of America* **109,** 6739–44. ISSN: 1091-6490 (Apr. 2012).

17. Gray, S. *et al.* The Krüppel-like factor KLF15 regulates the insulin-sensitive glucose transporter GLUT4. *The Journal of biological chemistry* **277,** 34322–8. ISSN: 0021-9258 (Oct. 2002).

18. Gray, S. *et al.* Regulation of Gluconeogenesis by Krüppel-like Factor 15. **5,** 305–312 (2007).

19. Chin, M. T. KLF15 and Cardiac Fibrosis: The Heart Thickens. *J Mol Cell Cardiol* **45,** 165–167. ISSN: 1878-5832 (2008).

20. Gao, X., Wu, G., Gu, X., Fu, L. & Mei, C. Kruppel-like factor 15 modulates renal interstitial fibrosis by ERK/MAPK and JNK/MAPK pathways regulation. *Kidney & blood pressure research* **37,** 631–40. ISSN: 1423-0143 (Jan. 2013).

21. Haldar, S. M. *et al.* Klf15 deficiency is a molecular link between heart failure and aortic aneurysm formation. *Science translational medicine* **2,** 26ra26. ISSN: 1946-6242 (Apr. 2010).

22. Luyckx, I. & Loeys, B. L. The genetic architecture of non-syndromic thoracic aortic aneurysm. *Heart* **101,** 1678–1684. ISSN: 1355-6037 (Oct. 2015).

23. Giardine, B. *et al.* Galaxy: a platform for interactive large-scale genome analysis. *Genome research* **15,** 1451–5. ISSN: 1088-9051 (Oct. 2005).

24. DePristo, M. A. *et al.* A framework for variation discovery and genotyping using next-generation DNA sequencing data. *Nature genetics* **43,** 491–8. ISSN: 1546-1718 (May 2011).

25. Vandeweyer, G., Loeys, B. L. & Van den Bulcke, T. VariantDB: A flexible annotation and filtering portal for NGS data. *Genome Med,* in press (2014).

26. Koressaar, T. & Remm, M. Enhancements and modifications of primer design program Primer3. *Bioinformatics* **23,** 1289–1291. ISSN: 13674803 (May 2007).

27. Untergasser, A. *et al.* Primer3-new capabilities and interfaces. *Nucleic Acids Research* **40,** e115. ISSN: 03051048 (Aug. 2012).

28. The UniProt Consortium. UniProt: a hub for protein information. *Nucleic Acids Research* **43,** D204–D212. ISSN: 0305-1048 (Jan. 2015).

29. Hiatt, J. B., Pritchard, C. C., Salipante, S. J., O'Roak, B. J. & Shendure, J. Single molecule molecular inversion probes for targeted, high accuracy detection of low frequency variation. *Genome research* **23,** 843–54. ISSN: 1549-5469 (2013).

30. Fisch, S. *et al.* Kruppel-like factor 15 is a regulator of cardiomyocyte hypertrophy. *Proceedings of the National Academy of Sciences of the United States of America* **104,** 7074–9. ISSN: 0027-8424 (Apr. 2007).

31. Svensson, E. C., Huggins, G. S., Dardik, F. B., Polk, C. E. & Leiden, J. M. A functionally conserved N-terminal domain of the friend of GATA-2 (FOG-2) protein represses GATA4-dependent transcription. *The Journal of biological chemistry* **275,** 20762–9. ISSN: 0021-9258 (July 2000).

32. Prosdocimo, D. A. *et al.* KLF15 and PPARα Cooperate to Regulate Cardiomyocyte Lipid Gene Expression and Oxidation. *PPAR Research* **2015.** ISSN: 1687-4757. doi:`10.1155/2015/201625` (2015).

33. Schneider, C. A., Rasband, W. S. & Eliceiri, K. W. NIH Image to ImageJ: 25 years of image analysis. *Nature methods* **9,** 671–5. ISSN: 1548-7105 (July 2012).

34. Cambridge, M. *Exome Aggregation Consortium (ExAC)*

35. Prosdocimo, D. a. *et al.* Kruppel-like factor 15 is a critical regulator of cardiac lipid metabolism. *J Biol Chem* **289,** 5914–5924. ISSN: 00219258 (Feb. 2014).

36. Zhan, B. *et al.* KLF15 Overexpression Protects β-Aminopropionitrile–Induced Aortic Rupture in Rodent Model via Inhibiting Connective Tissue Growth Factor. *The Thoracic and Cardiovascular Surgeon.* ISSN: 0171-6425. doi:`10.1055/s-0035-1566743` (2015).

37. Gillis, E., Van Laer, L. & Loeys, B. L. Genetics of thoracic aortic aneurysm: at the crossroad of transforming growth factor-β signaling and vascular smooth muscle cell contractility. *Circulation research* **113,** 327–40. ISSN: 1524-4571 (July 2013).

38. Neptune, E. R. *et al.* Dysregulation of TGF-beta activation contributes to pathogenesis in Marfan syndrome. *Nat Genet* **33,** 407–11. ISSN: 1061-4036 (Mar. 2003).

39. Habashi, J. P. *et al.* Angiotensin II type 2 receptor signaling attenuates aortic aneurysm in mice through ERK antagonism. *Science* **332,** 361–5. ISSN: 1095-9203 (Apr. 2011).

40. Wang, X., Lemaire, S. A., Chen, L. & Shen, Y. H. Increased Collagen Deposition and Elevated Expression of Connective Tissue Growth Factor in Human Thoracic Aortic Dissection Xinwen. *Vascular Surgery* **114,** 1–13 (2006).

41. Meng, Y., Tian, C., Liu, L., Wang, L. & Chang, Q. Elevated expression of connective tissue growth factor, osteopontin and increased collagen content in human ascending thoracic aortic aneurysms. *Vascular* **22,** 20–27. ISSN: 1708-5381 (Feb. 2014).

42. Yu, Y. *et al.* KLF15 Is an Essential Negative Regulatory Factor for the Cardiac Remodeling Response to Pressure Overload. *Cardiology* **130,** 143–152 (2015).

43. Mori, T. *et al.* Role of Krüppel-like factor 15 (KLF15) in transcriptional regulation of adipogenesis. *The Journal of biological chemistry* **280,** 12867–75. ISSN: 0021-9258 (Apr. 2005).

PART IV

Discussion

1   Unravelling the genetics of TAA and BAV

Studying the genetics of thoracic aortic aneurysms (TAA) over the years has
helped us to understand the pathogenesis of TAA tremendously.   But, even
though we have started to unravel the genetic determinants, we still struggle to
grasp the complete pathogenetic mechanisms underlying TAA. How do muta-
tions specifically lead to dysregulated transforming growth factor-beta (TGF-β)
signalling, which in turn affects the dilation of the aortic wall?   And how does
the myriad of interconnected pathways and mutations in their genes lead to disease?

FBN1, encoding fibrillin-1, was the first TAA gene to be discovered back in 1991
as the gene responsible for the Marfan syndrome (MFS)[1]. At that time, the most
plausible theory to explain how *FBN1* mutations cause TAA, was the weakening
aortic wall model. Fibrillins are important in the extracellular matrix (ECM) and
form the supporting structure of the aortic wall[2]. Thus, if fibrillins in the ECM
of the aortic wall weaken due to a *FBN1* mutation, this wall becomes more prone
to aneurysms and ruptures. Additionally, it explains the ectopia lentis observed
in MFS, because the weak fibrillin fibrils affect the ciliary apparatus. However,
the skeletal symptoms of overgrowth are hard to explain by the weakening wall
model. This structural deficiency theory was then complemented when Neptune et
al. discovered dysregulation of the TGF-β pathway in the lungs of MFS mice[3].
Subsequently, upregulation of TGF-β signalling was demonstrated in the aortic
walls of these MFS mice as well[4]. It was hypothesized that *FBN1* deficiency leads
to altered sequestration of the latent form of the TGF-β cytokine, making it more
accessible and hereby activating its signalling pathway. Additional evidence for this
hypothesis was gathered when more genes were identified for the syndromic forms
of TAA. Loeys-Dietz syndrome (LDS), a syndrome resembling MFS is caused by
mutations in *TGFBR1/2*[5]. Later on, *SMAD2*[6], *SMAD3*[7], *TGFB2*[8, 9] and
TGFB3[10] were added as causal genes. In recent years, even more genes from the
TGF-β pathway have been linked to other syndromic forms of TAA, for example
SKI for Shprintzen-Goldberg syndrome (SGS)[11] (Introduction; Table 1). Causal
missense mutations in *SMAD2*, *SMAD3*, *TGFB2* and *TGFB3* genes are located for
the most part in functionally important domains[12], and the additional presence
of nonsense mutations in or complete deletions of these genes, suggest that loss of

function (LOF) is the most probable pathogenetic mechanism in these subtypes of LDS. On top of that, most of the *TGFBR1* and *TGFBR2* mutations are also predicted to be LOF mutations. Paradoxically, the common observation in aortic wall tissue of TAA patients is that the TGF-β pathway is upregulated[6, 8, 10, 13, 14]. This finding is referred to as the TGF-β paradox. While *FBN1* deficiency could explain an upregulation of the TGF-β pathway by decreased sequestration, LOF mutations in the more downstream genes cannot be explained that easily.

Several theories have been proposed to explain this paradoxal upregulation[15]. Intitial theories focused on possible shifts in balances of the TGF-β pathway. For example, the altered use of different TGF-β ligands (TGF-β1, 2 or 3) or altered cycling of the TGF-β receptors on the cell surface can cause a boost of the pathway. In addition, the balance between the canonical (via SMAD proteins) and non-canonical (via ERK/JNK/p38 proteins) TGF-β signalling was demonstrated to be affected. Both pathways have been shown to be upregulated in diseased aortic human tissue and aorta from mouse MFS models[8, 10, 16]. More recent studies have gained insight into the LDS genes *TGFBR1/2* via human and mouse studies[16]. It was shown that pure haploinsufficiency of *TGFBR1/2* does not cause the LDS phenotype in mice[16]. Moreover, the smooth muscle cells (SMCs) in the aortic wall have different embryological origins dependent on their location. SMCs in the ascending aorta originate from the neural crest cells and second heart field cells. SMCs in the proximal descending aorta, on the other hand, derive from the somatic mesoderm, while the SMCs in the distal descending aorta originate from the splanchnic mesoderm[17]. Dependent on their origins, the aortic SMCs might respond differently to the disturbed TGF-β signalling[18]. Certain cell types might be more sensitive towards heterozygous LDS mutations, and subsequently overcompensate for the initial loss in TGF-β signaling by secreting excessive amounts of TGF-β ligand in their direct environment. This, in turn, could lead to an extreme overexpression of the TGF-β signaling pathway in neighboring cells with a different origin, which might be less vulnerable to those LDS mutations[16]. Because overexpression of pSMAD2 is also found in aortic media tissue of LDS patients, other TGF-β related pathways might be involved as well, for example the angiotensin II signalling pathway[19]. Importantly, the angiotensin II receptor 1 inhibitor losartan ameliorates aortic disease in LDS mice and it correlates with

pSMAD2 inhibition and the reduced expression of TGF-β ligand[16]. Therefore, the positive effect of losartan may not be solely dependent on its antihypertensive properties. Additionally, it might be involved in circumventing or suppressing whichever mechanism is driving increased TGF-β signalling in LDS mice[16]. While we are learning more about the possible mechanism of the TGF-β paradox, more research will be needed to unravel it completely.

Chapter 4 revealed *KLF15* as a possible new culprit for non-syndromic TAA. While there are potential links of KLF15 to the TGF-β pathway, its role is probably more complex. As a transcription factor it could potentially affect other pathways, disturbing expression of certain proteins and only indirectly affecting the balance of the TGF-β pathway. We have observed an increase in the non-canonical TGF-β pathway in the aortic wall of a patient carrying a *KLF15* mutation (but not of the canonical pathway), showing that both parts of the TGF-β pathway can be differentially affected. The effects of TGF-β signalling proved to be even more complex when researchers showed that mutations in the same gene (*FBN1*) could cause phenotypes opposite of MFS, like geleophysic dysplasia (OMIM 614185) and stiff skin syndrome (OMIM 184900)[20, 21]. These *FBN1* mutations affect specific FBN1 domains, namely the fourth and fifth LTBP-like domains. Interestingly, in both conditions, enhanced TGF-β signalling, similar to the one found in MFS, has been observed[20, 21]. This further indicates the importance of tissue and domain specific FBN1 effects on the TGF-β pathway.

In addition, both canonical and non-canonical TGF-β pathways are subject to epigenetic influences[22]. MicroRNAs (miRNA) play a role in RNA silencing and post-transcriptional gene regulation and are found to be implicated in vascular diseases[22]. For example, the miR-143/145 cluster is enriched in SMCs[23] and is involved in the communication between SMCs and endothelial cells. This communication is in itself also controlled by TGFB1[24], implicating that it might play a role in TAA development as well. Furthermore, several miRNAs have been found to be important in epigenetic regulation of specific genes within the TGF-β pathway[22]. Among these targets are *TGFB1*[25], *SMAD1*[26], *SMAD4*[26, 27] and *SMAD2*[27].

Non-syndromic forms of TAA have likewise been associated with increased TGF-β signalling. Aortic tissue of *ACTA2* and *MYH11* patients show dysregulated TGF-β signalling[28]. Overall, the current knowledge on the genes involved in the pathogenesis of TAA suggests that the identified SMC apparatus genes, extracellular matrix (ECM) genes and even transcription factors all seem to be linked to each other via their common denominator, the TGF-β pathway. With all the evolving different balances and interplay between pathways, a lot more research will be needed to unravel how these all connect and lead to TAA.

Remarkably, bicuspid aortic valve (BAV) patients have an increased risk of developing TAA. Although BAV has been described already by Leonardo da Vinci over 400 years ago[29], until recently, little was known about its genetics and the pathophysiological link with TAA. Historically, the disturbed flow model was deemed an interesting hypothesis. This theory states that the malformed (bicuspid) aortic valve causes a turbulent flow affecting the aortic wall. Nowadays, it is also accepted that BAV and TAA are linked genetically, based on a number of arguments. These include the common embryological origin, the worsening of TAA after valve replacement[30] and the fact that there are families with patients with BAV only, TAA only or combined BAV and TAA, spread over different generations[31]. Although the role of the TGF-β pathway has been established in TAA formation, its role in BAV/TAA is less well documented. Some studies showed enhanced TGF-β signalling in BAV aneurysms[32], while others showed that TGF-β signalling is silenced in BAV patients[33]. In chapter 3, we have contributed to the unravelling of the genetics of BAV/TAA, by focusing on the genes traditionally associated with BAV itself. By applying resequencing of a candidate gene panel, we revealed that BAV/TAA is not associated with *NOTCH1*, the only "established" BAV gene thus far. Based on the role of *NOTCH1* in aortic stenosis, it is likely that *NOTCH1* mutations are important for the early calcification of BAV but not for TAA. Our resequencing study has identified *SMAD6* as a strong candidate for BAV/TAA[34]. Eleven *SMAD6* variants were identified in 441 patients (2.5%) versus 450 *SMAD6* variants in 47,389 individuals (0.9%) in the ExAC control database. Surprisingly, 36.4% (n = 4/11) of the *SMAD6* mutations in the patient cohort were loss of function (LOF; frameshift, nonsense or splice site) mutations, and truncating *SMAD6* mutations were found in only 4.0% (n = 18/450) of the

ExAC control individuals. The enrichment of deleterious variations confirmed that *SMAD6* is an interesting candidate gene for BAV/TAA. Future research is needed to study the effect of these *SMAD6* mutations on the TGF-β pathway genes in aortic tissue of patients. The observation that so few genes have been associated with BAV/TAA thus far, points towards its enormous genetic heterogeneity. Most probably, multiple variations in different genes in a specific or even in a number of different pathways in combination with the person's specific altered flow pattern will make a person more prone to develop TAA in the presence of BAV and other common BAV-associated cardiovascular malformations.

As with TAA, it is expected that epigenetics have a possible effect on BAV. Genome-wide methylation studies showed differences in DNA methylation between BAV/TAA and TAV/TAA patients[35]. Moreover, miRNAs not only affect the TGF-β pathway (as described above) but they have been linked to mechano-transduction as well[36]. Recent studies have revealed the possible roles of shear stress-regulated miRNAs[36, 37]. This would fit with the mixed BAV/TAA hypothesis of genetics and hemodynamics. Indeed, the altered flow can contribute as environmental factor to the complex BAV/TAA genotype[38]. For example, BAV shape can influence flow patterns within the aorta[39]. They can even help aneurysm progression at different locations. For example the majority of patients with the right-left cusp fusion develop dilations at the tubular portion of the ascending aorta, while patients with right-non-coronary fusion will more likely develop aneurysms at the aortic root[39].

Shear stress on the other hand turns out to have an effect on gene expression[40]. For example, it can activate matrix metalloproteinases (MMPs) which in turn can degrade fibrillin-1 proteins[41]. Indeed, MMP2 has been observed to be increased in BAV/TAA aortas compared to TAV/TAA aortas[42]. Another example of the importance of shear stress are the *FOXE3* mutations in TAAD patients[43]. It was shown that FOXE3 deficiency causes increased SMC apoptosis and relative thinning of the aortic wall after mechanical stress induced by transverse aortic constriction[43]. Possibly, if BAV patients would have mutations in genes that can be affected by mechanical stress, they would be more prone to aneurysm formation. Additionally, when shear stress in the aorta is mapped, regions of wall

shear stress merge with regions of ECM dysregulation in aortas of BAV patients[44].

In general, the genetic heterogeneity and shear complexity of BAV is a tremendous challenge for scientists. At present, we don't even know how far this heterogeneity stretches. In addition, it is an oversimplification that common diseases are either caused by common alleles or by a lot of rare alleles. As professor Katsanis discussed in an opinion piece[45], our current methods of compartmentalising diseases is probably hindering our research efforts. Especially for complex diseases, we focus too much on a small group of genes. We would better start considering biological pathways as a whole instead of focusing on certain genes. A new idea is to see the pathway as the locus, not just the one variant. Complex statistics are needed to help generating models for looking at contribution of different factors, both genetic and environmental. BAV/TAA would be a perfect example with its complex genetics, epigenetics and hemodynamic influences. Another great help to improve our efforts is high-throughput functional testing. Analysing the effect of a disturbed pathway in a functional context would be most useful.

2 The future of genetics: whole genome sequencing

While many genes have already been linked to TAA (Introduction; table 1), about 70% of patients still await a proper diagnosis. One of the issues that may prevent a proper diagnosis is the set of techniques that are currently used both in research and diagnostic settings.

The story of chapter 1 is a clear example of the way genetic testing is evolving. It took over 10 years to properly diagnose this specific MFS family. Clinically diagnosed with MFS, *FBN1* was the obvious candidate. Sanger sequencing, high-pressure liquid chromatography, multiplex ligation-dependent probe amplification and even whole exome sequencing were employed in search of the causal mutation, but all failed to identify the pathogenic *FBN1* variant. Because our linkage analysis pointed to the *FBN1* gene once again, the mutation probably had been missed

despite all the effort and the different technologies that had been applied. The deep intronic mutation that was finally identified could only have been found using cDNA sequencing or whole genome sequencing (WGS). Techniques that are not regularly being used in the current diagnostic setting. However especially WGS will become the gold standard in the near future.

The field of genetics is rapidly evolving through next generation sequencing and third generation sequencing. In 2012, the Centre of Medical Genetics had implemented whole exome sequencing and targeted gene panels, which have been used throughout this thesis. Nowadays, WGS is becoming more and more feasible. This series of innovations brings a lot advantages, but also disadvantages. While WGS will pick up all variants in the entire genome, which would have been ideal for the family in chapter 1, it will also generate an enormous number of variants that will be very difficult to interpret. Our current knowledge of the non-coding genome, or even the coding genome, is not sufficient to explain all those variants. But with initiatives like gnomAD[46] and the increasing importance of bioinformatics, we are learning more about rare and common variants within the genome. It also stresses the importance of sharing data, which is most important and essential for the future of genetic research. On a positive note, WGS is hypothesis-free and thus shows no bias. Research on complex diseases is too often hypothesis-driven with a strong focus on a select number of genes. These are then placed into gene panels which will help gathering information about those particular genes, but finding new genes and pathways will be impossible with this approach. For patients, WGS will be an immense change. The use of WGS in future diagnostic settings will change genetic diagnostics from using genetic testing to find a diagnosis to having your genome sequenced before going to a doctor, and implementing those results in making a diagnosis[47]. On the other hand, a potential downside of WGS are the so-called incidental findings. Specific counselling rules on how much the patient wants or needs to know should be established. The identification of these findings and whether or not to tell patients spurs debate even between researchers, let alone the general public. With the upcoming genome age, the larger public needs to be informed more than ever. While the advances will be ground-breaking for disease knowledge and treatment, implications on everyday lives might be immense and will affect rules on data management, safety and privacy.

Because the functional effects of WGS variants are often unclear, there is an urgent
need to bring sequencing data and functional studies closer together. While it
is impossible to study every identified variant at the moment, it is important to
invest in high-throughput functional studies. For example, Starita et al[48], focused
on massive parallel functional testing of missense *BRCA1* mutations and their E3
ubiquitin ligase activity and their binding to the BARD1 RING domain. With
the rapid advances in CRISPR/Cas modelling, we are closer to developing animal
models with their corresponding mutations more accurately and easier than ever
before. Moreover, in the context of complex diseases it will be useful to test gene
interactions by introducing multiple mutations in the same animal. It is therefore
important to invest time and money in developing this bridge between molecular and
functional research. As it will, without doubt, become increasingly more relevant in
diagnostic settings.

3   The impact of genetics on patient management

Whether or not a patient's causal mutation is known, clinical management
and its development are immensely important. TAA patients usually undergo
annual surveillance imaging as the aortic diameter is the main predictor of aortic
dissection[49, 50]. Either echocardiography, computed tomographic angiography
(CTA), or magnetic resonance imaging (MRI), more specifically MRA (magnetic
resonance angiography) are used to measure the aortic diameters along the aorta.
Prophylactic treatment is used to help minimize aortic growth, however it is often
impossible to avoid surgery[51].

Historically, aortic diameters >55 mm were regarded as at high risk for dissection
as discussed in the introduction. However, nowadays family history, z-scores[52,
53] and the specific gene defects are taken into account. For example, for patients
with MFS syndrome, an echocardiography every year is preferred and if the aortic
diameter reaches >50 mm, aortic root surgery is recommended[54]. LDS patients
with a mutation in *TGFBR1* or *TGFBR2* should be operated when the diameter
of the aorta reaches 40 to 42 mm in adults. Patients with *SMAD3* mutations will

benefit from similar treatment guidelines, whereas the *TGFB2* and *TGFB3* patients seem to have milder aortic disease; but the experience within the latter group is small and specific treatment guidelines need more discussion. Patients with familial TAA, including those that have mutations in *MYH11*, *ACTA2*, *MYLK* and *PRKG1*, with relatives who have experienced an aortic dissection should be operated at a minimal dilatation of the thoracic aorta between 45 and 50 mm[55, 56]. For all other patients with TAAD, the American College of Cardiology recommends operating when the ascending aorta or aortic root reaches a threshold of 50 mm, in case of rapid growth of the aorta (±5 mm/year) or in the presence of severe aortic valve insufficiency or stenosis.

Follow-up guidelines for aortic surgery in BAV patients are historically based on ascending aorta diameter guidelines in connective tissue disorders (40-50 mm)[57, 58]. However, more and more studies show that the dilated aorta in BAV patients is distinctively different and that therefore clinical management should be specifically tailored to BAV/TAA patients[57]. For example, MFS aortas have a worse prognosis than BAV aortas[59]. Therefore, the cut-off for surgical indication has been changed to 50 mm for BAV/TAA patients, in contrast to TAV/TAA patients[58]. Additionally, BAV/TAA patients with aortic valve insufficiency might risk dissection at lower diameters than BAV/TAA patients with aortic valve stenosis[57, 60]. This only augments the complexity of BAV/TAA and its clinical management. With the recent identification of *SMAD6* mutations in BAV patients, it will be interesting to perform clinical evaluation of *SMAD6* patients and start to develop gene-specific guidelines for BAV/TAA patients with mutations in specific genes as well. Additionally, it is noted that *NOTCH1* mutations are more likely linked to calcified BAV[34], thus TAA guidelines might be different for *NOTCH1* patients, compared to those for *SMAD6* patients.

In addition, BAV patients will likely require replacement of their bicuspid aortic valve within their lifetime, and they may benefit from early valve replacement because this may reduce their risk of secondary aortic aneurysms influenced by turbulent flow. As discussed before, shear stress itself could have a contributing effect on aneurysm development[40]. However, in BAV patients with lower chance of TAA development, possibly *NOTCH1* patients, it might be appropriate to consider sparing the natural aortic valve as replacement might not be necessary to

diminish the risk for aneurysm progression and/or dissection.

The decision to perform aortic surgery currently depends on the aortic diameter, aortic z-score and its progression, family history, valve function and the causal gene. Additionally, identification of specific genetic modifiers might make this decision even more precise in the future. Moreover, not only the aortic diameter and the patient's gene defect will be taken into account before performing surgery, the aorta's biomechanical properties, such as tensile strength and aortic wall thickness, will help decide when an aorta is most at risk[61]. As such, the importance of an interdisciplinary management cannot be underestimated. Moreover, it is expected that epigenetics might get involved in this decision as well. Biomarker tests, for instance testing specific miRNA's, might be developed and may be used as non-invasive tests to predict aortic dissection risks. This may be especially interesting to detect high risk aortas in BAV patients.

Clinical follow-up is also important for relatives of TAA patients. Relatives of MFS patients undergo either clinical examination (if the familial mutation is unknown) or genetic testing (if the pathogenic mutation is known) to evaluate their risks[62]. For BAV/TAA patients there are no standard guidelines yet on genetic counselling for patients and their relatives, although clinical screening of first-degree relatives is recommended[63]. The biggest challenge is to find the asymptomatic family members that are most at risk.

Medical treatment aiming at reducing aortic wall stress consists mostly of anti-hypertensive drugs such as beta-blocker treatment[64]. Alternatively, angiotensin receptor blockers and angiotensin-converting-enzyme inhibitors are being used as well[65]. Besides reducing wall stress, some anti-hypertensive drugs may also play a role in reducing the rate of aortic wall growth. Losartan, an angiotensin receptor blocker and anti-hypertensive was investigated as a possible treatment in Marfan patients[66, 67]. As the angiotensin pathway is in itself a regulator for the TGF-β pathway, losartan was shown to diminish the accumulation of activated SMAD2 and also to reduce expression of TGFβ–responsive genes[68]. Several large randomized controlled trials have recently studied the effect of losartan on aortic

dilation growth in MFS during a 3-year period and have presented different results. First, the Pediatric Heart Network trial in which 608 young MFS patients were treated with losartan or atenolol, showed no significant differences between the effect of both treatments[69]. This study used very high dose of the beta-blocker atenolol or regular dose of losartan, suggesting that either could be used in clinical practice. Importantly, this study showed for the first time that earlier initiation of treatment (in both groups) has more favourable outcomes. While Groenink et al showed that losartan was able to reduce aortic dilation growth rate[67] in an adult MFS population, the Milleron study confirmed that the drug indeed decreased blood pressure in patients with MFS, but did not limit aortic dilatation[66]. The latter researchers stated that beta-blocker therapy should remain the standard first line of therapy in these patients. Interestingly, there is no evidence to show that beta-blockers are actually superior to other anti-hypertensive medications as a first-line treatment, because of the lack in randomized controlled trials that compare the two kinds of therapy[70].

Currently two other interesting studies are ongoing. Firstly, a meta-analysis in which 2.300 MFS patients from all finished trials in which angiotensin receptor blockers, such as losartan, versus placebo (or open-label control) and angiotensin receptor blockers versus β-blockers are being compared[71], had been started. Secondly, the first large trial investigating the benefits of irbesartan, which is another type of angiotensin receptor blocker[72] is being carried out in the UK. The results of these studies will hopefully shed more light on the optimal treatment strategy for MFS patients.

As expected, the focus of clinical research is moving towards personalized treatments. For example, the response to losartan was compared between MFS patients with haploinsufficient *FBN1* mutations and dominant negative *FBN1* mutations. Patients with haploinsufficient mutations seemed to have an increased inhibition of aortic root dilatation rate compared to patients with dominant negative mutations[73]. This result might offer a possible explanation for the discrepancies found in the results of the different clinical trials[66, 67] and show that standard trials should take into account information about the patient's genetic background. This also confirms that gene-tailored therapies will become the gold standard in the

future.

The importance of disease or gene-tailored guidelines cannot be underestimated. The reality of prescribing existing drugs for diseases without prior knowledge is highlighted by the recent findings on calcium channel blockers. Despite limited evidence for their efficacy and safety in the disorder, calcium channel blockers (CCBs) have also been prescribed to patients with MFS to slow down aortic aneurysm growth. However, MFS mice that were treated with CCBs have shown increased aneurysm growth, rupture, and premature lethality[74]. Indeed the CCB's amlodipine and verapamil increase aneurysm growth, while hydralazine (another CCB) is more tolerated. Thus, not all blood pressure lowering drugs can be used in TAA patients and excessive testing of existing therapeutics is extremely important.

Additionally, better insight in the pathogenesis of thoracic aortic disease opens up new perspectives for alternative treatments. For example, researchers have been looking into TGF-β neutralizing antibodies to undermine the increased TGF-β signalling pathway in TAA[75]. However results have been inconsistent, in fibrillin1 haploinsufficient mice and AngII-infused CXCL10 deficient mice, aneurysms would be reduced, while in fibrillin1 hypomorphic mice and in AngII-infused mice aortic rupture is accelerated[4, 75–77]. The possible target of matrix metalloproteinases (MMPs) has been selected for treatment as well. As described before, MMPs are important in degradation of FBN1 and the overall turnover of ECM proteins. Research showed that inhibitors of MMPs have an effect on vascular disease in animal models[78]. Another interesting approach consists of antagonizing the FBN1-derived GxxPG (Gly-x-x-Pro-Gly) fragments, these motifs can induce effects such as increased MMP activity by induction of signalling through the elastin-binding protein (EBP). Antagonizing these fragments has also been shown to ameliorate disease in MFS mice[79].

Finally, preclinical studies with stem cell therapy have been initiated[80]. It was shown that multipotent stem cells are abundant in affected TAAD tissue and that differentiation of these cells to VSMC and fibroblasts is not uncommon. Stem cells

might not only be involved in repair of medial degeneration tissue, but also in destructive modelling. In more recent research, it was shown that administration of mesenchymal stem cells in a mouse model slowed down aneurysm growth[81]. As these are only preliminary data, additional research will be required to assess the role and behaviour of stem cells in aortic tissue before treatment strategies can be developed.

The increasing knowledge gathered during the past few years provides opportunities for promising research at genetic, molecular, and hemodynamic levels, which in turn leads to new ways of approaching therapies. With every new TAA gene identified, the hope for new effective therapies increases. As a result of the growing evidence of the involvement of the TGF-β pathway, this remains the main focus. However, extended research will hopefully lead to a therapeutic regimen working on multiple pathways that in time will help prevent aortic dissection all together[82].

References

1. Dietz, H. C. *et al.* Marfan syndrome caused by a recurrent de novo missense mutation in the fibrillin gene. *Nature* **352,** 337–9. ISSN: 0028-0836 (July 1991).

2. Ramirez, F. & Sakai, L. Y. Biogenesis and function of fibrillin assemblies. *Cell Tissue Res* **339,** 71–82. ISSN: 1432-0878 (Jan. 2010).

3. Neptune, E. R. *et al.* Dysregulation of TGF-beta activation contributes to pathogenesis in Marfan syndrome. *Nat Genet* **33,** 407–11. ISSN: 1061-4036 (Mar. 2003).

4. Habashi, J. P. *et al.* Losartan, an AT1 antagonist, prevents aortic aneurysm in a mouse model of Marfan syndrome. *Science* **312,** 117–121. ISSN: 1095-9203 (Apr. 2006).

5. Loeys, B. L. *et al.* A syndrome of altered cardiovascular, craniofacial, neurocognitive and skeletal development caused by mutations in TGFBR1 or TGFBR2. *Nat Genet* **37,** 275–81. ISSN: 1061-4036 (Mar. 2005).

6. Micha, D. *et al.* SMAD2 Mutations Are Associated with Arterial Aneurysms and Dissections. *Human Mutation* **36,** 1145–1149. ISSN: 10597794 (Dec. 2015).

7. Van de Laar, I. M. B. H. *et al.* Mutations in SMAD3 cause a syndromic form of aortic aneurysms and dissections with early-onset osteoarthritis. *Nature genetics* **43,** 121–126. ISSN: 1061-4036 (Feb. 2011).

8. Lindsay, M. E. *et al.* Loss-of-function mutations in TGFB2 cause a syndromic presentation of thoracic aortic aneurysm. *Nat Genet* **44,** 922–7. ISSN: 1546-1718 (Aug. 2012).

9. Boileau, C. *et al.* TGFB2 mutations cause familial thoracic aortic aneurysms and dissections associated with mild systemic features of Marfan syndrome. *Nat Genet* **44,** 916–21. ISSN: 1546-1718 (Aug. 2012).

10. Bertoli-Avella, A. M. *et al.* Mutations in a TGF-β Ligand, TGFB3, Cause Syndromic Aortic Aneurysms and Dissections. *Journal of the American College of Cardiology* **65,** 1324–36. ISSN: 1558-3597 (Apr. 2015).

11. Doyle, A. J. *et al.* Mutations in the TGF-β repressor SKI cause Shprintzen-Goldberg syndrome with aortic aneurysm. *Nat Genet* **44,** 1249–54. ISSN: 1546-1718 (Sept. 2012).

12. Schepers, D. *et al.* A mutation update on the LDS-associated genes TGFB2/3 and SMAD2/3. *Human Mutation.* ISSN: 10597794. doi:`10.1002/humu.23407` (Mar. 2018).

13. Regalado, E. S. *et al.* Exome sequencing identifies SMAD3 mutations as a cause of familial thoracic aortic aneurysm and dissection with intracranial and other arterial aneurysms. *Circ Res* **109,** 680–6. ISSN: 1524-4571 (Sept. 2011).

14. Barbier, M. *et al.* MFAP5 Loss-of-Function Mutations Underscore the Involvement of Matrix Alteration in the Pathogenesis of Familial Thoracic Aortic Aneurysms and Dissections. *The American Journal of Human Genetics* **95,** 736–743. ISSN: 00029297 (Dec. 2014).

15. Luyckx, I. & Loeys, B. L. The genetic architecture of non-syndromic thoracic aortic aneurysm. *Heart* **101,** 1678–1684. ISSN: 1355-6037 (Oct. 2015).

16. Gallo, E. M. *et al.* Angiotensin II-dependent TGF-beta signaling contributes to Loeys-Dietz syndrome vascular pathogenesis. *Journal of Clinical Investigation* **124,** 448–460. ISSN: 00219738 (2014).

17. Majesky, M. W. Developmental Basis of Vascular Smooth Muscle Diversity. *Arteriosclerosis, Thrombosis, and Vascular Biology* **27,** 1248–1258. ISSN: 1079-5642 (June 2007).

18. Topouzis, S. & Majesky, M. W. Smooth Muscle Lineage Diversity in the Chick Embryo. *Developmental Biology* **178,** 430–445. ISSN: 00121606 (Sept. 1996).

19. Rodriguez-Vita, J. *et al.* Angiotensin II Activates the Smad Pathway in Vascular Smooth Muscle Cells by a Transforming Growth Factor- -Independent Mechanism. *Circulation* **111,** 2509–2517. ISSN: 0009-7322 (May 2005).

20. Loeys, B. L. *et al.* Mutations in fibrillin-1 cause congenital scleroderma: stiff skin syndrome. *Sci Transl Med* **2,** 23ra20. ISSN: 1946-6242 (Mar. 2010).

21. Le Goff, C. *et al.* Mutations in the TGFβ binding-protein-like domain 5 of FBN1 are responsible for acromicric and geleophysic dysplasias. en. *Am J Hum Genet* **89,** 7–14. ISSN: 1537-6605 (July 2011).

22. Forte, A., Galderisi, U., Cipollaro, M., De Feo, M. & Corte, A. Epigenetic regulation of TGF- 1 signalling in dilative aortopathy of the thoracic ascending aorta. *Clinical Science* **130,** 1389–1405. ISSN: 0143-5221 (2016).

23. Albinsson, S. & Swärd, K. Targeting smooth muscle microRNAs for thera-
     peutic benefit in vascular disease. *Pharmacological Research* **75,** 28–36. ISSN:
     10436618 (Sept. 2013).

24. Hergenreider, E. *et al.* Atheroprotective communication between endothelial
     cells and smooth muscle cells through miRNAs. *Nature Cell Biology* **14,** 249–
     256. ISSN: 1465-7392 (Feb. 2012).

25. Luna, C., Li, G., Qiu, J., Epstein, D. L. & Gonzalez, P. MicroRNA-24 regu-
     lates the processing of latent TGFβ1 during cyclic mechanical stress in human
     trabecular meshwork cells through direct targeting of FURIN. *Journal of Cel-
     lular Physiology* **226,** 1407–1414. ISSN: 00219541 (May 2011).

26. Leeper, N. J. *et al.* MicroRNA-26a is a novel regulator of vascular smooth
     muscle cell function. *Journal of Cellular Physiology* **226,** 1035–1043. ISSN:
     00219541 (Apr. 2011).

27. Cui, H. *et al.* MicroRNA-27a-3p Is a Negative Regulator of Lung Fibrosis by
     Targeting Myofibroblast Differentiation. *American journal of respiratory cell
     and molecular biology* **54,** 843–52. ISSN: 1535-4989 (June 2016).

28. Renard, M. *et al.* Novel MYH11 and ACTA2 mutations reveal a role for
     enhanced TGFβ signaling in FTAAD. *Int J Cardiol* **165,** 314–21. ISSN: 1874-
     1754 (Sept. 2013).

29. Braverman, A. C. *et al.* The bicuspid aortic valve. *Curr Probl in Cardiol* **30,**
     470–522. ISSN: 0146-2806 (Sept. 2005).

30. Jain, R. *et al.* Cardiac neural crest orchestrates remodeling and functional
     maturation of mouse semilunar valves. *J Clin Invest* **121,** 422–30. ISSN: 1558-
     8238 (Jan. 2011).

31. Loscalzo, M. L. *et al.* Familial thoracic aortic dilation and bicommissural
     aortic valve: a prospective analysis of natural history and inheritance. *Am J
     Med Genet* **143A,** 1960–7. ISSN: 1552-4825 (Sept. 2007).

32. Nataatmadja, M., West, J., Prabowo, S. & West, M. Angiotensin II Receptor
     Antagonism Reduces Transforming Growth Factor Beta and Smad Signaling
     in Thoracic Aortic Aneurysm. *The Ochsner journal* **13,** 42–8. ISSN: 1524-5012
     (Jan. 2013).

33. Paloschi, V. *et al.* Aneurysm Development in Patients With a Bicuspid Aortic Valve Is Not Associated With Transforming Growth Factor- Activation. *Arteriosclerosis, Thrombosis, and Vascular Biology* **35,** 973–980. ISSN: 1079-5642 (2015).

34. Gillis, E. *et al.* Candidate Gene Resequencing in a Large Bicuspid Aortic Valve-Associated Thoracic Aortic Aneurysm Cohort: SMAD6 as an Important Contributor. *Frontiers in physiology* **8,** 400. ISSN: 1664-042X (2017).

35. Shah, A. A. *et al.* Epigenetic profiling identifies novel genes for ascending aortic aneurysm formation with bicuspid aortic valves. *The heart surgery forum* **18,** E134–9. ISSN: 1522-6662 (Aug. 2015).

36. Marin, T. *et al.* Mechanosensitive microRNAs—role in endothelial responses to shear stress and redox state. *Free Radical Biology and Medicine* **64,** 61–68. ISSN: 08915849 (Sept. 2013).

37. Demolli, S. *et al.* Shear stress-regulated miR-27b controls pericyte recruitment by repressing SEMA6A and SEMA6D. *Cardiovascular Research* **113,** 681–691. ISSN: 0008-6363 (May 2017).

38. Nistri, S., Giusti, B., Pepe, G. & Cademartiri, F. Another piece in the puzzle of bicuspid aortic valve syndrome. *European Heart Journal – Cardiovascular Imaging,* jew169. ISSN: 2047-2404 (2016).

39. Mahadevia, R. *et al.* Bicuspid Aortic Cusp Fusion Morphology Alters Aortic Three-Dimensional Outflow Patterns, Wall Shear Stress, and Expression of Aortopathy. *Circulation* **129,** 673–682. ISSN: 0009-7322 (Feb. 2014).

40. Fedak, P. W. M. *et al.* Vascular matrix remodeling in patients with bicuspid aortic valve malformations: implications for aortic dilatation. *J Thorac Cardiovasc Surg* **126,** 797–806. ISSN: 0022-5223 (Sept. 2003).

41. Ashworth, J. L. *et al.* Fibrillin degradation by matrix metalloproteinases: implications for connective tissue remodelling. *The Biochemical journal* **340 (Pt 1,** 171–81. ISSN: 0264-6021 (May 1999).

42. Rabkin, S. W. Differential expression of MMP-2, MMP-9 and TIMP proteins in thoracic aortic aneurysm - comparison with and without bicuspid aortic valve: a meta-analysis. *VASA. Zeitschrift für Gefässkrankheiten* **43,** 433–42. ISSN: 0301-1526 (Nov. 2014).

43. Kuang, S.-Q. *et al.* FOXE3 mutations predispose to thoracic aortic aneurysms and dissections. *Journal of Clinical Investigation* **126,** 948–961. ISSN: 0021-9738 (Feb. 2016).

44. Guzzardi, D. G. *et al.* Valve-Related Hemodynamics Mediate Human Bicuspid Aortopathy: Insights From Wall Shear Stress Mapping. *Journal of the American College of Cardiology* **66,** 892–900. ISSN: 1558-3597 (Aug. 2015).

45. Katsanis, N. *et al.* The continuum of causality in human genetic disorders. *Genome Biology* **17,** 233. ISSN: 1474-760X (Dec. 2016).

46. Exome Aggregation Consortium *et al.* Analysis of protein-coding genetic variation in 60,706 humans. *Nature* **536,** 285–291 (2016).

47. Veltman, J. A. & Lupski, J. R. From genes to genomes in the clinic. *Genome Medicine* **7,** 78. ISSN: 1756-994X (Dec. 2015).

48. Starita, L. M. *et al.* Massively parallel functional analysis of BRCA1 RING domain variants. *Genetics* **200,** 413–422. ISSN: 19432631 (2015).

49. Losenno, K. L., Goodman, R. L. & Chu, M. W. a. Bicuspid aortic valve disease and ascending aortic aneurysms: gaps in knowledge. *Cardiol Res Pract* **2012,** 145202. ISSN: 2090-0597 (Jan. 2012).

50. Bonderman, D. *et al.* Mechanisms underlying aortic dilatation in congenital aortic valve malformation. *Circulation* **99,** 2138–43. ISSN: 1524-4539 (Apr. 1999).

51. Dudzinski, D. M. & Isselbacher, E. M. Diagnosis and Management of Thoracic Aortic Disease. *Current Cardiology Reports* **17,** 106. ISSN: 1523-3782 (Dec. 2015).

52. Kaiser, T., Kellenberger, C. J., Albisetti, M., Bergsträsser, E. & Valsangiacomo Buechel, E. R. Normal values for aortic diameters in children and adolescents–assessment in vivo by contrast-enhanced CMR-angiography. *J Cardiovasc Magn Reson* **10,** 56. ISSN: 1532-429X (Jan. 2008).

53. Devereux, R. B. *et al.* Normal limits in relation to age, body size and gender of two-dimensional echocardiographic aortic root dimensions in persons ≥15 years of age. *Am J Cardiol* **110,** 1189–94. ISSN: 1879-1913 (Oct. 2012).

54. Pepe, G. *et al.* Marfan syndrome: current perspectives. *The application of clinical genetics* **9,** 55–65 (2016).

55. Wang, L. *et al.* Mutations in myosin light chain kinase cause familial aortic dissections. *Am J Hum Genet* **87,** 701–7. ISSN: 1537-6605 (Nov. 2010).

56. Guo, D.-c. *et al.* Recurrent gain-of-function mutation in PRKG1 causes thoracic aortic aneurysms and acute aortic dissections. *American journal of human genetics* **93,** 398–404. ISSN: 1537-6605 (Aug. 2013).

57. Guzzardi, D. G., Verma, S. & Fedak, P. W. Bicuspid aortic valve aortopathy. *Current Opinion in Cardiology,* 1. ISSN: 0268-4705 (2016).

58. Lazar-karsten, P. Genetic Basis , Pathogenesis and Histopathology of Aortopathy in Bicuspid Aortic Valve and Marfan Syndrome (2015).

59. Sherrah, A. G. *et al.* Nonsyndromic Thoracic Aortic Aneurysm and Dissection: Outcomes With Marfan Syndrome Versus Bicuspid Aortic Valve Aneurysm. *Journal of the American College of Cardiology* **67,** 618–626. ISSN: 0735-1097 (Feb. 2016).

60. Girdauskas, E. *et al.* Aortic Dissection After Previous Aortic Valve Replacement for Bicuspid Aortic Valve Disease. *Journal of the American College of Cardiology* **66,** 1409–1411. ISSN: 07351097 (Sept. 2015).

61. Emmott, A. *et al.* Biomechanics of the Ascending Thoracic Aorta: A Clinical Perspective on Engineering Data. *Canadian Journal of Cardiology* **32,** 35–47. ISSN: 0828282X (Jan. 2016).

62. Dietz, H. *Marfan Syndrome* (University of Washington, Seattle, Oct. 2001).

63. Freeze, S. L., Landis, B. J., Ware, S. M. & Helm, B. M. Bicuspid Aortic Valve: a Review with Recommendations for Genetic Counseling. *Journal of genetic counseling* **25,** 1171–1178. ISSN: 1573-3599 (Dec. 2016).

64. Shores, J., Berger, K. R., Murphy, E. A. & Pyeritz, R. E. Progression of aortic dilatation and the benefit of long-term beta-adrenergic blockade in Marfan's syndrome. *N Engl J Med* **330,** 1335–41. ISSN: 0028-4793 (May 1994).

65. Judge, D. P. & Dietz, H. C. Marfan's syndrome. *Lancet* **366,** 1965–76. ISSN: 1474-547X (Dec. 2005).

66. Milleron, O. *et al.* Marfan Sartan: a randomized, double-blind, placebo-controlled trial. *European Heart Journal* **36,** 2160–2166. ISSN: 0195-668X (Aug. 2015).

67. Groenink, M. *et al.* Losartan reduces aortic dilatation rate in adults with Marfan syndrome: a randomized controlled trial. *European Heart Journal* **34,** 3491–3500. ISSN: 0195-668X (Dec. 2013).

68. Lindsay, M. E. & Dietz, H. C. Lessons on the pathogenesis of aneurysm from heritable conditions. *Nature* **473,** 308–16. ISSN: 1476-4687 (May 2011).

69. Lacro, R. V. *et al.* Atenolol versus Losartan in Children and Young Adults with Marfan's Syndrome. *New England Journal of Medicine* **371,** 2061–2071. ISSN: 0028-4793 (Nov. 2014).

70. Chan, K. K., Lai, P. & Wright, J. M. in *Cochrane Database of Systematic Reviews* (ed Chan, K. K.) 2, CD010426 (John Wiley & Sons, Ltd, Chichester, UK, Feb. 2014). doi:10.1002/14651858.CD010426.pub2.

71. Pitcher, A. *et al.* Design and rationale of a prospective, collaborative meta-analysis of all randomized controlled trials of angiotensin receptor antagonists in Marfan syndrome, based on individual patient data: A report from the Marfan Treatment Trialists' Collaboration. *American Heart Journal* **169,** 605–612. ISSN: 00028703 (May 2015).

72. Mullen, M. J. *et al.* A prospective, randomized, placebo-controlled, double-blind, multicenter study of the effects of irbesartan on aortic dilatation in Marfan syndrome (AIMS trial): study protocol. *Trials* **14,** 408 (Dec. 2013).

73. Franken, R. *et al.* Beneficial Outcome of Losartan Therapy Depends on Type of FBN1 Mutation in Marfan Syndrome. *Circulation: Cardiovascular Genetics* **8,** 383–388. ISSN: 1942-325X (Apr. 2015).

74. Doyle, J. J. *et al.* A deleterious gene-by-environment interaction imposed by calcium channel blockers in Marfan syndrome. *eLife* **4.** ISSN: 2050-084X. doi:10.7554/eLife.08648 (Jan. 2015).

75. Chen, X. *et al.* TGF-β Neutralization Enhances AngII-Induced Aortic Rupture and Aneurysm in Both Thoracic and Abdominal Regions. *PloS one* **11** (ed Aikawa, E.) e0153811. ISSN: 1932-6203 (Apr. 2016).

76. Pereira, L. *et al.* Targetting of the gene encoding fibrillin-1 recapitulates the vascular aspect of Marfan syndrome. *Nat Genet* **17,** 218–22. ISSN: 1061-4036 (Oct. 1997).

77. Cook, J. R. *et al.* Dimorphic Effects of Transforming Growth Factor-β Signaling During Aortic Aneurysm Progression in Mice Suggest a Combinatorial Therapy for Marfan SyndromeSignificance. *Arteriosclerosis, Thrombosis, and Vascular Biology* **35,** 911–917. ISSN: 1079-5642 (Apr. 2015).

78. Newby, A. C. Matrix metalloproteinase inhibition therapy for vascular diseases. *Vascul Pharmacol* **56,** 232–44. ISSN: 1879-3649 (2012).

79. Guo, G. *et al.* Antagonism of GxxPG fragments ameliorates manifestations of aortic disease in Marfan syndrome mice. *Hum Mol Genet* **22,** 433–43. ISSN: 1460-2083 (Nov. 2013).

80. Shen, Y. H. *et al.* Stem cells in thoracic aortic aneurysms and dissections: potential contributors to aortic repair. *Ann Thorac Surg* **93,** 1524–33. ISSN: 1552-6259 (May 2012).

81. Hawkins, R. B. *et al.* Abstract 16936: Mesenchymal Stem Cell Administration Attenuates Thoracic Aortic Aneurysm Formation. *Circulation* **134** (2016).

82. Milewicz, D. M., Prakash, S. K. & Ramirez, F. Therapeutics Targeting Drivers of Thoracic Aortic Aneurysms and Acute Aortic Dissections: Insights from Predisposing Genes and Mouse Models. *Annual review of medicine* **68,** 51–67. ISSN: 1545-326X (Jan. 2017).

Curriculum Vitae Elisabeth Gillis

Name: Elisabeth Gillis

Address: Lintsesteenweg 32, 2570 Duffel, Belgium

Tel: +32 498 70 58 35

Current position

HistoGeneX

Data Manager

2017 - present

Education

University of Antwerp, Centre for Medical Genetics

PhD in Medical Genetics

Dissertation: Contribution to elucidating the genetic aetiology of thoracic aortic aneurysms

2012-2016

University of Antwerp

Master in Biochemistry and biotechnology

2010-2012

University of Antwerp

Bachelor in Biochemistry and biotechnology

2007-2010

Research experience

McKusick-/Nathans Institute of Genetic Medicine, Johns Hopkins University, Baltimore, Maryland, USA

Visiting researcher with Prof. Dr. Harry C. Dietz

Jan 2015 - March 2015

Selected poster and oral presentations

European Society of human genetics 2015 Mutations in a TGF-β Ligand, *TGFB3*, Cause Syndromic Aortic Aneurysms and Dissections
Selected speaker

European Society of human genetics 2014 FBN1 deep intronic mutations: Can they explain the molecularly unresolved Marfan cases?
Selected poster

Belgian Society of human genetics 2014 FBN1 deep intronic mutations: Can they explain the molecularly unresolved Marfan cases?
Selected poster

Belgian Society of human genetics 2013 Mutations in the TGF-β repressor SKI cause Shprintzen-Goldberg syndrome with aortic aneurysm
Selected poster

Elastin, Elastic Fibers and Microfibrils 2013 Exclusion of TGFB1 and TGFBR3 as major candidate genes for syndromic thoracic aortic aneurysms
Selected poster

Publications

Gillis E, Kumar AA, Luyckx I, Preuss C, Cannaerts E, van de Beek G, Wieschendorf B, Alaerts M, Bolar N, Vandeweyer G, Meester J, Wünnemann F, Gould RA, Zhurayev R, Zerbino D, Mohamed SA, Mital S, Mertens L, Björck HM, Franco-Cereceda A, McCallion AS, Van Laer L, Verhagen JMA, van de Laar IMBH, Wessels MW, Messas E, Goudot G, Nemcikova M, Krebsova A, Kempers M, Salemink S, Duijnhouwer T, Jeunemaitre X, Albuisson J, Eriksson P, Andelfinger G, Dietz HC, Verstraeten A, Loeys BL, Mibava Leducq Consortium. Candidate

Gene Resequencing in a Large Bicuspid Aortic Valve-Associated Thoracic Aortic Aneurysm Cohort: SMAD6 as an Important Contributor. Frontiers of Physiology, 2017. 13;8:400.

Bertoli-Avella AM, **Gillis E**, Morisaki H, Verhagen JMA, de Graaf BM, van de Beek G, Gallo E, Kruithof BPT, Venselaar H, Myers LA, Laga S, Doyle AJ, Oswald G, van Cappellen GWA, Yamanaka I, van der Helm RM, Beverloo B, de Klein A, Pardo L, Lammens M, Evers C, Devriendt K, Dumoulein M, Timmermans J, Bruggenwirth HT, Verheijen F, Rodrigus I, Baynam G, Kempers M, Saenen J, Van Craenenbroeck EM, Minatoya K, Matsukawa R, Tsukube T, Kubo N, Hofstra R, Goumans MJ, Bekkers JA, Roos-Hesselink JW, van de Laar IMBH, Dietz HC, Van Laer L, Morisaki T, Wessels MW, Loeys BL. Mutations in a TGF-β ligand, TGFB3, cause syndromic aortic aneurysms and dissections. Journal of the American College of Cardiology, 2015. 7;65(13), p.1324-1336.

Gillis E, Kempers M, Salemink S, Timmermans J, Cheriex EC, Bekkers SC, Fransen E, De Die-Smulders CE, Loeys BL, Van Laer L. An FBN1 deep intronic mutation in a familial case of Marfan syndrome: an explanation for genetically unsolved cases? Human Mutation, 2014; 35(5), p.571-4.

Gillis E, Van Laer L, Loeys BL. Genetics of Thoracic Aortic Aneurysm: At the Crossroad of Transforming Growth Factor-β Signaling and Vascular Smooth Muscle Cell Contractility. Circulation Research, 2013; 113, p.327-340.

Doyle AJ, Doyle JJ, Bessling SL, Maragh S, Lindsay ME, Schepers D, **Gillis E**, Mortier G, Homfray T, Sauls K, Norris RA, Huso ND, Leahy D, Mohr DW, Caulfield MJ, Scott AF, Destrée A, Hennekam RC, Arn PH, Curry CJ, Van Laer L, McCallion AS, Loeys BL, Dietz HC. Mutations in the TGF-β repressor SKI cause Shprintzen-Goldberg syndrome with aortic aneurysm. Nature Genetics, 2012; 44(11), p.1249-54.